



*Midwest States Regional Pooled Fund Research Program  
Fiscal Year 2007 (Year 17)  
Research Project Number SPR-3(017)  
NDOR Sponsoring Agency Code RFPF-07-06*

**DEVELOPMENT AND RECOMMENDATIONS FOR A  
NON-PROPRIETARY, HIGH-TENSION, CABLE END  
TERMINAL SYSTEM**

Submitted by

Ryan J. Terpsma, M.S.M.E., E.I.T.  
Former Graduate Research Assistant

John D. Reid, Ph.D.  
Professor

Ronald K. Faller, Ph.D., P.E.  
Research Assistant Professor

Dean L. Sicking, Ph.D., P.E.  
Professor and MwRSF Director

**MIDWEST ROADSIDE SAFETY FACILITY**

Nebraska Transportation Center  
University of Nebraska-Lincoln  
130 Whittier Research Center  
2200 Vine Street  
Lincoln, Nebraska 68583-0853  
(402) 472-0965

Submitted to

**MIDWEST STATES REGIONAL POOLED FUND PROGRAM**

Nebraska Department of Roads  
1500 Nebraska Highway 2  
Lincoln, Nebraska 68502

MwRSF Research Report No. TRP-03-268-12

July 17, 2012

## TECHNICAL REPORT DOCUMENTATION PAGE

1. Report No. TRP-03-268-12	2.	3. Recipient's Accession No.	
4. Title and Subtitle Development and Recommendations for a Non-Proprietary, High-Tension, Cable End Terminal System		5. Report Date July 17, 2012	
		6.	
7. Author(s) Terpsma, R.J., Reid, J.D., Faller, R.K. and Sicking, D.L.		8. Performing Organization Report No. TRP-03-268-12	
9. Performing Organization Name and Address Midwest Roadside Safety Facility (MwRSF) Nebraska Transportation Center University of Nebraska-Lincoln 130 Whittier Research Center 2200 Vine Street Lincoln, Nebraska 68583-0853		10. Project/Task/Work Unit No.	
		11. Contract © or Grant (G) No. SPR-3(017) Supplement No. 38	
12. Sponsoring Organization Name and Address Midwest States Regional Pooled Fund Program Nebraska Department of Roads 1500 Nebraska Highway 2 Lincoln, Nebraska 68502		13. Type of Report and Period Covered Final Report: 2010 – 2012	
		14. Sponsoring Agency Code RPFPP-07-06	
15. Supplementary Notes Prepared in cooperation with U.S. Department of Transportation, Federal Highway Administration.			
16. Abstract (Limit: 200 words) <p>Cable guardrail systems have been increasing in popularity in recent years due to several perceived benefits over the commonly used W-beam guardrail. A non-proprietary design was desired as an alternative to the many proprietary designs available. A non-proprietary, high-tension, cable end terminal was necessary to accompany the non-proprietary, high-tension, cable guardrail system under development. The objective of this research project was to develop design recommendations for a non-proprietary, high-tension, cable end terminal. An analysis of several cable guardrail end terminals was undertaken to identify any common features that may prove to be beneficial or detrimental to end terminal designs. Next, a study of the non-proprietary, low-tension system was conducted to determine the cause of vehicle instabilities in full-scale testing. Since the high-tension and low-tension, cable end terminal designs are similar, it is likely that any issues with the low-tension design will also be evident in testing of the high-tension design.</p> <p>LS-DYNA modeling of current cable terminal anchor hardware was then accomplished and compared to bogie testing results. The anchor model proved to be sufficiently accurate to preliminarily analyze alternative cable anchor designs. A final, optimized, high-tension, cable anchor design was produced along with alternative terminal post recommendations for continuing development of the non-proprietary, high-tension, cable end terminal.</p>			
17. Document Analysis/Descriptors Highway Safety, Crash Test, Roadside Appurtenances, Compliance Test, MASH, High-Tension, Cable Guardrail, End Terminal, Cable Anchor Bracket		18. Availability Statement No restrictions. Document available from: National Technical Information Services, Springfield, Virginia 22161	
19. Security Class (this report) Unclassified	20. Security Class (this page) Unclassified	21. No. of Pages 186	22. Price

## **DISCLAIMER STATEMENT**

This report was completed with funding from the Federal Highway Administration, U.S. Department of Transportation. The contents of this report reflect the views and opinions of the authors who are responsible for the facts and the accuracy of the data presented herein. The contents do not necessarily reflect the official views or policies of the state highway departments participating in the Midwest States Regional Pooled Fund Program nor the Federal Highway Administration, U.S. Department of Transportation. This report does not constitute a standard, specification, regulation, product endorsement, or an endorsement of manufacturers.

## **ACKNOWLEDGEMENTS**

The authors wish to acknowledge several sources that made a contribution to this project:

(1) the Midwest States Regional Pooled Fund Program funded by the Illinois Department of Transportation, Iowa Department of Transportation, Kansas Department of Transportation, Minnesota Department of Transportation, Missouri Department of Transportation, Nebraska Department of Roads, Ohio Department of Transportation, South Dakota Department of Transportation, Wisconsin Department of Transportation, and Wyoming Department of Transportation for sponsoring this project; and (2) MwRSF personnel for constructing the barriers and conducting the crash tests.

Acknowledgement is also given to the following individuals who made a contribution to the completion of this research project.

### **Midwest Roadside Safety Facility**

J.C. Holloway, M.S.C.E., E.I.T., Test Site Manager  
K.A. Lechtenberg, M.S.M.E., E.I.T., Research Associate Engineer  
R.W. Bielenberg, M.S.M.E., E.I.T., Research Associate Engineer  
S.K. Rosenbaugh, M.S.C.E., E.I.T., Research Associate Engineer  
C.L. Meyer, B.S.M.E., E.I.T., Former Research Associate Engineer  
M. Mongiardini, Ph.D., Post-Doctoral Research Assistant  
A.T. Russell, B.S.B.A., Shop Manager  
K.L. Krenk, B.S.M.A., Maintenance Mechanic  
D.S. Charroin, Laboratory Mechanic  
S.M. Tighe, Laboratory Mechanic  
Undergraduate and Graduate Research Assistants

### **Illinois Department of Transportation**

David Piper, P.E., Safety Implementation Engineer (retired)  
Priscilla A. Tobias, P.E., State Safety Engineer/Bureau Chief

### **Iowa Department of Transportation**

David Little, P.E., Assistant District Engineer  
Deanna Maifield, P.E., Methods Engineer  
Chris Poole, P.E., Roadside Safety Engineer

**Kansas Department of Transportation**

Ron Seitz, P.E., Bureau Chief  
Rod Lacy, P.E., Metro Engineer  
Scott King, P.E., Road Design Leader

**Minnesota Department of Transportation**

Michael Elle, P.E., Design Standard Engineer

**Missouri Department of Transportation**

Joseph G. Jones, P.E., Engineering Policy Administrator

**Nebraska Department of Roads**

Amy Starr, P.E., Research Engineer  
Phil TenHulzen, P.E., Design Standards Engineer  
Jodi Gibson, Research Coordinator

**Ohio Department of Transportation**

Maria Ruppa, P.E., Roadway Safety Engineer  
Michael Bline, P.E., Standards and Geometrics Engineer

**South Dakota Department of Transportation**

David Huft, Research Engineer  
Bernie Clocksin, Lead Project Engineer

**Wisconsin Department of Transportation**

Jerry Zogg, P.E., Chief Roadway Standards Engineer  
John Bridwell, P.E., Standards Development Engineer  
Erik Emerson, P.E., Standards Development Engineer

**Wyoming Department of Transportation**

William Wilson, P.E., Architectural and Highway Standards Engineer

**Federal Highway Administration**

John Perry, P.E., Nebraska Division Office  
Danny Briggs, Nebraska Division Office

**TABLE OF CONTENTS**

TECHNICAL REPORT DOCUMENTATION PAGE ..... i

DISCLAIMER STATEMENT ..... ii

ACKNOWLEDGEMENTS ..... iii

TABLE OF CONTENTS ..... v

LIST OF FIGURES ..... viii

LIST OF TABLES ..... xi

1 INTRODUCTION ..... 1

    1.1 Problem Statement ..... 1

    1.2 Background ..... 2

    1.3 Research Objectives ..... 4

    1.4 Scope ..... 4

    1.5 Research Approach ..... 5

2 LITERATURE REVIEW ..... 7

    2.1 Introduction ..... 7

    2.2 Previously-Tested High-Tension, Cable End Terminal Designs ..... 7

        2.2.1 Texas Transportation Institute ..... 9

        2.2.2 Brifen ..... 12

        2.2.3 Gibraltar ..... 14

        2.2.4 Safence ..... 17

        2.2.5 Armorflex ..... 19

    2.3 Discussion ..... 22

3 EVALUATION OF THE LOW-TENSION, THREE-CABLE END TERMINAL TEST SERIES ..... 24

    3.1 Background ..... 24

    3.2 Simulation of the Low-Tension, Three-Cable End Terminal ..... 25

        3.2.1 Low-Tension, Three-Cable, Anchor Bracket Assembly ..... 25

        3.2.2 Slip Base Post No. 1 ..... 29

        3.2.3 Slip Base Line Posts ..... 31

        3.2.4 Cables ..... 32

            3.2.4.1 Pre-Tension ..... 32

        3.2.5 Vehicle Model ..... 32

        3.2.6 Model Construction ..... 33

        3.2.7 End Terminal Model Validation ..... 33

        3.2.8 Discussion ..... 40

            3.2.8.1 Vehicle Trajectory ..... 40

            3.2.8.2 Slip Base Post Performance Analysis ..... 42

                3.2.8.2.1 Full-Scale Testing Evaluation ..... 42

3.2.8.2.2	M4x3.2 (M102x4.8) Replacement Post Option .....	42
3.2.8.2.3	Modified S3x5.7 (S7x8.5) Post Option.....	44
3.2.8.2.4	Terminal Post Replacement Options Summary .....	47
3.3	Conclusions.....	48
4	CURRENT, HIGH-TENSION, CABLE ANCHOR BRACKET DESIGN .....	51
5	INITIAL COMPUTER SIMULATION .....	57
5.1	Introduction.....	57
5.2	Abbreviated, High-Tension, Cable End Terminal System Model.....	58
5.2.1	High-Tension, Cable Anchor Bracket Assembly.....	58
5.2.2	Slip Base Post Assembly .....	61
5.2.3	System Cables.....	62
5.2.4	Bogie Model.....	66
5.3	Bogie Test Simulation.....	67
5.4	Discussion.....	70
6	HIGH-TENSION, CABLE END TERMINAL BOGIE TESTING .....	71
6.1	Purpose.....	71
6.2	Scope.....	71
6.3	System Details .....	72
6.3.1	Cable Anchor Bracket Assemblies .....	72
6.3.2	Slip Base Post Assemblies.....	81
6.3.3	System Cables.....	82
6.4	Equipment and Instrumentation.....	83
6.4.1	Bogie.....	83
6.4.2	Accelerometer.....	84
6.4.3	Pressure Tape Switches.....	84
6.4.4	Digital Cameras .....	84
6.5	Data Processing.....	85
7	BOGIE TESTING – TEST NO. HTCT-1.....	86
7.1	Procedures.....	86
7.2	Test Description, Test No. HTCT-1 .....	86
7.3	System Damage .....	87
8	SIMULATION MODEL EVALUATION .....	101
8.1	Introduction.....	101
8.2	High-Speed Video Comparison .....	101
8.3	Accelerometer Data Comparison.....	103
8.4	Component Damage Comparison.....	105
8.5	Discussion and Conclusions .....	109
9	REDESIGN OF THE HIGH-TENSION, CABLE ANCHOR BRACKET ASSEMBLY .....	111
9.1	Introduction.....	111
9.2	Design Issues .....	111
9.2.1	Cable Release Lever .....	112

- 9.2.2 Cable Release Lever Rotation Point ..... 113
- 9.2.3 Cable Anchor Bracket Assembly Geometry ..... 116
- 9.3 Alternate Design Development ..... 119
  - 9.3.1 Redesigned, High-Tension, Cable Anchor Bracket Assembly Model Development ..... 119
    - 9.3.1.1 Cable Release Lever Rotation Brackets ..... 120
    - 9.3.1.2 Cable Anchor Bracket Assembly Rotation Support Brackets ..... 122
    - 9.3.1.3 Cable Release Lever Rotation Bolts ..... 122
  - 9.3.2 Model Development Simulations ..... 123
    - 9.3.2.1 Simulation No. 1 - Initial Anchor Bracket Assembly Model ..... 123
    - 9.3.2.2 Simulation No. 2 – Redesigned Support Bracket and Cable Release Lever Model ..... 124
    - 9.3.2.3 Simulation No. 3 – Redesign of Rotational Joint Hardware ..... 128
    - 9.3.2.4 Simulation No. 4 – Analysis of Release Lever Modification ..... 131
    - 9.3.2.5 Simulation No. 5 – Increased Cable Tension ..... 136
    - 9.3.2.6 Simulation No. 6 –Anchor Impact at Oblique Angle ..... 139
    - 9.3.2.7 Simulation No. 7 - Reverse Direction Impact ..... 141
- 9.4 Final Design and Simulation ..... 146
  - 9.4.1 Final Redesigned Cable Anchor Bracket Assembly ..... 146
  - 9.4.2 Simulation ..... 146
  - 9.4.3 Discussion ..... 157
- 10 SUMMARY, CONCLUSIONS, AND RECOMMENDATIONS ..... 162
  - 10.1 Summary ..... 162
  - 10.2 Conclusions and Recommendations ..... 164
    - 10.2.1 Future Work ..... 166
- 11 REFERENCES ..... 169
- 12 APPENDICES ..... 171
  - Appendix A. Initial Simulation Results - Metric ..... 172
  - Appendix B. Bogie Test Results - Metric ..... 174
  - Appendix C. Standard MwRSF Bogie Test Sheet, Test No. HTCT-1 ..... 179
  - Appendix D. Redesigned Cable Anchor Bracket Simulation Results – Metric ..... 182



## LIST OF FIGURES

Figure 1. TTI End Terminal.....	9
Figure 2. TTI End Terminal, Technical Drawing.....	10
Figure 3. TTI End Terminal, Technical Drawing.....	11
Figure 4. Brifen End Terminal, Technical Drawing.....	13
Figure 5. Gibraltar End Terminal.....	15
Figure 6. Gibraltar End Terminal, Technical Drawing.....	16
Figure 7. Safence End Terminal.....	17
Figure 8. Safence End Terminal, Technical Drawing.....	18
Figure 9. Armorflex End Terminal.....	20
Figure 10. Armorwire End Terminal, Technical Drawing.....	21
Figure 11. Low-Tension, Cable Anchor Bracket Assembly Details.....	26
Figure 12. Low-Tension, Cable Anchor Bracket Component Details.....	27
Figure 13. Low-Tension, Cable Anchor Bracket Component Details.....	28
Figure 14. Cable Anchor Bracket Assembly.....	29
Figure 15. Slip Base Post No. 1 Model.....	30
Figure 16. Slip Base Line Post Model.....	31
Figure 17. Geo Metro Vehicle Model.....	32
Figure 18. Shear Post Impact with Guide Flag, Test No. CT-4.....	35
Figure 19. Guide Flag/Shear Post Impact Force Diagram.....	36
Figure 20. Comparison of Actual and Simulated Vehicle Yaw – Test No. CT-4.....	36
Figure 21. Sequential Comparison at Post Impact Times, CT-4 and Simulation CT-4_13.....	37
Figure 22. Vehicle Trajectory Comparison – 500 ms After Impact.....	38
Figure 23. Geo Metro Overriding System Debris.....	39
Figure 24. Cable Interaction with Slip Base Post No. 1.....	41
Figure 25. Post Cross Section Dimensions.....	43
Figure 26. S3x5.7 (S76x8.5) Post with Cut Flanges.....	44
Figure 27. S3x5.7 (S76x8.5) Post with Weakening Holes.....	46
Figure 28. Cable Anchor Bracket Assembly Drawings.....	52
Figure 29. Cable Anchor Bracket Assembly Details.....	53
Figure 30. Cable Anchor Bracket Component Details.....	54
Figure 31. Cable Release Lever Assembly Details.....	55
Figure 32. Bill of Materials, Cable Anchor Bracket Assembly.....	56
Figure 33. Cable Anchor Bracket Component Mesh.....	59
Figure 34. Cable Anchor Bracket and Finite Element Model.....	60
Figure 35. Slip Base Post Assembly Component Mesh.....	63
Figure 36. Slip Base Post Assembly and Finite Element Model.....	64
Figure 37. Cable and End Fitter Component Model and Mesh.....	65
Figure 37 (continued). Cable and End Fitter Component Model and Mesh.....	66
Figure 38. Bogie Finite Element Model.....	66
Figure 39. Sequential Photographs, Bogie Test Simulation.....	69
Figure 40. Longitudinal Bogie Velocity, Initial Simulation.....	70
Figure 41. Bogie Test System Setup, Test No. HTCT-1.....	73
Figure 42. Bogie Test Layout, Test No. HTCT-1.....	74
Figure 43. Cable Anchor Bracket Assembly Details, Test No. HTCT-1.....	75

Figure 44. Slip Base Post Assembly Details, Test No. HTCT-1 .....	76
Figure 45. Slip Base Post Component Details, Test No. HTCT-1 .....	77
Figure 46. Slip Base Post Component Details, Test No. HTCT-1 .....	78
Figure 47. Cable End Fitters and Turnbuckle Details, Test No. HTCT-1 .....	79
Figure 48. Bill of Materials, Test No. HTCT-1 .....	80
Figure 49. Rigid Frame Bogie on Guidance Track.....	83
Figure 50. Sequential Photographs, Test No. HTCT-1.....	88
Figure 51. Documentary Photographs, Test No. HTCT-1 .....	89
Figure 52. System Damage, Test No. HTCT-1 .....	92
Figure 53. System Damage, Test No. HTCT-1 .....	93
Figure 54. System Damage, Test No. HTCT-1 .....	94
Figure 55. System Damage, Test No. HTCT-1 .....	95
Figure 56. System Damage, Test No. HTCT-1 .....	96
Figure 57. System Damage, Test No. HTCT-1 .....	97
Figure 58. System Damage, Test No. HTCT-1 .....	98
Figure 59. Force vs. Time, Test No. HTCT-1 .....	99
Figure 60. Longitudinal Velocity vs. Time, Test No. HTCT-1 .....	99
Figure 61. Energy vs. Time, Test No. HTCT-1 .....	100
Figure 62. Cable Release Event Comparison, Test No. HTCT-1 vs. Simulation.....	102
Figure 63. Sequential Comparison, Test No. HTCT-1 vs. Simulation.....	104
Figure 64. Bogie Velocity Comparison, Test No. HTCT-1 vs. Simulation .....	105
Figure 65. Upstream Cable Anchor Damage Comparison, Test No. HTCT-1 vs. Simulation....	106
Figure 66. S3x5.7 (S76x8.5) Post Damage Comparison, Test No. HTCT-1 vs. Simulation.....	107
Figure 67. Release Lever Interaction with System Cables, Test No. HTCT-1 vs. Simulation....	108
Figure 68. Simplified Free Body Diagram of Cable Release Lever During Cable Release.....	114
Figure 69. Rotation Point Comparison .....	115
Figure 70. Cable End Fitter Interference .....	117
Figure 71. Cable End Fitter Movement .....	118
Figure 72. Redesigned Cable Anchor Bracket Assembly Model .....	120
Figure 73. Cable Release Lever Rotation Bracket Model .....	121
Figure 74. Cable Anchor Bracket Assembly Rotation Support Bracket Model.....	122
Figure 75. Release Lever Disengaging from Assembly, Simulation No. 1 .....	124
Figure 76. Redesigned Cable Anchor Bracket Support Bracket Geometry.....	125
Figure 77. Redesigned Cable Release Lever, Angled Base Plate.....	126
Figure 78. Distorted Joint on Cable Anchor Bracket Assembly, Simulation No. 2 .....	127
Figure 79. Anchor Bracket Assembly Damage, Simulation No. 2.....	127
Figure 80. Anchor Bracket Assembly von Mises' Stress, Simulation No. 2 .....	128
Figure 81. Bolt Rotation with Washer .....	129
Figure 82. Anchor Bracket Assembly with Rod.....	129
Figure 83. Cable Anchor Bracket Assembly Deformation, Simulation No. 3 .....	130
Figure 84. Anchor Bracket Assembly Plastic Strain, Simulation No. 3 .....	131
Figure 85. Nodal Penetration in Rotation Bracket Contact .....	132
Figure 86. Typical Shell Element and Simulated Contact Surface.....	133
Figure 87. Rotation Bracket Contact Using Solid Elements.....	134
Figure 88. Deformation of Release Lever Assembly Components, von Mises' Stress.....	135
Figure 89. Cable Anchor Bracket Assembly von Mises' Stress, Simulation No. 4 .....	136

Figure 90. Cable Plate Plastic Strain, Simulation No. 5 .....	137
Figure 91. Impact Force Comparison, Increased Cable Tension vs. Design Tension .....	138
Figure 92. 15 Degree Impact Scenario Sequentials, Simulation No. 6.....	140
Figure 93. Cable Release Lever Plastic Strain, Simulation No. 6 .....	141
Figure 94. Bogie Impact Orientation, Simulation No. 7.....	142
Figure 95. Reverse Direction Impact Sequentials, Simulation No. 7 .....	144
Figure 96. Component Plastic Strain, Simulation No. 7.....	145
Figure 97. Redesigned, High-Tension, Cable Anchor Bracket Assembly Model.....	147
Figure 98. Redesigned, High-Tension, Cable Anchor Bracket Assembly .....	148
Figure 99. Cable Anchor Bracket and Cable Release Lever Assembly Details .....	149
Figure 100. Cable Anchor Bracket Component Details .....	150
Figure 101. Cable Release Lever Component Details .....	151
Figure 102. Redesigned, High-Tension, Cable Anchor Bracket Bill of Materials .....	152
Figure 103. Sequential Photographs, Final Redesign .....	154
Figure 104. Cable Anchor Bracket Assembly Damage, Final Redesign .....	155
Figure 105. Plastic Strain in Rotational Bolt, Final Redesign .....	156
Figure 106. Cable Anchor Components After Cable Release, Final Redesign .....	156
Figure 107. Bogie Velocity, Final Redesign.....	157
Figure 108. Comparison of Anchor Assembly von Mises' Stress Distribution .....	159
Figure 109. Anchor Bracket Assembly Simulations Velocity Comparison .....	160
Figure A-1. Bogie Velocity, Initial Simulation .....	173
Figure B-1. Force vs. Time, Test No. HTCT-1 .....	175
Figure B-2. Velocity vs. Time, Test No. HTCT-1 .....	176
Figure B-3. Energy vs. Time, Test No. HTCT-1 .....	177
Figure B-4. Bogie Velocity Comparison .....	178
Figure C-1. Results of Test No. HTCT-1 – English .....	180
Figure C-2. Results of Test No. HTCT-1 – Metric.....	181
Figure D-1. Impact Force Comparison, Increased Cable Tension vs. Design Tension.....	183
Figure D-2. Bogie Velocity, Final Redesign .....	184
Figure D-3. Anchor Bracket Assembly Simulations Velocity Comparison.....	185

**LIST OF TABLES**

Table 1. Comparison of MASH and NCHRP 350 Testing Criteria for Test Level 3 .....3  
Table 2. NCHRP 350 Crash Testing Results on Proprietary, High-Tension, Cable Barriers [8-12]  
.....8  
Table 3. Vertical Impact Forces, Cut Cable Post Bogie Testing [18].....45  
Table 4. Post Strength Properties.....48  
Table 5. Summary of Cable Anchor Bracket Model Properties .....59  
Table 6. Summary of Slip Base Post Model Properties.....62  
Table 7. Sequential Description of Impact Events, Initial Simulation .....68  
Table 8. Camera Locations, Speeds, and Lens Settings .....85  
Table 9. Sequential Description of Impact Events, Test No. HTCT-1 .....87  
Table 10. Summary of Redesigned Cable Anchor Bracket Assembly Model Properties .....121  
Table 11. Sequential Description of Impact Events, Final Redesign .....153  
Table 12. Recommended MASH Testing.....168

## 1 INTRODUCTION

### 1.1 Problem Statement

Cable guardrail has been in use along roadsides since the 1930's [1]. More recently, cable guardrails have become increasingly popular due to several benefits over the more common W-Beam guardrail [2] including:

- lower initial costs;
- easier repair after vehicle impacts;
- increased visibility behind the barriers (aesthetics and safety); and
- reduction or elimination of snow drifting against barrier.

In the 1980's and 1990's, all cable guardrail systems in use were low-tension systems. Recently, high-tension, cable guardrail systems have been developed and are gaining in popularity. High-tension systems have several advantages over low-tension systems [3]:

- lower system deflections;
- reduced maintenance costs; and
- ability to remain effective after vehicle impact.

There are numerous high-tension, cable guardrail designs available for installations along roadsides, all of which utilize one of the five currently-approved, high-tension, cable end terminal designs. However, all of the end terminal designs are proprietary. In 2006, a research program was begun at the Midwest Roadside Safety Facility (MwRSF) to develop a non-proprietary, high-tension, cable guardrail that would meet FHWA's crashworthiness requirements for a guardrail system. As part of that program, a new end terminal design is necessary that safely anchors and terminates the guardrail cables.

## 1.2 Background

In the early 2000's, a series of tests were conducted at MwRSF on a non-proprietary, low-tension, end terminal design [4]. Although the end result of the testing program produced an accepted design [5], high vehicle roll angles were observed during the 820C testing program which were caused by the interaction between the vehicle and the end terminal.

There are many similarities between high-tension and low-tension, cable guardrail end terminals. Therefore, it is reasonable to expect that some of the same issues experienced in low-tension end terminal testing will also occur in high-tension tests and should be taken into consideration with a high-tension, cable end terminal design.

Aside from the change from low cable tension to high cable tension, a change in testing criteria has also been implemented for end terminals after the testing of the low-tension, cable guardrail was conducted. The low-tension, end terminal tests were accomplished under National Cooperative Highway Research Program (NCHRP) Report No. 350 testing criteria [6]. The current testing criterion is specified in the *Manual for Assessing Safety Hardware* (MASH) [7]. Many of the test conditions and evaluation criterion are similar; however, one notable change is that the vehicles utilized under MASH criteria are significantly more massive than those used under NCHRP Report No. 350 criteria. The standard car mass increased from 1,808 to 2,425 lb (820 to 1,100 kg), and the standard pickup truck mass increased from 4,409 to 5,004 lb (2,000 to 2,270 kg). A comparison of the testing criteria specified by the two standards is shown in Table 1.

Although some of the test designation numbers were altered, the only new test added with the MASH testing criteria was test no. 3-38 which designates an end terminal impact with a 3,307-lb (1,500-kg) sedan. Many of the test conditions remained unchanged. Aside from the

Table 1. Comparison of MASH and NCHRP 350 Testing Criteria for Test Level 3

NCHRP 350						MASH					
Test No.	Terminal Type	Vehicle	Impact Speed mph (kph)	Impact Angle (deg)	Impact Location	Test No.	Terminal Type	Vehicle	Impact Speed mph (kph)	Impact Angle (deg)	Impact Location
3-30	G/NG	820C	62.1 (100)	0	Start of Terminal	3-30	G/NG	1100C	62.1 (100)	0	Start of Terminal
3-31	G/NG	2000P	62.1 (100)	0	Start of Terminal	3-31	G/NG	2270P	62.1 (100)	0	Start of Terminal
3-32	G/NG	820C	62.1 (100)	15	Start of Terminal	3-32	G/NG	1100C	62.1 (100)	15	Start of Terminal
3-33	G/NG	2000P	62.1 (100)	15	Start of Terminal	3-33	G/NG	2270P	62.1 (100)	15	Start of Terminal
3-34	G	820C	62.1 (100)	15	Critical Impact Point	3-34	G/NG	1100C	62.1 (100)	15	Critical Impact Point
3-35	G	2000P	62.1 (100)	20	Start of Length of Need	3-35	G/NG	2270P	62.1 (100)	25	Start of Length of Need
3-36	NG	820C	62.1 (100)	15	Start of Length of Need	3-36	G/NG	2270P	62.1 (100)	25	Critical Impact Point
3-37	NG	2000P	62.1 (100)	20	Start of Length of Need	3-37	G/NG	2270P	62.1 (100)	25	Reverse Direction
3-38	NG	2000P	62.1 (100)	20	Critical Impact Point	3-38	G/NG	1500A	62.1 (100)	0	Start of Terminal
3-39	G/NG	2000P	62.1 (100)	20	Reverse Direction						

G = Gating Terminal  
 NG= Non-Gating Terminal

3

increased vehicle masses, the impact angles for several of the truck tests (2000P vs. 2270P) were increased by 5 degrees which increases the impact severity of those tests.

### **1.3 Research Objectives**

The main research objective for this study was to evaluate cable guardrail end terminal designs and to produce recommendations for a high-tension, cable guardrail end terminal design that would safely perform under the Test Level 3 (TL-3) MASH crash testing criteria. A particular emphasis of the research efforts were placed on developing a design for the cable anchor hardware, as that component has a substantial influence on the overall safety performance of the end terminal system.

### **1.4 Scope**

The research effort began with a literature review of previous crash testing of high-tension, cable guardrail end terminals. An analysis of approved, proprietary designs was also conducted to identify any features that may improve or weaken system performance. Following the literature review, modeling and simulation efforts were undertaken to analyze the low-tension, cable end terminal design that was crash tested at MwRSF in the 2000's. This model was validated and studied to determine the causes of the degraded vehicle stability that was exhibited during full-scale crash testing.

Next, bogie testing and simulation was conducted on a high-tension, cable anchor design. Data from the testing and simulation was used to develop recommendations and a design for a new high-tension, cable anchor. Along with the anchor design, conclusions from the literature review and study of the low-tension, cable end terminal tests were combined to produce a final set of recommendations for a high-tension, cable end terminal design.



## **1.5 Research Approach**

A non-proprietary, high-tension, cable end terminal design was needed to safely terminate the non-proprietary high-tension, cable guardrail system. As an initial effort in the design process, a literature review was conducted to collect data on other high-tension designs, including testing on cable barrier designs that had failed or had not yet been approved. The results of the literature review are detailed in Chapter 2.

After the literature review was concluded, the non-proprietary, low-tension, cable end terminal that was previously tested at MwRSF was further evaluated. The evaluation consisted of a simulation study and analysis of the low-tension end terminal's performance during full-scale crash testing. The end terminal system was deemed satisfactory and was approved for use on roadsides; however, the vehicle/barrier interaction produced high vehicle roll and yaw angles and left room for future design improvements. The simulation study is presented in Chapter 3.

The history and development of the current, high-tension, cable anchor design was detailed and presented in Chapter 4. Technical drawings of the assembly are also provided in the chapter.

Next, an initial computer simulation study was conducted utilizing the current, high-tension, cable anchor bracket assembly. The simulation was utilized to evaluate the capability of the finite element code as a predictive evaluation tool. The development of the model and results of the simulation are presented in Chapter 5.

After the initial simulation of the current, high-tension, cable anchor bracket assembly, a bogie test was conducted to evaluate both the current design and the simulation results. The bogie test was designed to mimic the simulation model. The setup and methods used to conduct

the bogie test are provided in Chapter 6. Results and discussion of the bogie test are detailed in Chapter 7.

Next, the results of the physical bogie test and the initial simulation of the current high-tension, cable anchor bracket were compared and discussed. The results and findings are provided in Chapter 8.

Finally, the results of the literature review, low-tension end terminal analysis, initial simulation, and bogie testing were used to redesign the high-tension, cable anchor bracket. Simulation, 3-D modeling, and hand calculations were the primary tools utilized to evaluate modifications made to the cable anchor bracket assembly. The development of the cable anchor bracket design, results of the conducted simulations, and technical drawings for a redesigned, high-tension, cable anchor bracket are presented in Chapter 9.

Data and findings from the literature review, analysis of test results, and simulations results were then compiled and used to develop a final set of design recommendations for the high-tension, cable end terminal. Conclusions and recommendations are presented in Chapter 10.

## **2 LITERATURE REVIEW**

### **2.1 Introduction**

A preliminary review of high-tension, cable guardrail end terminals was conducted. Information pertaining to high-tension, cable end terminal designs, full-scale crash testing results, as well as high-tension, cable system characteristics were reviewed, and the relevant material is summarized in the ensuing section.

In order for roadside barrier hardware, cable or otherwise, to be utilized along federal-aid highways, that component and/or system must be crash tested using guidelines and requirements specified by the Federal Highway Administration (FHWA). Thus, all currently-approved, high-tension, cable guardrail end terminal designs were tested, evaluated, and granted acceptance using testing criteria published in the National Cooperative Highway Research Program (NCHRP) Report No. 350. The actual impact conditions under which the proprietary, high-tension end terminal designs were tested are listed and detailed in the current chapter.

A total of 7 crash tests were required to evaluate a gating end terminal design, while 8 crash tests were required for a non-gating end terminal design within the NCHRP Report No. 350 impact safety standards. Currently, all approved designs are gating end terminals. An NCHRP Report No. 350 test matrix for end terminal systems was previously shown in Table 1.

### **2.2 Previously-Tested High-Tension, Cable End Terminal Designs**

Currently, there are six approved, high-tension, cable end terminal designs, all of which are proprietary. The results of the full-scale testing required for system acceptance was tabulated for the sake of comparison and is shown in Table 2. Certain tests may be deemed unnecessary for a given design if another test is determined to be more critical. Note that due to the fact that these

designs are proprietary, the availability of results from full-scale crash testing is dependent on what is provided by the proprietors.

Table 2. NCHRP 350 Crash Testing Results on Proprietary, High-Tension, Cable Barriers [8-12]

Manufacturer	Testing Results									
	Test Designation	Test Vehicle	Impact Speed mph (kph)	Impact Angle (deg)	Impact Location	Exit Speed mph (kph)	% Speed Reduction	Max Roll (deg)	Max Pitch (deg)	Max Yaw (deg)
TTI	3-30	820c	62.9 (101.2)	0.3	At post no. 1	53.5 (86.1)	14.94	-9.7	4.8	6.2
	3-34	820c	62.3 (100.3)	15.2	42.9 in. (1090 mm) upstream of post no. 3	N/A	N/A	-27.9	4.9	21.9
	3-35	2000p	63.2 (101.7)	20.4	23.6 in. (599 mm) downstream of post no. 4	N/A	N/A	14.4	-10.4	21.1
	3-39	820c	63.4 (102.0)	20.5	At post no. 4, reverse direction	46.3 (74.5)	26.97	6.9	-10.2	-1.7
Brifen	3-30	820c	62.7 (100.9)	0.0	At post no. 1	N/A	N/A	38.9	N/A	20.7
	3-34	820c	61.5 (99.0)	14.0	Midspan between post nos. 1 and 2	N/A	N/A	-13.0	N/A	32.4
	3-35	2000p	61.8 (99.5)	23.0	63 in. (1600 mm) upstream from post no. 6	N/A	N/A	-6.2	N/A	20.0
	3-39	820c	63.1 (101.5)	21.5	Midspan between post nos. 4 and 5, reverse direction	N/A	N/A	12.4	N/A	41.9
Gibraltar	3-30	820c	62.3 (100.3)	0.0	At post no. 1	49.2 (79.2)	21.03	21.9	-12.8	8.9
	3-32	820c	64.1 (103.2)	15.0	At post no. 1	55.2 (88.8)	13.88	-27.1	-7.4	-19.2
	3-35	2000p	62.1 (100.0)	20	At post no. 5	23.7 (38.1)	61.84	44.2	7.7	51.0
	3-39	820c	61.5 (99.0)	20	At post no. 3, reverse direction	0 (0)	100.00	-53.9	-60.5	-15.5
Safence	3-30	820c	63.4 (102.0)	0.0	At post no. 1	60.3 (97.0)	4.89	47.6	15.8	9.0
	3-34	820c	63.1 (101.5)	15.0	Unknown	58.4 (94.0)	7.45	31.3	6.9	21.2
	3-35	2000p	63.3 (101.9)	20	Unknown	54.1 (87.1)	14.53	15.2	3.9	27.1
	3-39	820c	61.5 (99.0)	20	At post no. 11, reverse direction	39.1 (62.9)	36.42	14.4	11.6	81.1
Armorflex	3-30	820c	60.7 (97.7)	0	At post no. 1	N/A	N/A	-14.2	11.3	135.8
	3-32	820c	61.5 (99.0)	14.4	At post no. 1	57.5 (92.5)	6.50	14.2	-13.5	160.4
	3-35	2000p	63.2 (101.7)	20.3	Between post nos. 4 and 5	45.4 (73.1)	28.16	-7.1	-3.2	42.3
	3-39	820c	62.9 (101.2)	20	157.5 in. (4000 mm) upstream of terminal trigger post	N/A	N/A	7.5	-14.8	-45.4

N/A – Not Available

### 2.2.1 Texas Transportation Institute

The Texas Transportation Institute (TTI) designed and successfully tested a high-tension, cable barrier end terminal in 2002 [8]. TTI's end terminal incorporated proprietary breakaway posts in the end terminal section, followed by Rib-Bak, U-Channel posts for the line posts. The breakaway terminal posts are designated as Cable Release Posts (CRP). Each CRP is used to anchor one of the cable guiderails used in the system. The crash tested barrier system utilized three cables. The end terminal, as tested, is shown in Figure 1. Technical drawings of the system layout are shown in Figures 2 and 3.



Figure 1. TTI End Terminal

Although the system performed well in full-scale testing, some concerns arose during a review of the test data. The primary concern was associated with the alignment of the vehicle in test 3-30. That test calls for the vehicle to be aligned with the centerline of the system at 0 degrees using a  $\frac{1}{4}$ -point lateral offset of the vehicle's total width. From TTI's sequential

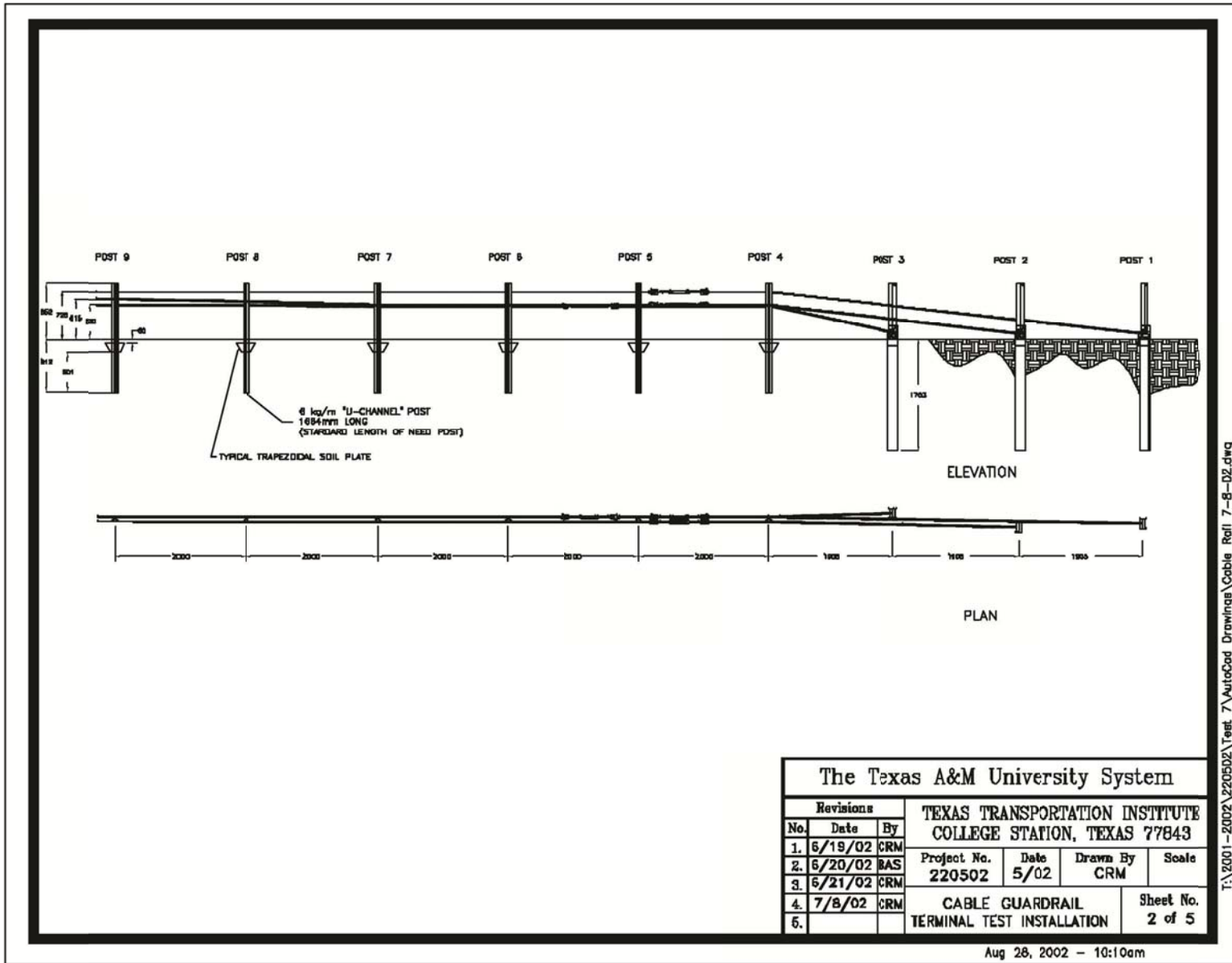
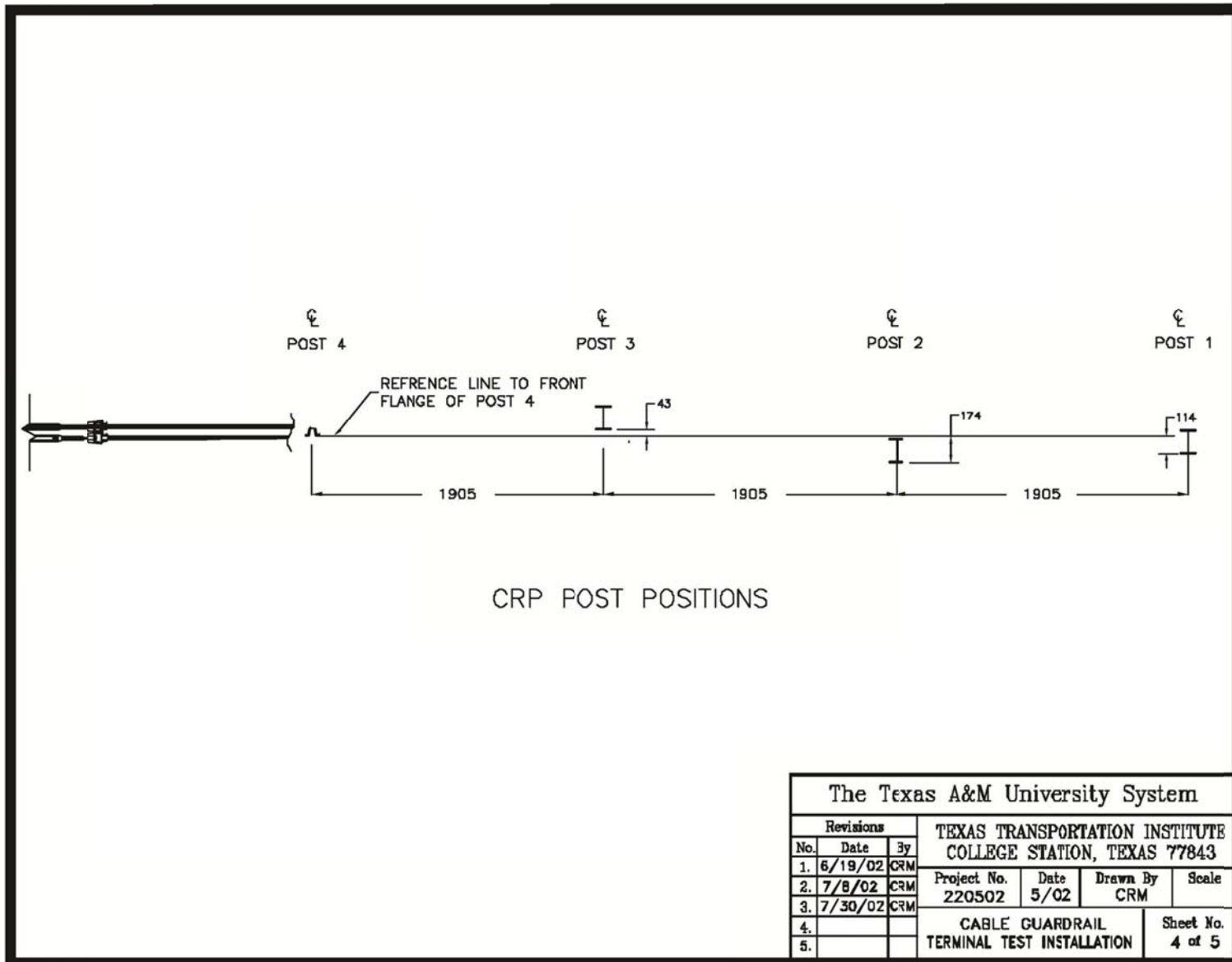


Figure 2. TTI End Terminal, Technical Drawing



T:\2001-2002\220502\test 7\AutoCad Drawings\Cable Roll 7-B-02.dwg

Figure 3. TTI End Terminal, Technical Drawing

photographs it appears that the vehicle was aligned with respect to CRP post no. 3 in the end terminal. CRP post no. 3 was offset from the tangent of the system and resulted in the vehicle's centerline being closely aligned with the centerline of the U-Channel line posts. This alignment resulted in a favorable vehicle trajectory after the vehicle had passed through the three breakaway terminal posts. The centerline vehicle impact with the line posts eliminated much of the yawing and instability concerns observed in other systems.

While this alignment is perfectly acceptable, it poses concern for increased vehicle instability should a vehicle strike the end terminal at a different lateral offset. One of the risks associated with an off-center impact is the inevitable yawing of the vehicle. With increased yaw motion, vehicle behavior will be much more similar to that seen in crash tests with other end terminal designs. As such, the trajectory of the vehicle will be more erratic and unpredictable after impact with the terminal. Beyond vehicle yawing and trajectory, it is unclear how the system's performance might be affected.

### **2.2.2 Brifen**

Brifen USA, Inc. successfully tested a high-tension end terminal design in the fall of 2003 [9]. Brifen's design incorporated an angled post no. 2 with proprietary "S" or "Z" posts for the remainder of the system. The cables were terminated using an anchor bracket that was secured to a buried, concrete block. The Brifen design utilized four system cables. A technical drawing of the system layout is shown in Figure 4.

The Brifen end terminal system performed satisfactorily under full-scale crash testing according to the NCHRP Report No. 350 requirements. In all tests, the vehicle was brought to a controlled stop without rollover, excessive decelerations, or excessive damage to the occupant compartment. However, there may be some issues that potentially degrade impact performance.



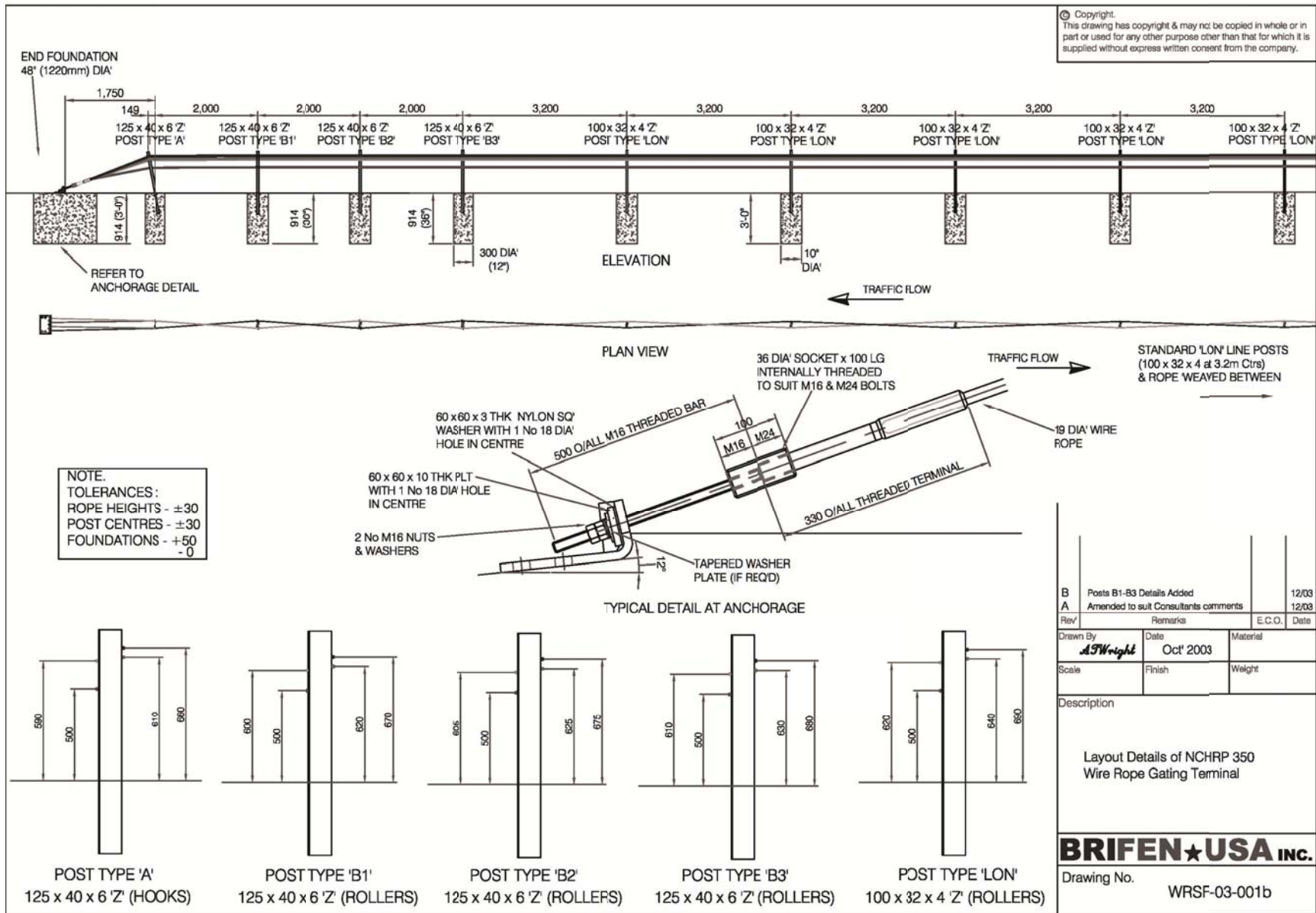


Figure 4. Brifen End Terminal, Technical Drawing

In test 3-30, the vehicle impacted the end terminal at a 0-degree angle and a ¼-point lateral offset. During the test, the vehicle ramped up the cables and rolled nearly 40 degrees. After ramping up and over angled post no. 2, the vehicle came back into contact with the ground off to the side of the system.

At the present, there is no mechanism to release the cables during end-on impacts with the terminal. In the case of a centerline vehicular impact on the end terminal system, it is possible that the vehicle could ramp up the cables and land on top of one or more line posts, possibly puncturing the undercarriage of the occupant compartment. Such an occurrence would be hazardous to occupants for several reasons. First, a penetrating post could directly cause harm to an occupant. Second, the airborne vehicle could become entangled within or snagged on system components, thus resulting in rapid decelerations and/or vehicle instabilities, such as rollover.

### **2.2.3 Gibraltar**

Gibraltar Cable Barrier Systems, L.P. designed and successfully tested a high-tension, three-cable end terminal in 2005 [10]. Gibraltar's design incorporated a cable release anchor post which was designed to release the cables in the case of an end-on impact with the terminal. The barrier system consisted of "C" section posts throughout the terminal region as well as for line posts. Post no. 2 was angled at 6 degrees with respect to vertical, and post nos. 2 and 3 utilized holes at ground level to weaken the terminal posts.

A Gibraltar cable barrier end terminal installed in a median application is shown in Figure 5. Technical drawings of the system layout and photographs of the constructed end terminal are shown in Figure 6.



Figure 5. Gibraltar End Terminal

Gibraltar's end terminal system exhibited good control of the vehicle and performed well in all end terminal testing. In test 3-30, the cable release anchor post functioned as designed and allowed the vehicle to travel through the system without ramping up the cables. However, the vehicle did rollover during this test, which was subsequently attributed to the vehicle's tires tripping on loose soil. Following a review of the test details, it was observed that the end terminal used in test 3-30 was a shortened version of the system. As such, there is concern that small car testing on a longer, more realistic system length may result in increased roll motion and vehicle instabilities. However, it is unknown as to how these changes would affect the stability of the vehicle and the overall success of the crash test.

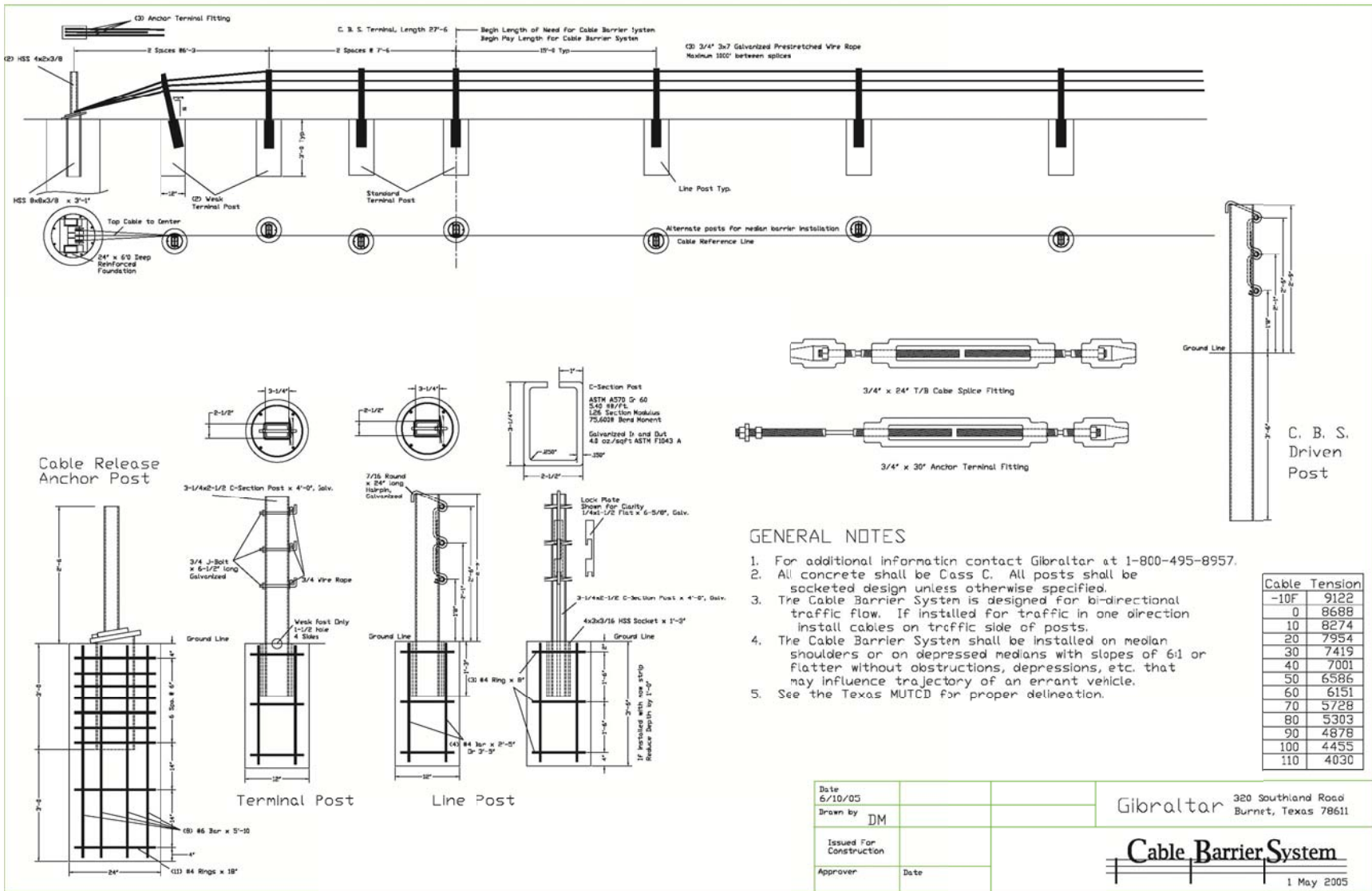


Figure 6. Gibraltar End Terminal, Technical Drawing

### 2.2.4 Safence

Safence, Inc. designed and successfully tested a high-tension, four-cable end terminal in 2005 [11]. The Safence end terminal design used 11 posts ranging in heights from 11.8 to 30.7 in. (300 to 780 mm) to transition the cables from the block anchor to the tangent system height. The system utilized a proprietary C-shaped section for both terminal and line posts. Like the Brifen design, Safence's design did not incorporate a method to release the system cables in the case of an end-on impact. As such, similar concerns to those noted for Brifen would exist for centered vehicle impacts on the end of the terminal.

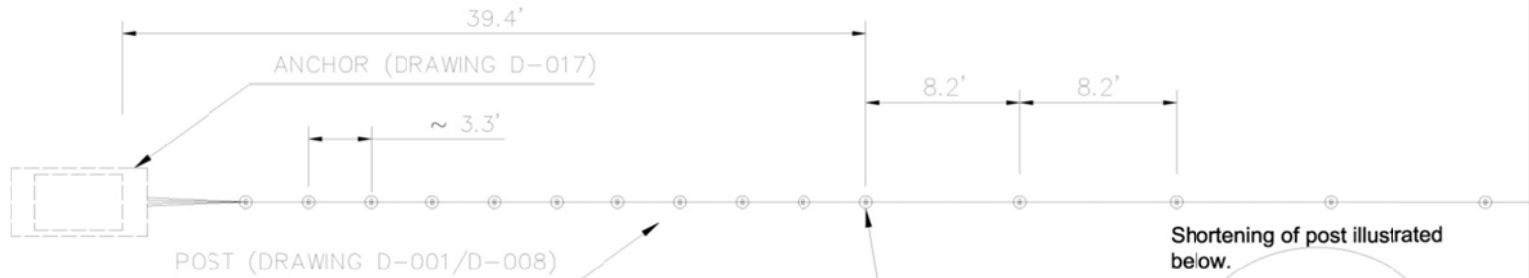
A Safence end terminal installed in a roadside application is shown in Figure 7. A technical drawing of the system layout is shown in Figure 8.



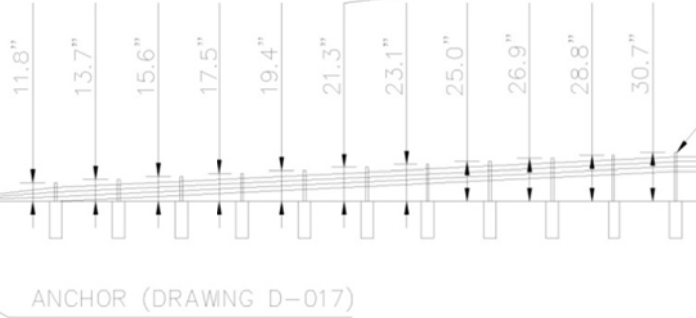
Figure 7. Safence End Terminal



TOP VIEW



All posts in the terminal are shortened to the specified length



SIDE VIEW

Designed <b>MH</b>	Drawn <b>NM</b>	Approved - date <b>2005-08-02</b>	Tolerance requirements	Units	Proj. 	Scale <b>1:100</b>
<b>BLUE SYSTEMS AB</b> Hälleforsgatan 24 S-426 58 Västra Frölunda SWEDEN Tel: +4631 207216 Fax: +4631 203065 E-post: info@bluesystems.se		Material		Issue	Sheet	File
		Name <b>SAFENCE 350 TL3 (Terminal)</b>		Drawing No. <b>SRB-011 imp</b>		

Figure 8. Safence End Terminal, Technical Drawing

Test 3-39, a reverse direction terminal impact, exhibited a controlled, safe vehicle interaction. There was no observable snag, and the vehicle passed through the anchor before coming to a controlled stop. In test 3-30, the vehicle rode up the cables before being deflected off to one side.

Safence's end terminal testing resulted in higher values of vehicle roll and pitch than were typically seen in other testing. However, considering the gradual slope of the cables, the vehicle exhibited more roll prior to losing contact with the system. Like Brifen's system, the vehicle was safely redirected, or allowed to pass through the system in all tests. The same potential for vehicle damage was evident. While test 3-30 successfully directed the vehicle out of the end terminal, it was determined that the successful redirection was in large part due to the ¼-point offset impact with the end terminal. A centerline vehicular impact with the terminal end could pose significant risk for the vehicle to land on top of posts, thus increasing the potential for penetration of the undercarriage and putting the occupants in considerable danger.

### **2.2.5 Armorflex**

Armorflex designed and successfully tested a high-tension, four-cable end terminal in 2008 [12]. The Armorflex end terminal consisted of a trigger post and line posts with oval shaped cross sections. The unique trigger post design consisted of an angled post assembly that was used to connect anchor cables to the line cables. The trigger post was designed to release the line cables when impacted by a vehicle. The trigger post assembly is shown in Figure 9. Technical drawings of the system layout and photographs of the constructed end terminal are shown in Figure 10.



Figure 9. ArmorflexEnd Terminal

The full-scale testing exhibited acceptable performance. The trigger post performed as designed in tests 3-30, 3-32, and 3-39. For test 3-35, the 2000P truck was smoothly redirected with no snag.

The Armorflex end terminal design prevented significant vehicle rolling or other instabilities that could have resulted in test failure. However, tests 3-30 and 3-32 did result in considerable yawing. Due to the lack of available test data, the exact causes for the increased yaw are unknown. However, upon examination of the system characteristics and comparing with other systems, the yawing is possibly due to the relatively high strength of the terminal and line posts. Off-center impacts with these posts would likely result in high forces imparted on the vehicle and induce substantial yawing in the vehicle.



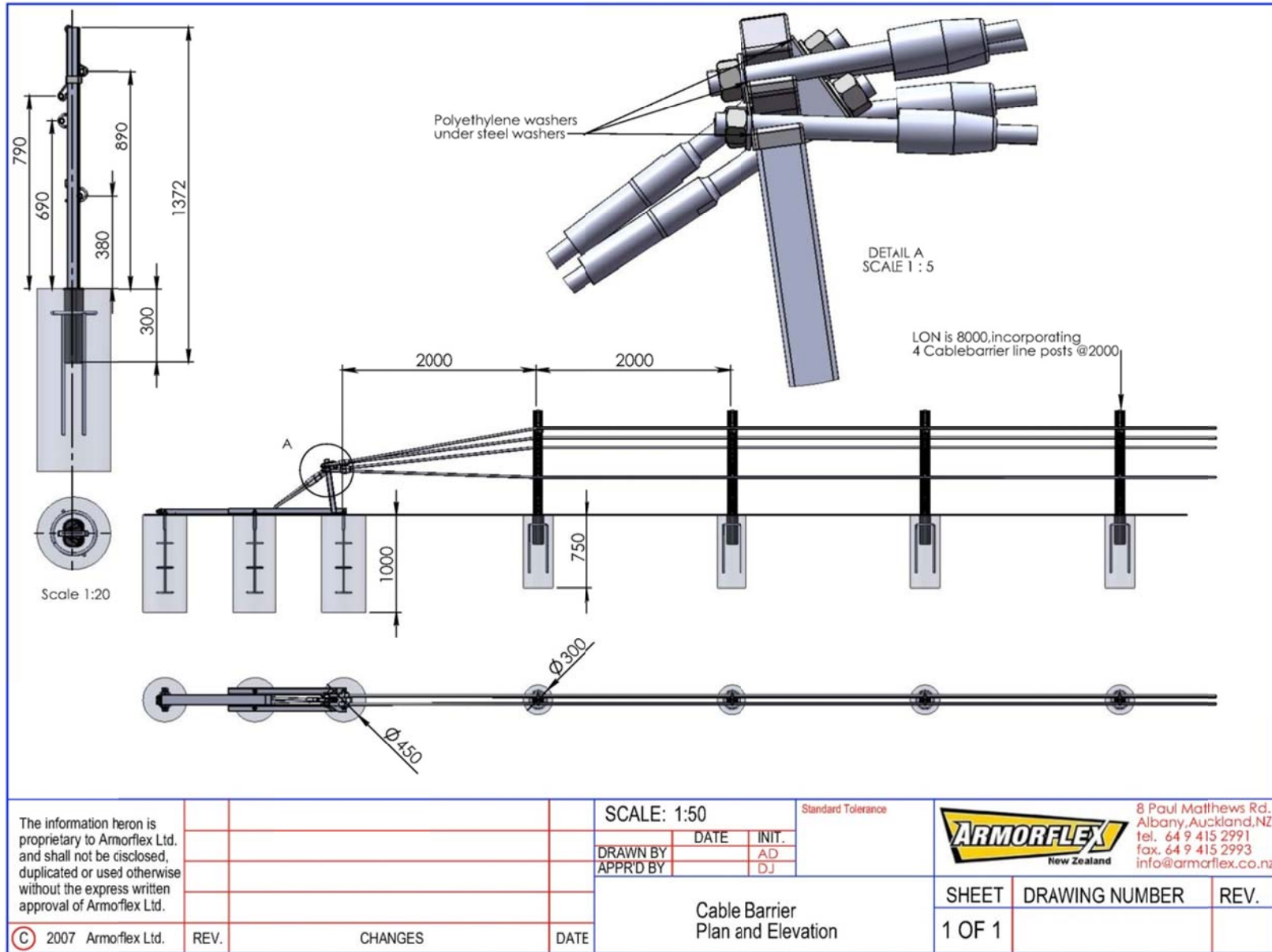


Figure 10. Armorwire End Terminal, Technical Drawing

## 2.3 Discussion

From the survey of various approved, high-tension end terminal designs, it is apparent that certain end terminal design features are beneficial for improving performance and some features have significant detrimental effects. Weak or weakened terminal posts performed well in TTI (with NUCOR posts) and Gibraltar's end terminal testing programs. In TTI's testing, the vehicle traveled down the centerline of the system without any induced roll or pitch that could potentially arise from the vehicle ramping up a post with stronger cross sectional properties. In systems with relatively close terminal post spacing, weak posts are especially important as any pitching or rolling effects from vehicle to post impacts will be compounded due to the shorter recovery time in between posts.

Terminal post spacing was found to range between 90 in. (2,286 mm) (Gibraltar) and 39.6 in. (1,006 mm) (Safence). Note that the one exception is the Armorflex system which transitioned directly from the anchor to the system posts and did not utilize any special terminal posts. The systems that utilized the shorter terminal post spacing exhibited higher roll and yaw angles than the systems with greater post spacing. The shorter post spacing undoubtedly directly contributed to degraded stability as frequent, off-centered impacts with terminal posts induced higher roll and yaw angles on the vehicle. The end terminal systems with increased terminal post spacing showed a more controlled vehicle trajectory, which may lead to even better vehicle stability. However, it is unclear as to whether an increased post spacing will negatively affect the redirective capabilities of the end terminal system.

The most noteworthy feature that was found during the literature review was the ability for the cables to release away from the end anchorage in the event of an inline, terminal impact. Three of the five approved high-tension end terminal designs have this ability. During testing,

the two designs that did not incorporate a mechanism to release the cables exhibited increased vehicle motions and more dangerous vehicle trajectories than observed for the other systems. Vehicle trajectories in those tests exhibited roll angles upwards of 40 degrees as well as excessive yawing. As noted earlier, different vehicle impact conditions (vehicle inline, for instance) could result in even more erratic vehicle behavior and potential harm to occupants.

### **3 EVALUATION OF THE LOW-TENSION, THREE-CABLE END TERMINAL TEST SERIES**

#### **3.1 Background**

In the early 2000s, MwRSF conducted four full-scale crash tests on a low-tension, three-cable end terminal design [4]. The first test, test no. CT-1, was conducted according to test designation 3-35. The final three tests were conducted according to test designation 3-30. Test nos. CT-2 and CT-3 failed due to vehicle rollover. The final test (test no. CT-4) was successful, although high roll and yaw angles were observed during vehicle trajectory. Other NCHRP Report No. 350 tests for the low-tension, three-cable end terminal were deemed unnecessary for the evaluation of the system design because previous full-scale testing of similar end terminals exhibited good crash performance.

Based on the safety performance exhibited by the low-tension, three-cable end terminal design, as well as the desire to utilize similar technology in a high-tension, four-cable barrier system, further analysis of the end terminal was conducted. Although there are differences between the low-tension, three-cable and the high-tension, four-cable end terminal systems, the design intent and expectation for performance are identical. Both systems must:

- 1) allow for the release of the cables when impacted by vehicles at the anchor end;
- 2) allow the impacting vehicle to safely traverse through the barrier system without an unstable vehicle trajectory; and
- 3) not pose undue risk to the vehicle occupants by means of excessive vehicle decelerations, penetration of the occupant compartment, or severe interior occupant compartment damage.

An increased understanding of the mechanisms that caused the poor performance observed in test nos. CT-2 and CT-3 as well as the high roll and yaw angles in test no. CT-4, was deemed necessary to improve the design for use in the high-tension, four-cable end terminal.

### **3.2 Simulation of the Low-Tension, Three-Cable End Terminal**

In order to analyze the effect that the different system components had on the performance of the low-tension, three-cable end terminal design, a validated end terminal finite element model was necessary. An end terminal model was constructed consisting of the low-tension, three-cable anchor bracket assembly, slip base post no. 1, five slip base terminal posts, and three wire rope cables. The terminal model was impacted by a Geo Metro vehicle model. Prior to assembling the end terminal, each component was individually constructed and simulated to simplify the eventual integration of the components. Each component model is described in detail herein. The modeling and analysis was accomplished using the explicit, non-linear finite element code LS-DYNA, developed by the Livermore Software Technology Corporation [13].

#### **3.2.1 Low-Tension, Three-Cable, Anchor Bracket Assembly**

Technical drawings of the low-tension, three-cable, anchor bracket assembly are shown in Figures 11 through 13. Shell elements were used to create all parts of the anchor bracket assembly. A Belytschko-Leviathan shell formulation was selected based on previous parameter testing [14]. The nodes on the base plate of the cable anchor bracket assembly were fully constrained to prevent any movement by the baseplate during the simulation. The model of the anchor assembly is shown in Figure 14.



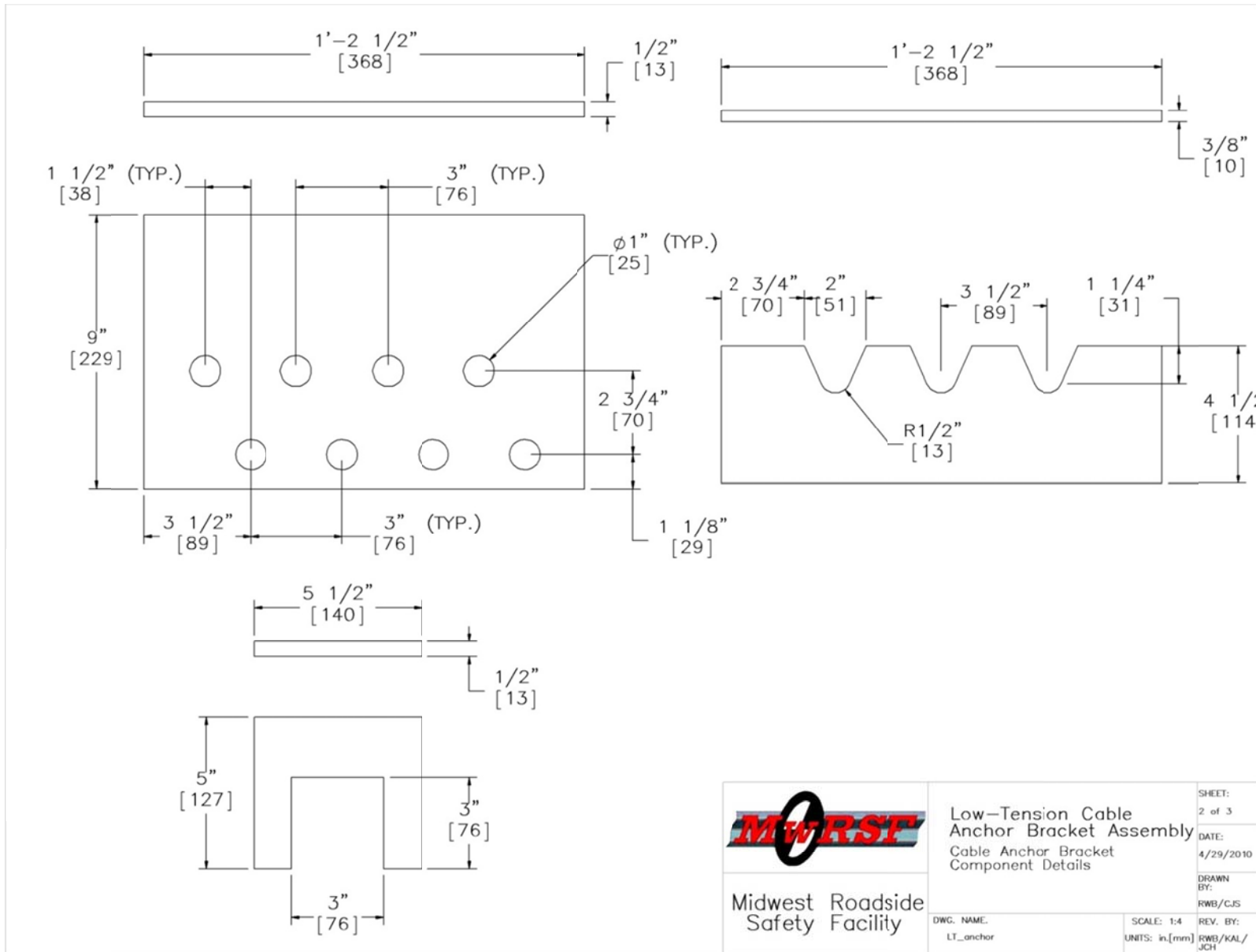


Figure 12. Low-Tension, Cable Anchor Bracket Component Details

	Low-Tension Cable Anchor Bracket Assembly Cable Anchor Bracket Component Details		SHEET: 2 of 3
	Midwest Roadside Safety Facility		DATE: 4/29/2010
DWG. NAME: LT_anchor	SCALE: 1:4 UNITS: in,[mm]	DRAWN BY: RWB/CJS	REV. BY: RWB/KAL/JCH

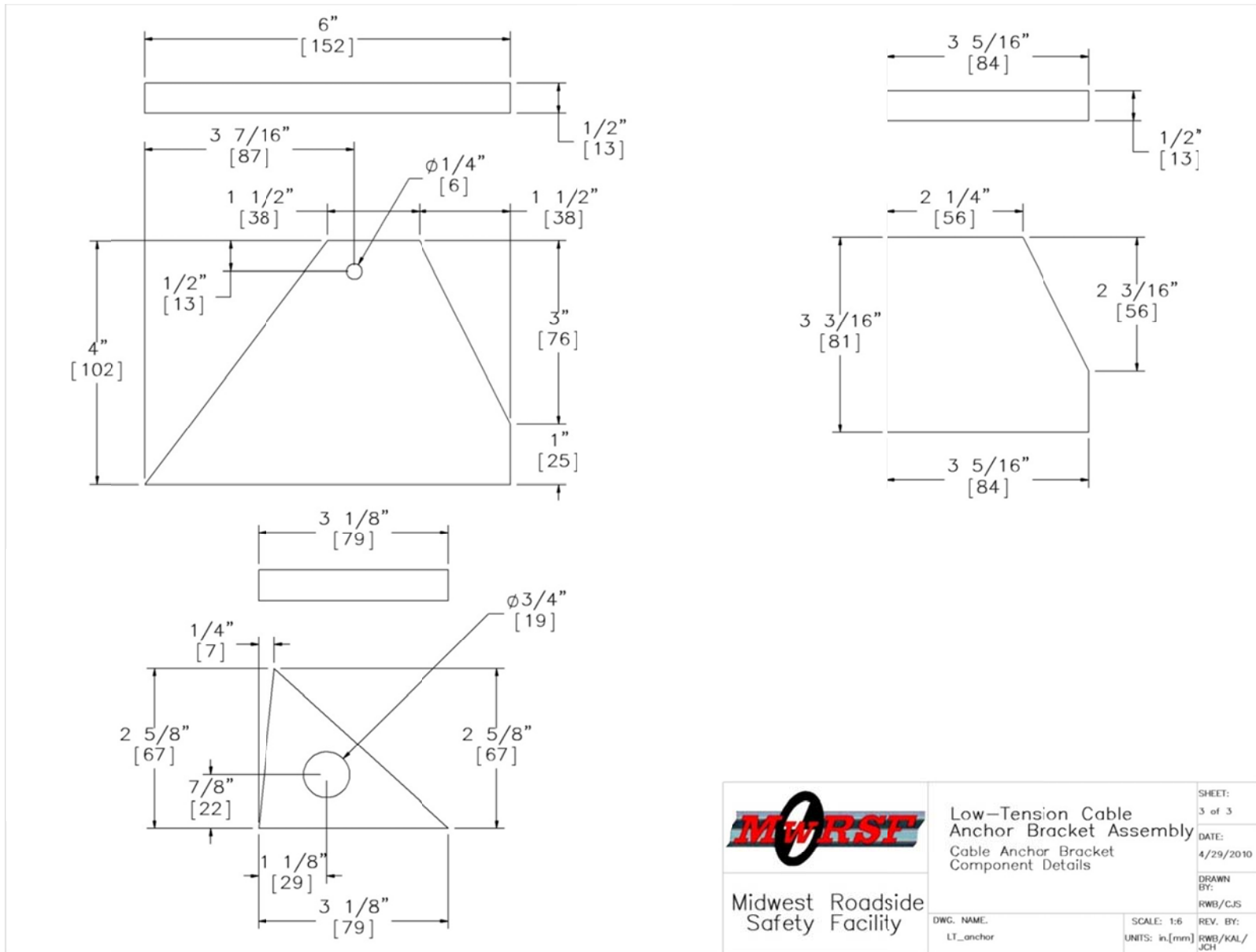


Figure 13. Low-Tension, Cable Anchor Bracket Component Details



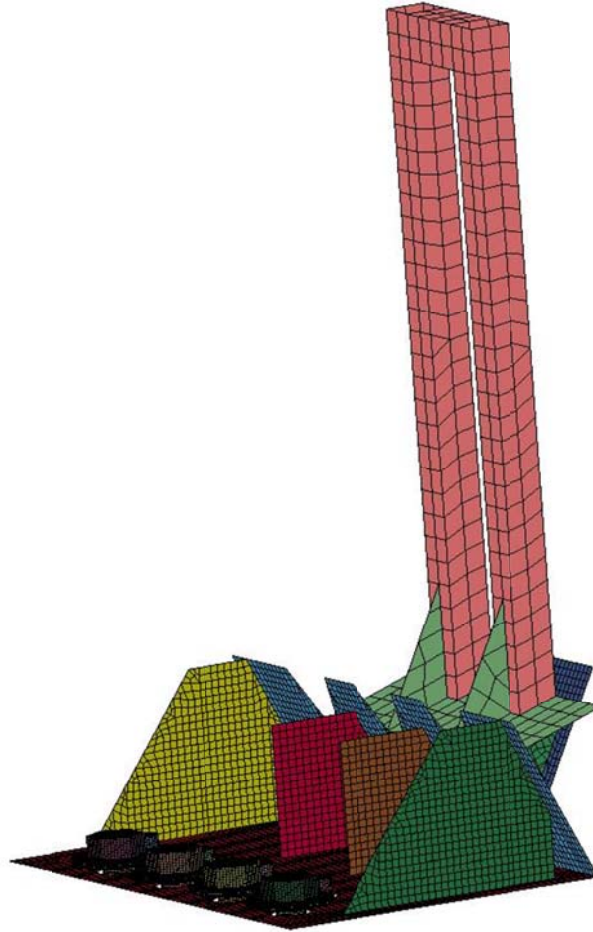


Figure 14. Cable Anchor Bracket Assembly

An elastic piecewise-linear, plastic material model was specified for all anchor bracket components. The yield strength, Young's Modulus, and Poisson's Ratio for the material model were specified as 54 ksi (372 MPa), 29,008 ksi (200 GPa), and 0.293, respectively, to reflect ASTM A36 steel material properties. Material properties for the anchor bracket model were taken from a previous study [15].

### **3.2.2 Slip Base Post No. 1**

The slip base post was the result of previously validated work. The primary purpose of the post was to support the cables as they transitioned from the horizontal, guardrail section, down to the anchor bracket. The difference between slip base post no.1 and the standard, slip

base terminal posts is the cable hanger that is welded to one of the flanges of the upper slip base post section. The cable hanger is necessary to withstand the vertical forces resulting from the redirection of the system cables. Post component details and a description of the development of the model can be found in Nick Hiser's Master's Thesis [15]. The post model is shown in Figure 15.

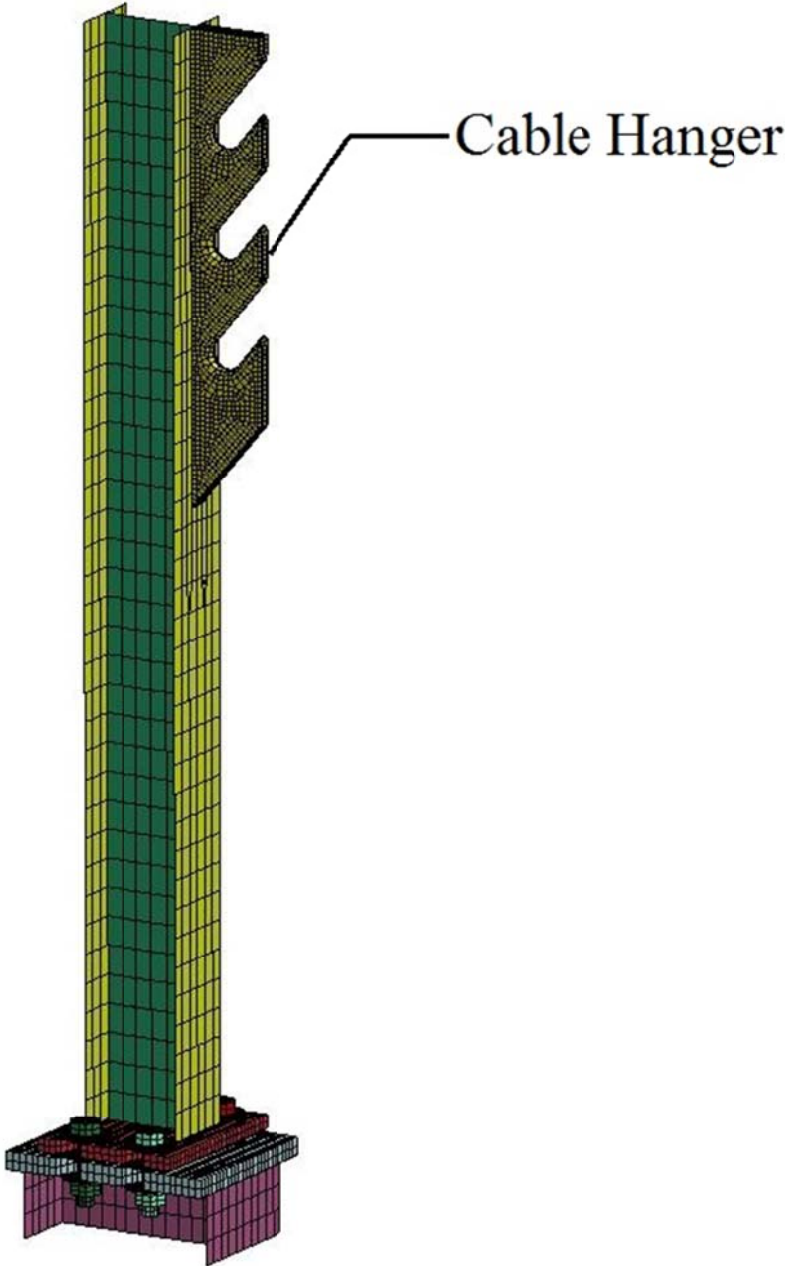


Figure 15. Slip Base Post No. 1 Model

### 3.2.3 Slip Base Line Posts

The slip base line post model was similar to the slip base post no. 1 model. However, the line posts utilized three cable hook bolts to secure the system cables to the post, in lieu of the cable hanger bracket. The hook bolt model had 9 solid elements in its cross section and was developed by Reid and Coon [16]. The slip base line post model is shown in Figure 16.

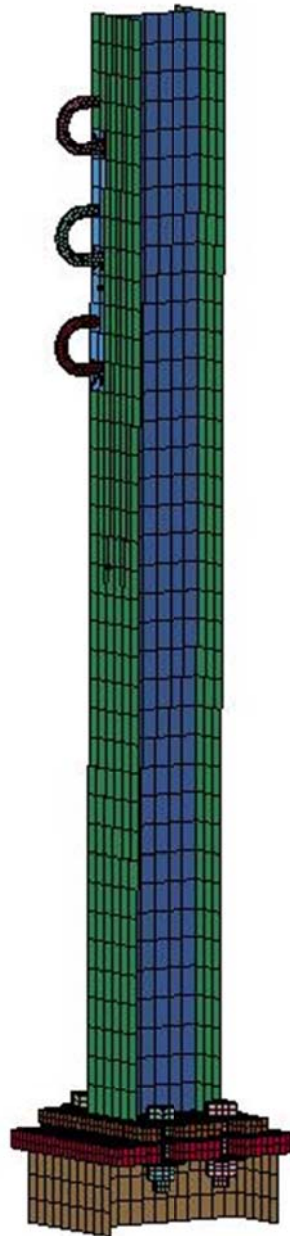


Figure 16. Slip Base Line Post Model

### 3.2.4 Cables

The cable model used in simulations was the same model used in the initial development of the three-cable end terminal model by Reid, Hiser, and Paulsen. The cable model consisted of beam elements surrounded by eight tetrahedron elements to serve as the contact surface. Specific details of the cable model and its development can be found in the technical paper *Simulation and Bogie Testing of a New Cable Barrier Terminal* [17].

#### 3.2.4.1 Pre-Tension

Cable pre-tension was defined as 900 lb (4 kN) per cable. This pre-tension value reflected what was specified in full-scale crash test no. CT-4. The cables were pre-tensioned by attaching discrete spring elements to the downstream ends of the cables.

### 3.2.5 Vehicle Model

A Geo Metro vehicle model was utilized as the impacting vehicle for the validation simulations. The Geo Metro model was obtained from Politecnico di Milano, Italy and subsequently modified for use in MwRSF's roadside safety applications. The original Metro model that was improved by Politecnico di Milano was developed by the National Crash Analysis Center (NCAC). The Geo model is shown in Figure 17.

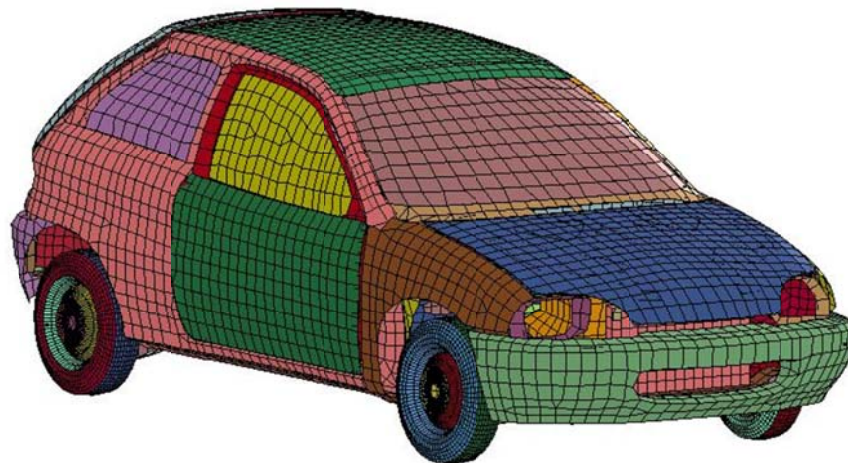


Figure 17. Geo Metro Vehicle Model

### **3.2.6 Model Construction**

Once each component model had been statically simulated to guarantee its individual efficacy, they were combined to create an abbreviated end terminal model identical to that used in full-scale crash test no. CT-4. The model included the cable anchor assembly, 3 system cables, slip base post no. 1, five slip base line posts, and the Geo Metro vehicle model. An automatic single surface contact was utilized as a global contact for system self-interaction as well as vehicle-system interaction. The Metro was given an initial velocity of 61.4 mph (98.8 km/h) and a ¼-point lateral offset toward the passenger side to reflect the impact conditions of test no. CT-4.

### **3.2.7 End Terminal Model Validation**

The main criteria used to evaluate and validate the end terminal model were:

- vehicle yaw data;
- vehicle trajectory; and
- visual comparison of component and vehicle damage.

During the initial simulations, the initial yaw of the Geo Metro did not match the test results obtained from CT-4. Upon further examination of the high-speed video from CT-4, it was determined that an initial yaw motion was imparted to the vehicle as a result of the tow and guidance process. As the vehicle neared the impact point, the guide flag, which maintains the vehicle's heading angle during towing, was detached from the vehicle. The guide flag release was accomplished through an impact with a shear post on the right side of the vehicle. Ideally the guide flag/shear post impact will be trivial. However, during test no. CT-4, the impact may have been significant enough that the vehicle began to yaw prior to impacting the cable anchor's release lever.

To further investigate the guide flag/shear post impact, the accelerometer data from the test was reanalyzed to examine events prior to the vehicle entering the guardrail system. At approximately the same time as the guide flag/shear post impact, there was a 1.8 g deceleration applied to the vehicle. At the point of the application of that deceleration, the applied force was approximately 2.5 kips (11.1 kN). Due to the off-center point of application, it is possible that the resultant force imparted an initial yawing motion to the vehicle. Overhead photographs of the guide flag impact are shown in Figures 18 and 19.

In order to match the initial yaw motion of the vehicle as it impacted the cable release lever, an initial yaw rate of 15 deg/s was applied to the Geo Metro model. After the initial yaw was applied to the vehicle, the simulated trajectory of the Geo Metro more closely matched that observed in test no. CT-4. Vehicle yaw data from the simulation and test no. CT-4 are shown in Figure 20. Sequential images for the simulated and actual vehicle trajectories are shown in Figure 21. Geo Metro vehicle positions at 500 ms after impact are compared between the actual test and simulation results and are shown in Figure 22.

Although the first portion of the simulation matched well with test no. CT-4, the vehicle trajectories began to diverge after 300 ms. A review of the high-speed video of test CT-4 revealed that this divergence in vehicle trajectories was partially due to vehicle contact with system debris. The debris included top sections of slip base posts, cable compensators, and the cable release lever from the end anchor. During test CT-4, this debris was overridden by the Geo Metro, thus resulting in increased vehicle yawing and also vehicle roll toward the driver's side that nearly led to rollover. As shown in Figure 23, the yawed vehicle has contacted and begun to override the system debris in test CT-4.



Impact



4 ms After Impact

Figure 18. Shear Post Impact with Guide Flag, Test No. CT-4

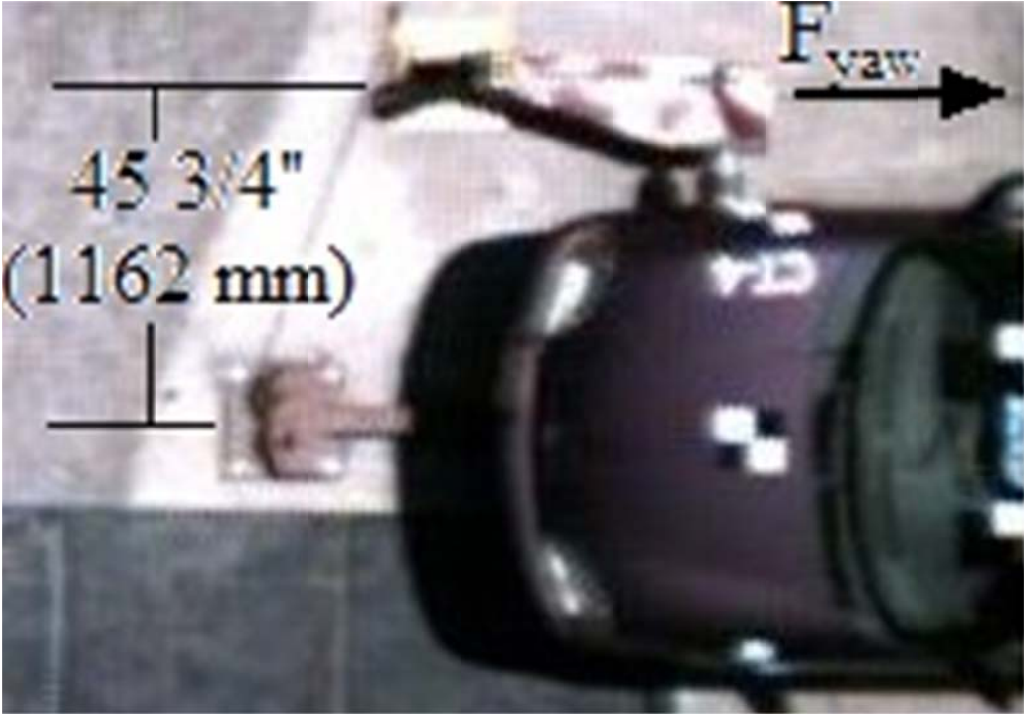


Figure 19. Guide Flag/Shear Post Impact Force Diagram

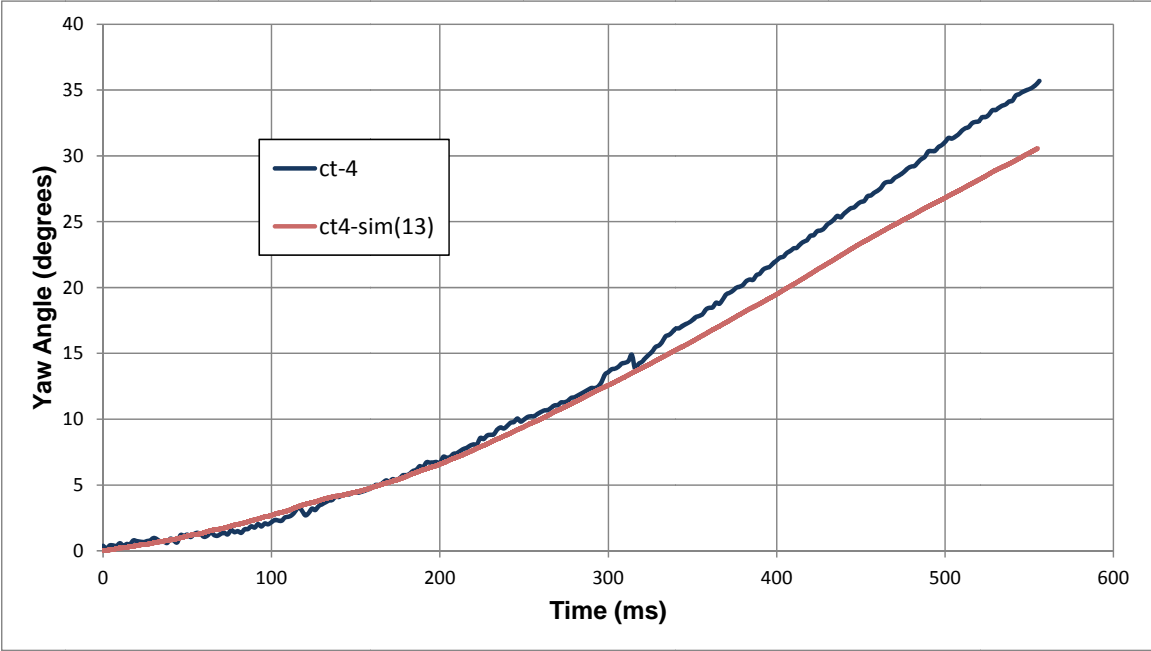


Figure 20. Comparison of Actual and Simulated Vehicle Yaw – Test No. CT-4



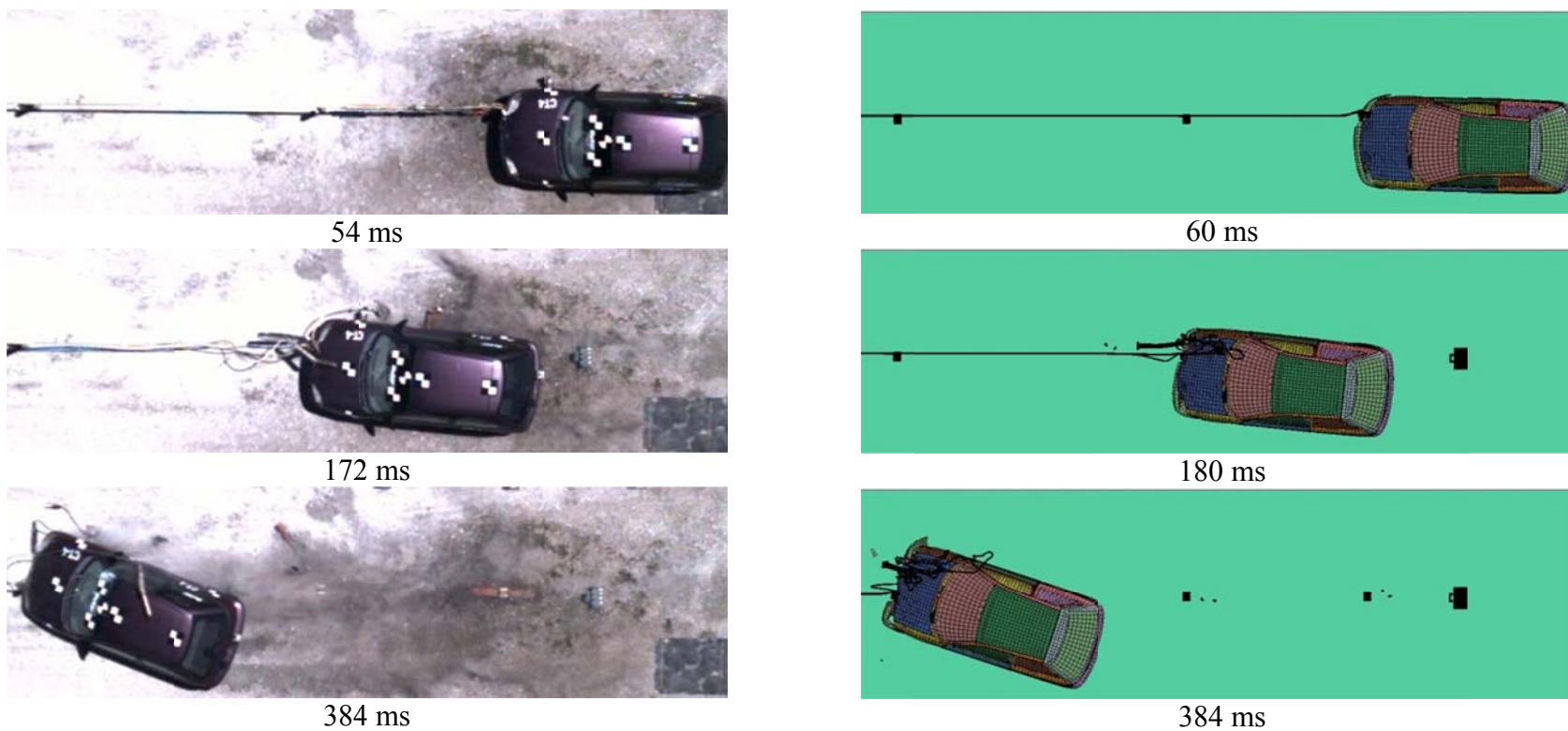
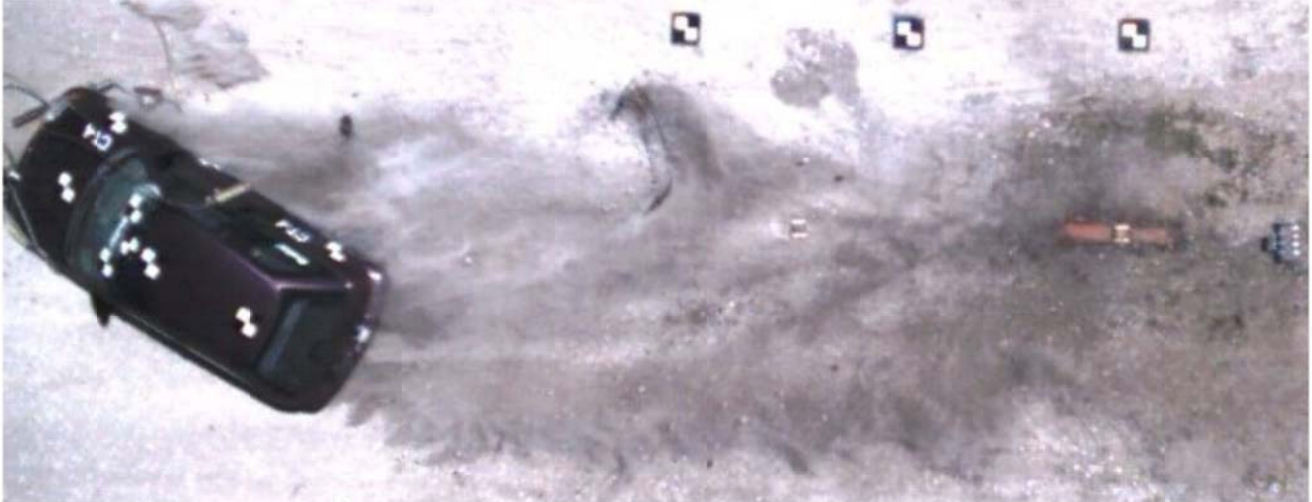


Figure 21. Sequential Comparison at Post Impact Times, CT-4 and Simulation CT-4\_13



500 ms



500 ms

Figure 22. Vehicle Trajectory Comparison – 500 ms After Impact



Figure 23. Geo Metro Overriding System Debris

### **3.2.8 Discussion**

#### **3.2.8.1 Vehicle Trajectory**

Through 300 ms, the simulated vehicle trajectory and yaw motion observed in the low-tension, three-cable end terminal model matched well with the actual results obtained in test CT-4. Although the trajectories began to diverge as the vehicles exited the terminals, valuable information was obtained from the simulation. The main cause of the divergent exit trajectories and near rollover in test no. CT-4 was likely due to the actual Geo Metro contacting and overriding the debris from detached end terminal components. The movement of the system debris and location of the vehicle-to-debris contact is highly dependent on ground conditions as well as bumper characteristics. As such, these vehicle-to-barrier interactions are very difficult to accurately simulate. Improvements to the simulation model could be made with further development of the ground and bumper models. For the current application, however, the utilized models proved sufficient.

Another sensitive part of the end terminal system was the interaction between the cable compensators and slip base post no. 1. In the “best” simulation model, it was discovered that the cables immediately downstream from slip base post no. 1 coiled on the downstream face of the web. This action forced the detached slip base post section up onto the hood of the vehicle, which prevented the simulated vehicle from overriding the post section. In test CT-4, the cable compensators located between slip base post nos. 1 and 2 similarly impacted the downstream face of the web on slip base post no. 1 and forced the post section onto the hood of the vehicle. The vehicle-to-post interactions for both the simulation and test CT-4 are shown in Figure 24.

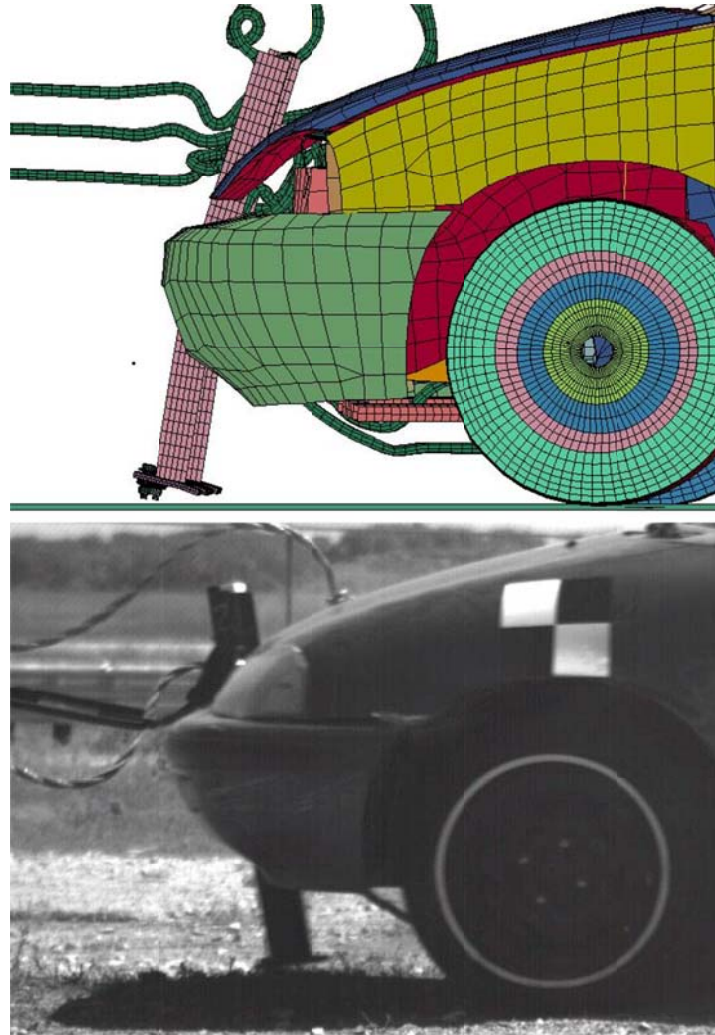


Figure 24. Cable Interaction with Slip Base Post No. 1

Throughout the study, many variations of the system were simulated including parameter studies on contact algorithms as well as cable pretension. In many of the simulations, the cables did not coil on the web of slip base post no. 1. For these scenarios, the detached section of slip base post no. 1 was overridden earlier in the simulation. The simulated trajectory of the vehicle as it overrode post sections was unpredictable. In some cases, the interaction significantly increased vehicle yawing and in other instances it hardly effected the vehicle trajectory at all.

### **3.2.8.2 Slip Base Post Performance Analysis**

#### **3.2.8.2.1 Full-Scale Testing Evaluation**

The slip base posts served their intended purpose by releasing upon impact in the weak-axis direction. This quick release prevented the vehicle from overriding and ramping up the post, as was seen in previous testing with other post options [4]. However, after the slip base post released, the detached top sections proved to be potentially hazardous debris. This behavior was exhibited in both simulations as well as physical testing. The detached post section trajectory was erratic and unpredictable. These detached posts have the potential to cluster together and cause vehicle instabilities, as seen in test no. CT-4. This hazard may be reduced if the post sections were retained or if a standard post with a decreased section modulus in the weak-axis direction were utilized in place of the slip base post assembly.

#### **3.2.8.2.2 M4x3.2 (M102x4.8) Replacement Post Option**

The S3x5.7 (S76x8.5) post has been used in previous, non-proprietary, cable end terminal designs. Full-scale testing showed that the S3x5.7 (S76x8.5) post has the propensity to cause vehicle rollover due to repeated impacts between terminal posts and the test vehicle. Therefore, a post with reduced weak-axis bending and/or shear strength is desired.

One terminal post replacement option is the M4x3.2 (M102x4.8) post section. The M4x3.2 (M102x4.8) section was selected to analyze due to its similar strong-axis bending strength as compared with the S3x5.7 (S76x8.5) section. The M4x3.2 (M102x4.8) section also has the greatest weak-axis bending strength reduction (compared to S3x5.7 (S76x8.5)) relative to other standard M section post options. The M4x3.2 (M102x4.8) section post has a 47 percent reduction in weak-axis bending strength, and an 18 percent reduction in bending strength in the strong-axis direction, as compared to the S3x5.7 (S76x8.5) post section.

The strength reduction in the weak-axis direction would reduce the likelihood of vehicle rollover as a result of repeated vehicle-to-post impacts. The section's strong-axis characteristics allow the post sufficient strength to provide resistance and support for the system cables in a redirection impact.

Although the M4x3.2 (M102x4.8) section has comparable strong-axis strength in pure bending as compared with the S3x5.7 (S76x8.5) post, the M4x3.2 (M102x4.8) section has an 86 percent reduction in torsional stiffness. The torsional stiffness of the terminal post section will have a significant effect on angled terminal impacts downstream of the cable anchor. With the reduced torsional stiffness, it is possible that posts downstream of the impact will twist due to cable deflection, thus reducing its strength. The reduction in post bending strength will reduce the likelihood of vehicle rollover, but it will also reduce the post's capacity to support the cables during redirection. Therefore, if an M4x3.2 (M102x4.8) section is selected for terminal posts, a relatively short post spacing may be necessary to adequately support the cables during redirection terminal impacts. A comparison of the S3x5.7 (S76x8.5) and M4x3.2 (M102x4.8) post cross sections is shown in Figure 25.

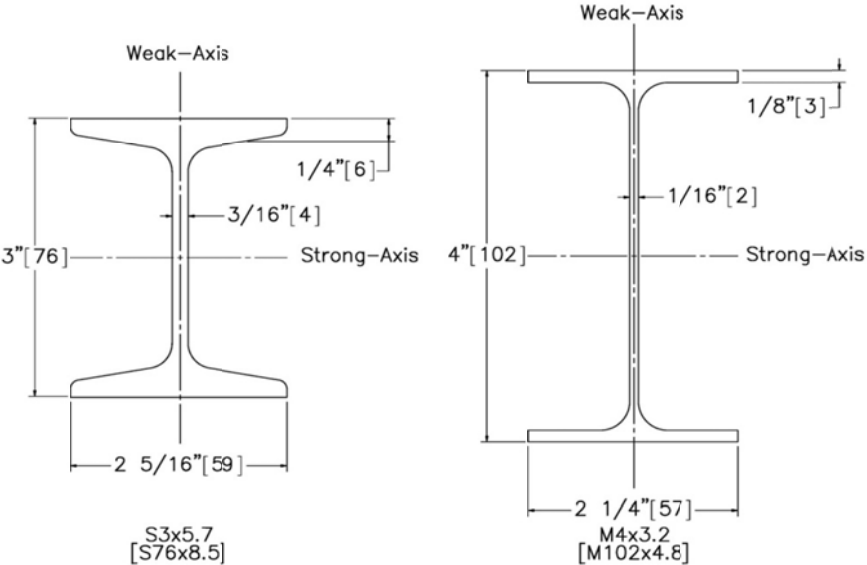


Figure 25. Post Cross Section Dimensions

### 3.2.8.2.3 Modified S3x5.7 (S7x8.5) Post Option

Another possible option to reduce weak-axis bending capacity would be to alter the strength characteristics of the S3x5.7 (S76x8.5) post. This strength reduction could be accomplished by incorporating horizontal cuts or holes into the post's cross section at the intended failure location. In this scenario, a failure in bending at the groundline would be ideal. This option would simplify system installation by using a uniform post type for the entirety of the system, as compared with a terminal that used a slip base post that would require assembly. The bending strength characteristics, however, are not as desirable as that of the M4x3.2 (M102x4.8) option due to the M4x3.2 (M102x4.8) section's reduced weak-axis bending strength and a strong-axis bending strength more comparable to standard S3x5.7 (S76x8.5) system line posts. Similarly, as noted previously for the M4x3.2 (M102x4.8) post, a modified S3x5.7 (S76x8.5) post would have reduced torsional stiffness as compared with an S3x5.7 (S76x8.5) section. Therefore, similar issues during redirection terminal impacts may be evident.

In 2004, a testing program was accomplished at MwRSF to evaluate the directional strength properties of modified S3x5.7 (S76x8.5) posts [18]. Posts with varying length cuts into the ends of the flanges were impacted in both strong-axis and weak-axis orientations. These results were compared with impact data obtained from unmodified S3x5.7 (S76x8.5) posts [19]. A technical drawing of a sample post modification is shown in Figure 26.

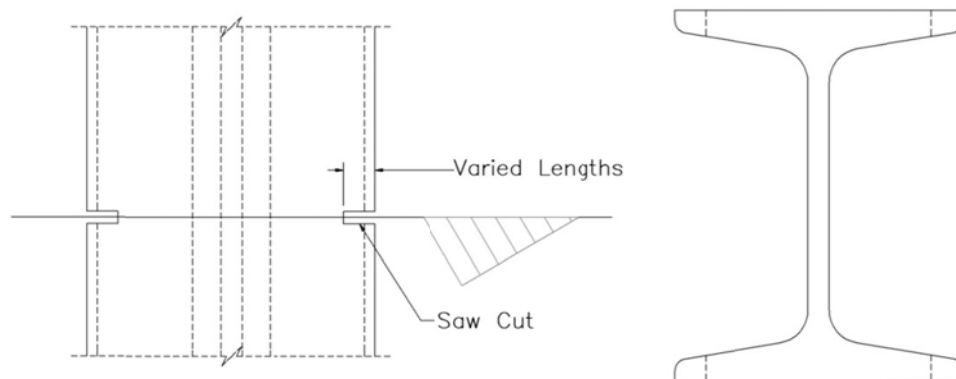


Figure 26. S3x5.7 (S76x8.5) Post with Cut Flanges



An S3x5.7 (S76x8.5) post with 1/8-in. (3.2-mm) cuts in each flange exhibited desirable strength characteristics for a terminal post. The modified post had similar maximum impact force values in both the strong-axis and the weak-axis orientations as compared with an unmodified S3x5.7 (S76x8.5) post. The vertical impact force, however, showed a 54 percent decrease in weak-axis strength. The vertical impact forces are important in this case since these are indicative of the posts ability to impart uplift forces on a vehicle and subsequently, could result in pitching and rolling if the force is high enough. Since the vertical impact forces were reduced by 54 percent in the weak-axis direction, the modified posts will be less likely to cause rollover in the event of a terminal impact. The vertical force data from bogie testing of the cut post section as compared to a non-cut section is shown in Table 3.

Table 3. Vertical Impact Forces, Cut Cable Post Bogie Testing [18]

Post Section	Plastic Section Modulus, Z in. <sup>3</sup> (mm <sup>3</sup> )		Vertical Impact Force kips (kN)	
	Strong-Axis	Weak-Axis	Strong Axis	Weak Axis
S3x5.7 (S76x8.5)	1.94 (31,791)	0.66 (10,816)	1.9 (8.5)	3.8 (16.9)
S3x5.7 (S76x8.5) with 1/8-in. Saw Cuts in Flanges	1.69 (27,694)	0.46 (7,538)	1.9 (8.5)	1.8 (8.0)

Although the S3x5.7 (S76x8.5) post with cut flanges showed favorable strength characteristics in the bogie testing program, the modified post was not selected for full-scale crash testing. There was some question as to whether the cuts in the flanges could be manufactured in a consistent manner and allow for predictable crack propagation. Another issue

that surrounded the modified posts was whether driving modified posts into soil would cause premature crack propagation at the cut flanges, thus excessively weakening the terminal posts.

These manufacturing and installation concerns eliminated the modified cut post from consideration for the non-proprietary, low-tension end terminal. However, these issues were speculative, and the cut cable post was never investigated further.

An alternate means of reducing the bending strength of the S3x5.7 (S76x8.5) post could be accomplished by drilling weakening holes into the flanges of the post. Although the cut flanges option would yield a greater reduction in weak-axis bending strength, the weakening holes would alleviate concerns of crack propagation during post installation. It would also improve the manufacturability of the terminal posts.

Weakening holes measuring 3/8-in. (9.5-mm) in diameter would result in a weak-axis bending strength reduction of 40 percent, and a 25 percent reduction in the strong-axis bending strength. The decreased weak-axis bending strength would aid in the reduction of vehicle roll motion. Unlike the cut flanges option, no bogie tests have been performed on S3x5.7 (S76x8.5) posts with weakening holes. Thus, physical testing and evaluation will be required prior to moving forward with this option. The weakening hole option is shown in Figure 27.

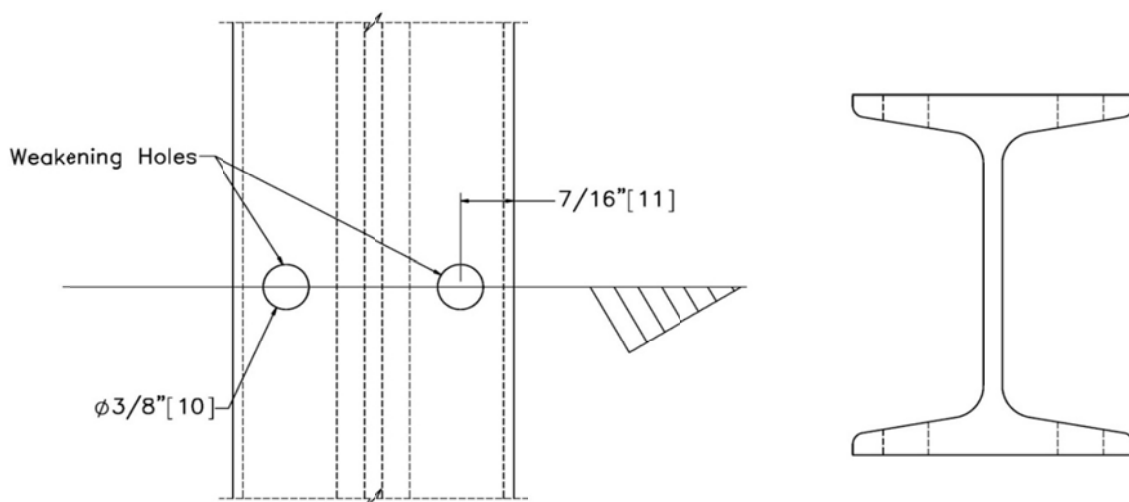


Figure 27. S3x5.7 (S76x8.5) Post with Weakening Holes

#### **3.2.8.2.4 Terminal Post Replacement Options Summary**

The slip base post assembly utilized in the non-proprietary, low-tension, cable end terminal led to significant vehicular roll and yaw motions during the full-scale crash testing. Potential replacement options include an M4x3.2 (M102x4.8) post or a weakened S3x5.7 (S76x8.5) post. The M4x3.2 (M102x4.8) post is similar to the S3x5.7 (S76x8.5) in strong-axis bending strength. However, its weak-axis bending strength is significantly reduced, which diminishes its propensity to cause vehicle rollover. The weakened S3x5.7 (S76x8.5) post may be preferable because it simplifies the construction of the non-proprietary cable guardrail system. However, its strength characteristics are not as desirable as that of the M4x3.2 (M102x4.8) post section. Both the M4x3.2 (M102x4.8) section post and modified S3x5.7 (S76x8.5) post options have reduced torsional stiffness as compared with the S3x5.7 (S76x8.5) section. The reduction in torsional stiffness may require a relatively close terminal post spacing in order to adequately support cables during a terminal redirection impact, however this issue requires further investigation. A comparison of the post strength is shown in Table 4.

The use of one of the replacement post options could potentially increase the robustness of the end terminal design by eliminating the unpredictable interactions between detached post sections and the impacting vehicle. As a result, the overall safety performance and ease of assembly of the end terminal design would be improved.

Table 4. Post Strength Properties

Post Section	Plastic Section Modulus, Z in. <sup>3</sup> (mm <sup>3</sup> )		Plastic Bending Moment kip-in. (kN-m)		Impact Force kips (kN)		Torsional Strength kip-in. (N-m)
	Strong-Axis	Weak-Axis	Strong-Axis	Weak-Axis	Strong-Axis	Weak-Axis	
S3x5.7 (S76x8.5)	1.94 (31,791)	0.66 (10,816)	104.8 (11.8)	35.6 (4.0)	6.9 (30.7)	2.3 (10.2)	1.0* (113.0)
S3x5.7 (S76x8.5) with 1/8-in. Saw Cuts in Flanges	1.69 (27,694)	0.46 (7,538)	91.3 (10.3)	24.8 (2.8)	6.5 (28.9)	2.7 (12.0)	0.8* (90.4)
S3x5.7 (S76x8.5) with ø3/8-in. (9.5-mm) Weakening Holes	1.45 (23,761)	0.39 (6,391)	78.3 (8.8)	21.1 (2.4)	5.2* (2.3)	1.4* (6.2)	-
M4x3.2 (M102x4.8)	1.68 (27,530)	0.35 (5,735)	90.7 (10.2)	18.9 (2.1)	5.7* (2.5)	1.2* (5.2)	0.1* (11.3)
Slip Base Post	-	-	-	-	-	4.3 (19.1)	-

\*Theoretically Derived Values

### 3.3 Conclusions

An investigation of the vehicle trajectory and stability exhibited in the low-tension, cable end terminal test series (CT series) was undertaken. To analyze the system, a model of the low-tension, cable end terminal system was developed using finite element software. The model was then validated using test data from the physical crash test no. CT-4.

Analysis of the simulation results revealed that the vehicle had an initial yaw prior to impact with the system. The initial yaw was due to the impact between the vehicle's guide flag and the shear post on the tow line. This initial yaw intensified the yawing that was generated by off-centered anchor and post impacts once the vehicle entered the system. The vehicle yaw, while not solely responsible for the near vehicle rollover, contributed to the erratic vehicle trajectory.

The vehicle impacted the system and began to yaw. As mentioned previously, the yaw alone was not cause for concern as the vehicle will still remain stable and balanced. The vehicle then overrode a cluster of system debris. System debris included cable compensators, detached, top sections of slip base post assemblies, and the cable release lever. The interaction between the right-front vehicle tire and undercarriage with the system debris caused abrupt vehicle decelerations, sharp increases in yaw rate, and induced a roll toward the driver side of the vehicle. This resulted in the near vehicle rollover that occurred in test no. CT-4.

Since cable end terminal components and features are similar regardless of the designed cable tension, it is possible that the non-proprietary, high-tension, cable end terminal will exhibit similar vehicle trajectory, yaw, and roll angles if no modifications are made to the end terminal design. While the cable anchor served its intended purpose, the crashworthiness of the design would be improved if the cable anchor was redesigned. The cable release lever was allowed to detach from the assembly post-cable release. The detached release lever's trajectory was unpredictable, and in the case of test no. CT-4, the interaction between the release lever and the vehicle contributed to high vehicle roll and yaw angles. These angular motions nearly resulted in vehicle rollover.

The slip base posts also activated as intended. However, much like the cable release lever, interaction between the vehicle and the detached top post sections resulted in unintended vehicle decelerations, yaw, and roll. Although the slip base post assembly has several features that are beneficial to satisfactory terminal performance, the unpredictability of the detached post sections makes it less than ideal to use slip base posts in future systems.

Alternate options for the slip base post assemblies include an M4x3.2 (M102x4.8) post and modified S3x5.7 (S76x8.5) post options. The alternate post options have lower weak-axis

bending strength as compared to the S3x5.7 (S76x8.5) post. Thus, it would be less likely to induce vehicle rollover. The replacement options also would not introduce system debris into the vehicle path that could cause vehicle instabilities. A detailed investigation including bogie testing, full-scale crash testing, and further simulation would be necessary to verify that either the M4x3.2 (M102x4.8) post section or one of the modified S3x5.7 (S76x8.5) post sections are indeed viable replacement options.

#### **4 CURRENT, HIGH-TENSION, CABLE ANCHOR BRACKET DESIGN**

With the ongoing development of high-tension, cable median barriers for use in ditch applications, it was deemed necessary to also continue to develop a crashworthy cable end terminal system for anchoring the cables. As noted previously, MwRSF developed, crash tested, and obtained FHWA's acceptance of a low-tension, cable guardrail end terminal. Subsequently, the anchor bracket assembly was adapted for use with a high-tension, four-cable end terminal system. In the low-tension end terminal testing, the anchor bracket and cable release mechanism performed well. During testing, there was no indication that the end terminal would not perform well in high-tension applications as well as with more cables.

Therefore, the anchor bracket assembly was modified for a high-tension, four-cable system. Modifications included:

- widening the entire anchor bracket assembly to accommodate an extra system cable;
- adding a 4th slot on the cable plate to accommodate 4th system cable;
- adding extra internal gussets to strengthen the assembly against increased cable loading;
- increasing the height of outer gussets to provide extra support for the cable plate; and
- altering the release lever and release lever support geometry to accommodate the revised slope of the end cables that are terminated at the cable bracket assembly.

Detailed drawings of the high-tension, cable anchor bracket assembly are shown in Figures 28 through 32.

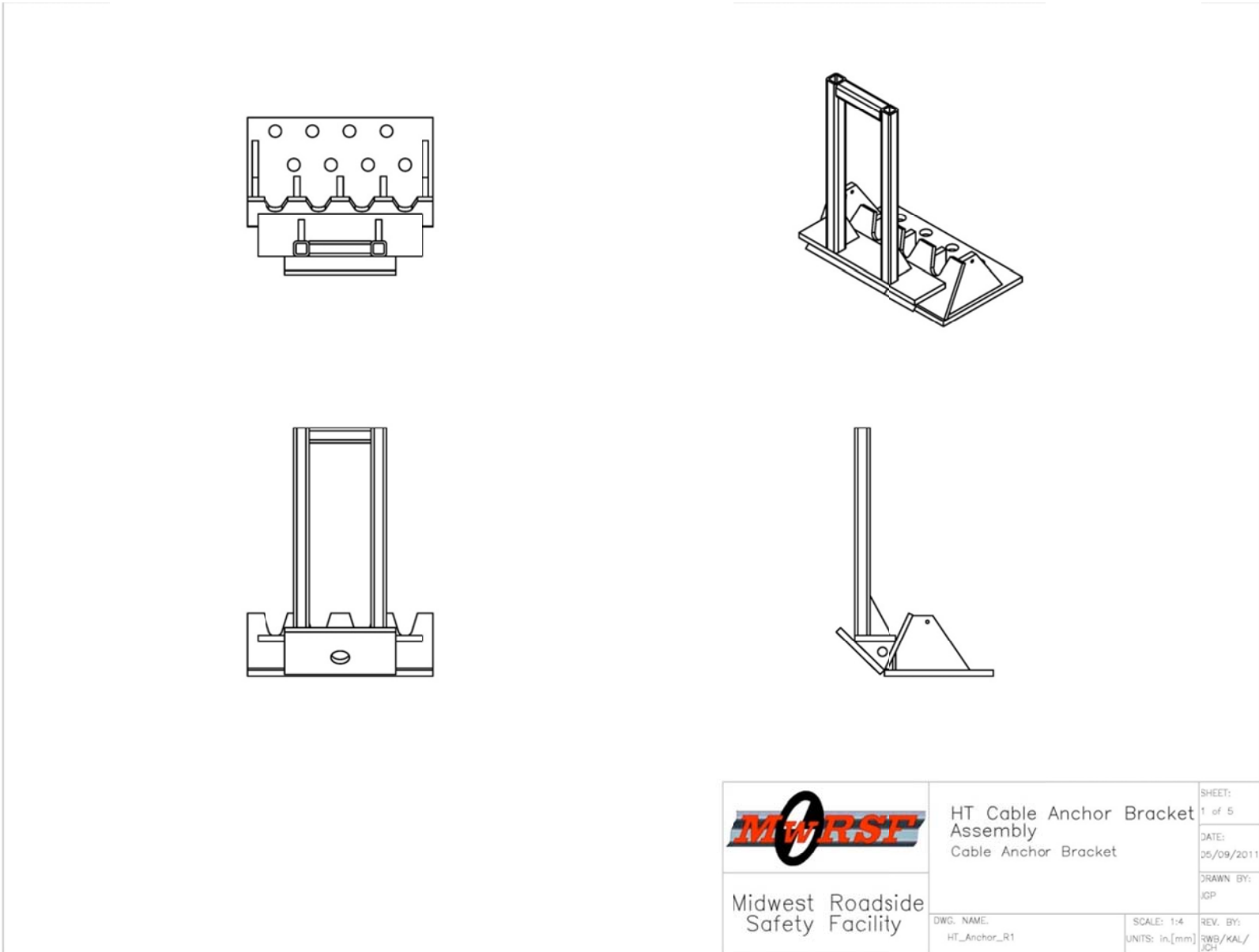


Figure 28. Cable Anchor Bracket Assembly Drawings



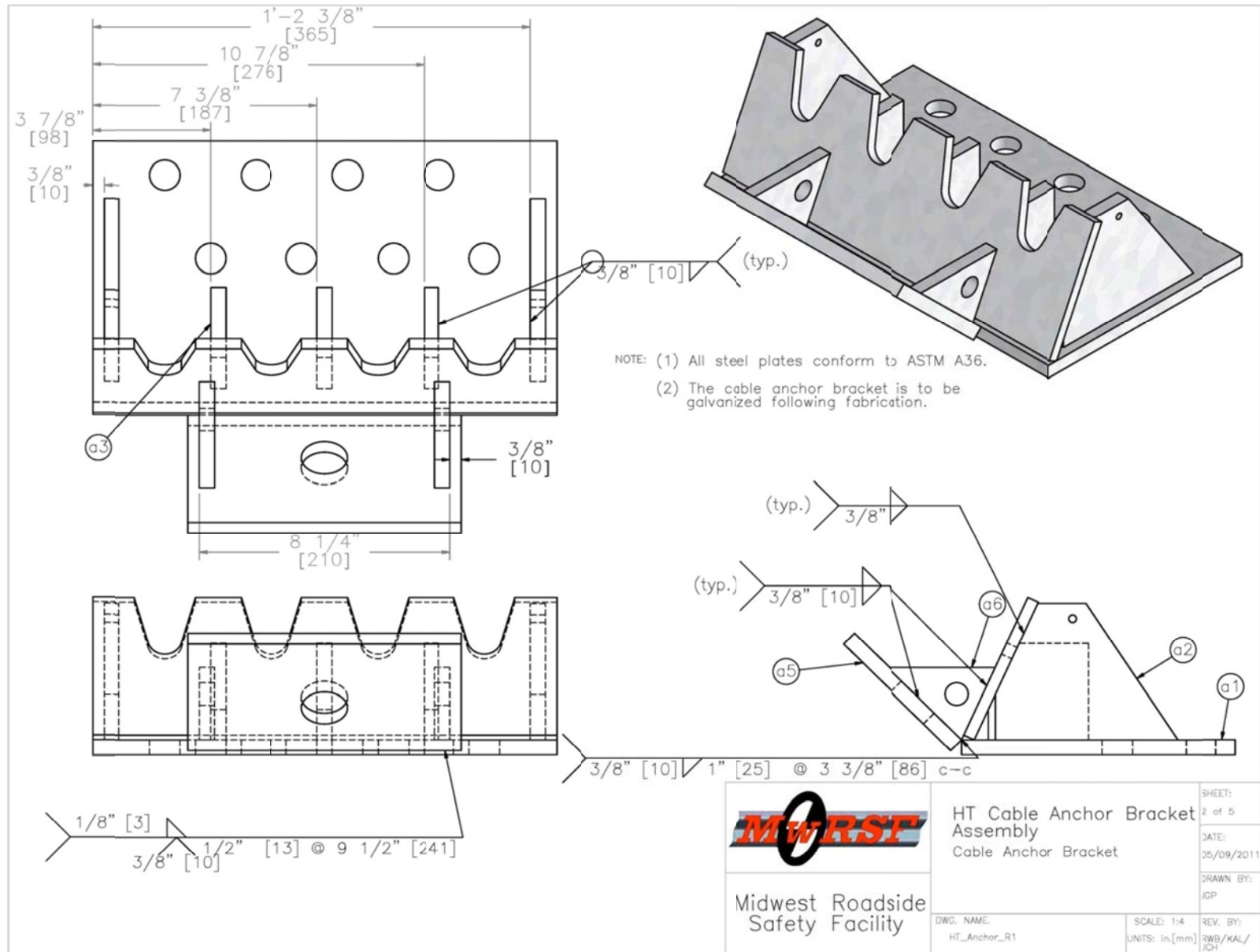


Figure 29. Cable Anchor Bracket Assembly Details

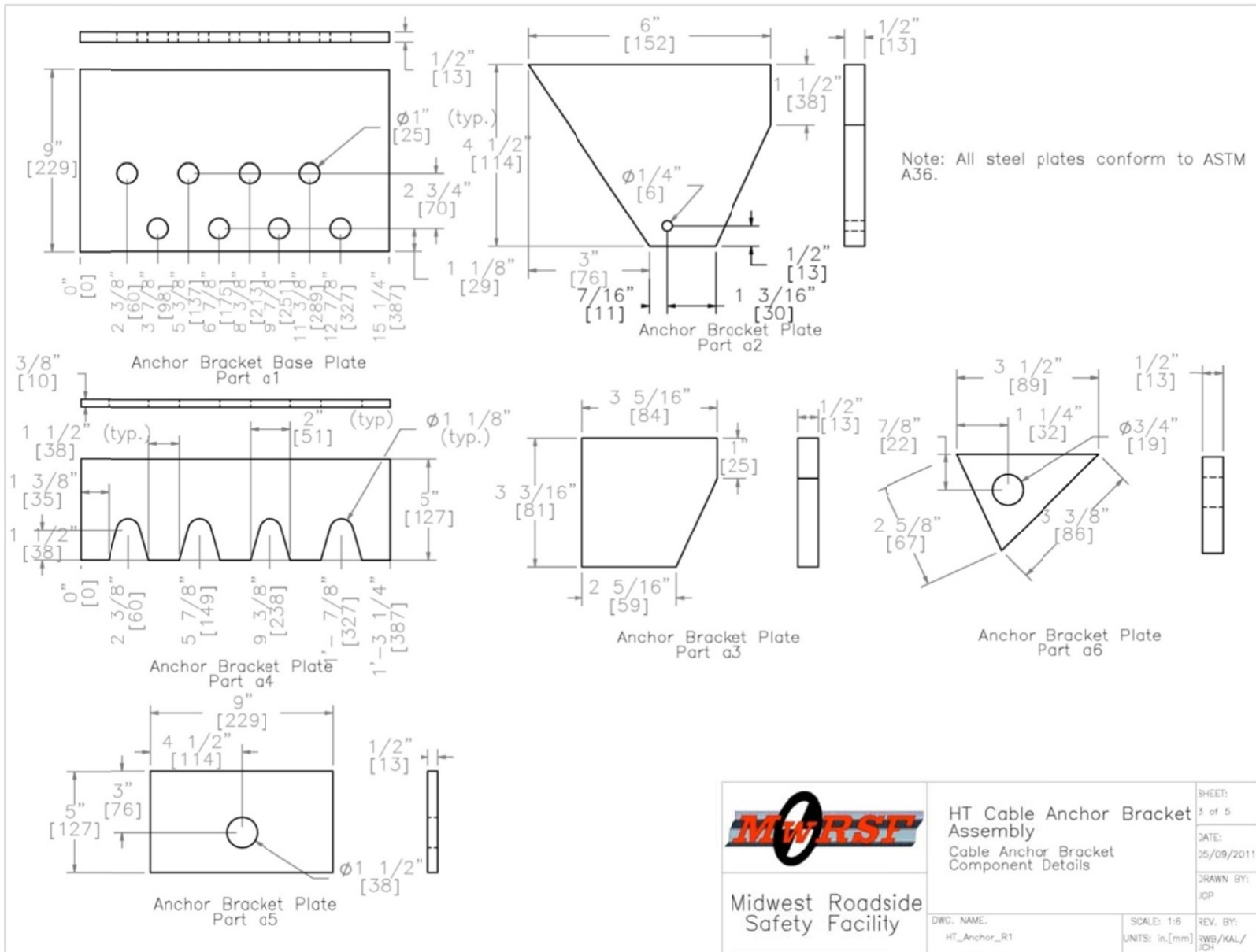


Figure 30. Cable Anchor Bracket Component Details

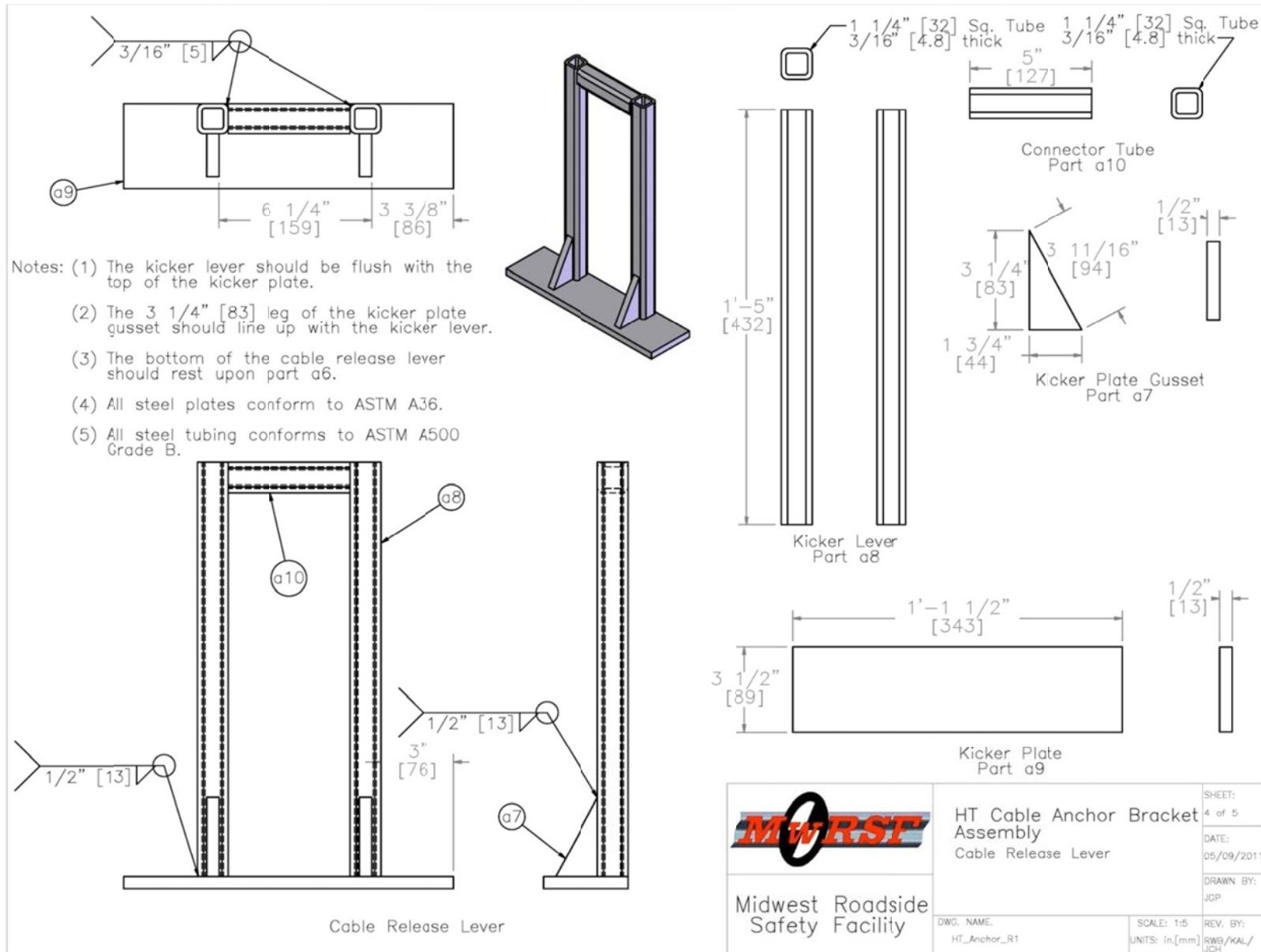


Figure 31. Cable Release Lever Assembly Details

Item No.	QTY.	Description	Material Specification
a1	2	Cable Anchor Base Plate	ASTM A36 Steel
a2	4	Exterior Cable Plate Gusset	ASTM A36 Steel
a3	6	Interior Cable Plate Gusset	ASTM A36 Steel
a4	2	Anchor Bracket Plate	ASTM A36 Steel
a5	2	Release Lever Plate	ASTM A36 Steel
a6	4	Release Gusset	ASTM A36 Steel
a7	4	CT kicker – gusset	ASTM A36 Steel
a8	4	1.25x1.25x0.1875" TS CT Kicker Lever Tube	ASTM A500 Grade B
a9	2	3x10x0.5" Kicker Plate	ASTM A36 Steel
a10	2	1.25x1.25x0.1875" TS CT Kicker Lever Connecting Tube	ASTM A 500 Grade B

 Midwest Roadside Safety Facility	HT Cable Anchor Bracket Assembly Bill of Materials	SHEET: 5 of 5
	DWG. NAME: HT_Anchor_R1	SCALE: 1:5 UNITS: in.[mm]
		DRAWN BY: JGP
		REV. BY: RWB/KAL/ JCH

Figure 32. Bill of Materials, Cable Anchor Bracket Assembly

## 5 INITIAL COMPUTER SIMULATION

### 5.1 Introduction

Finite element modeling can be a useful tool in the design process. If an accurate model is obtained, it can be used in place of costly physical testing to evaluate potential designs. A finite element model of the high-tension, cable anchor bracket assembly was created in order to assess the capability of finite element modeling as a predictive design tool. Simulations were conducted with an abbreviated finite element model of the high-tension, cable end terminal. Subsequent physical bogie testing of the anchor was used to evaluate the current, high-tension, cable anchor design as well as the predictive capabilities of the finite element model.

During the low-tension end terminal validation, the model closely replicated the mechanics of the cable anchor bracket assembly during the release of the cables. After the successful modeling of the low-tension, cable anchor bracket and end terminal, it was hoped that the high-tension, cable anchor bracket model would be replicated as well.

Many of the system components in the high-tension, cable end terminal are similar to components in the low-tension, cable end terminal. One difference, however, is that the cable compensators utilized in low-tension systems are not necessary in high-tension systems. The elimination of the cable compensators reduces the amount of debris that could possibly cause vehicle instabilities observed during end-on terminal impacts. The only other significant difference between the two systems is small variations in component geometry. Materials used for fabricating many of the components were unchanged from the low-tension system to the high-tension system. As such, the material models and element formulations were reused from the low-tension end terminal model and applied to the high-tension model.

## **5.2 Abbreviated, High-Tension, Cable End Terminal System Model**

To evaluate the high-tension, cable anchor bracket model, an abbreviated high-tension, cable end terminal model was created. This system was then impacted with a bogie vehicle model to simulate a dynamic component test. The abbreviated high-tension, cable end terminal model consisted of four main components:

- the high-tension, cable anchor bracket assembly;
- one slip base post assembly;
- four system cables; and
- bogie model.

Detailed descriptions of the individual components and the techniques used to model them are discussed in the ensuing sections.

### **5.2.1 High-Tension, Cable Anchor Bracket Assembly**

The cable anchor bracket was modeled using a combination of three-noded and four-noded shell elements. The cable release lever was also modeled using shell elements. Eight-noded hexagonal elements were used to model the anchor bolts and their associated washers. ASTM A36 steel material properties were specified for all components of the cable anchor bracket model, and ASTM A307 steel material properties were used for the bolts. A Belytschko-Leviathan element formulation was specified for all shell elements and a Fully Integrated S/R solid element formulation was used for all solid elements. A summary of the anchor bracket assembly components and their associated element and material types is shown in Table 5. A comparison of the physical cable anchor bracket and its finite element model as well as a close up of the component meshing is shown in Figures 33 and 34.

Table 5. Summary of Cable Anchor Bracket Model Properties

Part Name	Element Type	Element Formulation	Material Type	Material Formulation
Interior Cable Plate Gusset	Shell	Belytschko-Leviathan	ASTM A36	Piecewise, Linear Plastic
Exterior Cable Plate Gusset	Shell	Belytschko-Leviathan	ASTM A36	Piecewise, Linear Plastic
Base Plate	Shell	Belytschko-Leviathan	ASTM A36	Piecewise, Linear Plastic
Cable Plate	Shell	Belytschko-Leviathan	ASTM A36	Piecewise, Linear Plastic
Release Lever Support Plate	Shell	Belytschko-Leviathan	ASTM A36	Piecewise, Linear Plastic
Release Lever Support Gusset	Shell	Belytschko-Leviathan	ASTM A36	Piecewise, Linear Plastic
Release Lever Vertical Tube	Shell	Belytschko-Leviathan	ASTM A36	Piecewise, Linear Plastic
Release Lever Connecting Tube	Shell	Belytschko-Leviathan	ASTM A36	Piecewise, Linear Plastic
Release Lever Base Plate	Shell	Belytschko-Leviathan	ASTM A36	Piecewise, Linear Plastic
Release Lever Gusset	Shell	Belytschko-Leviathan	ASTM A36	Piecewise, Linear Plastic
Anchor Bolts	Solid	Fully Integrated, S/R	ASTM A307	Piecewise, Linear Plastic
Washers	Solid	Fully Integrated, S/R	ASTM A36	Rigid

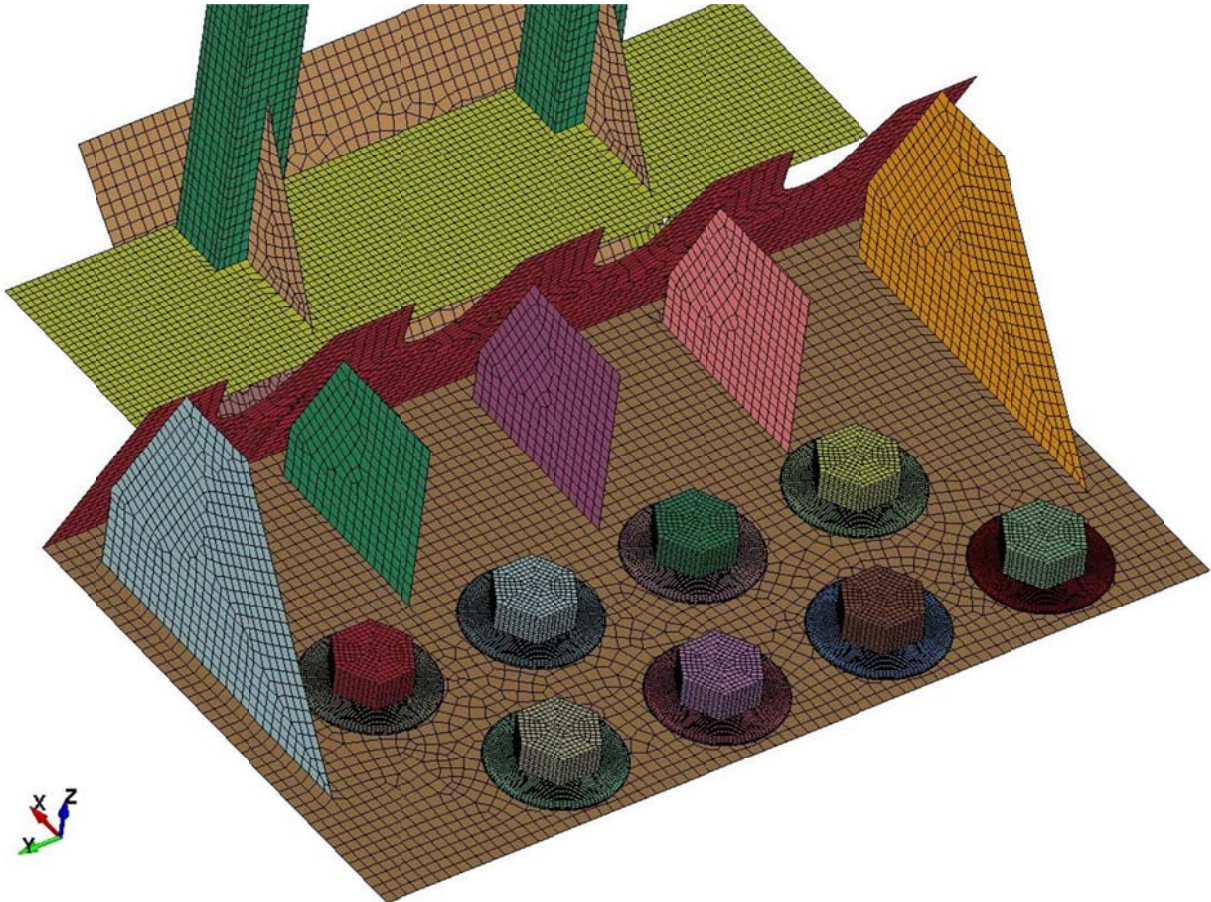


Figure 33. Cable Anchor Bracket Component Mesh

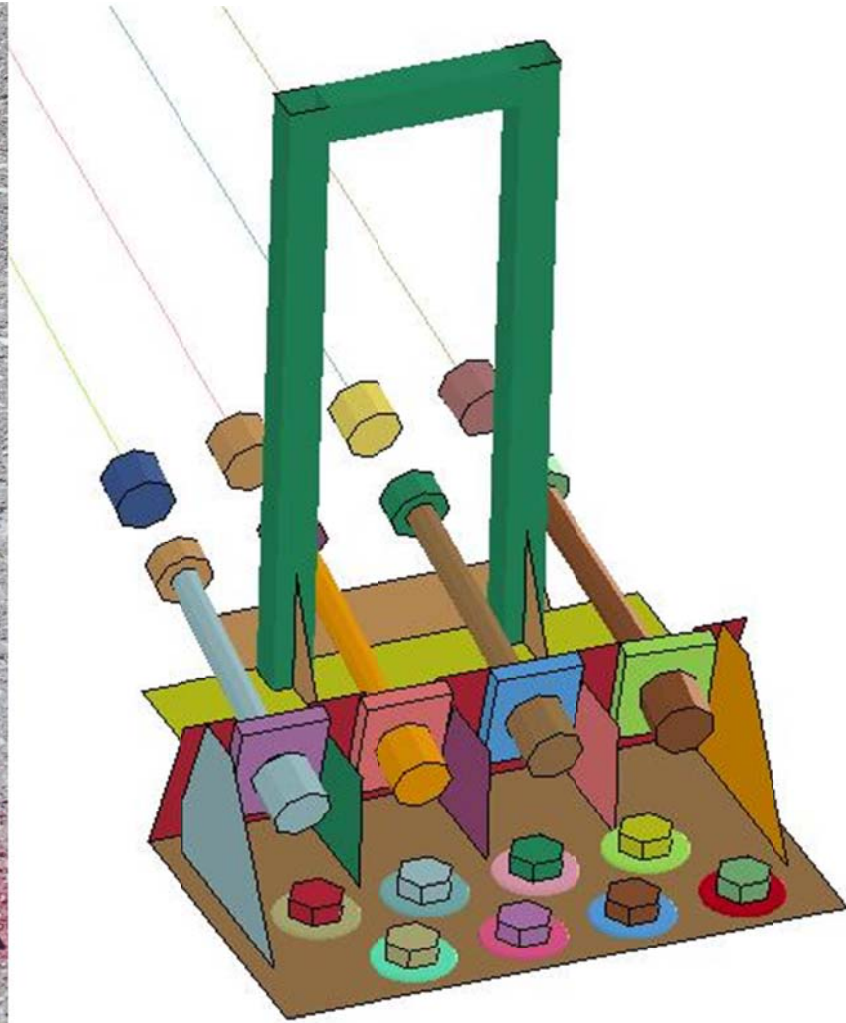


Figure 34. Cable Anchor Bracket and Finite Element Model



### **5.2.2 Slip Base Post Assembly**

The slip base post assembly utilized in the end terminal simulation was modeled to reflect the geometry and slip characteristics of the physical post assembly. The S3x5.7 (S76x8.5) portion of the post was meshed with three-noded and four-noded shell elements. A Belytshcko-Leviathan element formulation was specified for the post elements. The cable hangar attached to the post was meshed with three-noded shell elements. Various physical tests have shown this component to be very robust; therefore, a rigid material type was applied to reduce computational time.

The base plate components that comprised the slip interface were modeled with solid elements. A Fully Integrated S/R solid element formulation was used. Solid elements were used to model the slip connection to better define the contact surfaces. The bolts and washers utilized in the slip connection were also meshed with solid elements and a Fully Integrated S/R element formulation. The washers utilized between the slip plates and under the bolt heads and nuts were specified as rigid. Note that although the component modeling was accomplished for this simulation effort, the slip connection model was taken from a previous study [15].

The slip connection support plates, as well as the assembly base plate, were meshed with three-noded and four-noded shell elements. A Fully Integrated shell element formulation was specified for both the supports and the base plate. The wedge bolts and washers used to anchor the assembly were meshed with solid elements. Fully Integrated S/R element formulations were used for both the bolts and the washers. The washers were again specified as rigid. ASTM A36 steel material properties were specified for all steel plate components and ASTM A307 steel material properties were used for the slip base bolts and the wedge bolts. Component modeling information is tabulated in Table 6. A comparison of the physical cable anchor bracket and its

finite element model, as well as a close up of the component meshing, is shown in Figures Figure 35 and Figure 36.

Table 6. Summary of Slip Base Post Model Properties

Part Name	Element Type	Element Formulation	Material Type	Material Formulation
S3x5.7 Post	Shell	Belytschko-Leviathan	ASTM A36	Piecewise, Linear Plastic
Cable Hangar	Shell	Belytschko-Leviathan	ASTM A36	Rigid
Top Slip Base Plate	Shell	Belytschko-Leviathan	ASTM A36	Piecewise, Linear Plastic
Bottom Slip Base Plate	Shell	Belytschko-Leviathan	ASTM A36	Piecewise, Linear Plastic
Slip Base Bolts	Solid	Fully Integrated, S/R	ASTM A307	Piecewise, Linear Plastic
Slip Base Washers	Solid	Fully Integrated, S/R	ASTM A36	Rigid
Slip Base Support Plates	Shell	Belytschko-Leviathan	ASTM A36	Piecewise, Linear Plastic
Post Assembly Base Plate	Shell	Belytschko-Leviathan	ASTM A36	Piecewise, Linear Plastic
Wedge Bolt Anchors	Solid	Fully Integrated, S/R	ASTM A307	Piecewise, Linear Plastic
Anchor Washers	Solid	Fully Integrated, S/R	ASTM A36	Rigid

### 5.2.3 System Cables

The cable model used in the high-tension simulation differed from the model used for the low-tension end terminal validation. The cable model used in the current component test simulation model was the result of a previous study [20]. However, at the time of the low-tension end terminal validation there were some issues with the cable model that prevented its use. Since then, the issues were corrected and the model was available for use. The new cable model has several advantages over the older model, including accuracy and usability. The cables main purpose in the simulation is to provide a load on the cable anchor bracket. Thus, it is reasonable to assume that changing cable models would have a negligible effect on the performance of the anchor or the simulation in general.

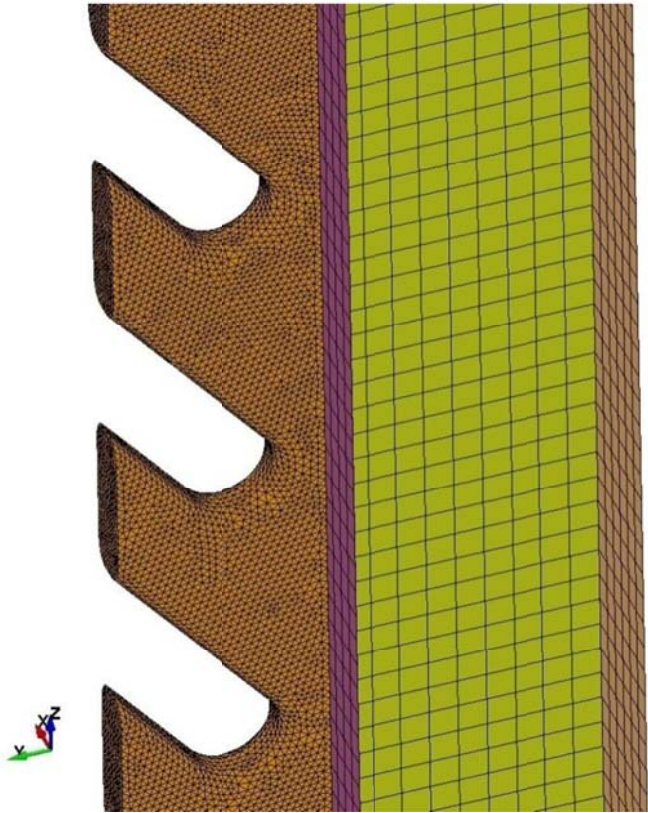
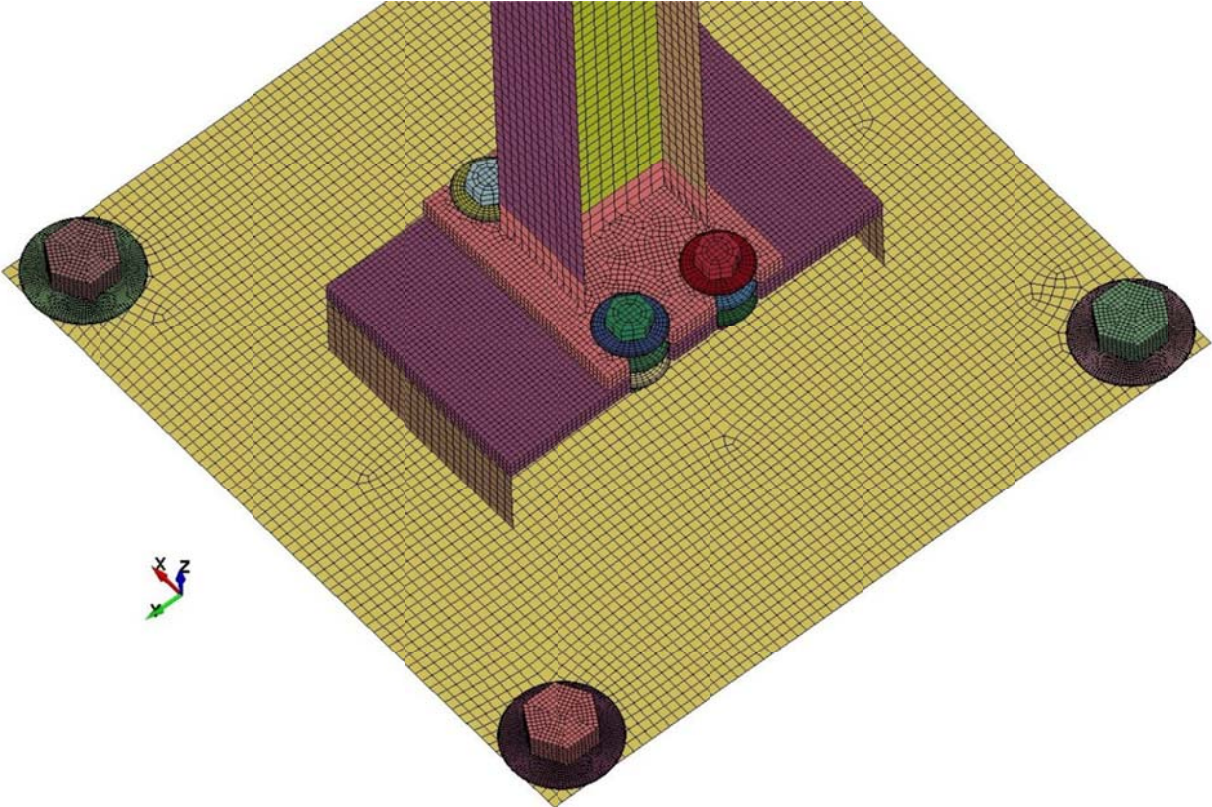


Figure 35. Slip Base Post Assembly Component Mesh

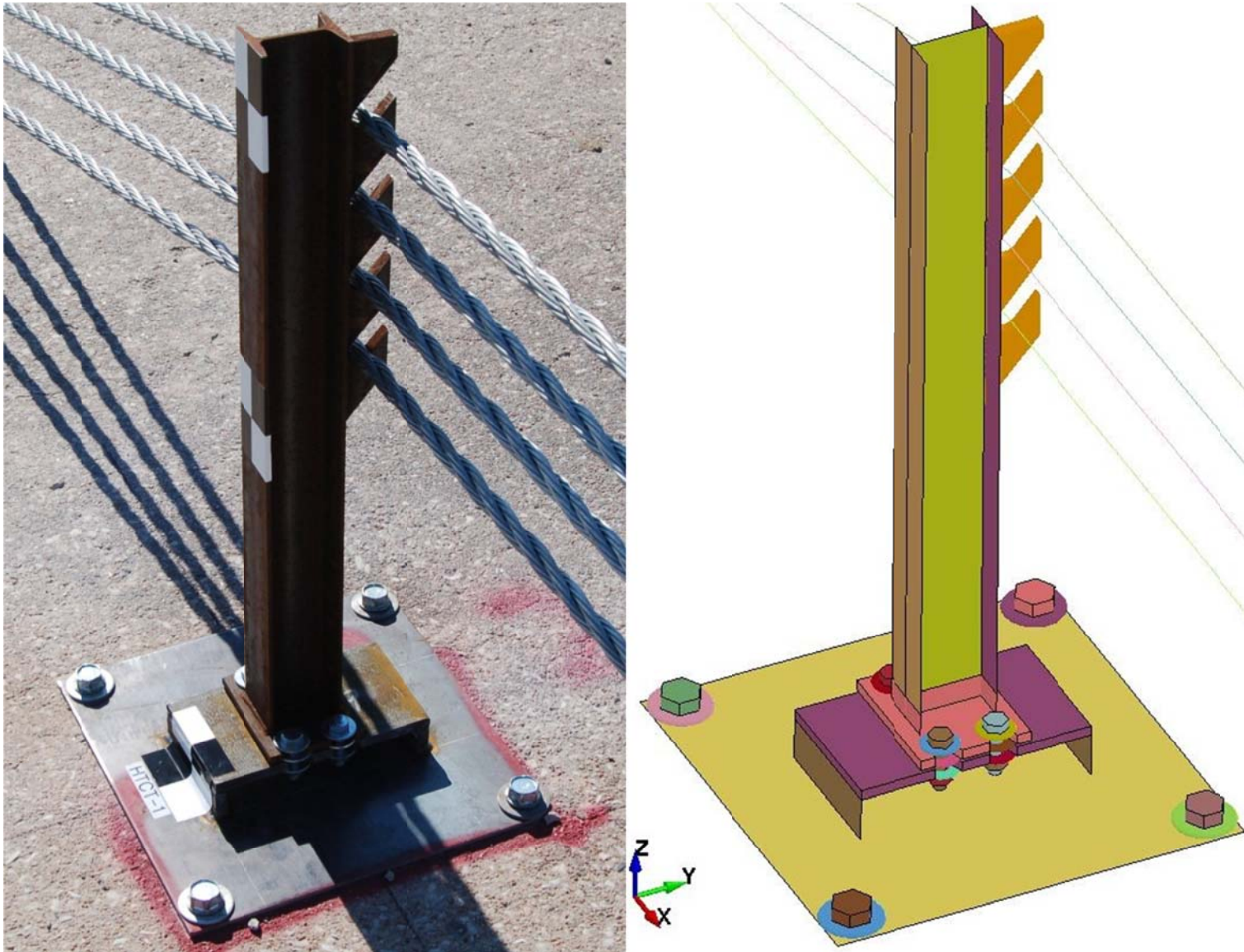


Figure 36. Slip Base Post Assembly and Finite Element Model

Discrete spring elements were used to tension the cables. One end of each spring element was attached to the downstream end of a cable and the other end was fixed. The springs were given an initial offset so that when the system had reached equilibrium, the tension in each cable was 4,200 lb (18.7 kN).

One significant change from the low-tension, cable anchor bracket to the high-tension, cable anchor bracket was in the type of washer used on the cable end fitters. The low-tension, anchor bracket utilized a typical round washer, while the high-tension, anchor bracket required a stronger plate washer to resist deformations from the higher static cable loads. The plate washers also provided increased surface area, which required greater displacement in order to release away from the slots on the anchor bracket.

The plate washers were modeled using 8-noded solid elements. It was expected that the plate washers would not sustain any plastic deformation; therefore a rigid material type was specified to reduce computational time. Subsequent physical testing was later used to verify this assumption. A comparison of the physical system components and their finite element models is shown in Figure 37.



Figure 37. Cable and End Fitter Component Model and Mesh

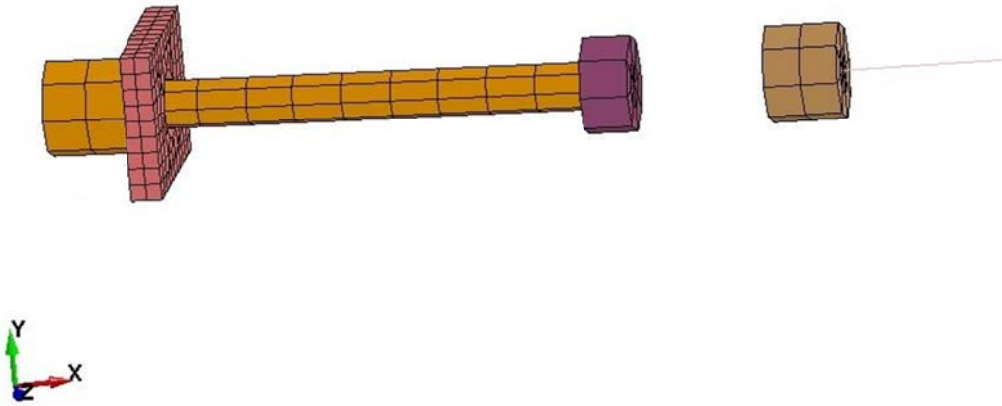


Figure 37 (continued). Cable and End Fitter Component Model and Mesh

**5.2.4 Bogie Model**

The bogie model used for the simulation was previously developed by the MwRSF. Only slight modifications were made to the bogie model (i.e. impact head mounting height and bogie mass) in order to more closely represent the physical bogie. The final mounting height of the impact head was 19 in. (483 mm) and the bogie weight was 1,794 lb (814 kg). The bogie model is shown in Figure 38.

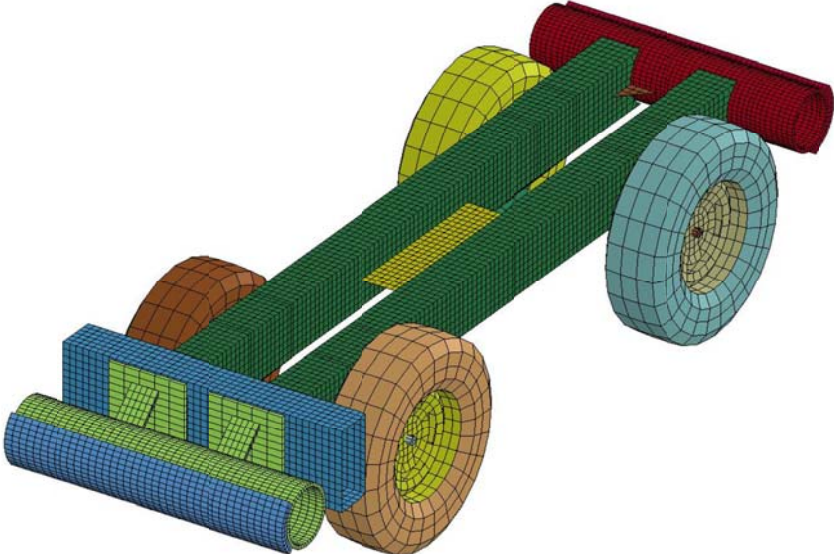


Figure 38. Bogie Finite Element Model

### 5.3 Bogie Test Simulation

The bogie model was given an initial velocity of 45.0 mph (72.4 km/h). The centerline of the bogie impact head was aligned with the vertical centerline of the cable release lever. An automatic single surface contact was used to specify contact between the slip base post assembly, cable anchor bracket assembly, and the bogie's impact head. An automatic nodes to surface contact was used with the cable model to better capture the cable interaction with the cable hangar, bogie impact head, and any other system components that may contact the cables.

Initial impact was between the center of the bogie head and the center of the cable release lever. A sequential description of the simulated impact events is contained in Table 7. Sequential images of the simulation are shown in Figure 39.

The bogie velocity in the simulation was captured to analyze the impact events between the bogie, cable anchor assembly, and slip base post. To capture the bogie velocity, a node located at the bogie's center of mass was tracked throughout the simulation.

After the bogie impact with the anchor bracket, the bogie's longitudinal velocity remained constant for a short time before contacting the system cables and other detached anchor bracket components. The simulated bogie velocity after impact with the cable anchor bracket stabilized to 44.4 mph (71.5 km/h). The associated change in velocity due to the anchor impact was 0.6 mph (1.0 km/h). The bogie head impact with the system cables resulted in a linear decrease in velocity beginning at roughly 61 ms. The total loss in velocity from the cable impact was 0.5 mph (0.8 km/h). The bogie then impacted the slip base post, thus resulting in an additional bogie velocity reduction of 0.9 mph (1.4 km/h). The velocity data from the simulation is shown in Figure 40.

Table 7. Sequential Description of Impact Events, Initial Simulation

TIME (sec)	EVENT
0.000	The cable release lever began to rotate backwards as the bogie impacted and entered the system. The cable end fitters began to translate upwards and out of their respective slots as the cable release lever rotated backwards.
0.019	The cable end fitters fully released from the cable anchor bracket.
0.024	The cross bar on the cable release lever assembly impacted the middle two system cables, causing the cables to begin to wrap around the cross bar.
0.026	The cable release lever assembly lost contact with the cable anchor bracket.
0.052	The top of the cable release lever impacted the ground. The middle two system cables are still wrapped around the cross bar of the cable release lever assembly and continued to pull the assembly downstream.
0.053	The bogie head impacted the top system cable.
0.063	The bogie head simultaneously impacted the middle two system cables.
0.066	The bottom cable impacted the bogie head. All four cables began to coil on the front of the bogie head.
0.110	The bogie head impacted the upstream edge of the slip base post.
0.129	The bottom slip base plate separated from the slip base supports due to element failure along the component boundary. The element failure occurred due to the slip base mechanism failing to activate. The failure of the plate-support boundary marked the end of the simulation.



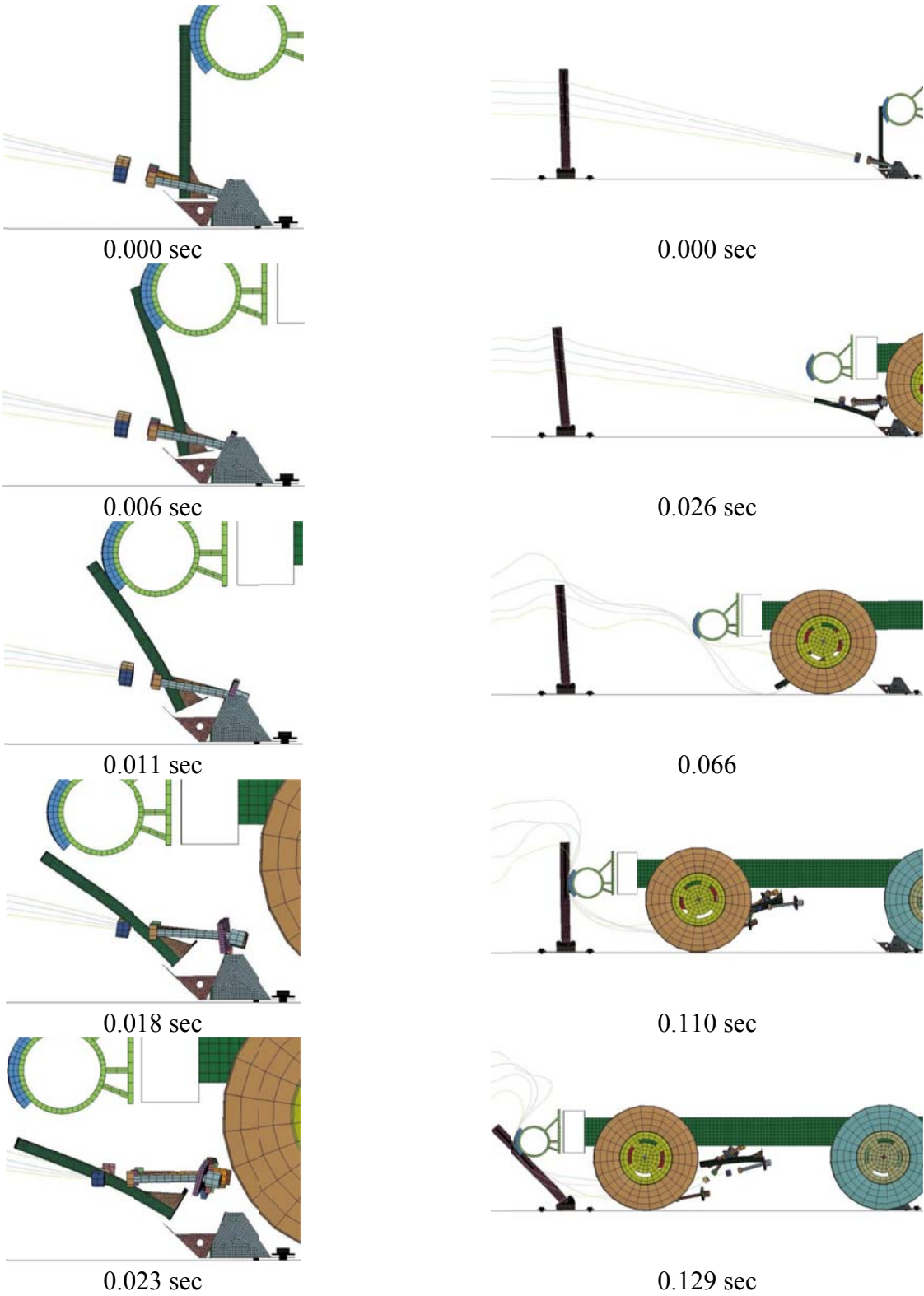


Figure 39. Sequential Photographs, Bogie Test Simulation

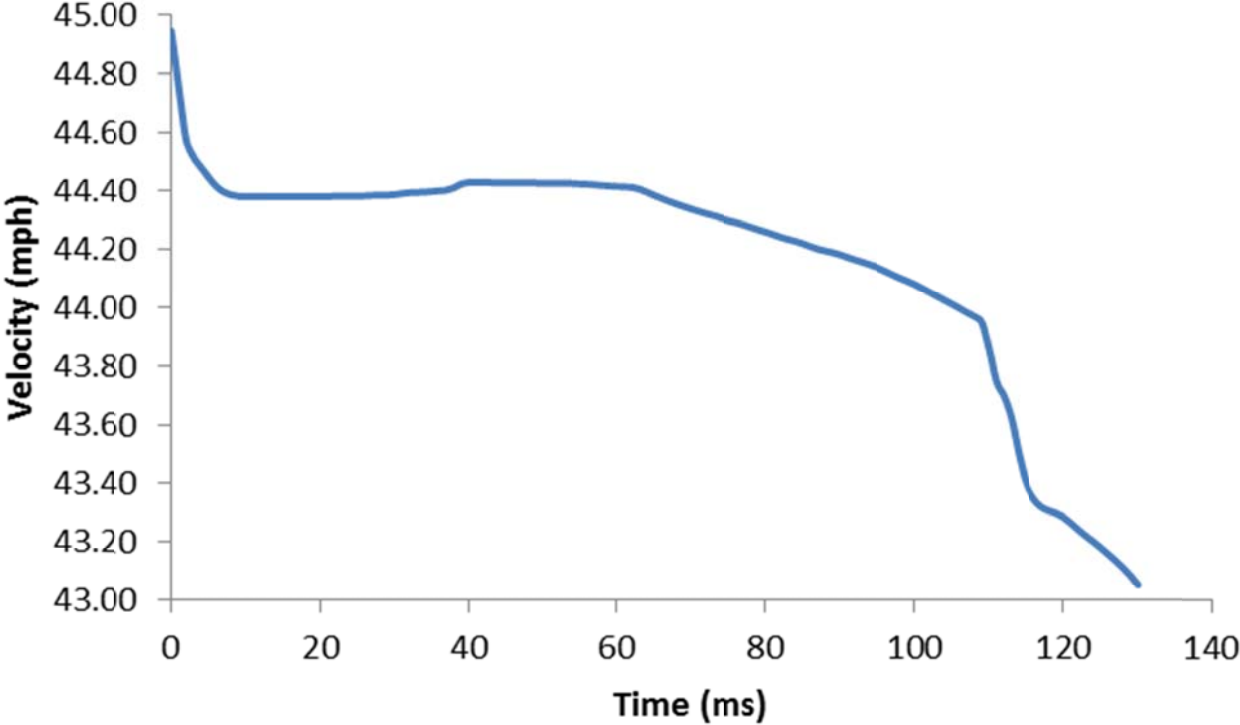


Figure 40. Longitudinal Bogie Velocity, Initial Simulation

**5.4 Discussion**

A finite element model of the current, high-tension, cable anchor bracket was created and analyzed using a simulated dynamic bogie test. The simulation was conducted in order to obtain a numerical model to compare to subsequent physical bogie testing. The initial simulation of the current, high-tension, cable anchor bracket exhibited good cable release mechanics as the cable release lever was impacted and rotated backwards, releasing the system cables as designed.

A physical bogie test using a test setup identical to the simulation model was next conducted. If results from the physical bogie test are deemed to be in relatively good agreement with initial simulation results, the model can be used with confidence to evaluate alternative high-tension, cable anchor bracket designs and modifications.

## **6 HIGH-TENSION, CABLE END TERMINAL BOGIE TESTING**

### **6.1 Purpose**

In order to evaluate the current design and to validate the simulation, bogie testing was performed on an identical terminal system. The test results were needed to evaluate anchor design performance, structural adequacy, and potential for damage or failure. If the design worked well and the model proved accurate, then other simulations with alternate high-tension anchor designs could be analyzed with confidence.

An evaluation of the structural capacity of the current, high-tension, cable anchor bracket was previously incorporated into numerous barrier systems that were subjected to full-scale crash testing. However, the impact performance of the anchor bracket assembly has never been investigated during vehicle impacts on the end terminal. Based on investigation of the low-tension end terminal system, there are concerns with some design aspects of the low-tension, cable anchor bracket that were utilized in the current, high-tension, cable anchor bracket. These features could increase the propensity for vehicle instabilities in small car impacts with the high-tension end terminal system.

With this in mind, component testing was used to verify assumptions, investigate concerns, and determine if design modifications were necessary. The dynamic testing was conducted at the MwRSF Proving Grounds in Lincoln, Nebraska.

### **6.2 Scope**

A bogie test was conducted on an abbreviated version of a high-tension, cable end terminal. The abbreviated system consisted of two high-tension, cable anchor brackets, two slip base post assemblies, and four system cables. The system was installed on a concrete tarmac at MwRSF's outdoor testing facility. The target test conditions consisted of an impact speed of 45

mph (72.4 km/h) with the bogie's impact head centered and aligned with the center of the cable release lever on the cable anchor bracket. The targeted impact height for the test was 19 in. (483 mm), as measured from the ground to the horizontal centerline of the bogie impact head. This height was selected to simulate the bumper height of a Kia Rio.

### **6.3 System Details**

The cable barrier test system used for the bogie test consisted of three main components: (1) cable anchor bracket assemblies; (2) slip base post assemblies; and (3) system cables. Descriptions of each of these assemblies and the components that comprise the assembly can be found in the following sections. Photographs of the system prior to testing are shown in Figure 41. Design drawings for the test articles are shown in Figures 42 through 48.

#### **6.3.1 Cable Anchor Bracket Assemblies**

The cable anchor bracket assemblies consisted of five components: (1) cable release lever; (2) anchor baseplate; (3) anchor cable plate; (4) anchor support gussets; and (5) release lever support gussets. The cable release lever consisted of two 17-in. (432-mm) long, 1 1/4-in. x 1 1/4-in. x 3/16-in. (32-mm x 32-mm x 4.8-mm) thick steel tubes welded to a 3 1/2-in. x 13 1/2-in. x 1/2-in. (89-mm x 343-mm x 12.7-mm) thick steel baseplate. Two 3 1/4-in. x 1 3/4-in. x 1/2-in. (83-mm x 44-mm x 12.7-mm) thick, triangular steel gussets were welded between the baseplate and the steel tubes to increase the bending capacity of the connection. A 5-in. long (127-mm), 1 1/4-in. x 1 1/4-in. x 3/16-in. (32-mm x 32-mm x 4.8-mm) steel tube was welded between the two vertical tubes to aid in the distribution of forces throughout the assembly.

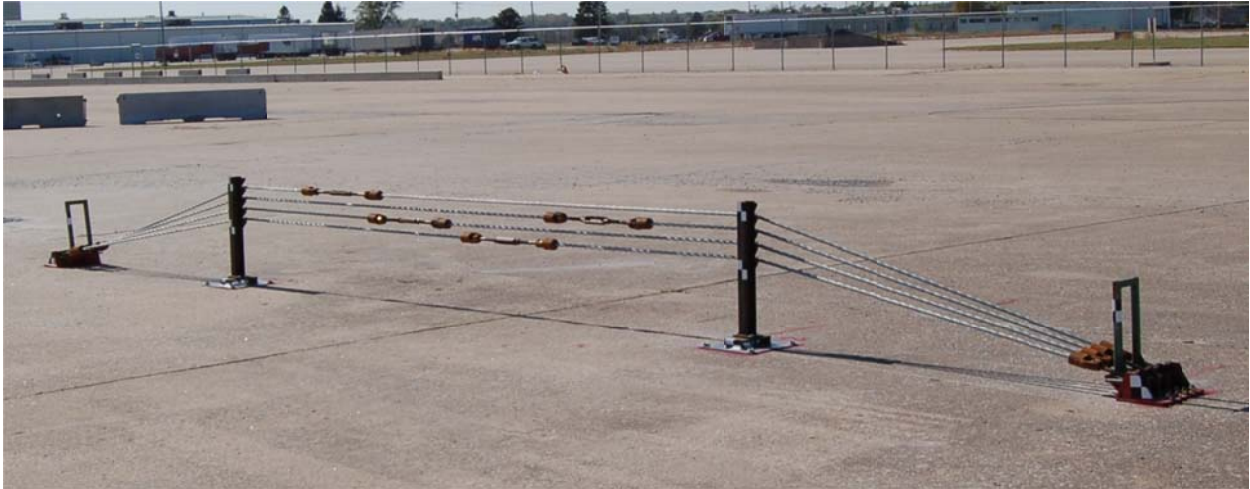


Figure 41. Bogie Test System Setup, Test No. HTCT-1

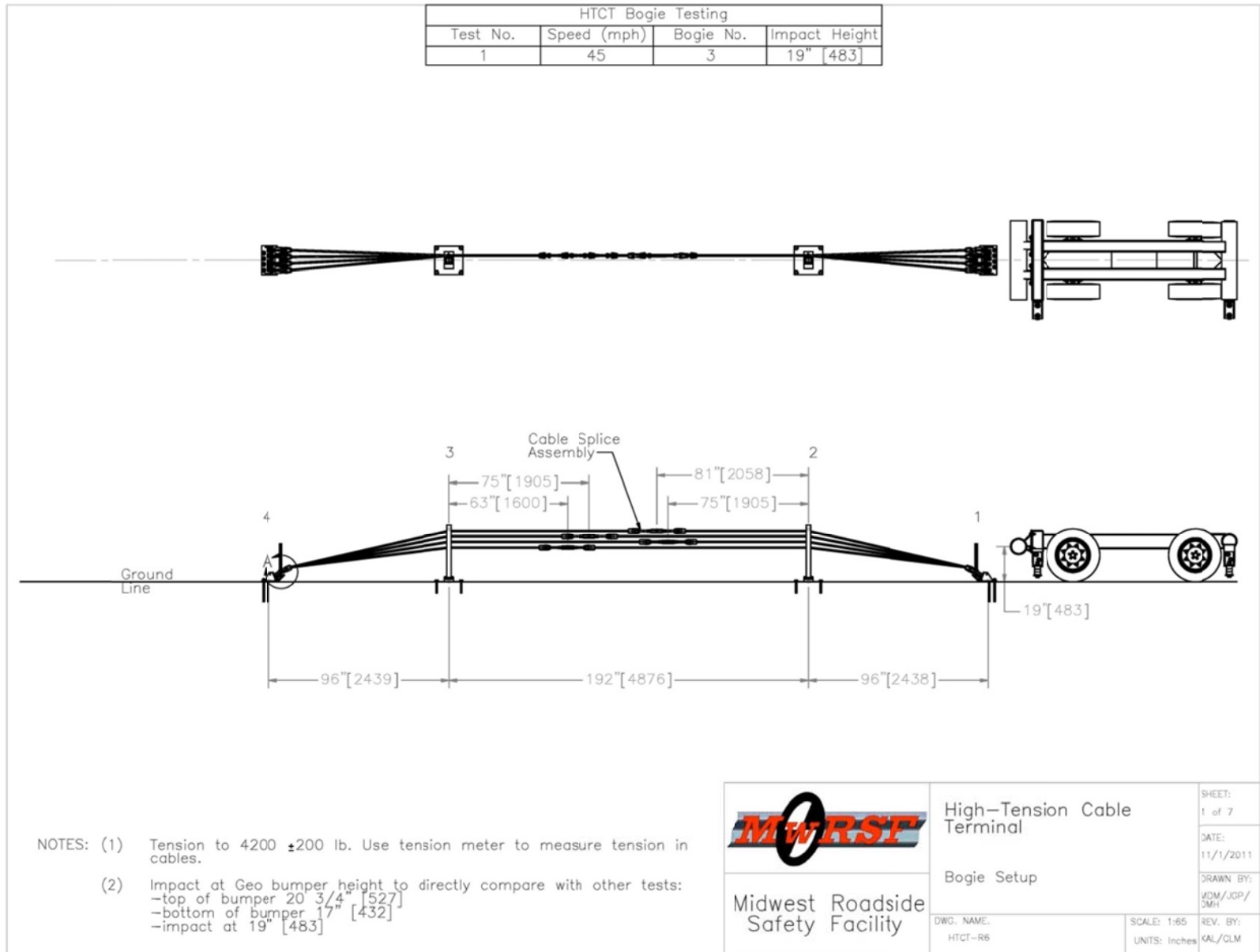


Figure 42. Bogie Test Layout, Test No. HTCT-1

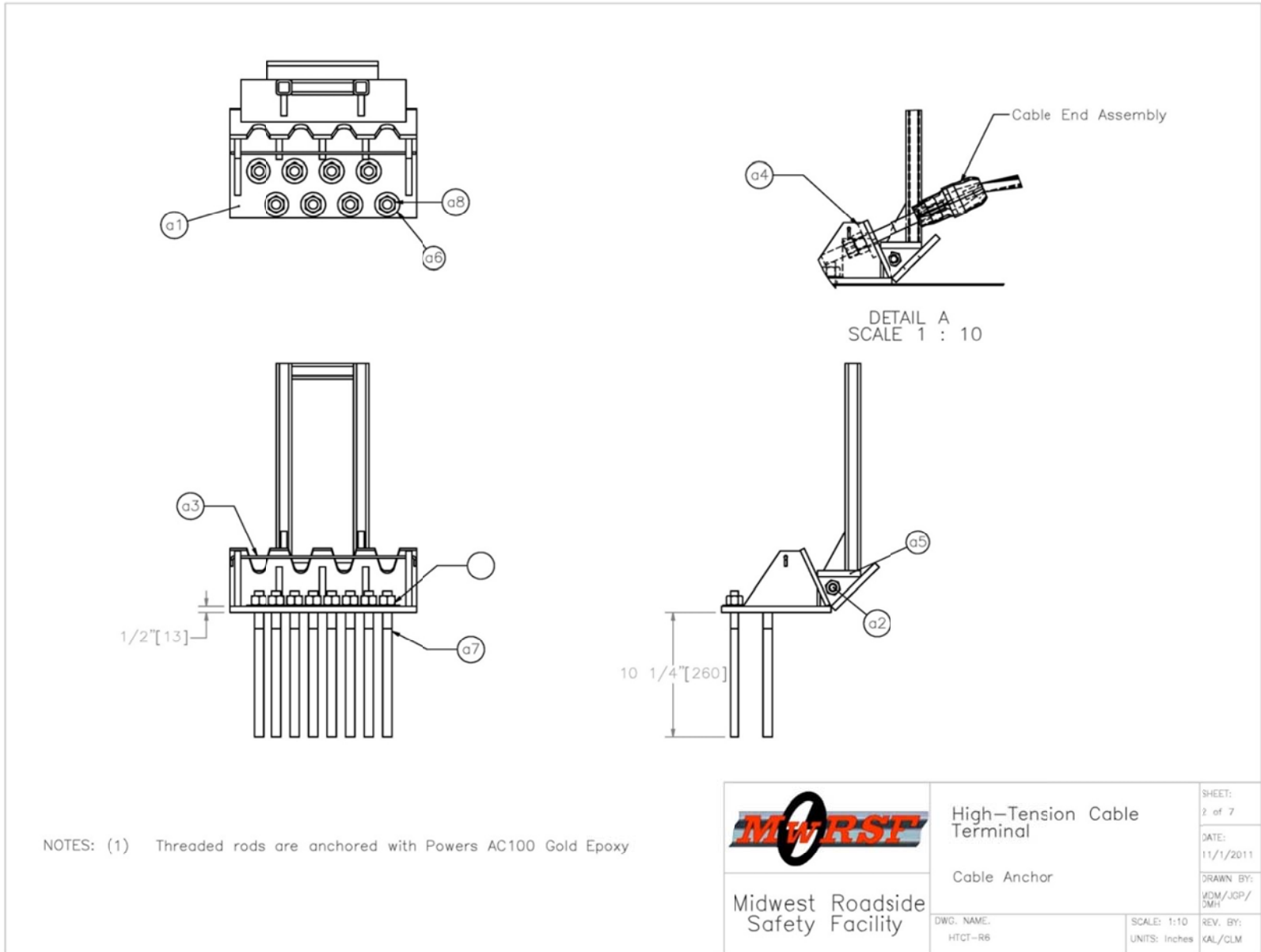


Figure 43. Cable Anchor Bracket Assembly Details, Test No. HTCT-1

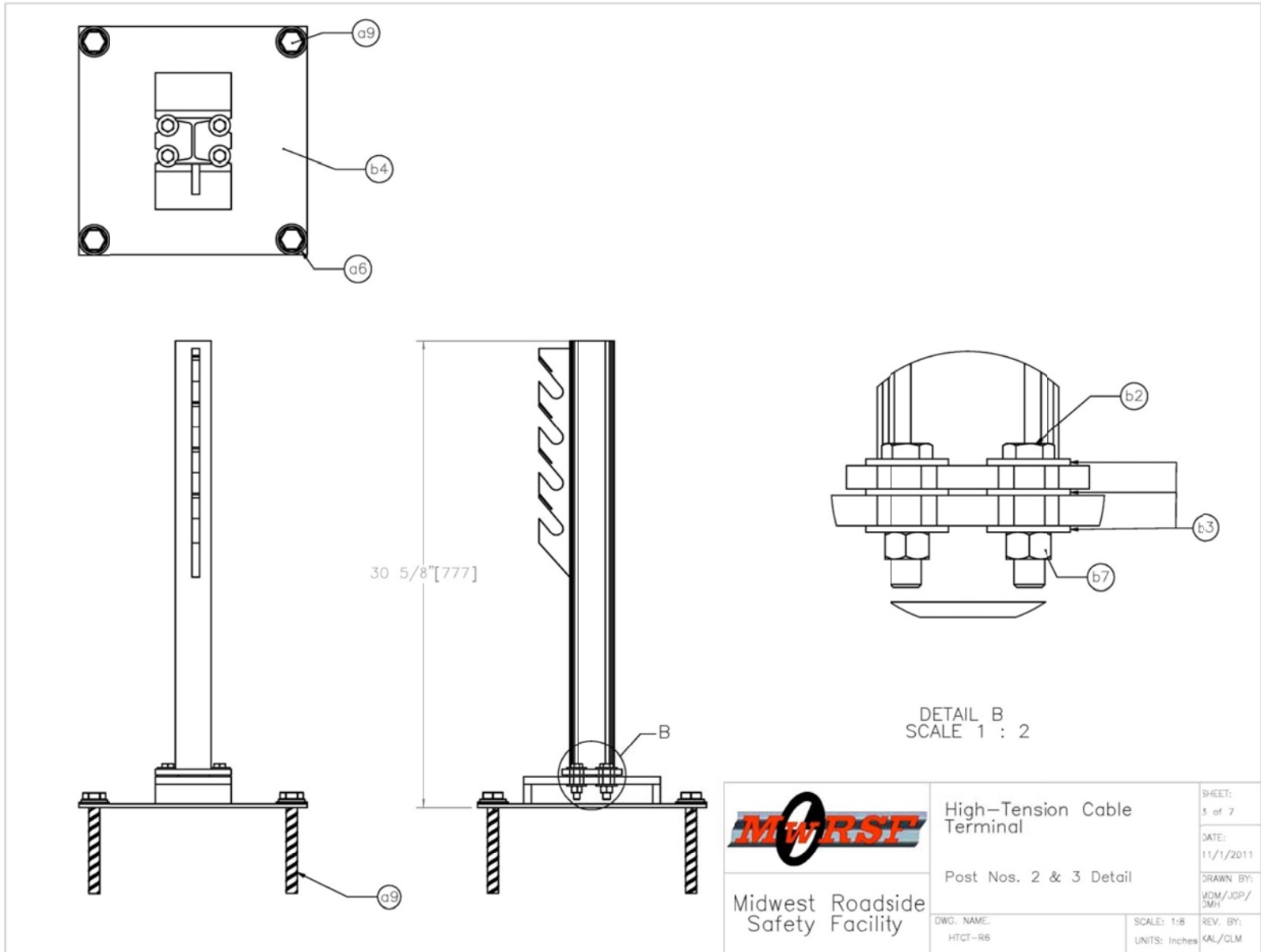


Figure 44. Slip Base Post Assembly Details, Test No. HTCT-1



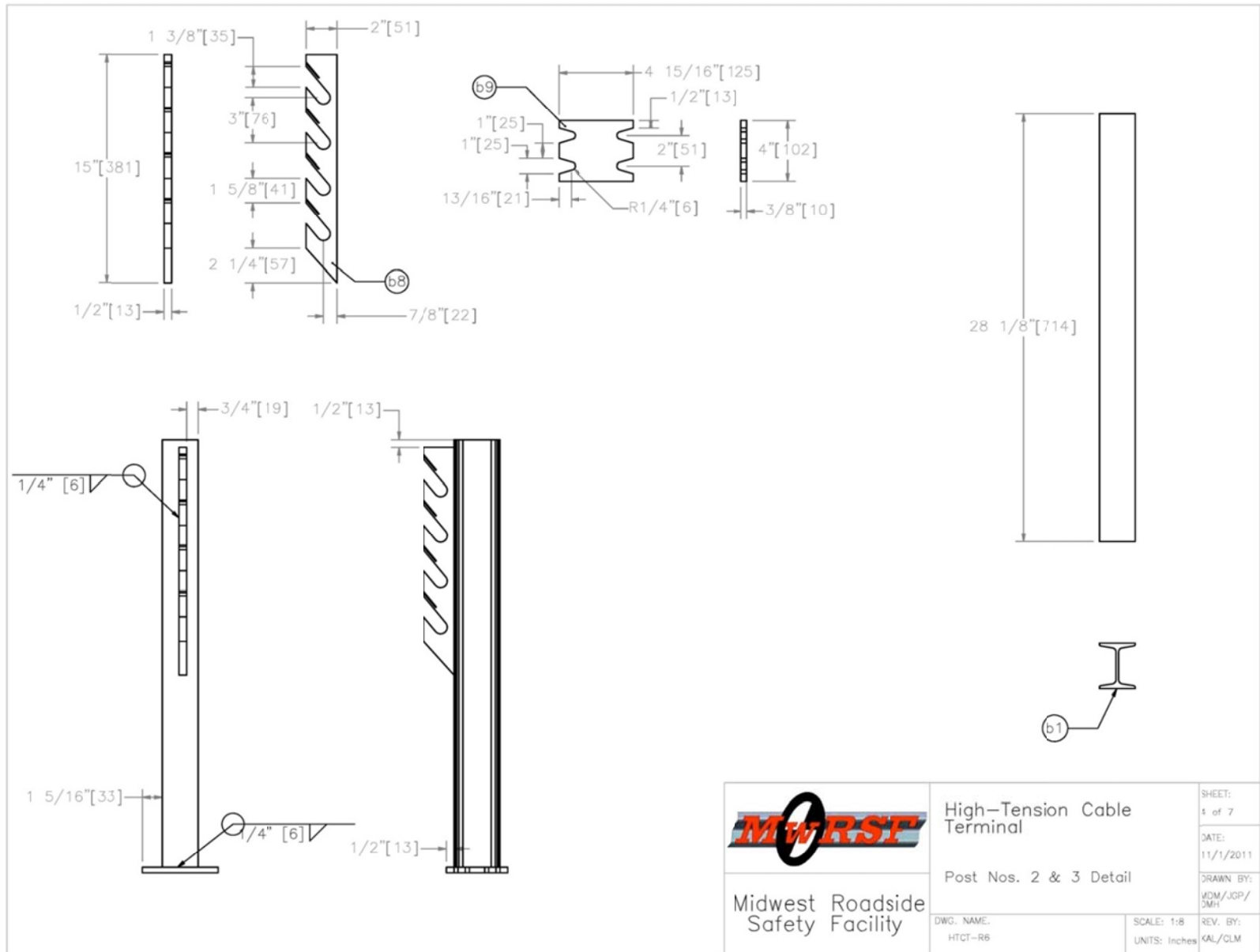


Figure 45. Slip Base Post Component Details, Test No. HTCT-1



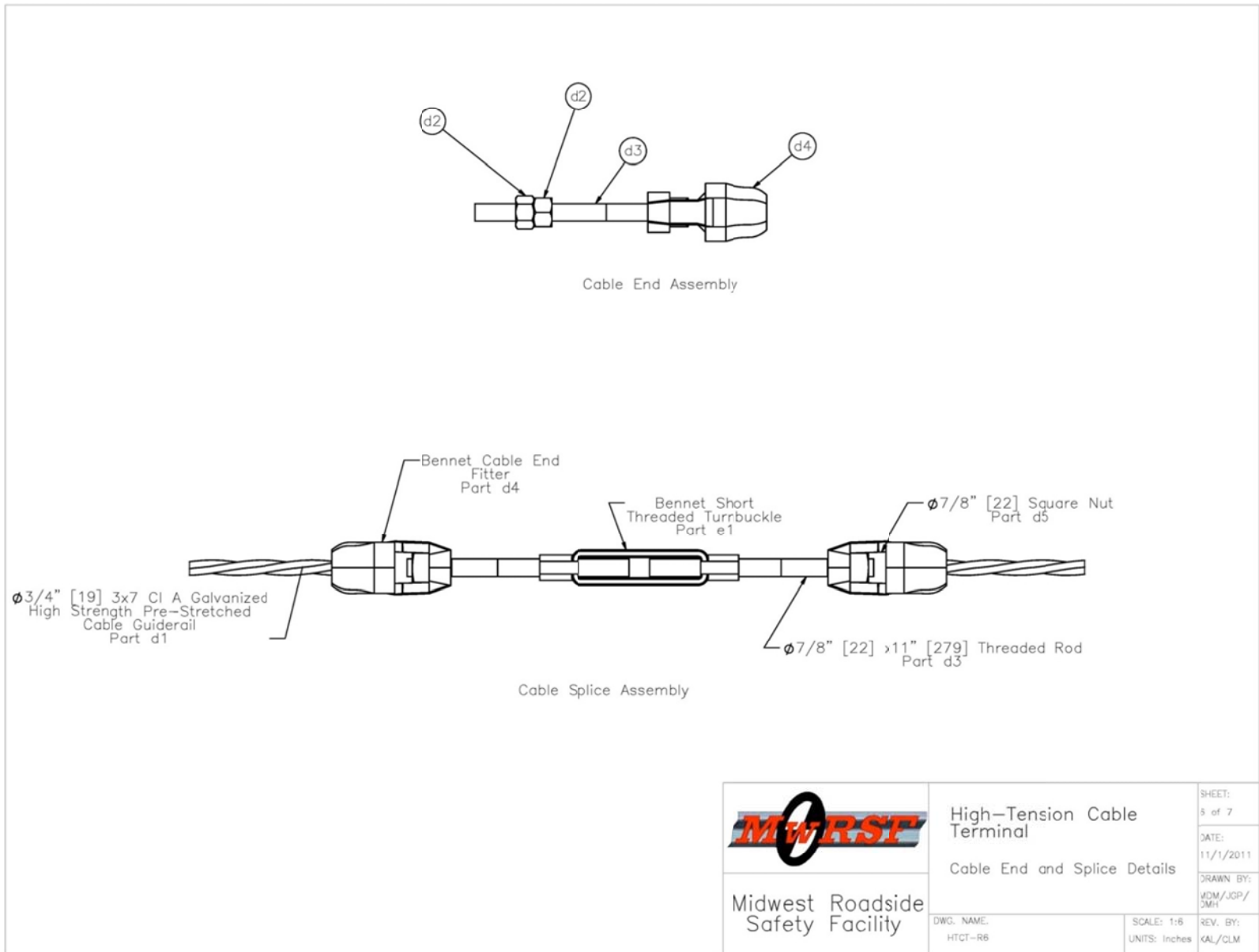


Figure 47. Cable End Fitters and Turnbuckle Details, Test No. HTCT-1

Item No.	QTY.	Description	Material Specifications	Hardware Guide
a1	2	Cable Anchor	ASTM A36	–
a2	2	Ø5/8" x 9 1/2" Long Hex Bolt and Nut	A307 & A563M	FBX16a
a3	2	Ø3/16" Brass Keeper Rod, 14" long	Brass Alloy 260	–
a4	8	CMB High Tension Anchor Plate Washer	ASTM A36	–
a5	2	Kicker Plate	ASTM A36	–
a6	24	Ø3/4" Flat Washer	Grade 2	FWC20a
a7	16	Ø3/4" dia. by 12" Long Threaded Rod	ASTM A193 Grade B7	–
a8	16	Ø3/4" Hex Nut	Grade 8	–
a9	8	3/4" Dia. by 6" Long Wedge-Bolt Anchor	Galvanized, Carbon Steel	–
b1	2	S3x5.7 Post – 28 1/8" Long	ASTM A572 GR50-07	–
b2	8	Ø1/2" x 2" long Hex Bolt	ASTM A307	FBX14a
b3	24	Ø1/2" Washer	ASTM A307	FWC14a
b4	2	15"x15"x0.25" Base Plate	ASTM A36	–
b5	4	1 1/4"x4 15/16"x1/2" Post Base Side	ASTM A36	–
b6	2	9"x4 15/16"x1/2" Top Base Plate	ASTM A36	–
b7	8	Ø1/2" Hex Nut	ASTM A563M	FBX14a
b8	2	2nd Post Cable Hanger	ASTM A36	–
b9	2	2nd Post Base Plate	ASTM A36	–
d1	4	Ø3/4" Cable	AASHTO M30 Type 1 Class A	–
d2	16	Ø7/8" Hex Nut	ASTM A563M	RCE03
d3	16	Cable End Threaded Rod	ASTM-A449	RCE03
d4	16	Bennet Cable End Fitter	ASTM-A47	RCE03
d5	16	Ø7/8" Square Nut	Grade 5	FNS20
e1	4	Bennet Short Threaded Turnbuckle	Not Specified	–
–	–	Powers AC100 Gold Epoxy	–	–

 Midwest Roadside Safety Facility	High-Tension Cable Terminal	SHEET: 7 of 7
	Bill of Materials	DATE: 11/1/2011
DWG. NAME: HTCT-RB	SCALE: None UNITS: Inches	DRAWN BY: MDM/JGP/ DMH
		REV. BY: KAL/CLM

Figure 48. Bill of Materials, Test No. HTCT-1

The cable anchor bracket consisted of a 9-in. x 15 1/4-in. x 1/2-in. (229-mm x 387-mm x 12.7-mm) thick steel baseplate with a 5-in. x 15 1/4-in. x 3/8-in. (127-mm x 387-mm x 9.5-mm) thick steel cable plate welded at a 65-degree angle. Eight 1-in. (25-mm) diameter holes were drilled into the baseplate in order to anchor the assembly. Four 1 1/8-in. (29-mm) diameter notches were cut into the cable plate in order to secure the cables to the assembly. Two 4 1/2-in. x 6-in. x 1 1/2-in. (114-mm x 152-mm x 38-mm) thick gussets were welded to the baseplate and the cable plate at the edges of the assembly. Three smaller gussets, each measuring 3 3/16-in. x 3 5/16-in. x 1/2-in. (81-mm x 84-mm x 12.7-mm), were welded to the cable plate and base plate at interior locations. On the front of the assembly, two rectangular gussets, measuring 3 1/2-in. x 2 3/8-in. x 1/2-in. (89-mm x 60-mm x 12.7-mm), were welded to the cable plate. A 9-in. x 5-in. x 1/2-in. (229-mm x 127-mm x 12.7-mm) thick support plate was also welded to the front gussets. A 3/4-in. (19.1-mm) diameter hole was cut into each gusset as well as a 1 1/2-in. (38-mm) diameter hole in the support plate to aid in the galvanization process. The gussets and the support plate provided the surface for rotation of the cable release lever.

The cable anchor brackets were secured to the testing surface using eight 3/4-in. (19.1-mm) diameter x 12-in. (305-mm) long ASTM A193 Grade B7 threaded rods with hex nuts and washers. The threaded rods were epoxied 10 1/2-in. (267-mm) into the concrete.

All steel plate used in the cable anchor bracket assembly conformed to ASTM A36 specifications. All steel tubing used in the assembly conformed to ASTM A500 Grade B specifications.

### **6.3.2 Slip Base Post Assemblies**

The slip base post assemblies consisted of two sub-assemblies: (1) top post section and (2) base assembly. The top post section was comprised of a 28 1/8-in. (714-mm) long, S3x5.7

(S76x8.5) steel post that was welded to a 4 15/16-in. x 4-in. x 3/8-in. (125-mm x 102-mm x 9.5-mm) thick steel base plate. A cable hanger was welded to the outer surface of a flange of the S3x5.7 (S76x8.5) post to support the cables. The cable hanger was machined out of a 2-in. x 15-in. x 1/2-in. (51-mm x 381-mm x 12.7-mm) thick steel plate.

The base of the slip base post assembly was comprised of a 15-in. x 15-in. x 1/4-in. (381-mm x 381-mm x 6.4-mm) steel base plate with two 4 15/16-in. x 1 1/4-in. x 1/2-in. (125-mm x 32-mm x 12.7-mm) thick steel plates welded to the top surface. A 4 15/16-in. x 9-in. x 1/2-in. (125-mm x 229-mm x 12.7-mm) thick steel slip base plate was welded to the top of the two plates to provide a support surface for the top post section. The base assembly was secured to the concrete tarmac using four 3/4-in. (19.1-mm) diameter wedge bolt anchors and washers.

The top post section and base section were then assembled using four 1/2-in. (12.7-mm) diameter x 2-in. (51-mm) long ASTM A307 bolts with washers and nuts used to form the slip base connection. All steel used to fabricate the slip base post assembly conformed to ASTM A36 specifications.

### **6.3.3 System Cables**

Four 3/4-in. (19.1-mm) diameter, 3x7 wire rope cables were used in the barrier system. The cables were tightened through the use of cable turnbuckles. The ends of the cable contained threaded rod fittings that terminated in the cable anchor bracket. Each threaded rod was secured in a cable anchor slot with a 3-in. x 2 3/8-in. x 1/2-in. (76-mm x 60-mm x 12.7-mm) thick plate washer and two 3/4-in. (19.1-mm) diameter heavy hex nuts.

## 6.4 Equipment and Instrumentation

A variety of equipment and instrumentation was used to record and collect data.

Equipment and instruments utilized in this testing included:

- Bogie
- Accelerometer
- Pressure Tape Switches
- Digital Photographic Cameras

### 6.4.1 Bogie

A rigid frame bogie was used to impact the system. The bogie impact head was constructed of 8-in. (203-mm) diameter, 1/2-in. (12.7-mm) thick, standard steel pipe, with 3/4-in. (19.1-mm) thick neoprene belting wrapped around the pipe to prevent local damage to the post from the impact. The bogie with the impact head is shown on the guidance track in Figure 49. The weight of the bogie with the addition of the mountable impact head was 1,794 lb (814 kg). The impact head contacted the release lever at 19-in. (483-mm) above the ground. The target speed for the test was 45 mph (72.4 km/h).



Figure 49. Rigid Frame Bogie on Guidance Track

A pickup truck with a reverse cable tow and guide rail system was used to propel and direct the bogie. The bogie was accelerated toward the system along the guidance system, which consisted of a steel pipe anchored above the tarmac. The bogie wheels were aligned for caster and toe-in values of zero so that the bogie would track properly. When the bogie reached the end of the guidance system, it was released from the tow cable, allowing it to be free rolling when it struck the cable release lever. A remote braking system was installed on the bogie to provide for safe deceleration of the bogie after the test.

#### **6.4.2 Accelerometer**

One tri-axial, piezo-resistive, accelerometer system Model EDR-3 with a range of  $\pm 200$  g's was developed by Instrumented Sensor Technology (IST) of Okemos, Michigan and was mounted on the frame on the bogie near its center of gravity. Data sampling was at 3,200 Hz with a 1,120 Hz Butterworth low-pass filter with a -3 dB cut-off. Computer software, "DynaMax 1 3/4" and a customized "Microsoft Excel" worksheet were used to analyze and plot the accelerometer data [21].

#### **6.4.3 Pressure Tape Switches**

Four pressure tape switches, spaced at 3-ft (0.9-m) intervals and placed near the end of the bogie track, were used to determine the speed of the bogie before the impact. As the right-front tire of the bogie passed over each tape switch, a strobe light was fired sending an electronic timing signal to the data acquisition system. Test speeds were determined by dividing the measured distance between the switches by the time between the electronic signals.

#### **6.4.4 Digital Cameras**

Three high-speed AOS XPRI digital video cameras, each with operating speeds of 500 frames/sec, were used to film the bogie test. Three JVC digital video cameras, each with an



operating speed of 29.97 frames/sec, were also used to film the bogie test. Camera locations and camera lens information is shown in Table 8.

Table 8. Camera Locations, Speeds, and Lens Settings

	Camera No.	Type	Operating Speed (frames/sec)	Lens/Setting	Location/Distance
High-Speed Video	5	Vitcam X-PRI	500	Fujinon 50 mm Fixed	70 in. Away, Perpendicular to Upstream Anchor, and 35 in. Downstream
	6	Vitcam X-PRI	500	Canon 17-102 / 102	237 in. Away, Perpendicular to Upstream Anchor
	7	Vitcam X-PRI	500	Nikon 50 mm Fixed	344 in. Away, Perpendicular to First Slip Base Post
Digital Video	2	JVC - GZ - MG27u (Everio)	29.97	-	567 in. Away, Perpendicular with the Center of the System
	3	JVC - GZ - MG27u (Everio)	29.97	-	344 in. Away, Perpendicular to First Slip Base Post
	4	JVC - GZ - MG27u (Everio)	29.97	-	344 in. Away, Perpendicular to First Slip Base Post

## 6.5 Data Processing

The electronic accelerometer data obtained in dynamic testing was filtered using the SAE Class 60 Butterworth filter conforming to the SAE J211/1 specifications [22]. The pertinent acceleration signal was extracted from the bulk of the data signals. The processed acceleration data was then multiplied by the mass of the bogie to get the impact force using Newton's Second Law. Next, the acceleration trace was integrated to find the change in velocity versus time. Initial velocity of the bogie, calculated from the pressure tape switch data, was then used to determine the bogie velocity, and the calculated velocity trace was integrated to find the bogie's displacement. Combining the previous results, a force vs. deflection curve was plotted for each test. Finally, integration of the force vs. deflection curve provided the energy vs. deflection curve for each test.

## **7 BOGIE TESTING – TEST NO. HTCT-1**

### **7.1 Procedures**

From the bogie test, information was desired to analyze the mechanics and structural adequacy of the cable anchor bracket assembly. Characterization of the bogie deceleration and force loading on the cable anchor bracket and lever arm was also of utmost importance in the test.

Although the acceleration data was applied from the bogie impact location, the data came from the center of gravity of the bogie. Error was added to the data since the bogie was not perfectly rigid and sustained vibrations. The bogie may have also rotated during impact, causing differences in accelerations between the bogie center of mass and the bogie impact head. While these issues may affect the data, the data was deemed sufficiently valid. Filtering procedures were applied to the data to smooth out vibrations, and the rotations of the bogie during test were minor.

The accelerometer data for the bogie test was processed in order to obtain acceleration, velocity, and deflection curves. The values described herein were calculated from the EDR-3 data curves.

### **7.2 Test Description, Test No. HTCT-1**

Test no. HTCT-1 was performed at 0 degrees and 44.9 mph (72.3 km/h) with the bogie impact head centered on the cable release lever. A sequential description of the impact events is contained in Table 9. During the test, the guide bracket and roller bearing on the bogie snagged on a concrete edge after exiting the test setup, and the bogie came to a rest roughly 43 ft (13.1 m) downstream from the downstream anchor bracket. Time-sequential documentary photographs of the test are shown in Figures 50 and 51.

Table 9. Sequential Description of Impact Events, Test No. HTCT-1

TIME (sec)	EVENT
0.000	The cable release lever began to rotate backwards, forcing the cable end fitters up and out of their respective slots on the cable anchor bracket.
0.006	Slip base post no. 1 began to deflect upstream due to the stretching of the cables from the prying action of the release lever.
0.018	Cables have been fully released from their respective slots.
0.040	The system cables began to coil on the front of the bogie's impact head.
0.116	The bogie impacted slip base post no. 1.
0.118	Baseplate of slip base post no. 1 began to buckle as the slip connection did not immediately activate.
0.124	The welds between the top S3x5.7 post section and the slip plate broke causing the post to fail prior to activation of the slip base mechanism.
0.200	The bogie head impacted the cable turnbuckle from the second highest mounted cable.
0.370	The bogie impacted the second slip base post.
0.380	The welds between the top S3x5.7 post section and the slip plate on the second slip base post assembly broke prior to activation of the slip base mechanism, at roughly this time.
0.510	Bogie impacted the downstream cable release lever.
0.530	The left-front tire of the bogie impacted the downstream cable anchor bracket, causing the bogie to roll.
0.770	The bogie exited the field of view.

### 7.3 System Damage

The damage to system components in test no. HTCT-1 was moderate. Both of the slip base post assembly bases buckled under impact loading, and the top S3x5.7 (S76x8.5) post sections fractured off of the lower assembly due to weld failure in both cases. The detached S3x5.7 (S76x8.5) post sections exhibited some plastic bending in the impact region.



0.000 sec



0.006 sec



0.014 sec



0.018 sec



0.024 sec



0.000 sec



0.018 sec



0.046 sec



0.116 sec



0.130 sec

Figure 50. Sequential Photographs, Test No. HTCT-1

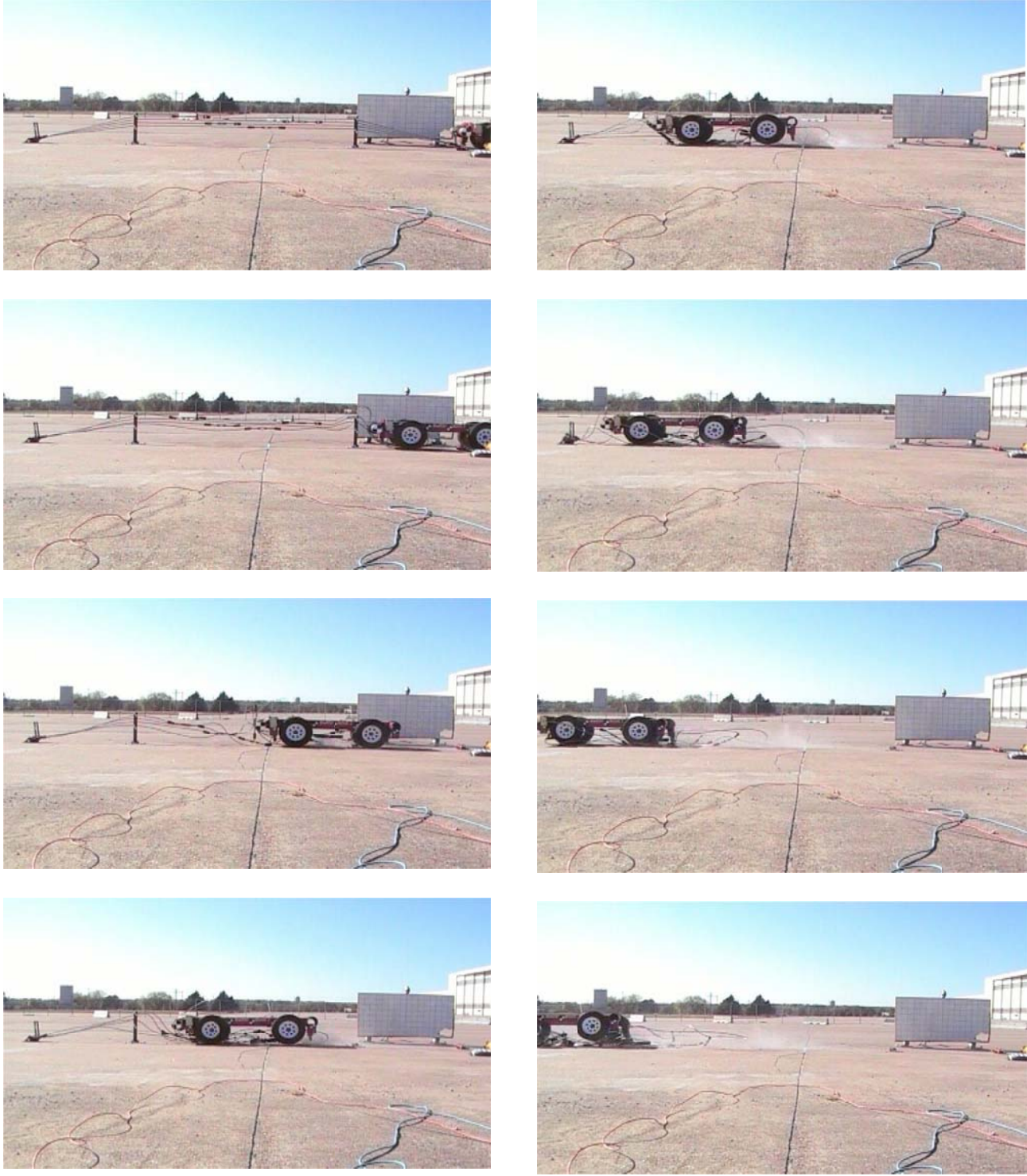


Figure 51. Documentary Photographs, Test No. HTCT-1

The upper edges of the cable slots on the upstream cable anchor bracket assembly showed some plastic bending as the cables were forced out of the slots. Other components of the cable anchor bracket assembly were undamaged. There was some contact and/or gouging on the base plate of the upstream cable release lever due to highly concentrated contact forces with the cable end fitters. However, there was no plastic bending in the base plate or the vertical impact tubes. Damage photos are shown in Figures 52 through 58.

Force, velocity, and energy dissipation curves for the bogie test were created from accelerometer data and are shown in Figures 59, 60, and 61, respectively. Also, standard MwRSF bogie test documentation sheets can be found in Appendix C.

The maximum force during the test was due to the bogie impacting the two slip base posts. Peak force levels of 14.6 kips (65.0 kN) at 120 ms and 15.3 kips (68.1 kN) at 387 ms were experienced for the first and second slip base posts, respectively. Recall that in both cases, the slip base mechanism did not activate but rather the assembly failed due to weld fracture at the base of the upper post section and the support plate buckling. Had the slip base post functioned as designed it could be expected that the force levels would be lower.

The peak force for the bogie impact with the upstream cable anchor assembly was 5.0 kips (22.2 kN) which occurred at approximately 5 ms. Although the peak force was significant, the duration of the impact event was relatively short, which resulted in only 21.8 kip-in. (2.5 kN-m) of energy being dissipated. The energy loss equates to a 0.3 mph (0.5 km/h) decrease in bogie velocity. The bogie impacts with the slip base posts absorbed an average of 43 kip-in. (4.9 kN-m) per impact. The impacts resulted in an average speed loss of 0.7 mph (1.1 km/h) per impact.

At approximately 270 ms after impact, the bogie head impacted one of the cable turnbuckles. This impact resulted in a 6.5-kip (28.9-kN) force on the bogie. At approximately

520 ms, the bogie head impacted the downstream cable release lever. The peak force from impact was 3.2 kips (14.2 kN), or 32 percent less than that of the impact with the upstream anchor.

One reason for the significantly reduced peak impact force on the downstream cable anchor assembly was that the cable tension had been reduced to 0 after the release of the cables from the upstream anchor. The majority of the resistive force from impact with the cable anchor bracket assemblies comes from the prying action of the cables from the slots. In order to release the cables from the slots, the release lever must overcome the force of friction caused by the cable tension on the cable plate. Since the cables had been released, there was no friction force to overcome, thus resulting in a lower resistive force.

The bogie's left-front wheel impacted the downstream cable anchor bracket at approximately 573 ms. The impact resulted in a peak force of 9.2 kip (40.9 kN). After the bogie impact with the downstream cable anchor bracket, the bogie continued out of the system before coming to a stop downstream of the test setup.



Figure 52. System Damage, Test No. HTCT-1





Upstream Cable Anchor Bracket Assembly – Pre-Test



Upstream Cable Anchor Bracket Assembly – Post-Test

Figure 53. System Damage, Test No. HTCT-1



Upstream Slip Base Post Assembly



Upstream Slip Base Post Assembly



Upstream Slip Base Post Assembly

Figure 54. System Damage, Test No. HTCT-1



Upstream Slip Base Post Assembly



Upstream Slip Base Post Assembly

Figure 55. System Damage, Test No. HTCT-1



Downstream Slip Base Post Assembly



Downstream Slip Base Post Assembly

Figure 56. System Damage, Test No. HTCT-1



Downstream Slip Base Post Assembly



Downstream Slip Base Post Assembly

Figure 57. System Damage, Test No. HTCT-1



Downstream Cable Anchor Bracket Assembly – Pre-Test



Downstream Cable Anchor Bracket Assembly – Post-Test

Figure 58. System Damage, Test No. HTCT-1

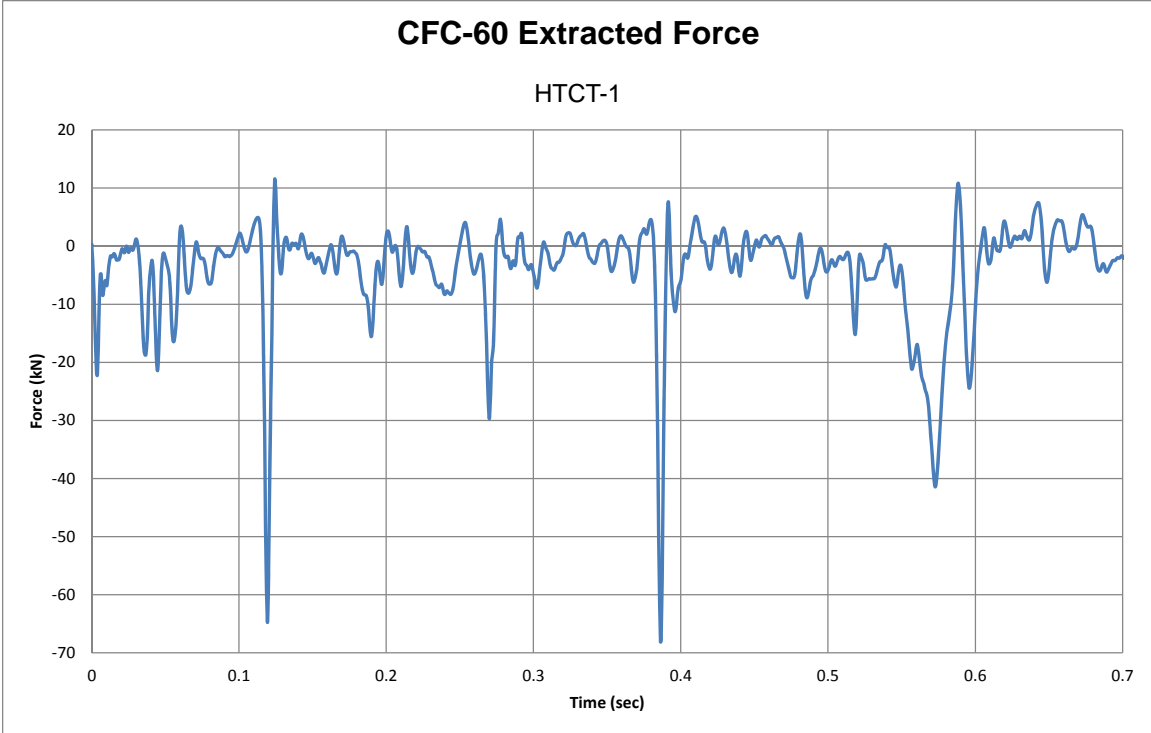


Figure 59. Force vs. Time, Test No. HTCT-1

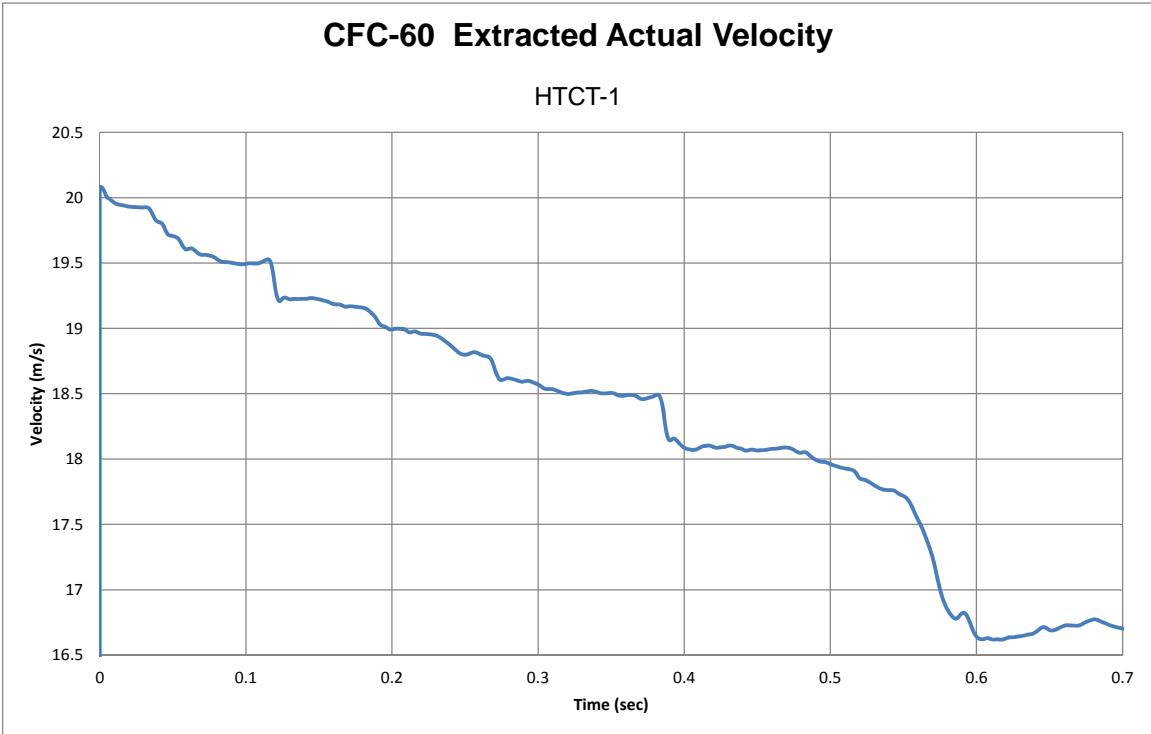


Figure 60. Longitudinal Velocity vs. Time, Test No. HTCT-1

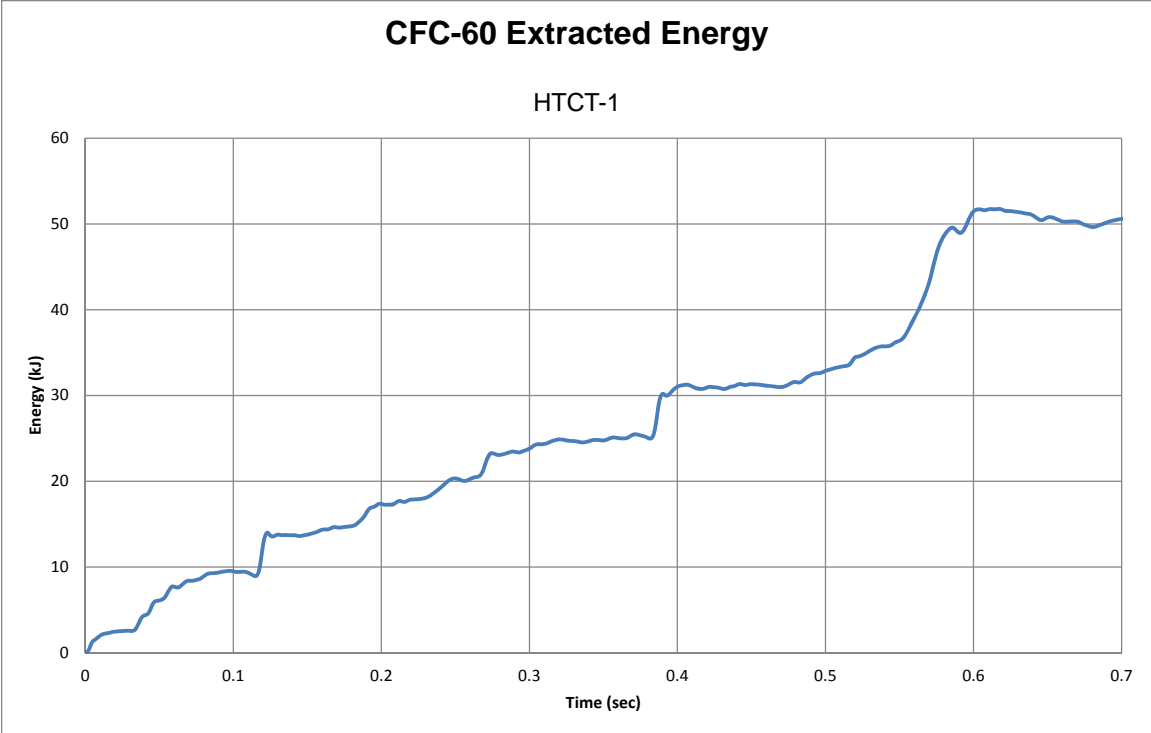


Figure 61. Energy vs. Time, Test No. HTCT-1



## **8 SIMULATION MODEL EVALUATION**

### **8.1 Introduction**

The results from the cable end terminal simulation and the associated physical bogie testing were compared to determine the effectiveness and accuracy of the simulation model. If the model showed good initial agreement with the physical testing, alternate high-tension, cable anchor bracket designs could be modeled and evaluated with confidence.

The main criteria used to evaluate the end terminal model were:

- mechanics of the cable release process;
- impact times of major system components;
- accelerometer data; and
- component damage.

### **8.2 High-Speed Video Comparison**

High-speed video from test no. HTCT-1 was used to incrementally compare the release mechanics of the cables from the cable anchor bracket to the mechanics observed in the simulation model. A sequential comparison of the cable release event is shown in Figure 62. The cables showed smooth release without snag in both the simulation as well as the physical test. The cables fully released from the cable anchor bracket at roughly 18 ms as compared to 20 ms in the physical test. The error in release times could partially be attributed to frame rate limitations in physical testing. The frame rate on the actual high-speed cameras was 500 frames/sec. While this limitation is likely not the sole cause of the error, it could have contributed to the difference in release time.

The timing of the bogie impact with the slip base post correlated well between the simulation and the physical test. The bogie in the simulation impacted the slip base post at 111

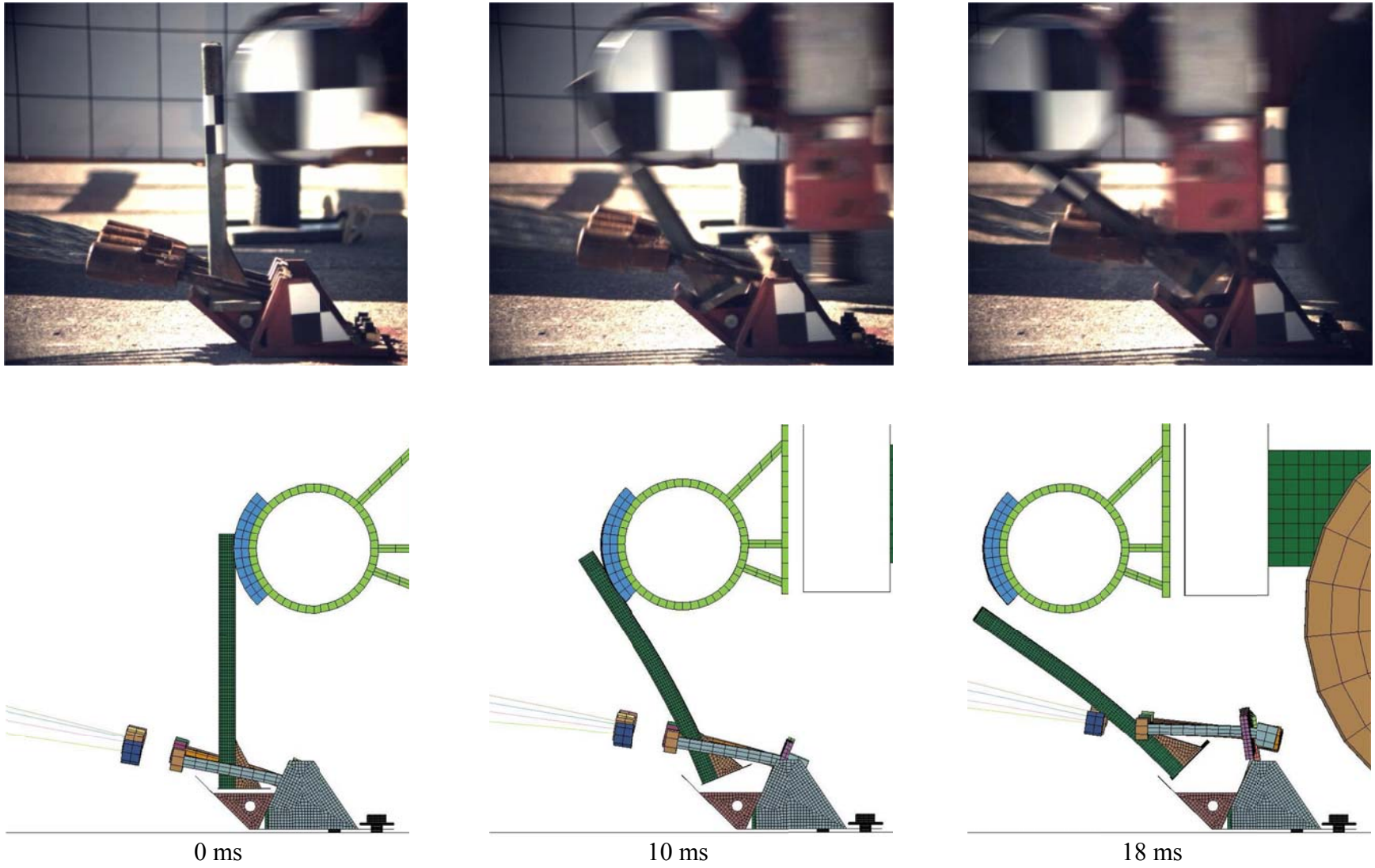


Figure 62. Cable Release Event Comparison, Test No. HTCT-1 vs. Simulation

ms. The bogie in test no. HTCT-1 impacted the slip base post at 116 ms. The error could again be partially attributed to frame rate limitations with the high-speed cameras or simplifications and assumptions made in the simulation model that led to a divergence from actual component behavior. Differences in cable material properties and interactions with the bogie impact head could have resulted in higher longitudinal changes in bogie velocity ( $\Delta v$ 's) and also contributed to the error. The higher  $\Delta v$ 's would increase the time between the initial impact with the cable lever arm and the impact with the slip base post. A sequential comparison of test no. HTCT-1 and the associated simulation is shown in Figure 63.

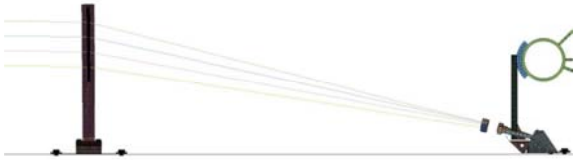
### **8.3 Accelerometer Data Comparison**

Bogie velocity was also used to evaluate the accuracy of the simulation model. Accelerometer data captured during the actual and simulated bogie tests was processed in order to calculate and compare bogie velocities. The bogie velocities for the simulation and physical test are shown in Figure 64. The velocity trace is plotted through the impact with the upstream cable anchor assembly. However, it is cut off prior to the bogie's impact with the slip base post. Although similar failure modes were exhibited in both the simulation and the physical testing, the main focus of the comparison is the modeling of the cable anchor bracket and its release mechanics.

The velocity data agreed well between the physical bogie test and the simulation. The average error in velocity between the physical test and numerical simulation was 0.79 percent. After the anchor bracket impact, the bogie velocity in both the simulation and physical test stabilized for a short time before small impacts with the system cables and other detached anchor bracket components. These secondary impacts caused small velocity reductions at roughly 35 ms after initial impact. The stabilized velocity in test no. HTCT-1 after impact with the cable anchor



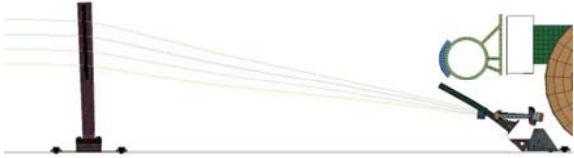
0.000 sec



0.000 sec



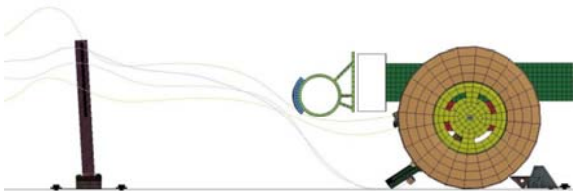
0.020 sec



0.020 sec



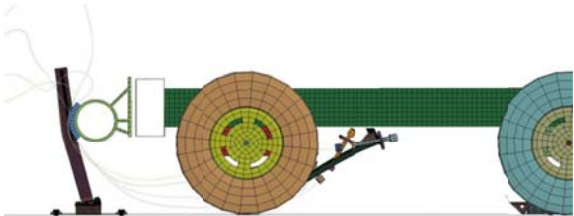
0.058 sec



0.058



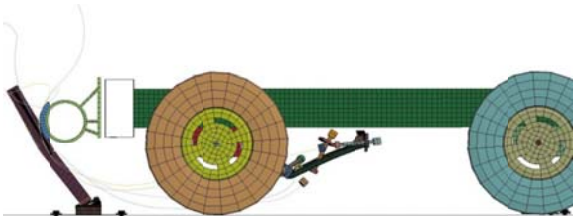
0.116 sec



0.116 sec



0.124 sec



0.124 sec

Figure 63. Sequential Comparison, Test No. HTCT-1 vs. Simulation

bracket was 44.6 mph (71.8 km/h), compared with 44.3 mph (71.3 km/h) observed in the simulation. The resulting error in the  $\Delta v$  from the impact was 0.7 percent.

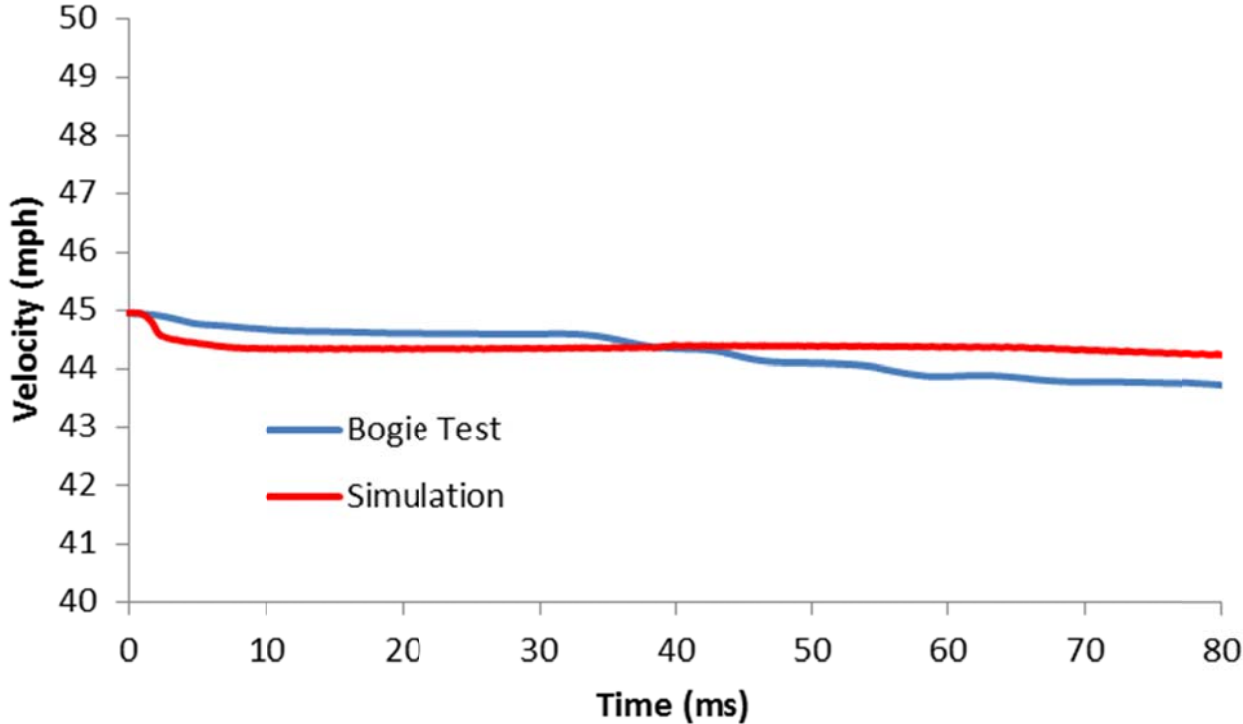


Figure 64. Bogie Velocity Comparison, Test No. HTCT-1 vs. Simulation

### 8.4 Component Damage Comparison

There was relatively little component damage to the cable anchor bracket assembly in both the physical testing and the simulation. The only permanent deformation to the assembly was plastic bending in the cable plate. The S3x5.7 (S76x8.5) post section on the first slip base post assembly sustained some plastic deformation in the impact region during the physical test and the simulation. A comparison of the damage is shown in Figures 65 and 66. Although the cable release lever did not sustain any damage, it was pulled downstream with the bogie after several of the system cables wrapped around the assembly’s crossbar. This behavior occurred in both the simulation and the physical test, as shown in Figure 67. Although the dynamics and

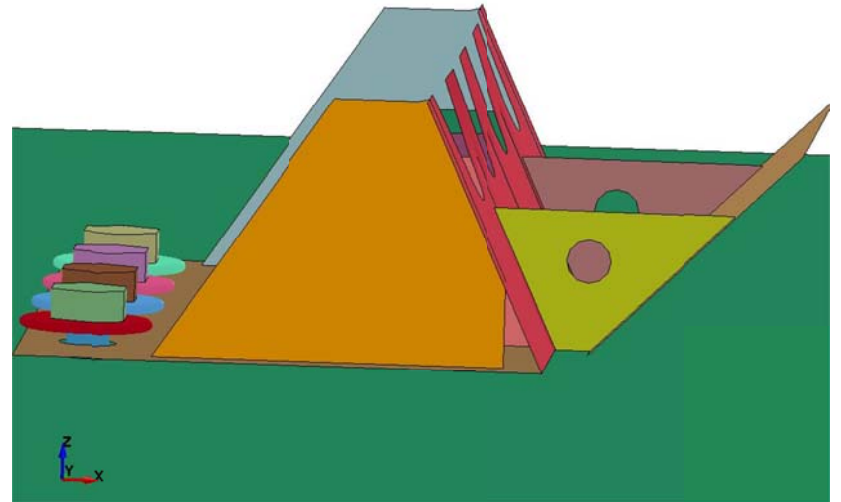
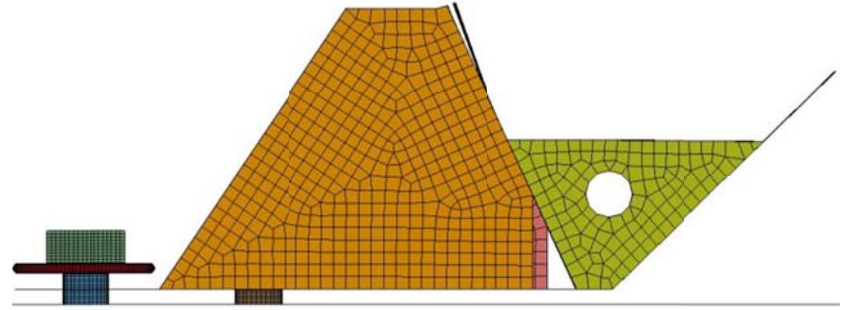


Figure 65. Upstream Cable Anchor Damage Comparison, Test No. HTCT-1 vs. Simulation



Figure 66. S3x5.7 (S76x8.5) Post Damage Comparison, Test No. HTCT-1 vs. Simulation

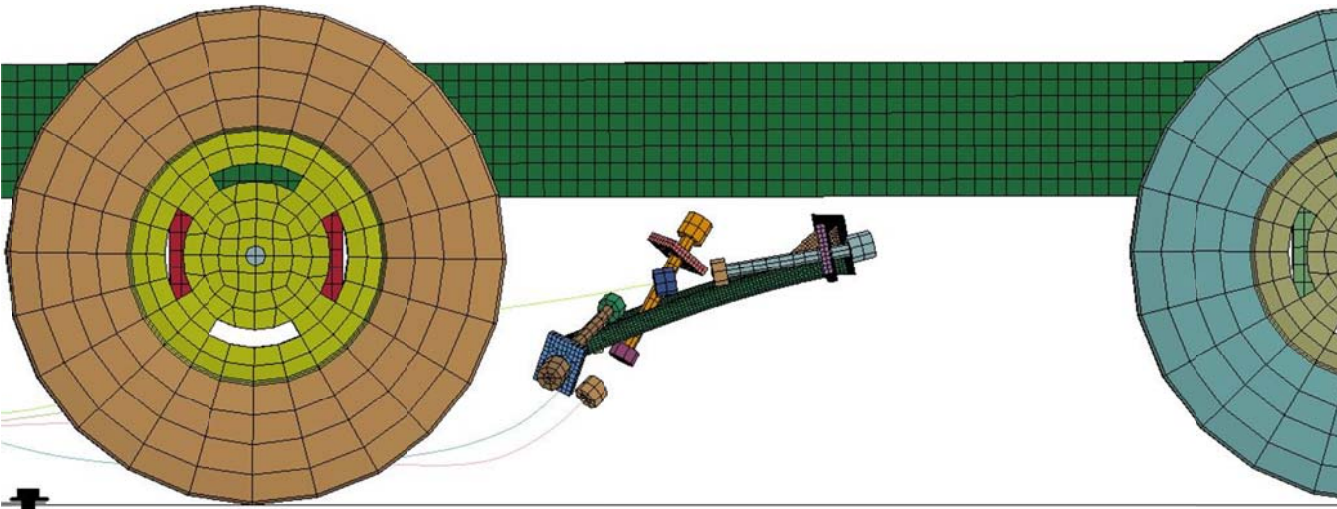


Figure 67. Release Lever Interaction with System Cables, Test No. HTCT-1 vs. Simulation



trajectory of the lever do not match exactly between the simulation and physical test, the fact that the cables wrapped around the crossbar in both events further support that the cable release event is being simulated accurately.

## **8.5 Discussion and Conclusions**

Data from the simulation of the high-tension, cable anchor bracket and abbreviated end terminal model was compared with physical data from component testing. The timing of the cable release mechanism correlated well between the physical test and simulation. The cable release times and the bogie impact times with the slip base post in the physical test and the simulation were within 2 ms and 6 ms of each other, respectively. The velocity data obtained from the physical test and the simulation also compared well with less than 1 percent error in the bogie's  $\Delta v$  after impact with the cable anchor bracket assembly.

The discrepancy between the impact times can partially be attributed to differences in system cable dynamics and trajectory as they impacted the bogie head. The cables appeared to coil more on the bogie head during the physical test, which would have resulted in a greater  $\Delta v$ . Frame rate limitations with the high-speed cameras used in the bogie test could have also introduced some uncertainty with exact event times.

There was very little component damage to the cable anchor bracket during test no. HTCT-1. Damage that did occur to the anchor bracket was concentrated in the cable plate. The deformation to the cable plate on the anchor bracket was replicated well during the simulation. No other permanent deformation to the anchor bracket or its components occurred during the bogie test.

In both the simulation and the physical test, the system cables wrapped around the cable release lever and pulled it downstream. The trajectory and dynamics of the release lever were not

replicated very accurately. The trajectory, however, is highly dependent on the lever's interaction with the system cables, among other things. The cable model is sufficiently accurate for its intended use in simulations. However, there are differences and simplifications used to model the cables that would unrealistically effect its interaction with other system components. Small differences in mass distribution over the cable lever could also have large effects on the dynamics and trajectory of the assembly.

With the agreement between the results of the simulation and the subsequent test no. HTCT-1, the simulation model can be used with confidence. Moving forward, alternate anchor bracket designs and modifications can be first evaluated using the model.

Although simulation is a powerful tool, it cannot be used to definitively evaluate designs. Physical testing is still the most important aspect of the design process. The model is, however, sufficiently accurate to identify potential problems with prospective high-tension, cable anchor bracket designs. Once the most promising design candidates have been identified, they can then be further evaluated with component and full-scale testing to definitively assess their effectiveness.

## **9 REDESIGN OF THE HIGH-TENSION, CABLE ANCHOR BRACKET ASSEMBLY**

### **9.1 Introduction**

The current, high-tension, cable anchor bracket assembly design was modeled to function much like the previously-tested, low-tension, cable anchor bracket assembly. Unlike the low-tension, cable anchor bracket assembly, the high-tension design has not been fully evaluated in full-scale crash testing. Since the designs are similar, however, it can be expected that the high-tension, cable anchor bracket assembly will perform comparably to the low-tension design in many aspects. As such, any issues that were exposed during full-scale testing of the low-tension, cable anchor bracket assembly will also likely be evident with the high-tension design.

With this in mind, a redesign of the high-tension, cable anchor bracket assembly was necessary to ensure that future testing would not be subject to the same issues as its low-tension counterpart. Alternative designs for the high-tension, cable anchor bracket assembly were modeled and evaluated. The finite element code LS-DYNA was the primary evaluation tool utilized in the design process.

Simulation results with the current design showed good initial agreement. Therefore, it is reasonable to assume that modeling alternative designs can be used as a good initial evaluation of potential designs. Data obtained from test no. HTCT-1 was also used to support alternative design components and features. Design methodology, criteria, and results are summarized in the ensuing chapter.

### **9.2 Design Issues**

The first step in the redesign of the high-tension, cable anchor bracket assembly was to identify areas for improvement from the previous design as well as the current design. The new design should not pose any additional concerns. Data from previous testing as well as simulation

results were used to detect issues and concerns with the low-tension, cable anchor bracket assembly and the current, high-tension, cable anchor bracket assembly design.

It is important to remember that there are several desirable features of the low-tension, cable anchor bracket assembly. Primarily, it performed well in full-scale crash testing as it smoothly released the system cables upon vehicle impact with the cable release lever. The anchor bracket assembly also successfully anchored the system cables during system strength tests. The high-tension design has been used with tangent system tests and has proved to be structurally adequate [23]. The current cable anchor bracket assembly demonstrated positive structural performance during full-scale crash testing beyond the length-of-need as part of several research and development programs. Thus, the structural features of the cable anchor bracket assembly were kept intact with only minimal changes to component geometry.

### **9.2.1 Cable Release Lever**

Based on crash testing performance, the low-tension, cable end terminal was approved for roadside implementation. The vehicle trajectory and interaction with the system resulted in high roll and yaw angles and caused some concern over vehicle stability. The cable anchor assembly contributed to the exhibited trajectory as the cable release lever impacted the underside of the vehicle and wedged into the ground. The impact resulted in increased vehicle decelerations and a yaw and roll force being applied to the right side of the vehicle. To eliminate any secondary impacts, the cable release lever must not be pulled downstream by the system cables. This change would eliminate any unintended, secondary impacts between the cable release lever and the vehicle, thereby reducing the magnitude of yaw and roll exhibited by the impacting vehicle.

To protect against the cable release lever being pulled downstream, it could be secured to the cable anchor bracket assembly with a rotational joint. There would still be potential for the cable release lever to be pulled downstream, however, since previous testing showed that the cables consistently wrapped around the lever's cross arm. This behavior resulted in the cable release lever being pulled downstream as the cables retracted from the downstream tension. Therefore, the cross arm of the cable release lever was eliminated.

The cross arm was a precautionary component in the original design to ensure a distributed load was applied to the release lever base plate in order to allow for a smooth, even rotation and release of the cables. In previous testing, however, there was never any indication that the cross arm was necessary for the successful release of the cables. Based on these observations, it is assumed that the elimination of the cross arm will have little to no effect on the release mechanics or overall performance of the cable anchor bracket assembly.

### **9.2.2 Cable Release Lever Rotation Point**

Another issue that was identified in the simulation of the current, high-tension, cable anchor design was that the release of the cables occurred over a period of 18 ms, while the release of the cables in the low-tension design took only 8 ms. Both designs successfully released the cables; however, a longer release time may result in greater decelerations and increased yaw imparted to the vehicle. While vehicle yaw alone is not a concern, minimizing it is preferred to obtain a stable vehicle trajectory.

The increased release time is partially due to a higher friction force that must be overcome during the rotation of the cable release lever assembly. The higher friction force results from the increased cable tension and the additional system cable. A free body diagram of the forces involved in the release of the cables is shown in Figure 68.

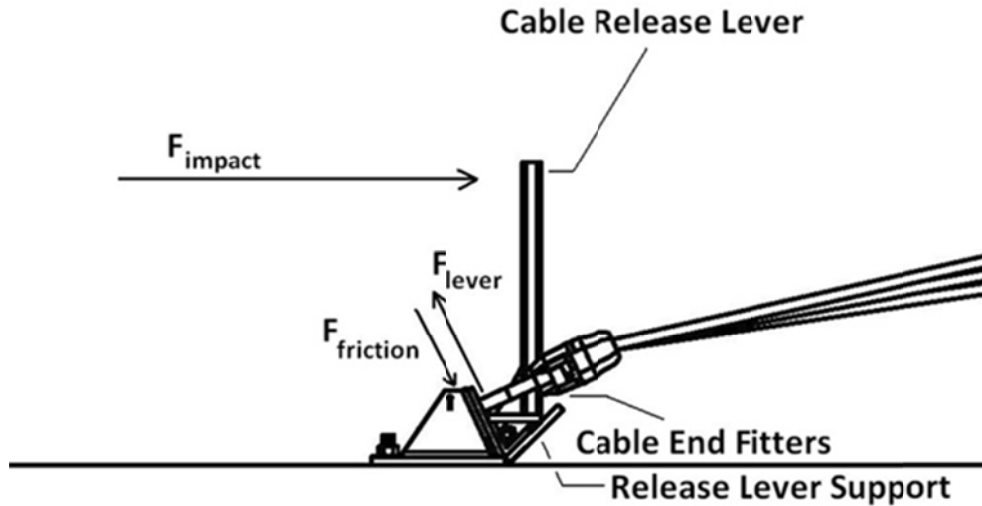


Figure 68. Simplified Free Body Diagram of Cable Release Lever During Cable Release

In order for the cable release lever to begin to rotate, the lever force,  $F_{\text{lever}}$ , must be greater than the friction force due to the contact between the plate washers on the cable end fitters and the cable plate. The lever force is generated as a result of a moment force applied by the impacting vehicle,  $F_{\text{impact}}$ , and the corresponding upward prying action. The friction force between one of the washers and the cable plate can be calculated using Equation 1.

$$F_{\text{friction}} = F_{\text{normal}} \cdot \mu_{\text{static-dynamic}} \quad (\text{Eq. 1})$$

where

$$F_{\text{friction}} = \text{Friction Force}$$

$$F_{\text{normal}} = \text{Normal Force}$$

$$\mu_{\text{static-dynamic}} = \text{Coefficient of Static or Dynamic Friction}$$

The normal force in Equation 1 can be approximated as the cable tension. The static/dynamic coefficient will remain constant between the low-tension and high-tension tests. Therefore, the total normal force will increase from 2.7 to 16.8 kips (12.0 to 74.7 kN) with the

addition of one cable and an increase in cable tension from roughly 900 to 4,200 lb/cable (4 to 19 kN/cable).

Another reason for the increased release time pertains to the geometry of the cable anchor bracket assemblies. The two cable anchor bracket assemblies are shown in Figure 69. The rotation point for the cable release lever on the low-tension, cable anchor bracket assembly was located 5/8-in. (15.9-mm) above the bottom of the cable slots on the cable plate. The rotation point for the cable release lever on the high-tension, cable anchor bracket assembly was located 1/2-in. (12.7-mm) below the bottom of the cable slots on the cable plate. The low-tension, cable anchor bracket assembly's geometry allowed for more upward movement of the cables with less rotation of the release lever due to the higher rotation point.

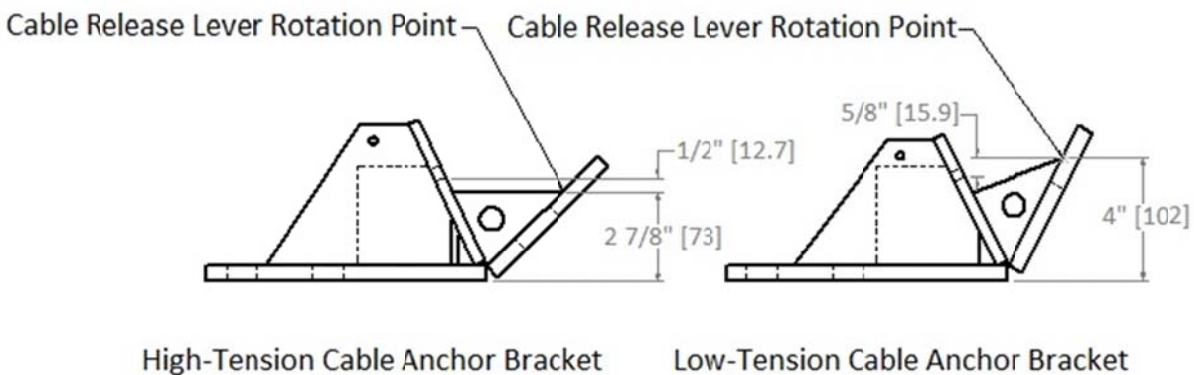


Figure 69. Rotation Point Comparison

Both anchor bracket assemblies exhibited smooth release of the cables in physical testing. However, a quicker release is more desirable as it would reduce the contact time between the vehicle and the anchor assembly. The reduced contact time could reduce yaw and potentially lead to a more controlled vehicle trajectory. Thus, minimizing the contact time between the cable anchor bracket assembly and an impacting vehicle was a goal of the redesign effort.

### **9.2.3 Cable Anchor Bracket Assembly Geometry**

The overall dimensions (i.e., height and width) of the current, high-tension, cable anchor bracket assembly design also raised some concerns. MASH specifies that a breakaway device shall have a stub height of no higher than 4-in. (102-mm) [7]. While the cable anchor bracket assembly is not technically a breakaway device, the fixed anchor portion of the assembly could pose some risk of undercarriage damage to the impacting vehicle if it is too high. The current height of the assembly is 5-in. (127-mm). In order to mitigate risks of undercarriage damage and occupant risk, the gusset and cable plate height should be decreased by 1-in. (25-mm) so that the assembly would meet the MASH specification.

Another concern regarding the geometry of the current, high-tension, cable anchor bracket assembly pertains to its overall width. The current assembly is shown in Figure 70. During the assembly of the four cables and end fitting hardware and placement into the cable anchor bracket assembly, space may be somewhat limited. This could potentially result in difficult system construction.

In the current design, four cable end fitters are placed side by side in their respective slots, thus leaving very little room for adjustments within the assembly. Cable tension is achieved by tightening the inline cable turnbuckles and cable end fitters. As cable tension is increased, the cable end fitters move closer together horizontally, thus reducing the spacing between them. This movement is exhibited in Figure 71.

The smaller the spacing between the end fitters, the more difficult it is to assemble the anchor bracket. There is also a limit to how much slack can be taken up in the end fitters since the end fitters will eventually contact each other and cause flexural deformations in the threaded rods.



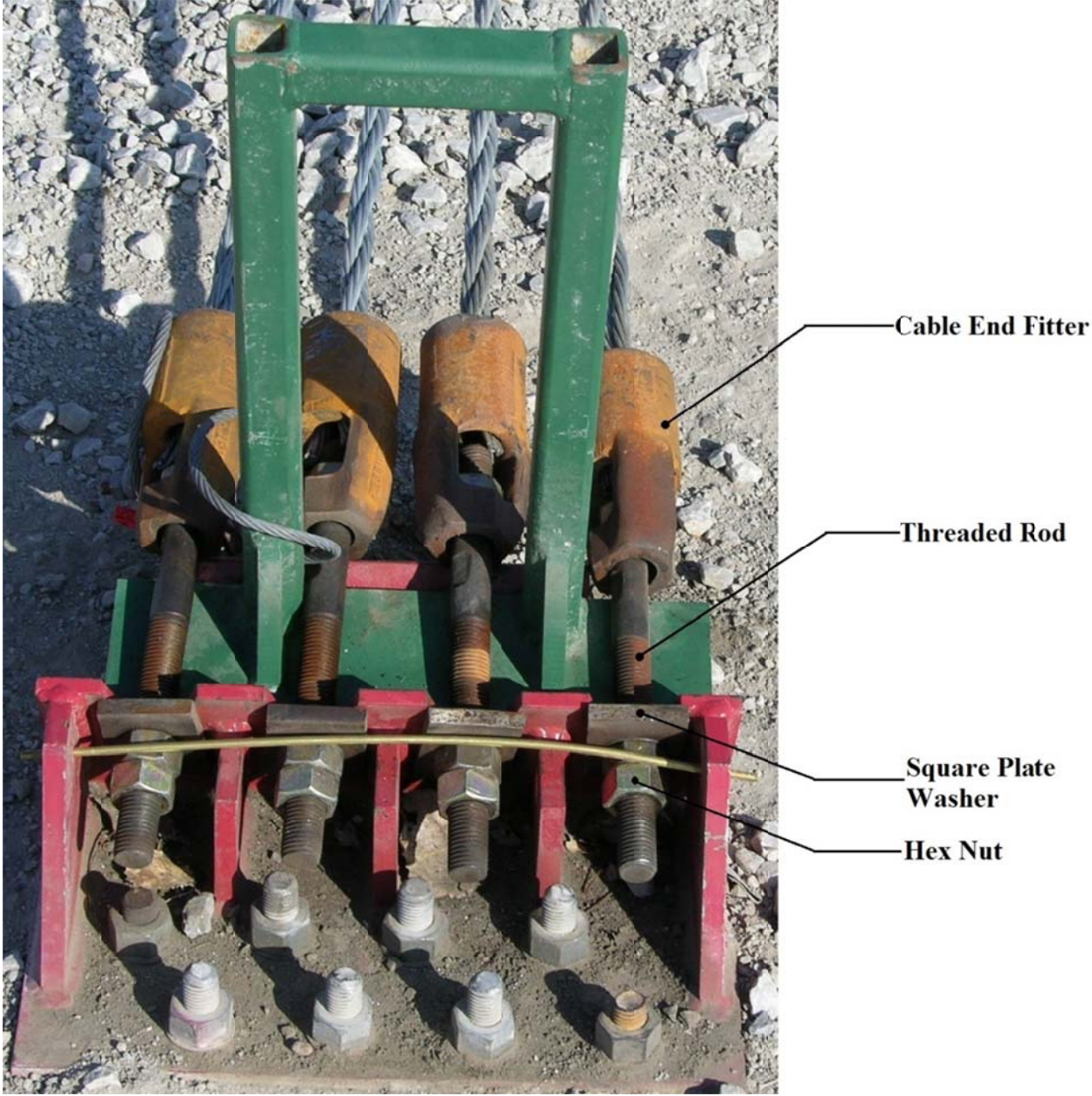
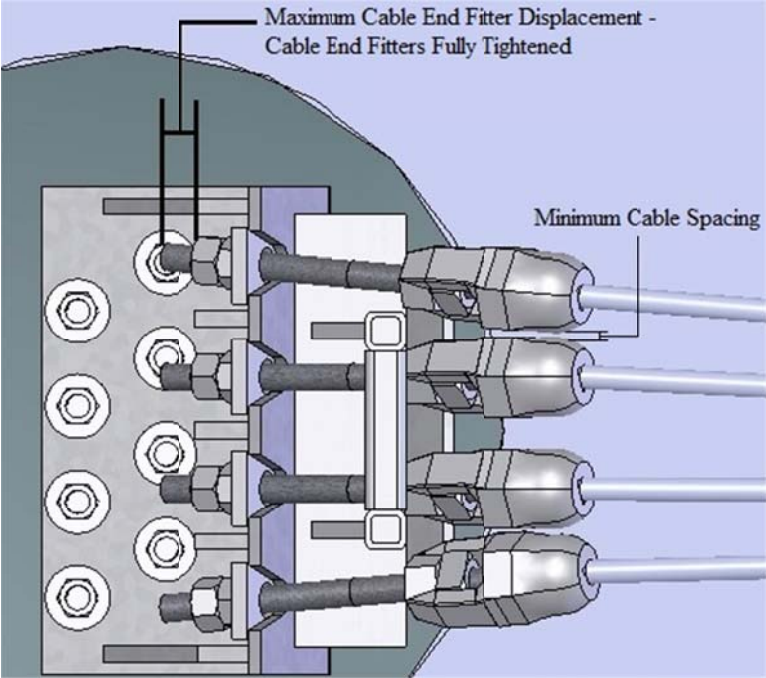
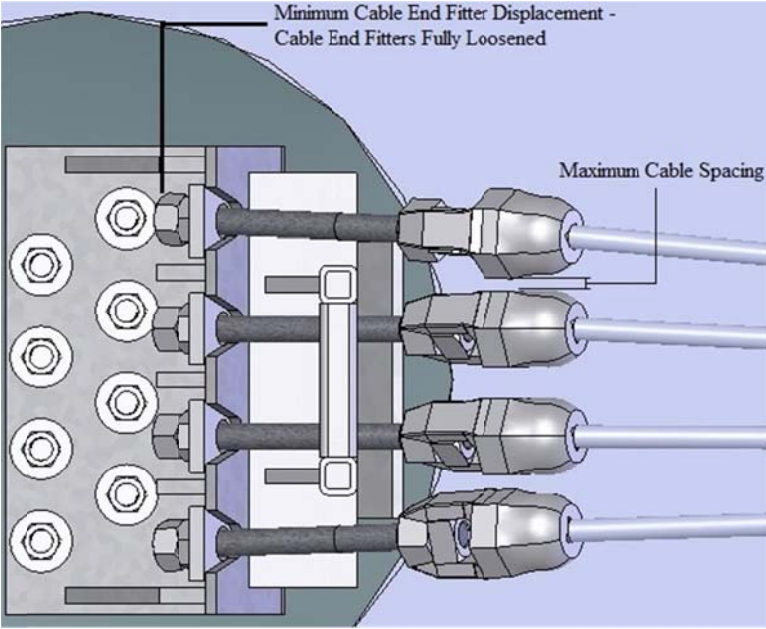


Figure 70. Cable End Fitter Interference

Aside from issues with tensioning the cables, the cable end fitters could also inhibit the rotation of the cable release lever if they are spaced too closely together. Although it is possible that the cables could still release, bogie testing of this scenario would be required to verify that this configuration would not significantly alter the cable release mechanics.



Cable End Fitters at Minimum Cable Spacing



Cable End Fitters at Maximum Spacing

Figure 71. Cable End Fitter Movement

To eliminate any uncertainty with the performance of the cable anchor bracket assembly, the new design for the cable anchor bracket assembly should be widened. Widening the anchor bracket assembly would also improve the ease of assembly of the anchor bracket and cable end fitters, as well as allow for sufficient play in the cable end fitter assemblies.

### **9.3 Alternate Design Development**

Based on the investigation of the low-tension, cable end terminal tests as well as in-field cable anchor bracket assembly observations, the following design aspects were incorporated into a redesign of the high-tension, cable anchor bracket assembly:

- rotating cable release lever with means of retention during impact;
- increased height of rotation point for cable release lever relative to cable slots;
- reduced overall height of cable anchor bracket assembly to 4-in. (102-mm); and
- widened cable anchor bracket assembly from 15 1/4-in. to 19 3/4-in. (387-mm to 502-mm).

#### **9.3.1 Redesigned, High-Tension, Cable Anchor Bracket Assembly Model**

##### **Development**

In order to evaluate potential designs and modifications, a finite element model was developed for use with the LS-DYNA FE code. An initial, finite element model of the redesigned cable anchor bracket assembly is shown in Figure 72.

The primary purpose of the redesigned, high-tension, cable anchor bracket assembly was to release the system cables when the cable release lever was impacted by a vehicle. Since the mechanics enabling the release of the cables was similar to those in the previous design, many of the element and material formulations were reused. Geometric modifications had to be made to many components to incorporate the previously-outlined design changes.

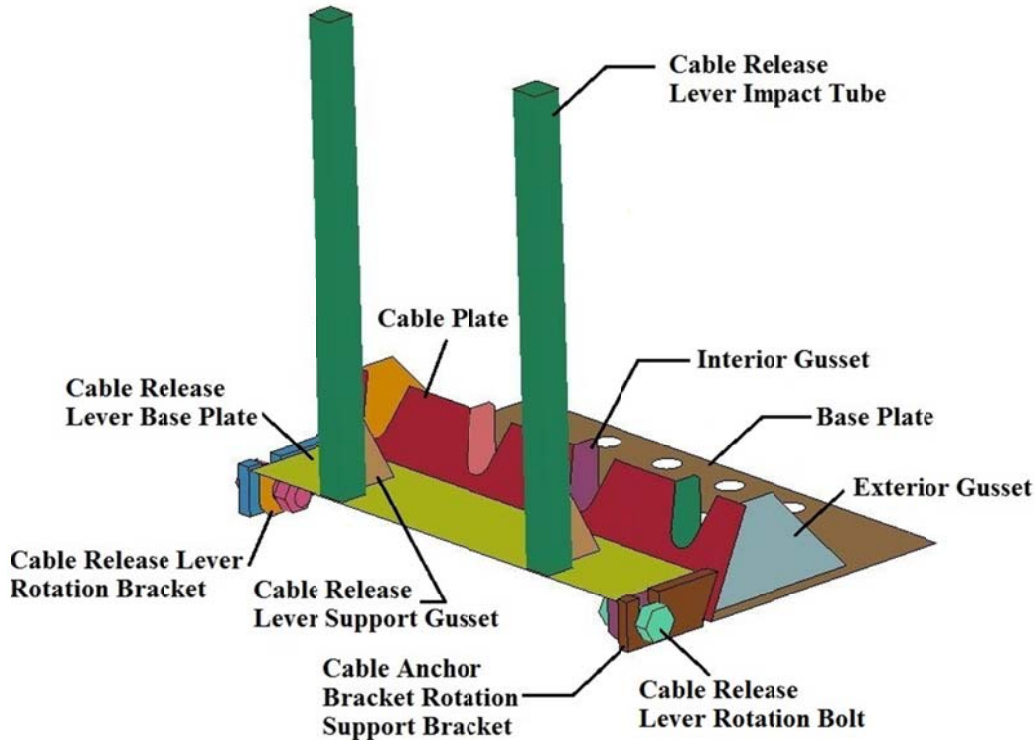


Figure 72. Redesigned Cable Anchor Bracket Assembly Model

It was necessary to model several new components used in the assembly. These components are described in the following subsections. A summary of the redesigned, anchor bracket assembly components and their associated element and material types is shown in Table 10.

### 9.3.1.1 Cable Release Lever Rotation Brackets

Brackets needed to be attached to the cable release lever assembly in order to retain the release lever after the release of the cables. To accomplish this, two brackets were modeled and attached to the underside of the release lever base plate. An initial bracket model was discretized using three-noded and four-noded shell elements. A piecewise-linear, plastic material model with ASTM A36 steel material properties was specified for the bracket. A Belytschko-Leviathan element formulation was specified for the shell elements. The bracket model is shown in Figure 73.

Table 10. Summary of Redesigned Cable Anchor Bracket Assembly Model Properties

Part Name	Element Type	Element Formulation	Material Type	Material Formulation
Interior Gusset	Shell	Belytschko-Leviathan	ASTM A36	Piecewise, Linear Plastic
Exterior Gusset	Shell	Belytschko-Leviathan	ASTM A36	Piecewise, Linear Plastic
Base Plate	Shell	Belytschko-Leviathan	ASTM A36	Piecewise, Linear Plastic
Cable Plate	Shell	Belytschko-Leviathan	ASTM A36	Piecewise, Linear Plastic
Cable Anchor Bracket Rotation Support	Solid	Fully Integrated S/R	ASTM A36	Piecewise, Linear Plastic
Release Lever Support Gusset	Shell	Belytschko-Leviathan	ASTM A36	Piecewise, Linear Plastic
Cable Release Lever Impact Tube	Shell	Belytschko-Leviathan	ASTM A36	Piecewise, Linear Plastic
Cable Release Lever Rotation Bracket	Shell	Belytschko-Leviathan	ASTM A36	Piecewise, Linear Plastic
Release Lever Base Plate	Shell	Belytschko-Leviathan	ASTM A36	Piecewise, Linear Plastic
Cable Release Lever Rotation Bolt	Solid	Fully Integrated, S/R	ASTM A307	Piecewise, Linear Plastic

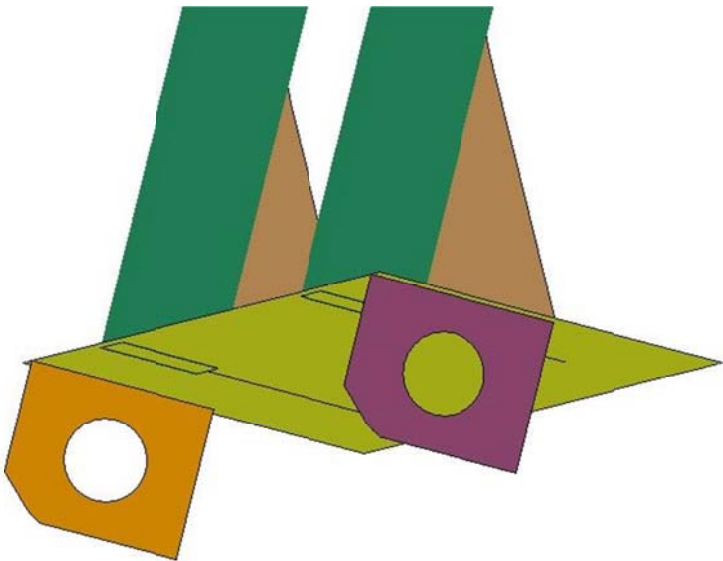


Figure 73. Cable Release Lever Rotation Bracket Model

### 9.3.1.2 Cable Anchor Bracket Assembly Rotation Support Brackets

A new bracket was necessary to support and accommodate the rotation of the cable release lever assembly during the cable release. Two brackets were attached to the front of the cable plate to create a rotational joint on the front of the cable anchor bracket assembly. A preliminary design was modeled using eight-noded hexagonal elements. A piecewise-linear, plastic material model with ASTM A36 steel material properties was specified for the bracket model. A Fully Integrated S/R solid element formulation was used for the solid elements. The bracket model is shown in Figure 74.

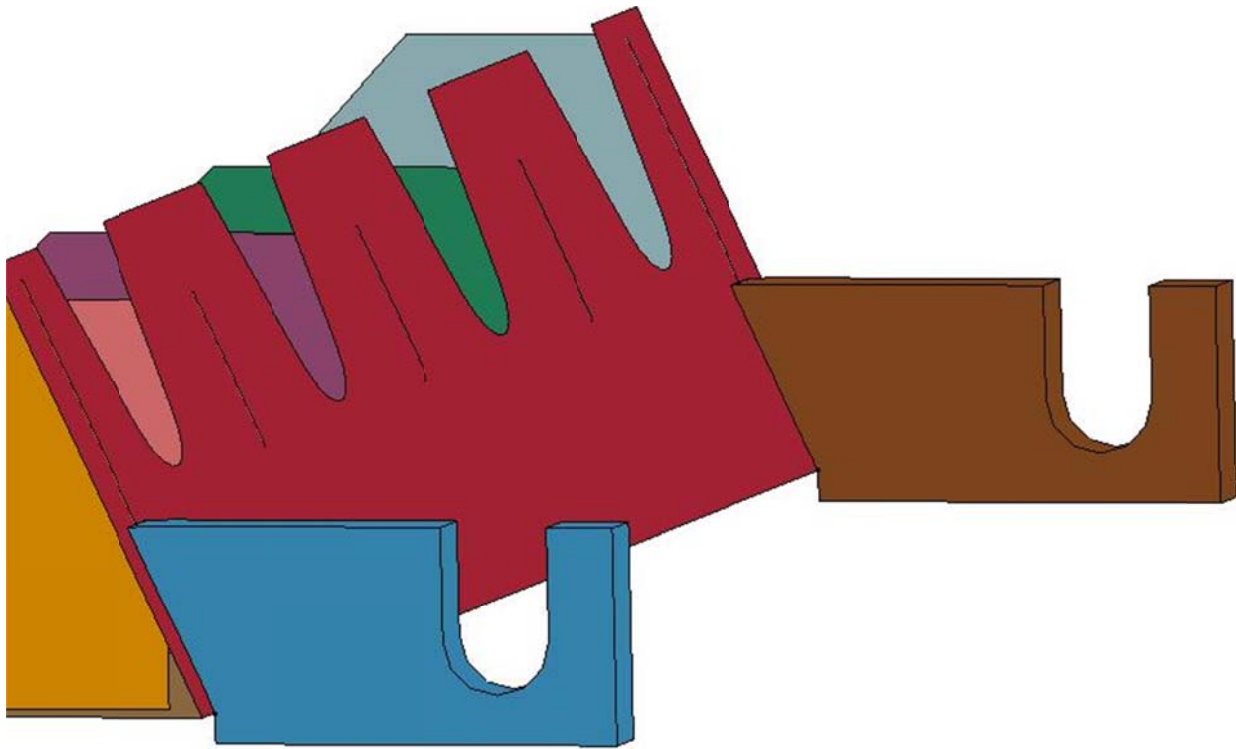


Figure 74. Cable Anchor Bracket Assembly Rotation Support Bracket Model

### 9.3.1.3 Cable Release Lever Rotation Bolts

Two 3/4-in. (19.1-mm) diameter x 2-in. (51-mm) long ASTM A307 hex bolts were specified to attach the release lever brackets to the support brackets. The bolts were modeled

using eight-noded hexagonal elements. A piecewise-linear, plastic material model with ASTM A307 steel material properties was specified for the bolt model. A Fully Integrated S/R solid element formulation was used for the solid elements.

### **9.3.2 Model Development Simulations**

Once a finite element model of the redesigned, high-tension, cable anchor bracket assembly had been completed, the model was inserted into the previously-constructed bogie test simulation model. The current design of the high-tension, cable anchor bracket assembly model used in the validated simulation was replaced with the redesigned anchor model to evaluate its performance and identify any potential design issues. Similar bogie impact conditions were used.

#### **9.3.2.1 Simulation No. 1 - Initial Anchor Bracket Assembly Model**

Initial simulations with the redesigned, cable anchor bracket assembly resulted in questionable performance. Although the assembly did release the cables, the cable release lever was not retained. The retention of the cable release lever was one of the primary goals of the redesign. The cable release lever as it is detaching from the anchor bracket assembly during the simulation is shown in Figure 75.

It was determined that the cable anchor bracket rotation support bracket's geometry and performance was the primary cause for the cable release lever not being retained. Deformation in the bracket slot as well as the bracket height allowed for the cable release lever rotation bolts to slide upwards out of the slot. It was concluded that the bracket's geometry was the primary reason the cable release lever was able to disengage from the rest of the assembly.

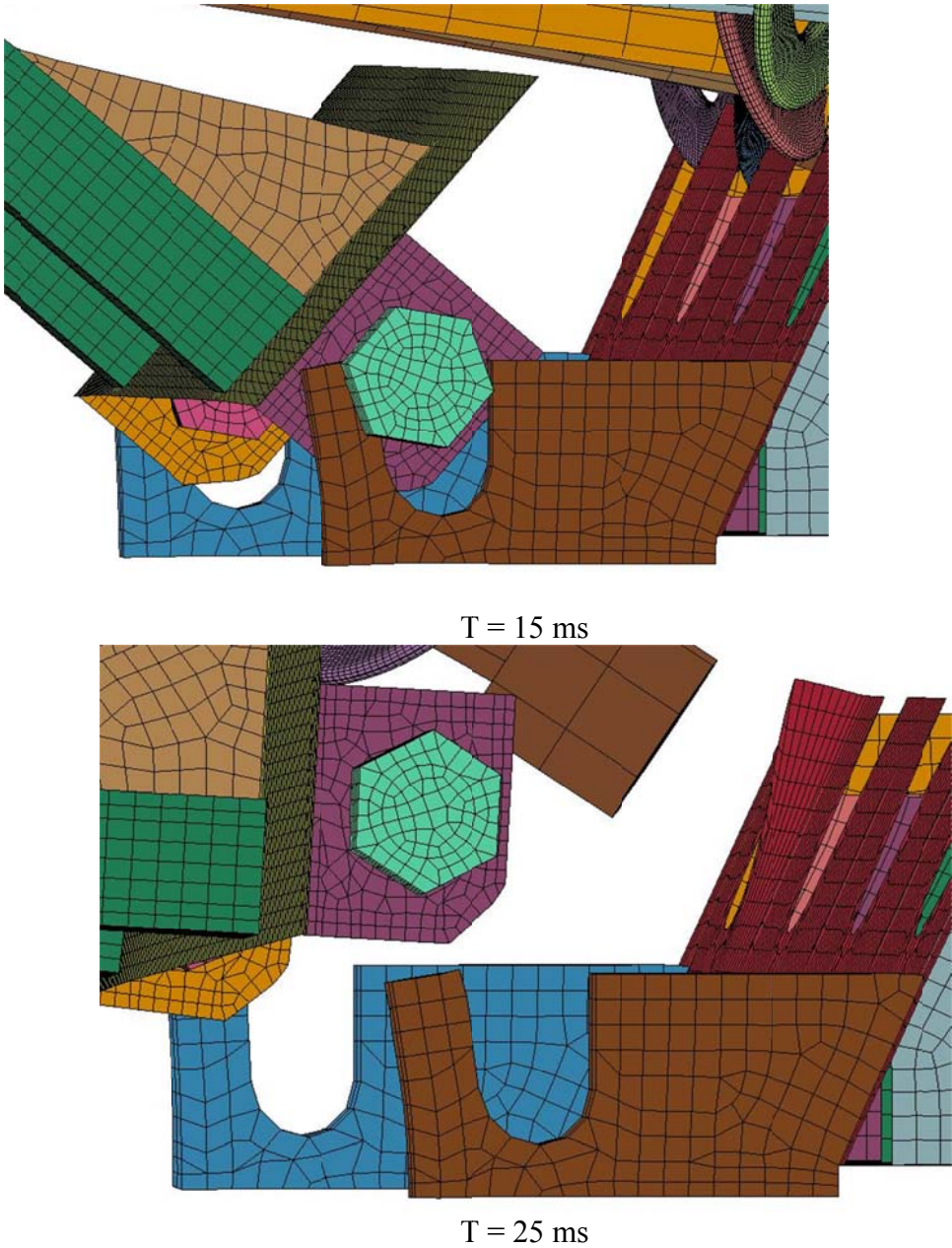


Figure 75. Release Lever Disengaging from Assembly, Simulation No. 1

**9.3.2.2 Simulation No. 2 – Redesigned Support Bracket and Cable Release**

**Lever Model**

Following the poor performance observed in the initial simulation attempt, the cable anchor bracket rotation support bracket’s geometry was redesigned in an attempt to retain the



cable release lever. The results and behavior of the previous simulation were studied and numerous component simulations with varying bracket geometries were conducted. Alternate cable release lever concepts were also analyzed in order to determine the design which resulted in optimum cable release mechanics. Release lever concepts investigated included rotation brackets with slots instead of holes, varying the location of the impact tubes and support gussets, and changing the angle of the cable release lever base plate.

It was determined that a taller support bracket would perform better. The slot in the support bracket was also angled back towards the anchor bracket to inhibit the bolt from riding up in the slot. A cable release lever base plate with a mounting angle of 11.5 degrees was selected to use with the updated model. Initial analysis of the new configuration showed that the angled baseplate would reduce the cable release time and result in better cable release mechanics. The redesigned bracket and cable release lever are shown in Figures 76 and 77, respectively. The new design was then inserted into the bogie model and simulated.

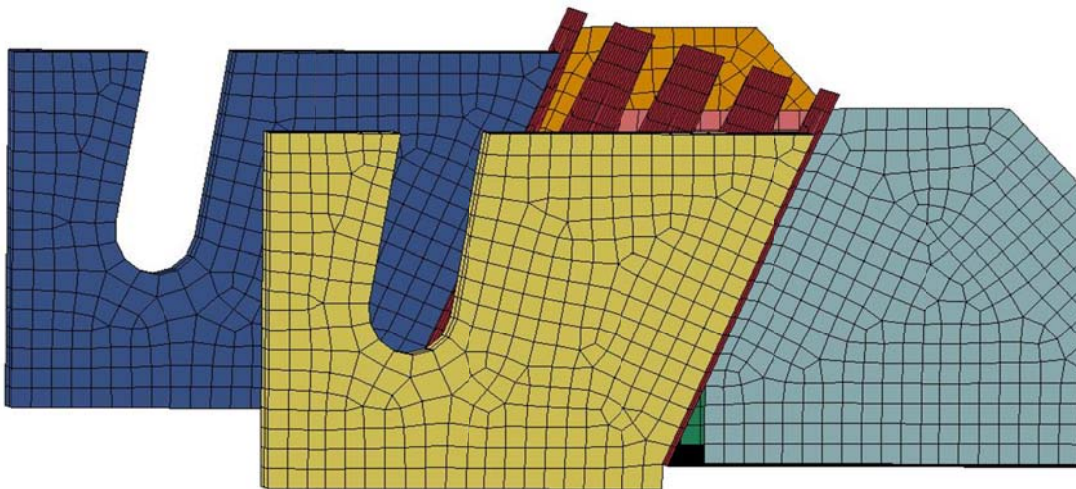


Figure 76. Redesigned Cable Anchor Bracket Support Bracket Geometry

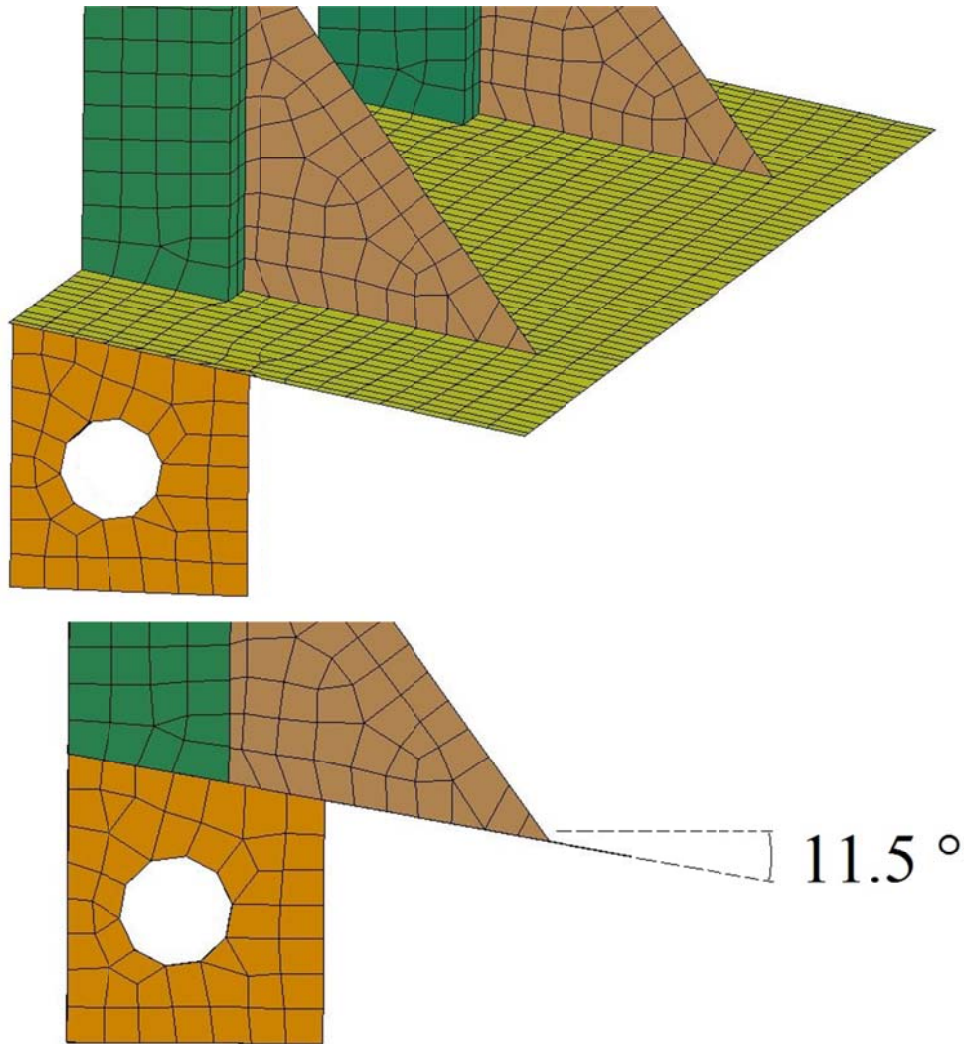


Figure 77. Redesigned Cable Release Lever, Angled Base Plate

The redesigned cable anchor bracket assembly encountered several issues during the second round of simulation. During simulation no. 2, the cables were released successfully. However, there was severe damage to the anchor bracket assembly. The release of the cables took much longer than in previous simulations as well.

The poor release mechanics were primarily due to the release lever assembly binding up upon impact. The binding was caused when the bolts which connect the release lever rotation brackets to the cable anchor rotation support brackets rotated downward. This created a distorted

rotational joint on the front of the cable anchor bracket. The distorted joint resulted in deformation in the release lever base plate. The base plate deformation delayed the cable release and led to high impact forces being imparted to the rest of the assembly. This behavior resulted in the damage to the cable release lever assembly as well as the support brackets. Hardware damage and rotation behavior are shown in Figures 78 through 80.

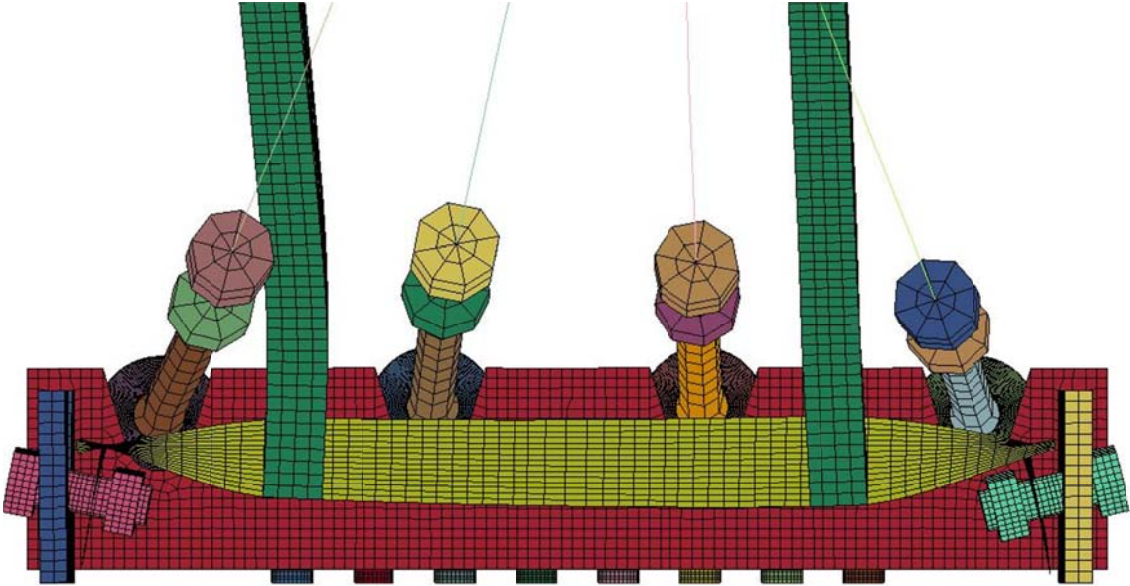


Figure 78. Distorted Joint on Cable Anchor Bracket Assembly, Simulation No. 2

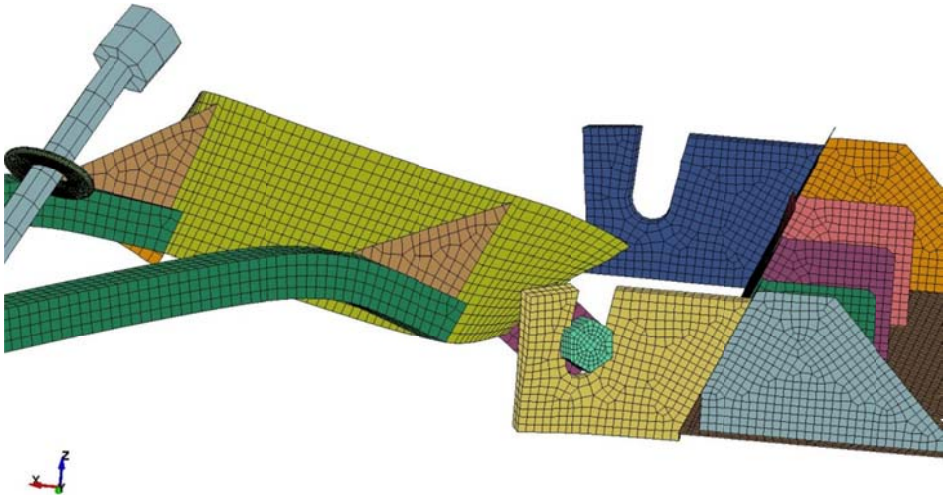


Figure 79. Anchor Bracket Assembly Damage, Simulation No. 2

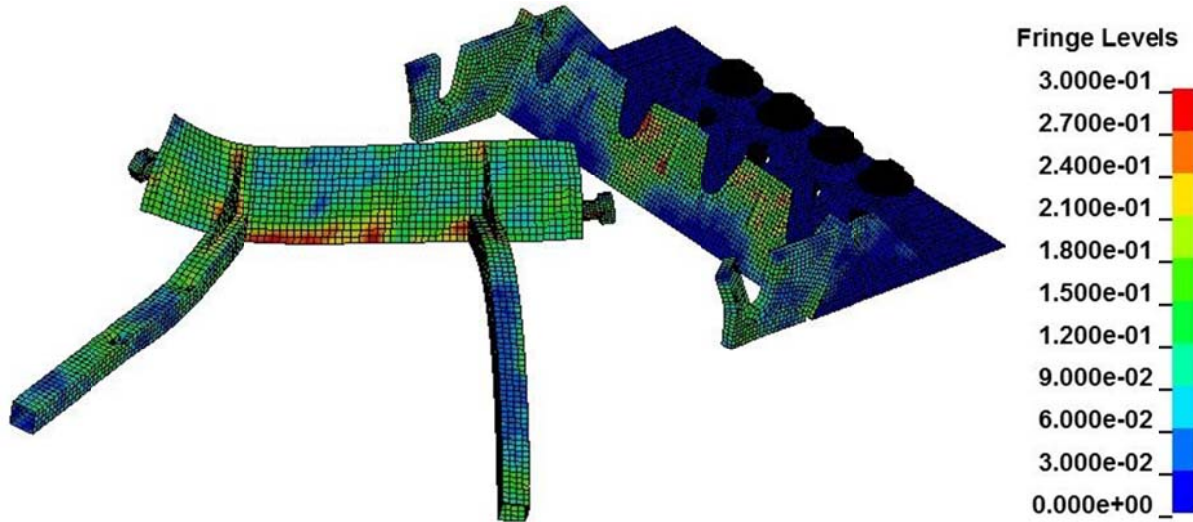


Figure 80. Anchor Bracket Assembly von Mises' Stress, Simulation No. 2

While the results of simulation no. 2 were ultimately unacceptable, the support brackets exhibited much better performance. The taller brackets held the release lever in place, although this is partially what contributed to the severe damage. Since the release lever assembly could not slide upwards in the support bracket slot, the bolts rotated downwards, which initiated the rotation issues. As the cable anchor rotation support brackets served their intended purpose, no modifications were made to their design.

### 9.3.2.3 Simulation No. 3 – Redesign of Rotational Joint Hardware

To address the rotation issues, several possible solutions were investigated. Washers were placed in between the bolt head and the outer face of the support bracket. While this improved the stability of the rotational joint, there was still some bolt rotation. This led to similar damage to the anchor bracket and release lever assembly, although not to the same extent as seen in simulation no. 2. The bolt rotation with inserted washers is shown in Figure 81.

After the washers did not correct the issue, the two bolts were exchanged for one long, steel rod with threaded ends. As long as the rod does not fail, the rotational joint should remain intact. The washers were used again between the nuts at each end of the rod and the outer surface

of the support brackets. The washers were reused to ensure that there was no pullout of the rod in the support bracket slots. The anchor bracket assembly with the rod and washers is shown in Figure 82.

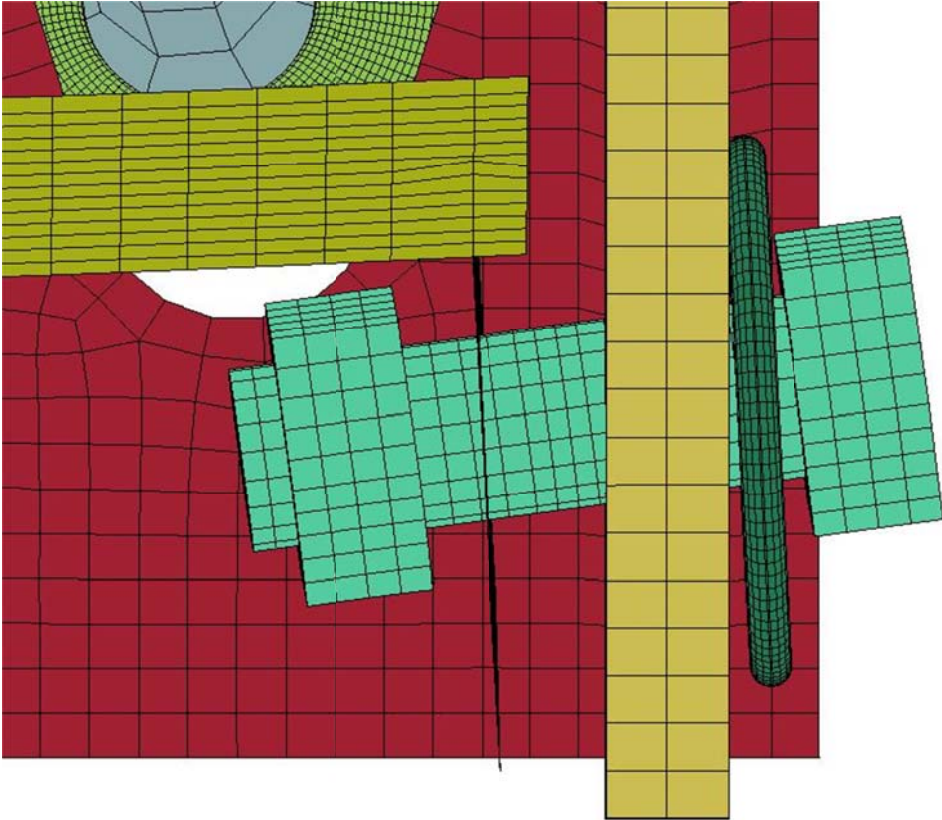


Figure 81. Bolt Rotation with Washer

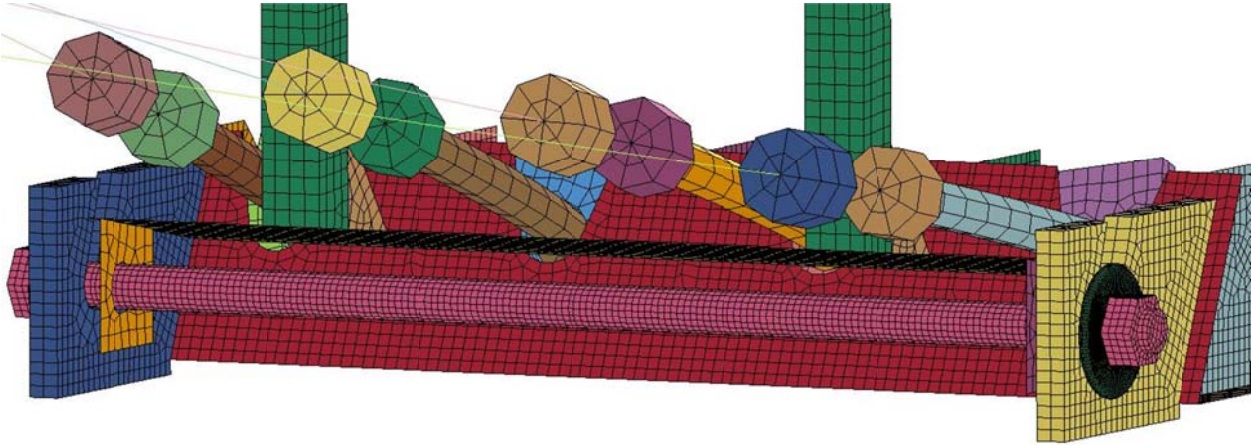


Figure 82. Anchor Bracket Assembly with Rod

During simulation no. 3, the cable release lever rotated smoothly during impact. The cables were released evenly and without incident. At the conclusion of the simulation, the cable release lever was successfully retained. There was some slight deformation to the vertical release lever tubes, and extensive deformation to the angled cable plate. The support brackets and remainder of the anchor bracket assembly were undamaged during the simulation. The cable anchor bracket assembly at the conclusion of simulation no. 3 is shown in Figure 83.

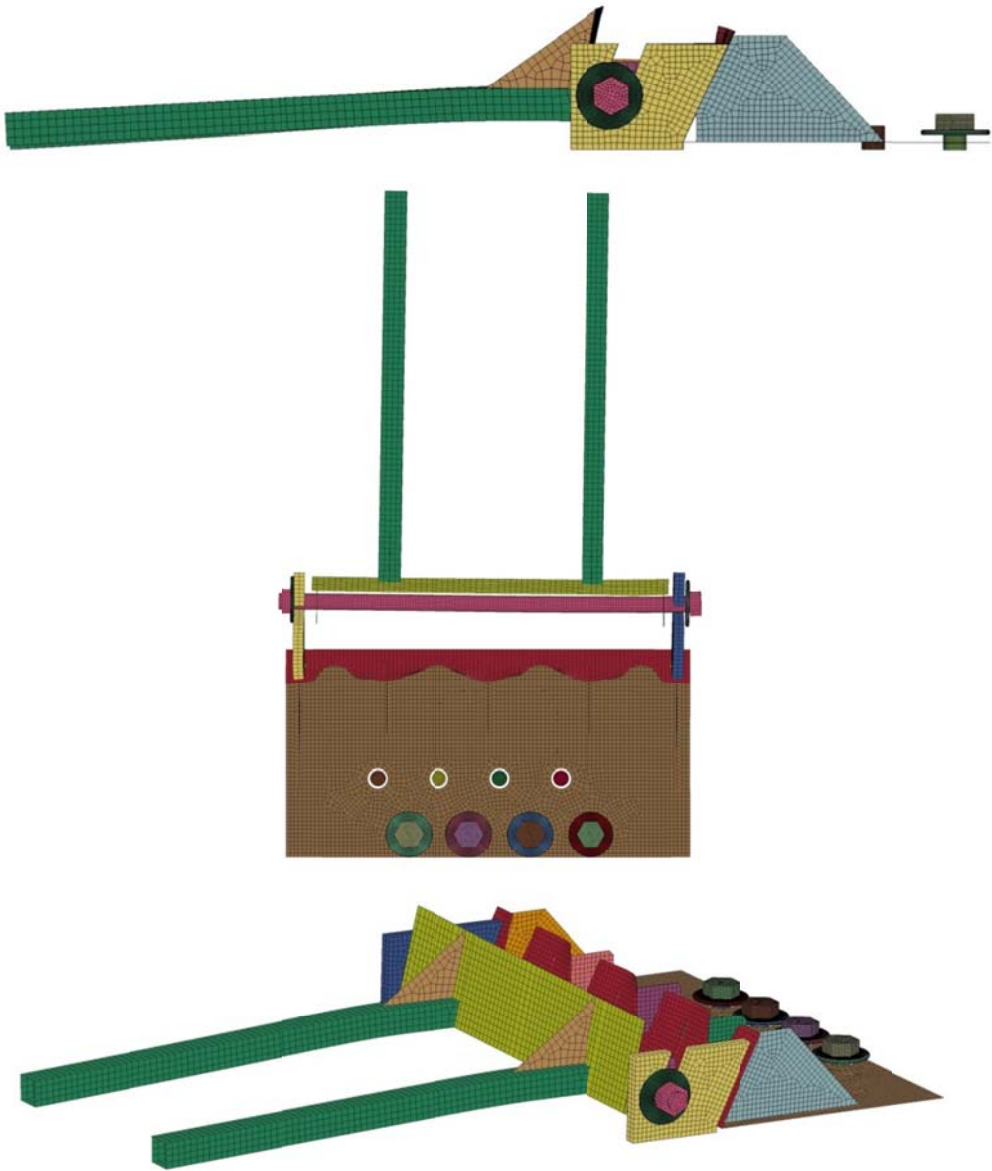


Figure 83. Cable Anchor Bracket Assembly Deformation, Simulation No. 3

The cable plate sustained severe plastic deformation in such a manner that the entire anchor bracket assembly would require replacement before the terminal could safely function. The robustness of the high-tension, cable end terminal design as a whole would be greatly aided by an anchor that was reusable or required minimal repair following an impact event. The plastic strain distribution in the anchor assembly after the release of the cables is shown in Figure 84.

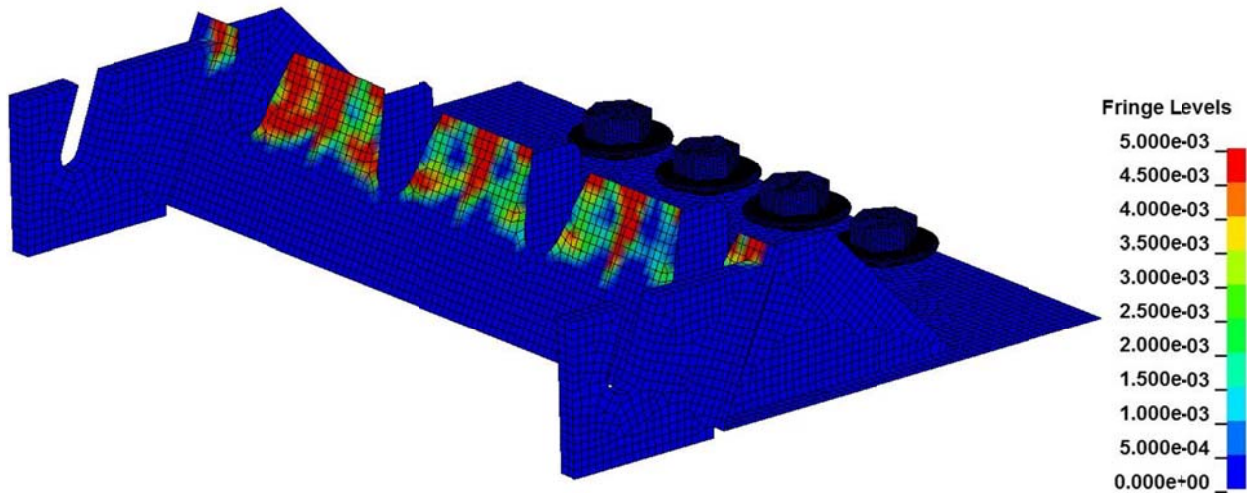


Figure 84. Anchor Bracket Assembly Plastic Strain, Simulation No. 3

#### 9.3.2.4 Simulation No. 4 – Analysis of Release Lever Modification

The elimination of the cross bar on the cable release lever assembly was necessary to prevent the assembly from being pulled downstream after release of the cables in an anchor impact. There was some concern how the modified release lever would perform in the instance that a vehicle impacts only one of the vertical tubes either end-on or at an oblique angle. Without the crossbar to distribute the impact force, all of the load will be concentrated in a single tube. That tube needed to be strong enough to withstand the impact forces and still be able to release the system cables from the slots on the cable plate. If only one tube was unable to successfully release the cables, the vehicle could potentially ramp up the unreleased cable or cables and produce a hazardous vehicle trajectory, including rollover.

To evaluate the redesigned anchor in this scenario, a simulation was conducted with one of the vertical tubes removed from the contact definition. Modifications were made to several cable anchor bracket assembly components to correct issues that were identified after the completion of simulation no. 3.

The primary concern that arose from analysis of the results from simulation no. 3 was deformation to the cable plate. To eliminate the plastic deformation in the cable plate flanges, the interior cable anchor gussets were extended upwards to the top of the cable plate. The extended gussets provide more support for the flanges and increased the available weld area for the connection between the cable plate and the interior gussets. The cable plate thickness was also increased from 3/8-in. to 5/8-in. (9.5-mm to 15.9-mm) to further guard against deformation.

Initial simulations with the updated anchor bracket assembly model revealed several problems with the design and the modeling techniques. Significant nodal penetrations were evident in the contact between the cable release lever rotation brackets and the steel rod. The node penetrations resulted in non-physical deflection of the cable release lever, poor rotation mechanics, and ultimately the cables were not released during the simulated interaction between the cable anchor bracket assembly and the bogie. The node penetration between one of the rotation brackets and the steel rod is shown in Figure 85.

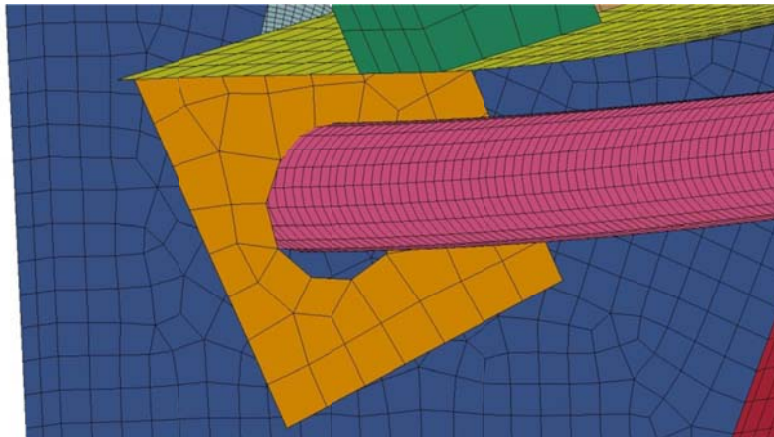


Figure 85. Nodal Penetration in Rotation Bracket Contact



To correct the contact issue, the rotation brackets were remodeled using solid elements. While shell elements are more computationally efficient and easy to use, solid element contact is much more robust and omnidirectional.

The primary issue with shell contacts arises in the instance when a shell edge contacts another element of any type. While solid elements have well defined surfaces for contacts, shell elements utilize artificially created “thicknesses” as contact surfaces on edges. In order to simulate a smooth contact surface, the contact thickness is radially projected around the edge of a shell element boundary. These artificial surfaces can create edge and node penetration issues, which in some cases can yield unrealistic contact behavior and misleading simulation results. For this reason, solid elements are the more reliable option, although more computationally expensive. An example of a typical shell element and its simulated element thickness is shown in Figure 86.

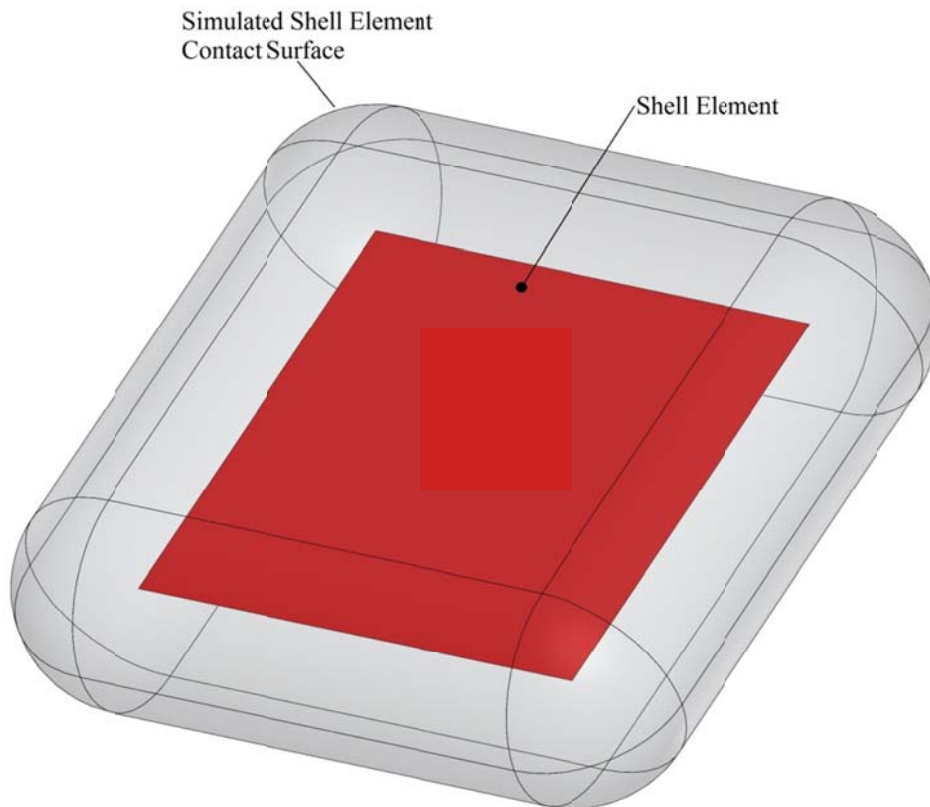


Figure 86. Typical Shell Element and Simulated Contact Surface

Another simulation was conducted with the updated cable anchor bracket assembly model. The solid element rotation brackets improved the contact between the brackets and the steel rod. The updated contact is shown in Figure 87.

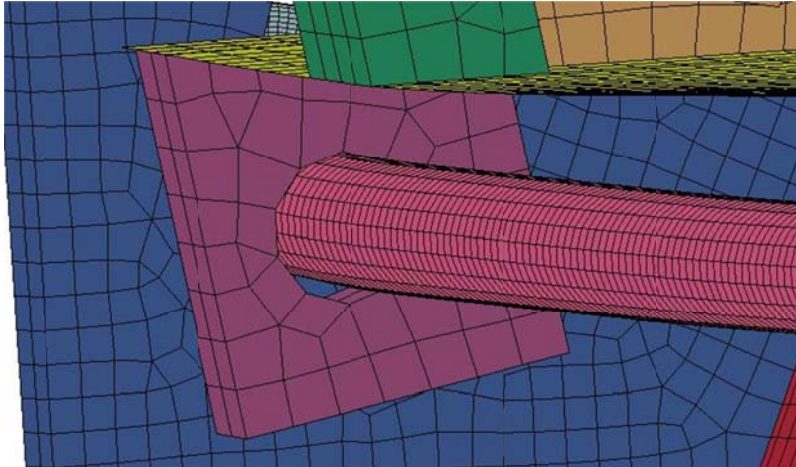


Figure 87. Rotation Bracket Contact Using Solid Elements

The anchor bracket assembly again failed to release the cables. Deformation to the vertical tube as well as torsion in the release lever assembly base plate prevented the cables from releasing during the bogie impact. The tube bending prevented the release lever from fully rotating and the torsion in the base plate caused one side of the plate to deflect downward. The deflection in turn prevented the cable end fitters from fully translating up and out of their respective slots on the cable plate. Fringe plots of the damaged components are shown in Figure 88.

In order to successfully release the cables, the torsion and deformation to the release lever assembly needed to be alleviated. Therefore, the vertical tubes were strengthened by replacing the 1 1/4-in. x 1 1/4-in. x 3/16-in. (32-mm x 32-mm x 4.8-mm) section tubes with 1 1/2-in. x 1 1/2-in. x 1/4-in. (38-mm x 38-mm x 6.4-mm) section tubes. The steel base plate size was also increased from 1/2-in. to 5/8-in. (12.7-mm to 15.9-mm) thick.

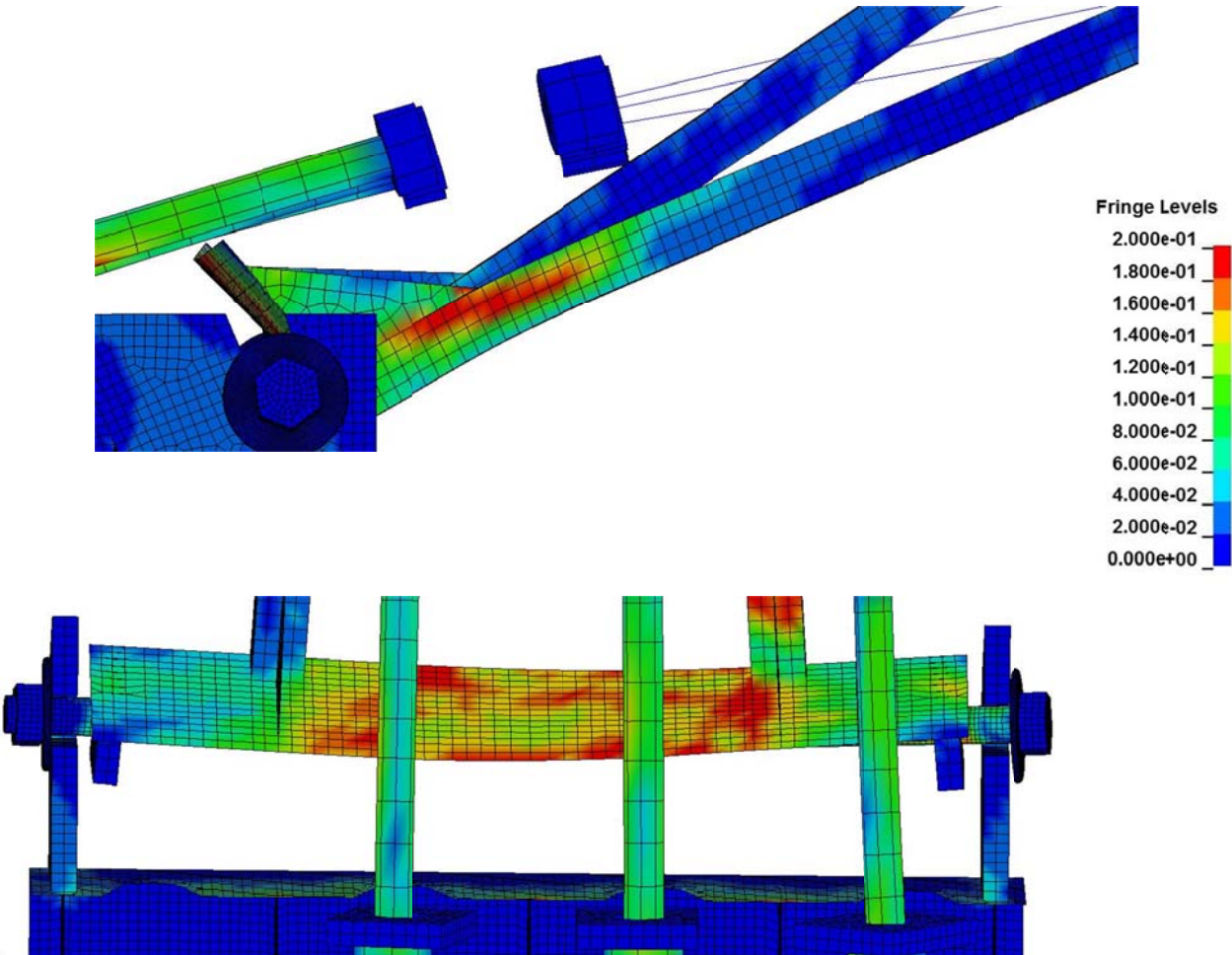


Figure 88. Deformation of Release Lever Assembly Components, von Mises' Stress

After the previously described modifications had been made to the model of the cable anchor bracket assembly, the simulation was conducted again to evaluate the changes. The updated cable anchor bracket assembly model exhibited better rotation mechanics and resulted in the smooth release of the cables during the simulation.

There was still some bending in the vertical tube as well as torsion in the base plate of the cable release lever assembly. The deformation, however, was mitigated by the strengthened components. The deformed components did not exhibit any potential to effect the release mechanics of the redesigned, cable anchor bracket assembly. Therefore, this deformation is considered acceptable. Note also that the cable release lever assembly was the only component

of the anchor bracket that would require replacement post impact. The damage in the cable anchor bracket assembly at the instant the cables fully released is shown in Figure 89.

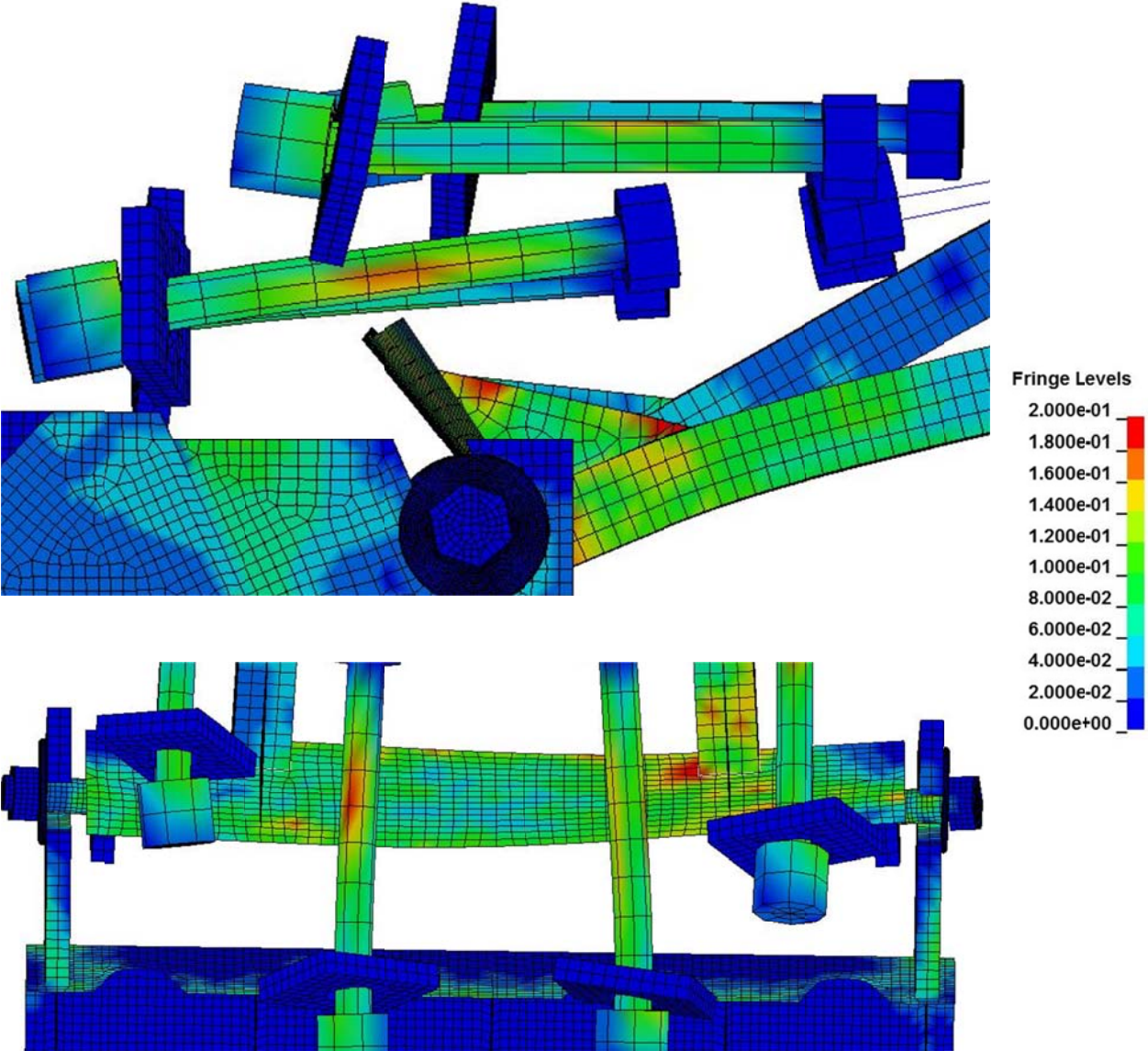


Figure 89. Cable Anchor Bracket Assembly von Mises' Stress, Simulation No. 4

**9.3.2.5 Simulation No. 5 – Increased Cable Tension**

Although the design tension for the system cables is 4,200 lb (18.7 kN), temperature fluctuations could result in increased cable tension. A simulation was conducted in which the cable tension was doubled to 8,400 lb/cable (37.4 kN/cable). The goal of the simulation was to

analyze the effects that increased cable tension would have on the cable release mechanics. The bogie head was centered on the cable anchor and an impact speed of 45.0 mph (72.4 km/h) was used in the simulation.

The bogie head impacted the cable release lever and rotated the cables out of their respective slots on the cable plate. The duration of the cable release process was roughly 6 ms longer as compared to simulation no. 3. Significant plastic deformation in the cable plate flanges occurred due to the prying action of the cables during impact. The maximum plastic strain in the cable plate was 0.65. Since the simulation represents a worst case scenario, however, this deformation was deemed acceptable. The plastic strain in the cable plate at the conclusion of the simulation is shown in Figure 90.

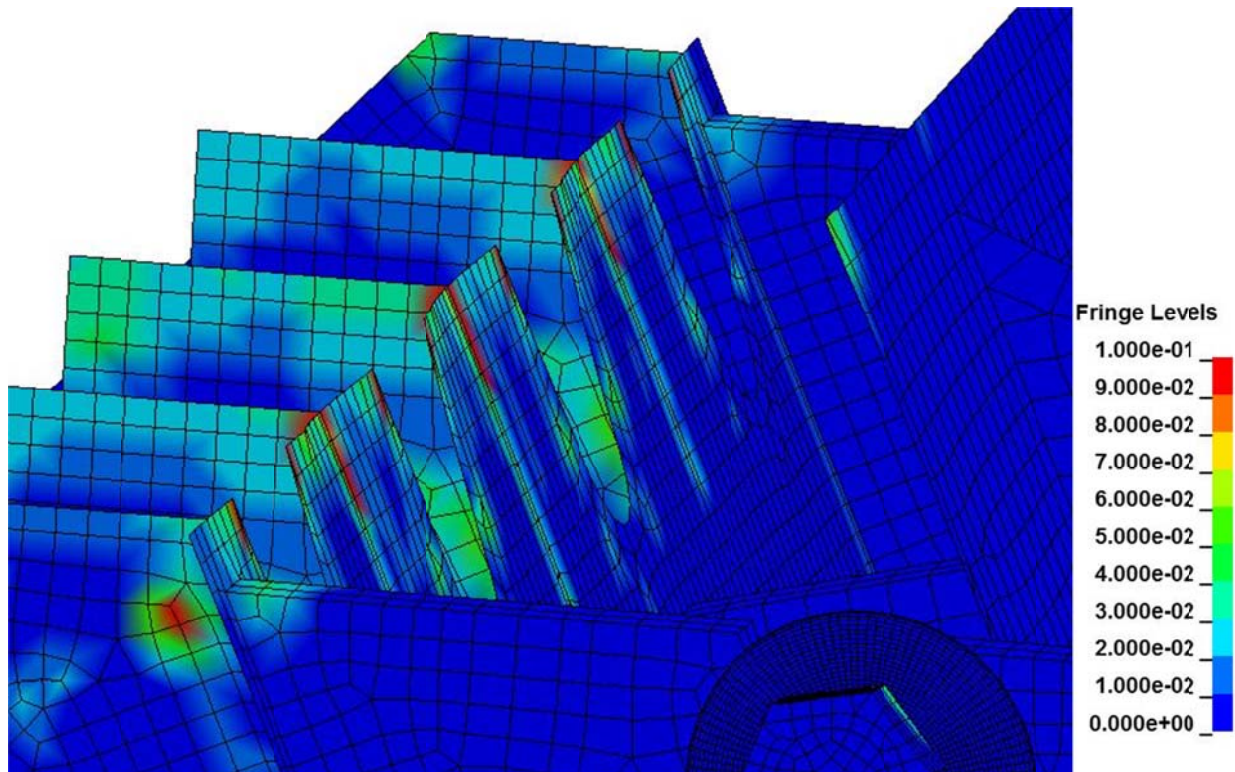


Figure 90. Cable Plate Plastic Strain, Simulation No. 5

Although the cable tension was doubled, the maximum impact force imparted to the bogie was only 1 percent higher as compared with the simulation with the design tension. This is in part due to anchor component deformation that occurred in the simulation with increased cable tension. Although the normal force was increased significantly, plastic deformation in the cable release lever and cable plate absorbed energy reducing the peak impact forces. No plastic deformation to the cable anchor bracket assembly was seen in the simulation with the design tension. The average force after the maximum in the simulation with double tension was 1.5 kips (6.7 kN) as compared to 1.2 kips (5.3 kN) in the simulation with design tension. The increased average force and elongated cable release time also resulted in more energy dissipation by the bogie due to the larger sliding friction force. The simulation resultant forces on the bogie head from initial impact are shown in Figure 91.

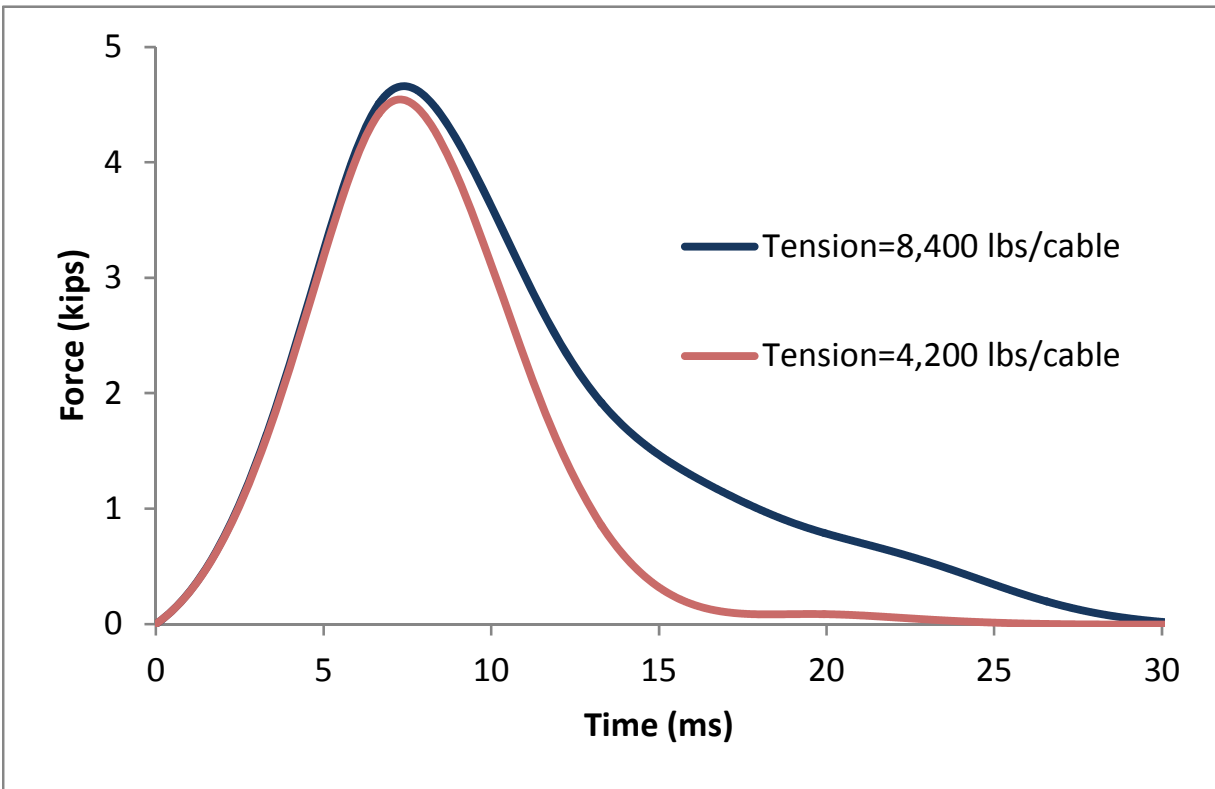


Figure 91. Impact Force Comparison, Increased Cable Tension vs. Design Tension

### **9.3.2.6 Simulation No. 6 –Anchor Impact at Oblique Angle**

The redesigned, high-tension, cable anchor bracket has exhibited good performance and release mechanics with inline impacts, however the likelihood of a perfectly aligned vehicle orientation in a roadside impact is minimal. Roadside vehicle interactions with anchors will more commonly be oblique impacts. Because of this, the cable release mechanics must function in the event that the cable anchor bracket assembly is impacted at an oblique angle.

To evaluate the robustness of the redesigned cable anchor bracket assembly's cable release mechanics, a simulation was conducted with the bogie impacting the anchor assembly at an angle of 15 degrees. The bogie head was aligned with the center of the redesigned anchor assembly. The impact angle was selected to reflect impact orientation requirements for MASH Test No. 3-33. An impact speed of 45.0 mph (72.4 km/h) was used.

The bogie impacted one of the vertical release lever tubes and smoothly rotated the cables out of their respective slots on the cable plate. The cable release lever base plate exhibited noticeable bending during the cable release process, primarily due to the forces exerted on the impact tubes out of plane with the rotational joint. There was some permanent deformation in the vertical impact tubes at the conclusion of the simulation, however, since the cables were released smoothly and the oblique impact scenario is a worst case scenario, the deformation was deemed acceptable. Sequential images of the oblique impact simulation are shown in Figure 92. The plastic deformation in the cable release lever assembly is shown in Figure 93.

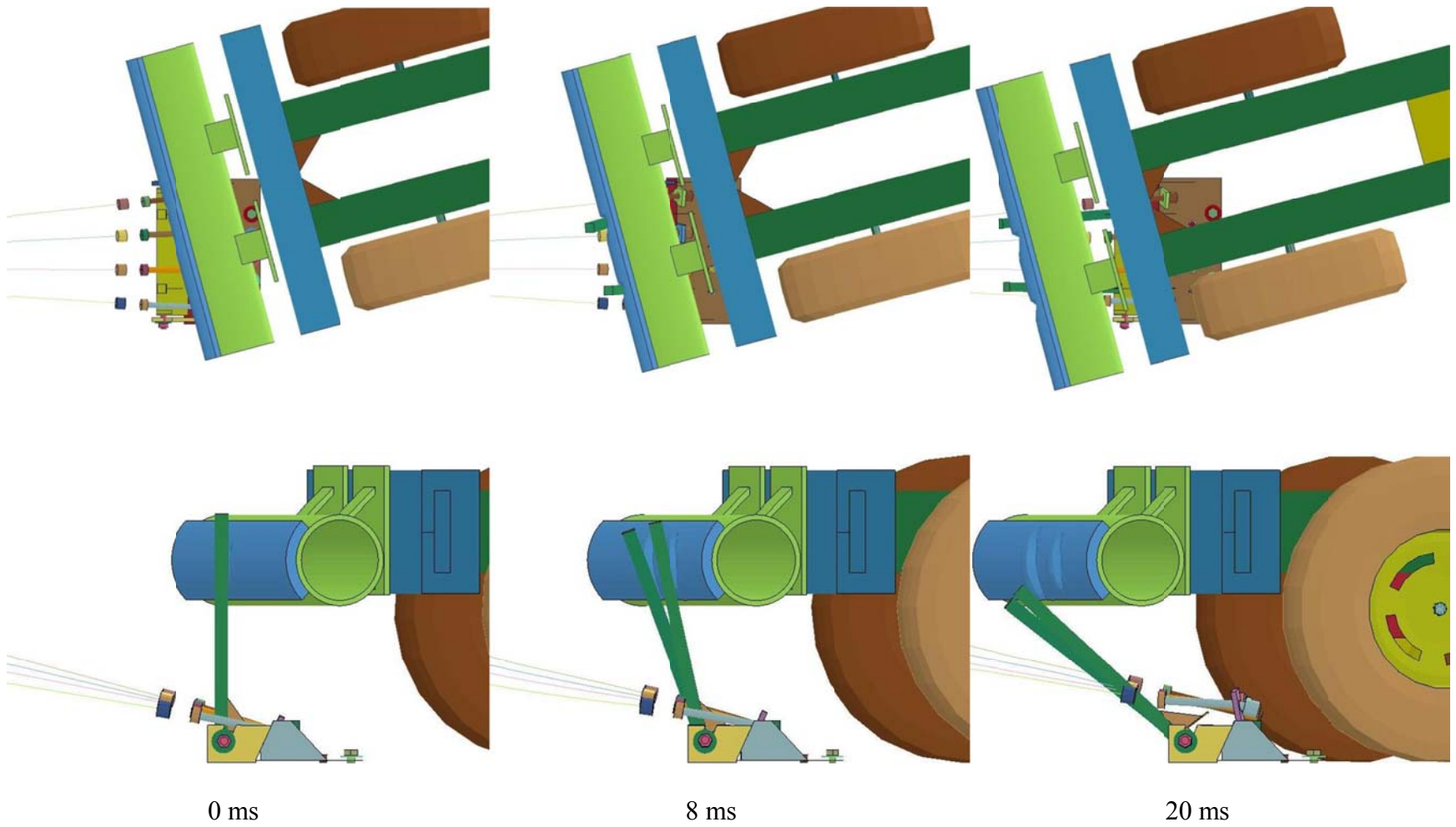


Figure 92. 15 Degree Impact Scenario Sequentials, Simulation No. 6



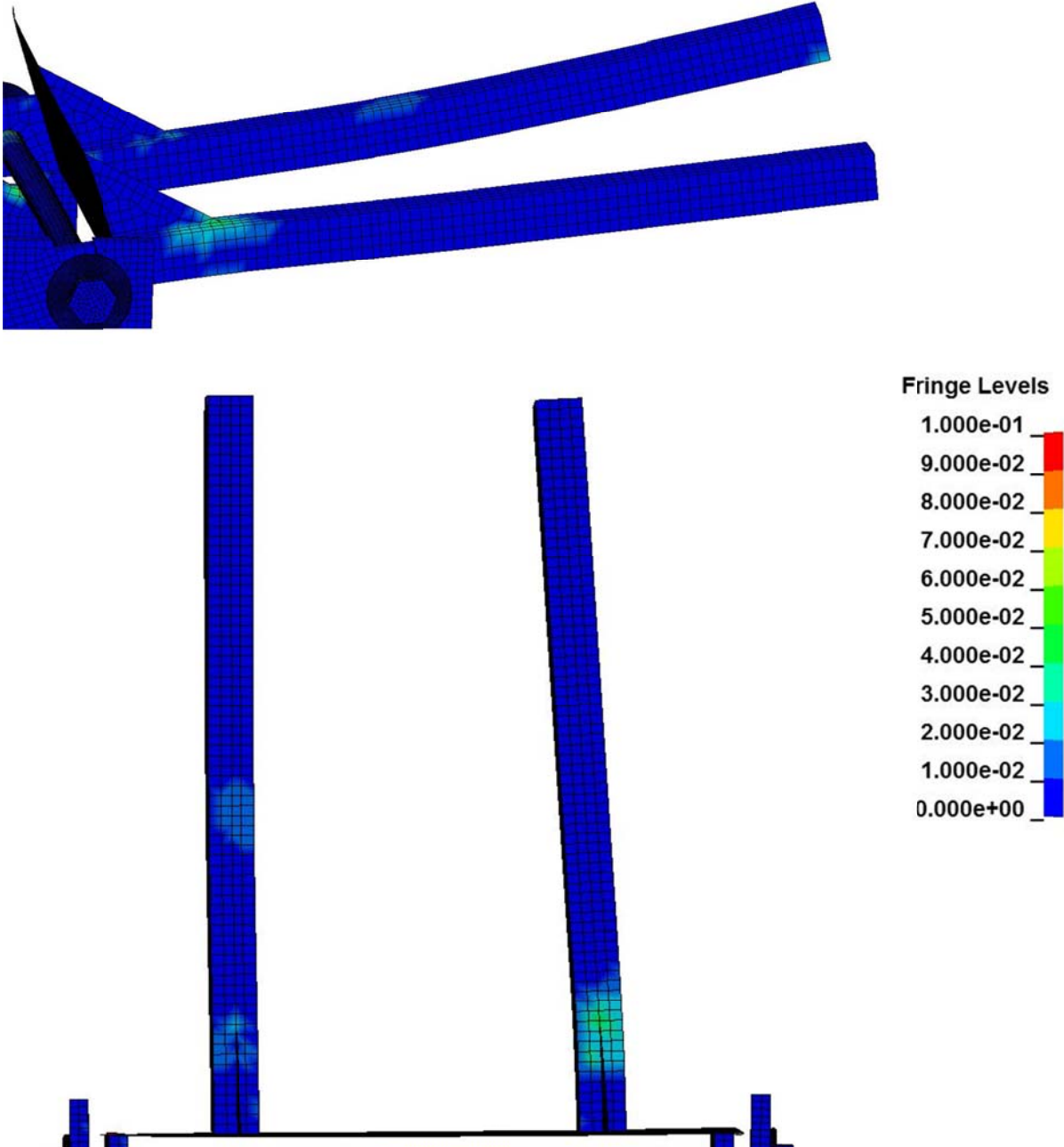


Figure 93. Cable Release Lever Plastic Strain, Simulation No. 6

**9.3.2.7 Simulation No. 7 - Reverse Direction Impact**

Since the redesigned cable anchor bracket assembly is intended to be used in median applications, the possibility exists that the anchor will be subjected to a reverse direction impact.

To analyze this scenario, the bogie model was oriented behind the cable anchor bracket assembly at an angle of 25 degrees. The bogie head was aligned with the center of the redesigned anchor bracket assembly. The 25 degree impact angle was selected to reflect impact orientation requirements for MASH Test No. 3-37. The initial model setup is shown in Figure 94.

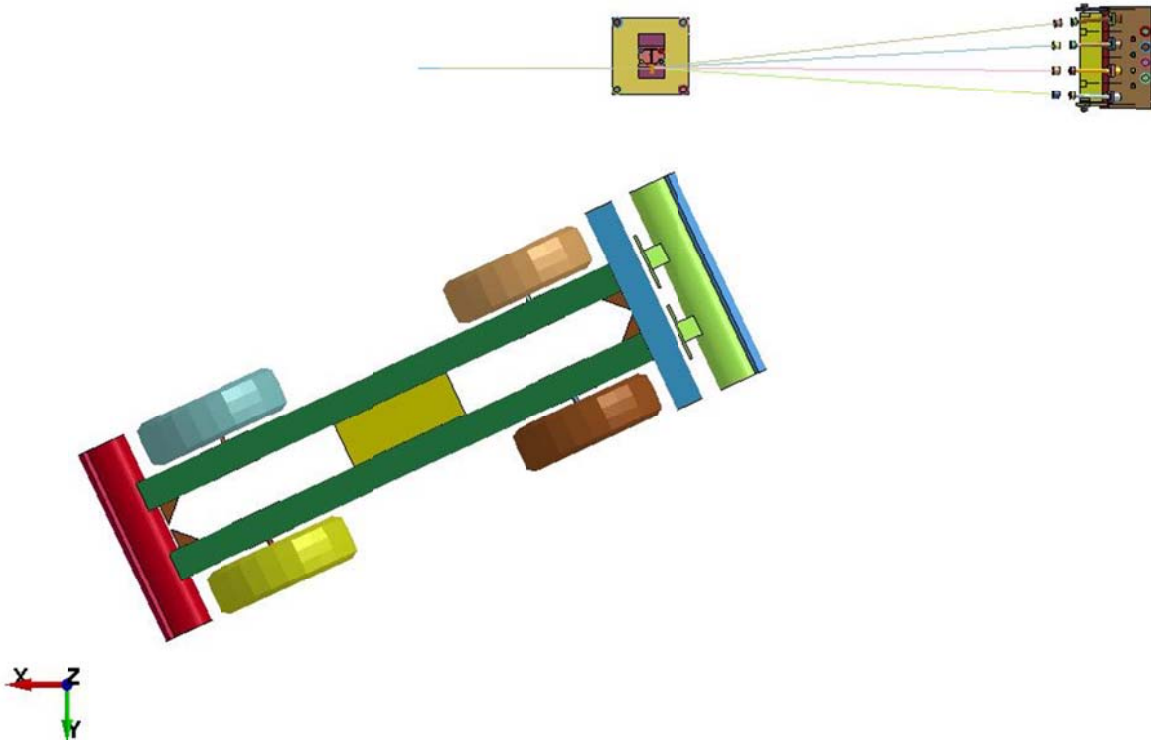


Figure 94. Bogie Impact Orientation, Simulation No. 7

Due to the orientation of the bogie and the nature of the simulation, the left-front bogie wheel made initial contact with the system, impacting the system cables in between the anchor and the slip base post. This impact rotated the cable end fitters in the cable slots on the anchor and resulted in slightly increased cable tension at impact, however it had no other significant effect on the simulation. The bogie head impacted one vertical impact tube and began to bend it backwards. The rotational bolt began to slide upwards in the support bracket immediately after impact. The cable release lever rotated backwards as it translated up in the slot. Due to geometric

constraints, the upward motion of the cable release lever was facilitated by deformation in both the support bracket slots and deformation in the rotational bolt. The bolt was fully removed from the slots in both brackets roughly 18 ms after initial bogie impact with the vertical impact tube.

As the cable release lever was displaced upwards, it also began to force the cables end fitters out of their respective slots on the cable plate. The cables were fully released from the cable plate at roughly 21 ms after initial bogie impact with the vertical impact tube. Sequential images of the simulation are shown in Figure 95. Note that in the side view of the simulation, the right-front wheel of the bogie has been hidden to clarify the behavior of the release lever assembly.

There was significant plastic bending in the vertical impact tube that was initially impacted as well as the cable release lever cable plate. Both support brackets and the rotation bolt also sustained significant plastic deformation. The permanent damage to the cable release lever assembly, support brackets, and rotation bolt is shown in Figure 96.

Although the anchor bracket assembly would require significant repair after impact, the release lever was allowed to disengage from the anchor bracket assembly during the reverse direction impact. This ability greatly reduces any concerns that a vehicle will snag on the cables or impact lever in a reverse direction impact. Although the redesigned anchor bracket assembly model exhibited potential in the reverse direction impact simulation, physical testing is still necessary to definitively evaluate the reverse direction release mechanics.



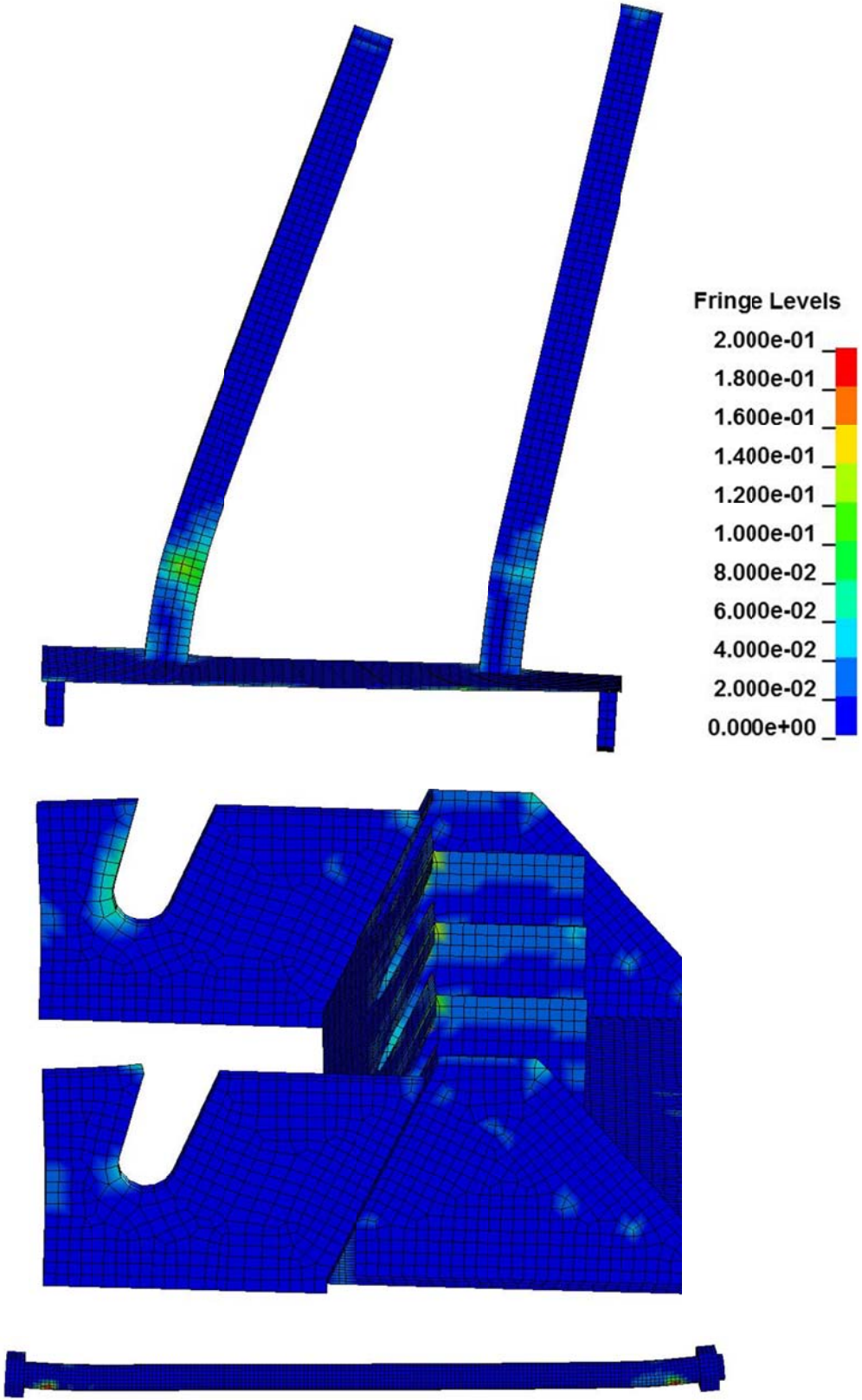


Figure 96. Component Plastic Strain, Simulation No. 7

## **9.4 Final Design and Simulation**

### **9.4.1 Final Redesigned Cable Anchor Bracket Assembly**

The simulation of the redesigned cable anchor bracket assembly exhibited good mechanics and behavior in simulation nos. 4, 5, 6, and 7. To fully evaluate the final design, the scenario when both vertical tubes were impacted was simulated. Results from the final simulation could also be used to compare the final design to initial concepts as well as the current, high-tension, cable anchor bracket assembly. The final finite element model of the cable anchor bracket assembly is shown in Figure 97. Technical drawings of the cable anchor bracket assembly are shown in Figures 98 through 102.

### **9.4.2 Simulation**

The bogie model was given an initial velocity of 45.0 mph (72.4 km/h). The center of the bogie's impact head was aligned with the center of the release lever. An automatic single surface contact was used to specify contact between the slip base post assembly, cable anchor bracket assembly, and the bogie impact head. An automatic nodes to surface contact was used with the cable model to better capture the cable interaction with the cable hangar, bogie impact head, and any other system components that may contact the cables.

Initial impact was between the center of the bogie head and the center of the cable release lever. A sequential description of the impact events is contained in Table 11. Sequential images of the simulation are shown in Figure 103. Note that the outer wheel of the bogie is not shown to clarify the release mechanics of the anchor assembly.

Damage to the cable anchor assembly was minimal. The cable plate sustained no plastic deformation. The rotational joint for the cable release lever remained intact throughout the impact event. The only component of the rotational joint that sustained permanent damage was

the rotational bolt. Other structural components of the anchor assembly had no deformation. Post-test images of the anchor bracket assembly at the conclusion of simulation are shown in Figures 104 through 106.

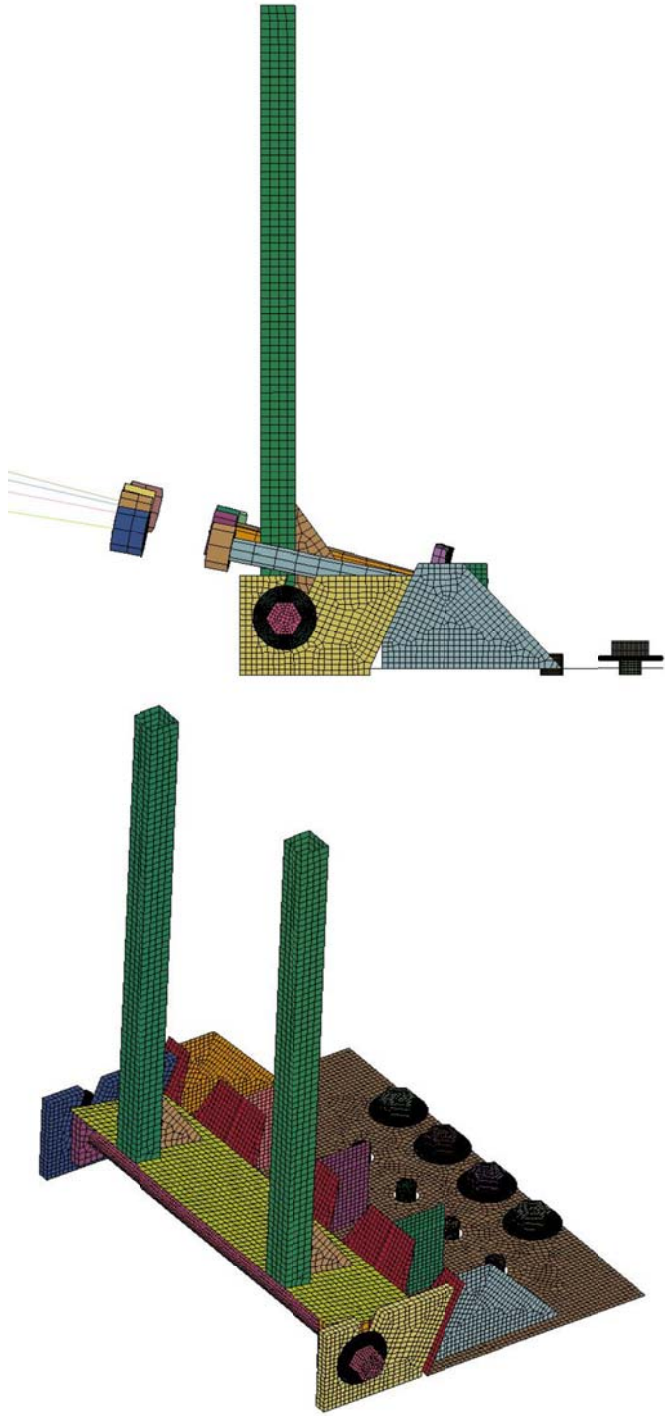


Figure 97. Redesigned, High-Tension, Cable Anchor Bracket Assembly Model

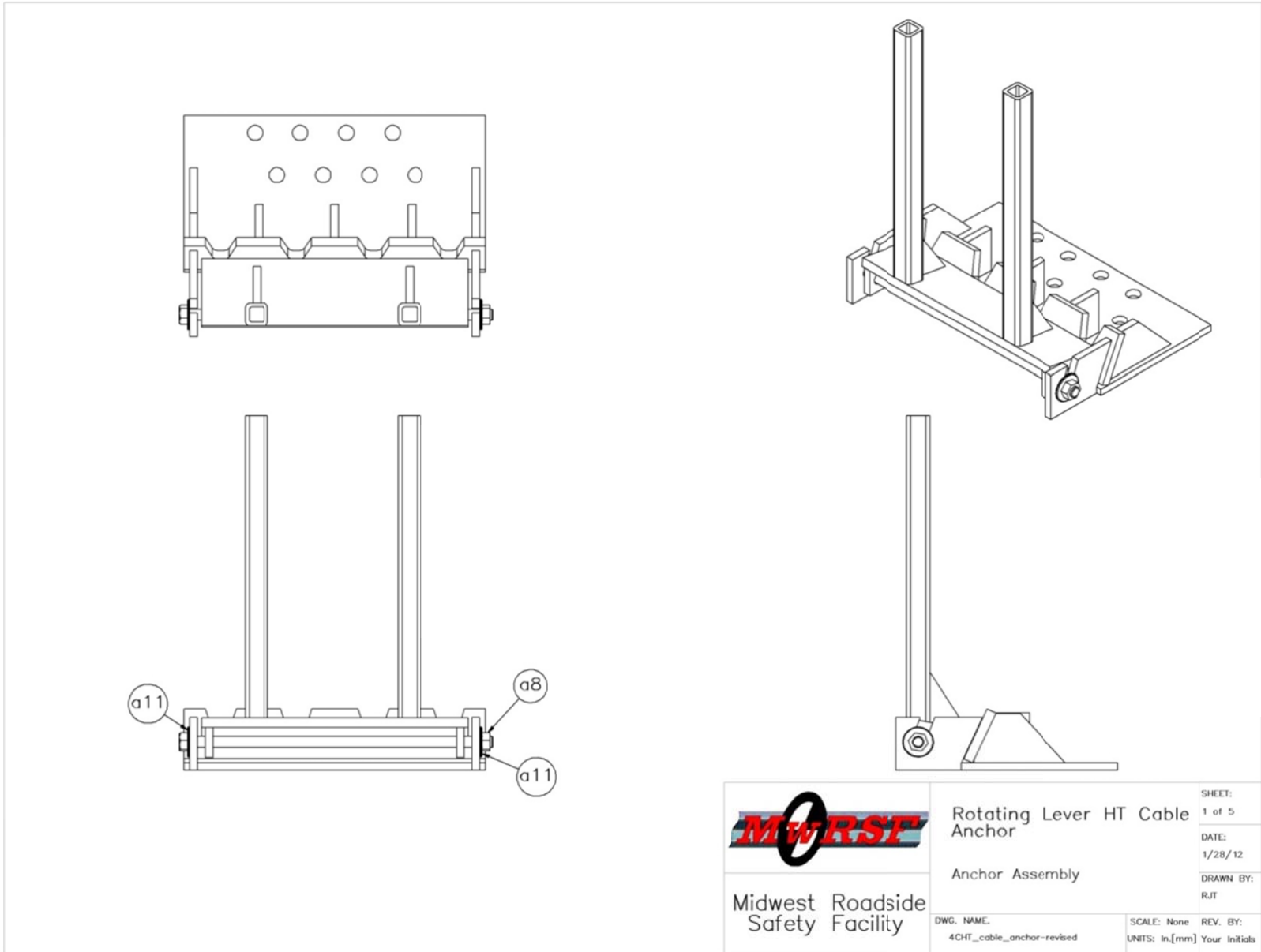


Figure 98. Redesigned, High-Tension, Cable Anchor Bracket Assembly



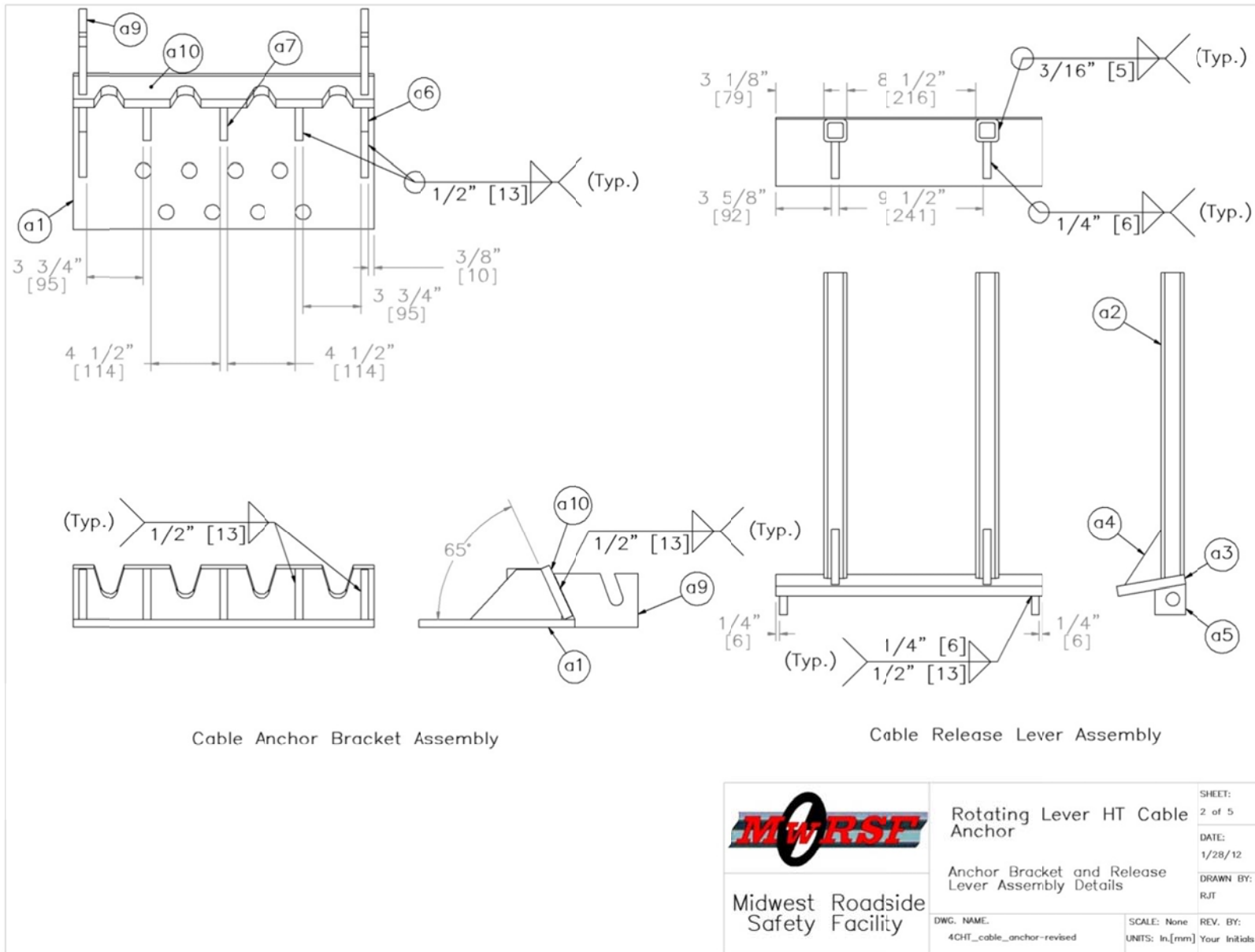


Figure 99. Cable Anchor Bracket and Cable Release Lever Assembly Details

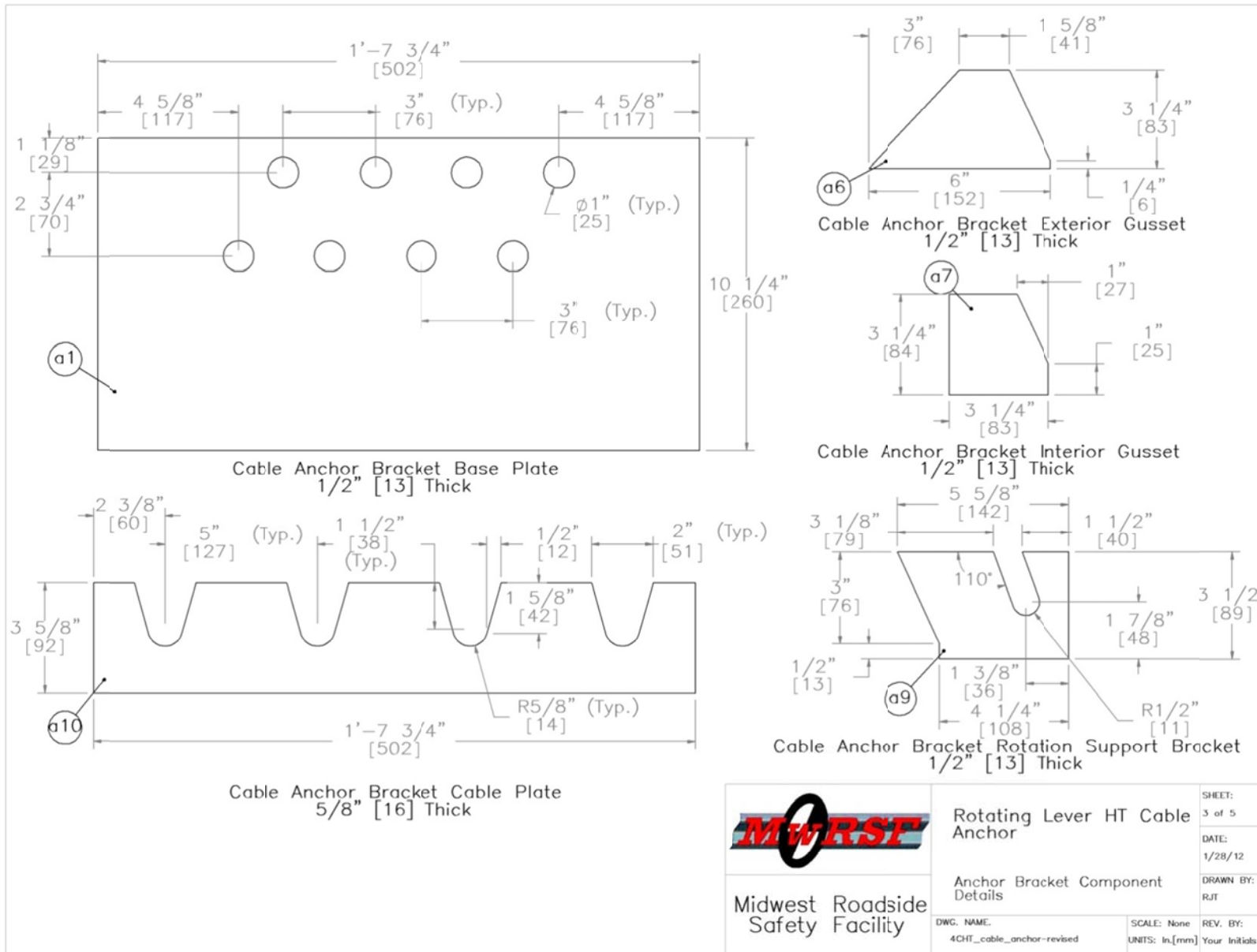


Figure 100. Cable Anchor Bracket Component Details

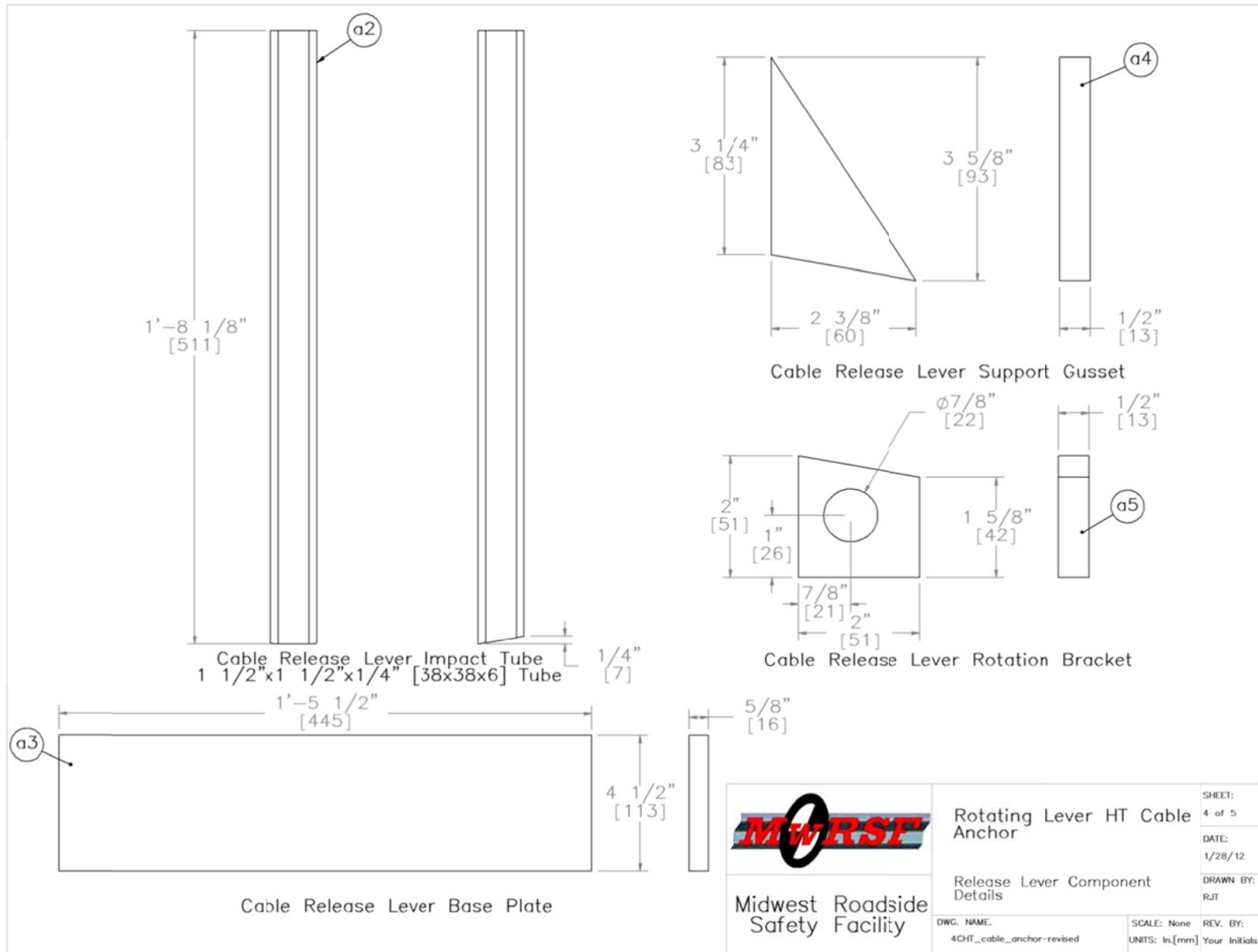


Figure 101. Cable Release Lever Component Details

Item No.	QTY.	Description	Material Specification
a1	1	Cable Anchor Bracket Base Plate	ASTM A36 Steel
a2	2	Cable Release Lever Impact Tube	ASTM A500 Grade B
a3	1	Cable Release Lever Base Plate	ASTM A36 Steel
a4	2	Cable Release Lever Support Gusset	ASTM A36 Steel
a5	2	Cable Release Lever Rotation Bracket	ASTM A36 Steel
a6	2	Cable Anchor Bracket Exterior Gusset	ASTM A36 Steel
a7	3	Cable Anchor Bracket Interior Gusset	ASTM A36 Steel
a8	1	ϕ3/4" Rod with Threaded Ends and Nuts	ASTM A307
a9	2	Cable Anchor Bracket Rotation Bracket	ASTM A36 Steel
a10	1	Cable Anchor Bracket Cable Plate	ASTM A36 Steel
a11	2	ϕ3/4" Flat Washer	ASTM F844


	Rotating Lever HT Cable Anchor	SHEET: 5 of 5
	Bill of Materials	DATE: 1/28/12
Midwest Roadside Safety Facility	DWG. NAME: 4CHT_cable_anchor-revised	SCALE: 1:100 UNITS: In,[mm]
		REV. BY: Your Initials

Figure 102. Redesigned, High-Tension, Cable Anchor Bracket Bill of Materials

Table 11. Sequential Description of Impact Events, Final Redesign

TIME (sec)	EVENT
0.000	The cable release lever began to rotate backward smoothly and evenly immediately after initial impact with the bogie head.
0.022	All four system cables have been released from their respective slots on the cable anchor bracket.
0.044	The top of the cable release lever impacted the ground. After the lever rebounded, it remained connected to the cable anchor bracket assembly.
0.061	The bogie head impacted the top system cable.
0.065	The bogie head impacted the remaining three system cables simultaneously. All four cables are now in contact with the bogie head and begin to coil against it.
0.107	The bogie head impacted the upstream side of the slip base post.
0.125	The bottom slip base post base plate separated from the slip base post support plates. The failure of the slip base post was due to element erosion along the boundary between the bottom slip base post plate and the slip base post support plates.

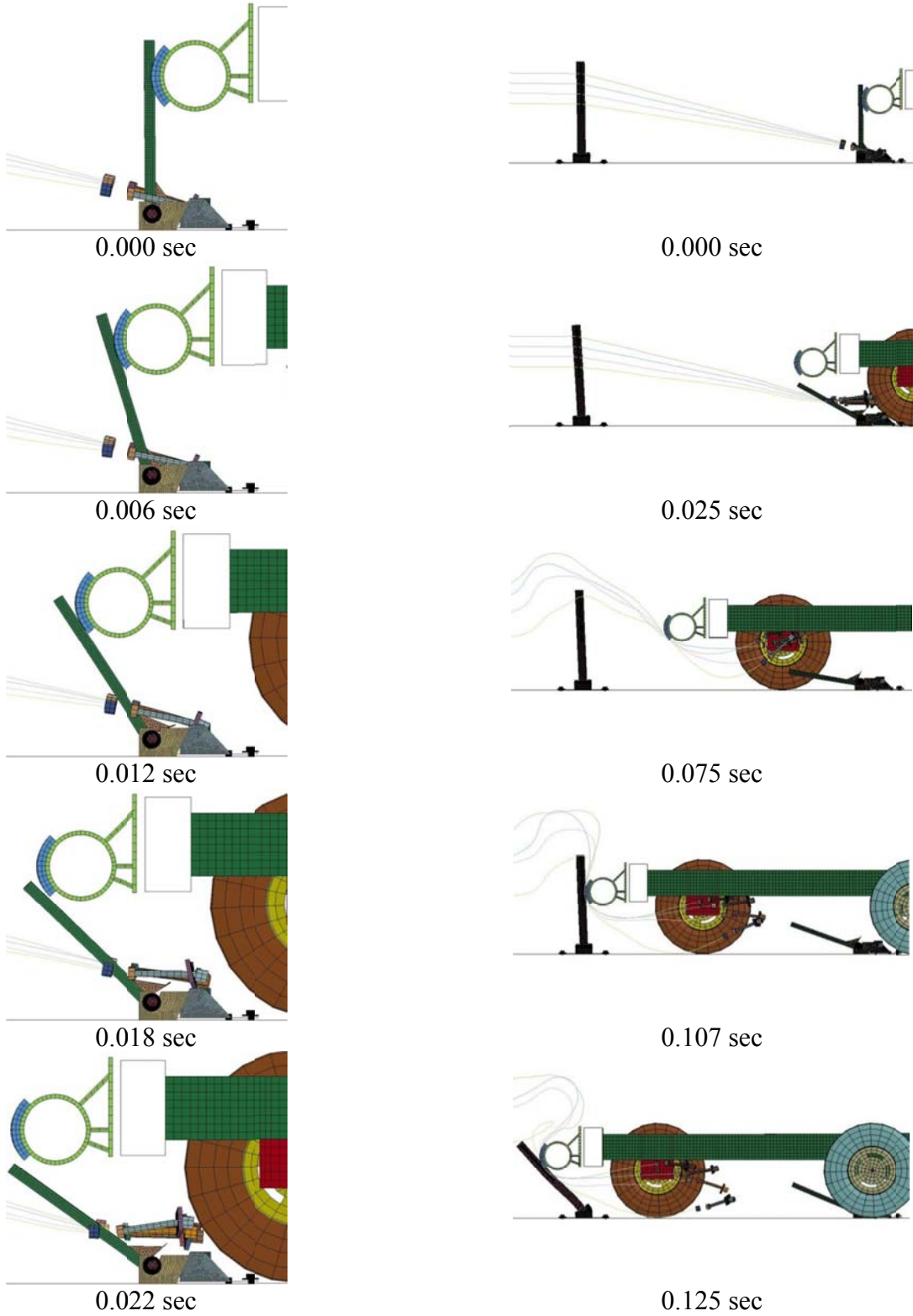


Figure 103. Sequential Photographs, Final Redesign

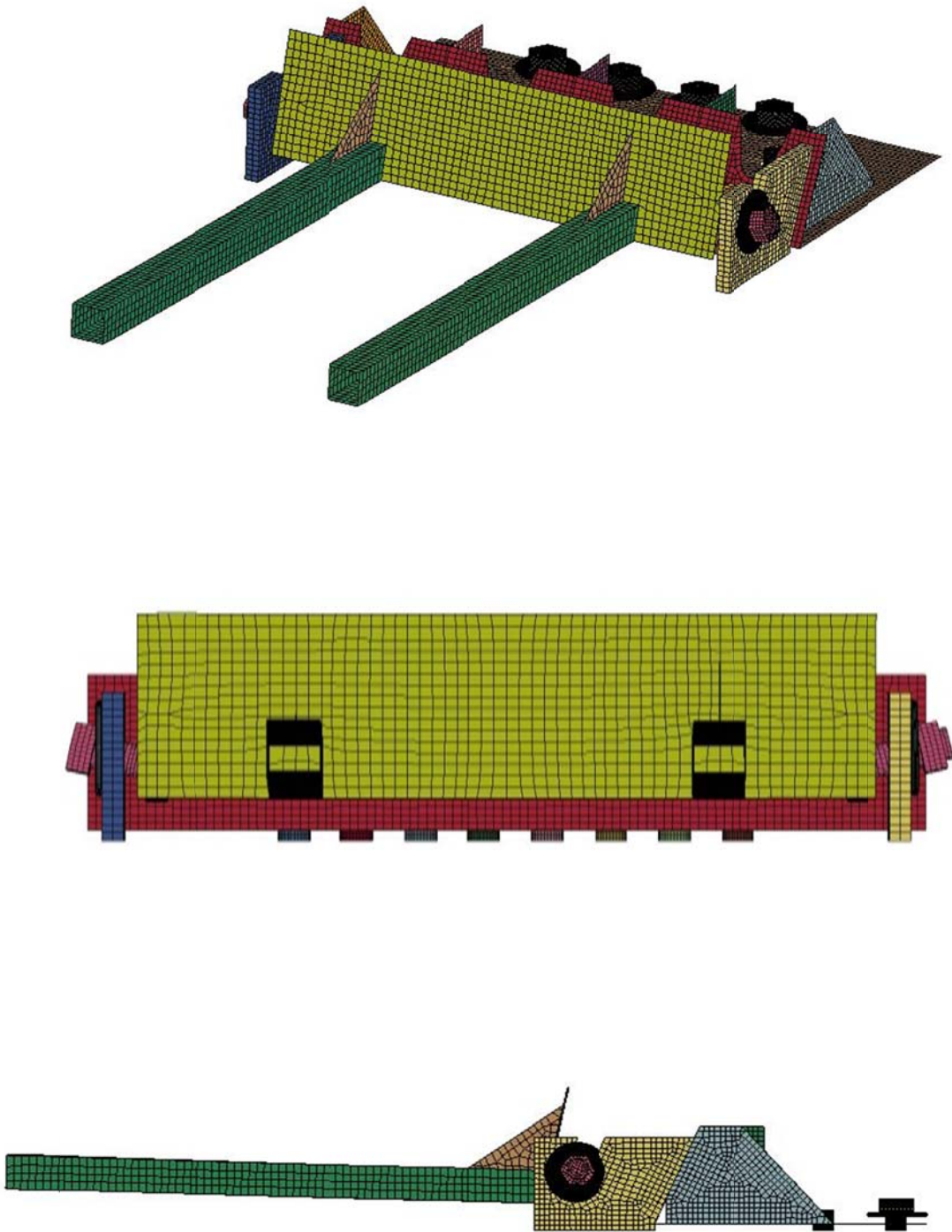


Figure 104. Cable Anchor Bracket Assembly Damage, Final Redesign

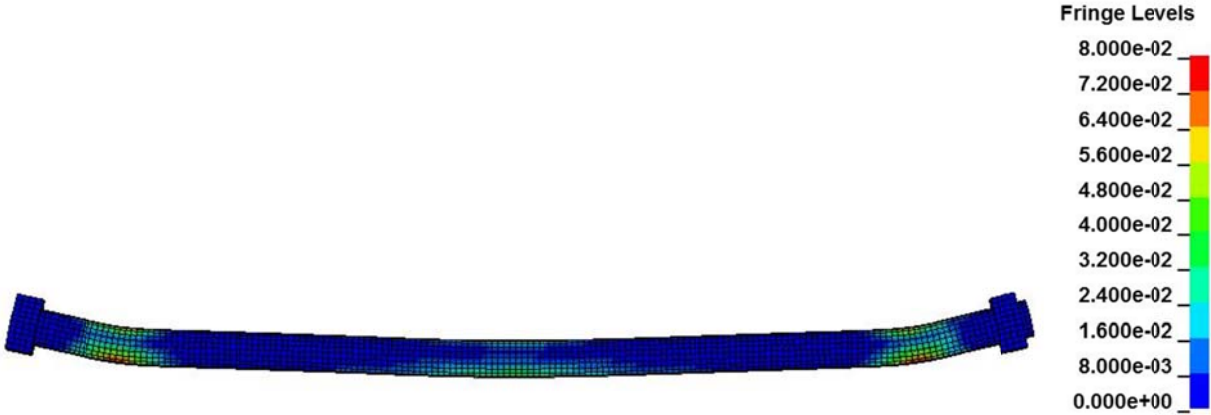


Figure 105. Plastic Strain in Rotational Bolt, Final Redesign

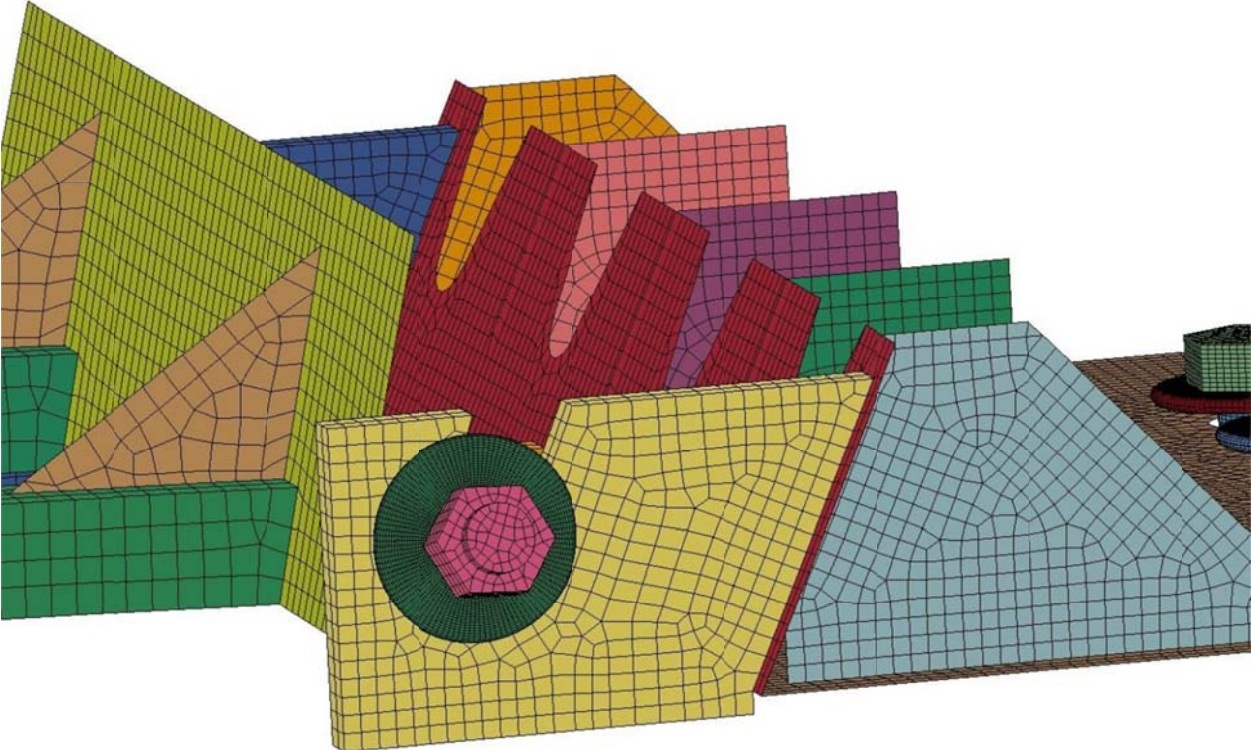


Figure 106. Cable Anchor Components After Cable Release, Final Redesign

After impact, the change in velocity due to impact with the anchor bracket assembly and the release of the cables was 0.48 mph (0.77 km/h). After the release of the cables, the bogie maintained a velocity of roughly 44.5 mph (71.6 km/h). The bogie experienced a linear decrease in velocity due to the cables coiling against the impact head beginning at roughly 63 ms. The



cable interaction resulted in a total  $\Delta v$  of 0.38 mph (0.61 km/h). The bogie then impacted the slip base post which resulted in a  $\Delta v$  of 1.25 mph (2.01 km/h). The bogie's velocity during the simulation is shown in Figure 107.

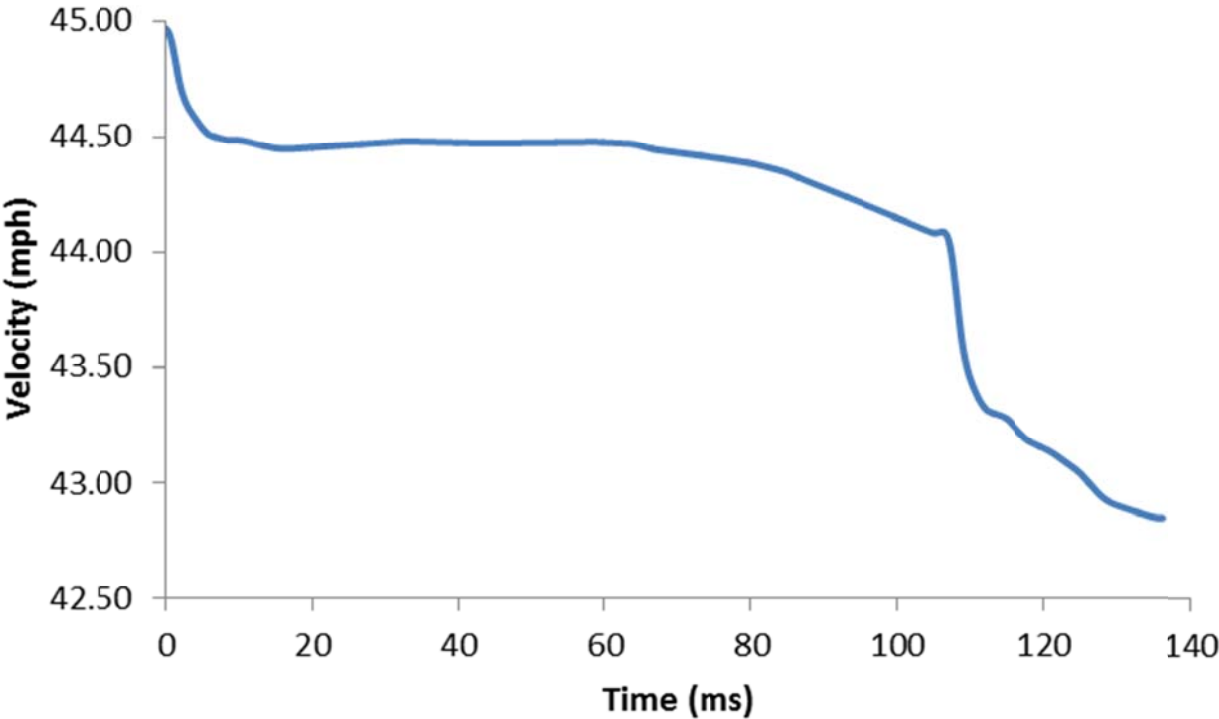


Figure 107. Bogie Velocity, Final Redesign

**9.4.3 Discussion**

The rotating lever released the cables as designed, eliminating any risk of the vehicle riding up the cables and potentially causing injury to vehicle occupants. At the conclusion of the simulation, the cable release lever was successfully retained by the cable anchor bracket assembly. By retaining the cable release lever assembly, any risk of the vehicle overriding the assembly and causing unstable trajectories or undercarriage damage would be eliminated.

Another goal of the redesign was to make the cable anchor bracket assembly reusable. The current, high-tension, cable anchor design as well as previous designs exhibited plastic

deformation in the cable plate flanges after release of the cables. To eliminate the damage, the thickness of the cable plate was increased. The structural cable anchor gussets used to support the cable plate were also modified to reduce any bending in the cable plate flanges. The height of the interior gussets was increased to provide extra support during the release of the cables. The increased gusset height also increased the weldable area between the structural gussets and the cable plate.

These modifications eliminated much of the plastic deformation to the assembly, and in many impact scenarios would ultimately allow the assembly to be reused through multiple impacts. The maximum von Mises' stress in the cable plate was reduced from 58.5 to 48.4 ksi (403.3 to 333.7 MPa). The final simulation showed no permanent deformation to the cable anchor bracket assembly. Based on analysis of the simulation results and engineering judgment, a replacement of the rotational bolt would allow the assembly to be reused without concern for structural adequacy or unintended release mechanics upon impact. Substituting the currently specified bolt in the assembly with one fabricated from a higher grade steel could potentially eliminate the deformation entirely, and is also an option. The maximum stress in the anchor bracket components are shown in Figure 108.

The bogie velocity from the simulation with the current, high-tension, cable anchor bracket assembly design as well as that of the redesigned anchor bracket assembly exhibited similar trends. The  $\Delta v$  due to impacts were 0.48 mph (0.77 km/h) and 0.56 mph (0.90 km/h) for the redesign and current simulations, respectively. As such, the impact severity due to the bogie's impact with the cable release lever was reduced in the redesigned anchor bracket assembly simulation as compared to the simulation with the current anchor bracket assembly. The impact severity from the redesigned, high-tension, cable anchor bracket assembly was

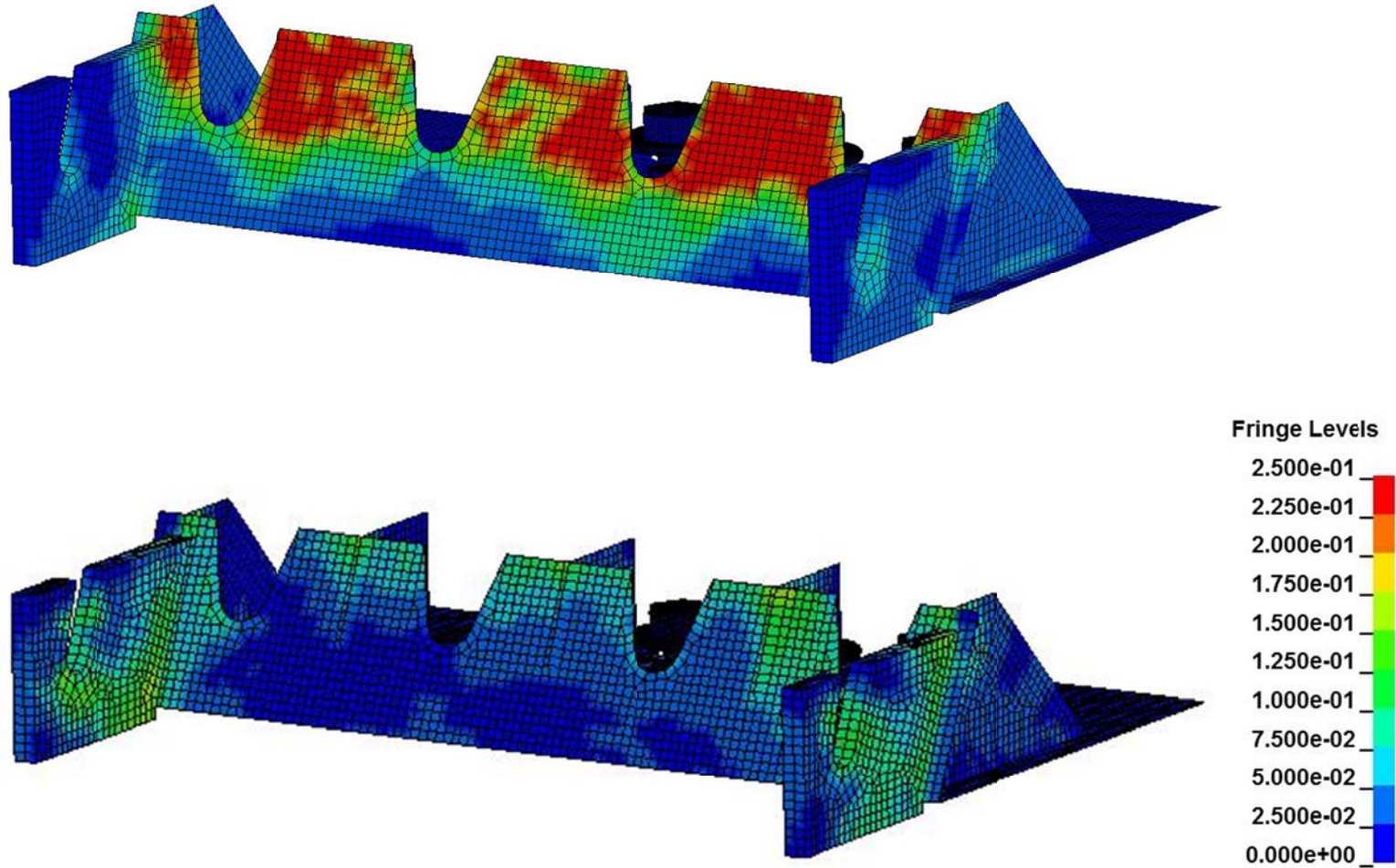


Figure 108. Comparison of Anchor Assembly von Mises' Stress Distribution

166.44 lb-in. (18.81 N-m) compared to 225.72 lb-in. (25.50 N-m) for the current anchor bracket assembly. The differences in impact severities resulted in a 26 percent reduction between the current design and the redesigned cable anchor bracket assembly. A comparison of the bogie velocity in the current, high-tension, cable anchor bracket assembly simulation and the redesigned, high-tension, cable anchor bracket assembly simulation is shown in Figure 109.

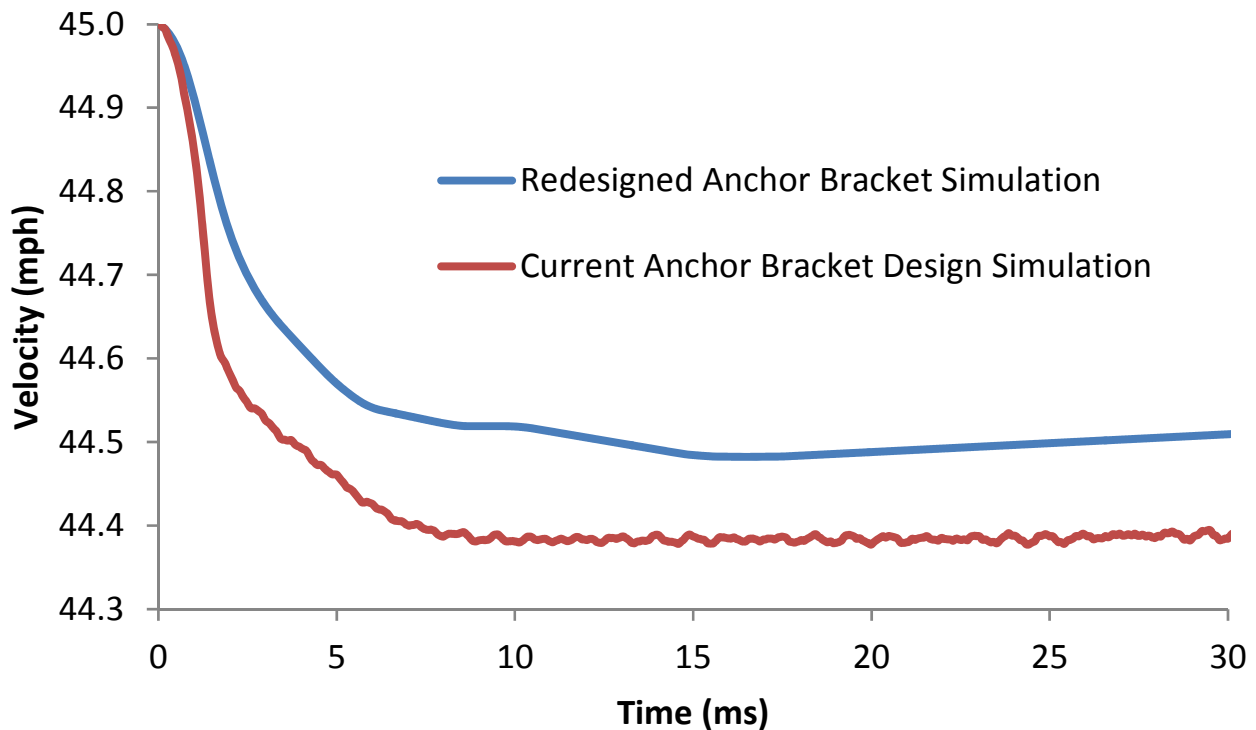


Figure 109. Anchor Bracket Assembly Simulations Velocity Comparison

The primary reason for the reduction in impact severities was due to the change in the overall height in the cable anchor bracket assembly. Since the whole assembly was restricted to a 4-in. (102-mm) maximum height, the anchor point for the cables on the cable plate had to be lowered. The cable release lever support assembly was also lowered to properly align with the cable slots. By lowering the cables and the cable release lever assembly, the moment arm for the impacting vehicle was increased. The increased moment arm allows impacting vehicles to

release the cables with less applied force, thus lowering decelerations and  $\Delta v$ . One consequence of increasing the moment arm is that the vertical, cable release tubes will be subjected to higher bending stresses. However, after review of the simulation results, there was no indication that tube deformation would be a potential issue.

The redesigned, high-tension, cable anchor bracket assembly performed well in simulations with an abbreviated cable end terminal model. The redesigned hardware eliminated many of the crash performance issues that were identified with the current, high-tension, cable anchor bracket assembly. Although the new design has only been evaluated through numerical modeling, previous comparisons between simulation models and physical testing yielded good initial agreement. Therefore, it is recommended that the redesigned cable anchor bracket assembly be subjected to physical component testing to further evaluate its crashworthiness.

## **10 SUMMARY, CONCLUSIONS, AND RECOMMENDATIONS**

### **10.1 Summary**

A new, non-proprietary, high-tension, cable end terminal design was investigated to provide State DOT's with an alternate option to the proprietary designs that are currently available. A literature review of high-tension, cable end terminals revealed that cable anchors with a means of releasing the system cables provided a more crashworthy and robust end terminal system. Terminal post characteristics were also critical to the success of the system. Weak-sectioned terminal posts reduced the threat of vehicle rollover in the case of end-on, terminal impacts.

A study of the non-proprietary, low-tension end terminal system developed by MwRSF was conducted. The high vehicle roll and yaw angles exhibited in test no. CT-4 were the result of a combination of initial vehicle yaw motion as well as vehicle interaction with system debris, including detached slip base post sections and the cable release lever.

Due to the contribution of the low-tension, cable anchor bracket assembly to the vehicle trajectory in test no. CT-4, and the similarities between the low-tension, anchor bracket and the current, high-tension, cable anchor bracket design, a further analysis of the high-tension, anchor bracket assembly was deemed necessary. Simulation and bogie testing were used to study the assembly. Analysis showed that the current, high-tension, cable anchor bracket assembly exhibited similar behavior and cable release mechanics as the previously-tested, low-tension, cable anchor bracket assembly. Thus, there was concern that similar vehicle instabilities may be witnessed during full-scale crash testing of the current design.

Therefore, the high-tension, cable anchor bracket assembly was redesigned to improve the crashworthiness of the assembly and end terminal system as a whole. The redesigned

assembly was shortened to conform to MASH stub height criteria for breakaway devices. The front end of the assembly was redesigned in order to retain the cable release lever. The redesigned cable anchor bracket assembly was modeled, simulated, and analyzed. The assembly released the cables in a similar manner as both the non-proprietary, low-tension and current, high-tension, cable anchor bracket assemblies. The anchor bracket assembly successfully retained the cable release lever after release of the cables. The retention of the cable release lever eliminates any potential for undercarriage damage or vehicle interaction with the lever further into the system. Additionally, the modified design reduced the impact severity between the vehicle and the vertical, cable release tubes by 26 percent, as compared with the current, non-proprietary, cable anchor design.

Various alternate impact simulations were conducted including scenarios where only one vertical tube was impacted, reverse direction impacts, angled, frontal impacts, and impacts with cable tensions at higher than design specification. Although there was some plastic deformation exhibited in alternate impact simulations, the cables were released as intended, or in the case of the reverse direction impact, the cable release lever disengaged from the anchor bracket as designed. Since these scenarios represent non-ideal impact situations, the plastic deformation was deemed acceptable. Technical drawings for the assembly were provided in Section 9.4.1.

The investigation of test no. CT-4 also showed that the slip base post may be a less than ideal option for terminal applications. Although the initial impacts with slip base posts did not produce rollover, secondary impacts with slip base post assembly debris resulted in high roll angles and vehicle instabilities.

An analysis of the standard M4x3.2 (M102x4.8) post or a weakened S3x5.7 (S76x8.5) post showed that they may be viable replacement options for the slip base post in the terminal.

All alternate post sections have a diminished bending strength in the weak-axis direction, as compared with an S3x5.7 (S76x8.5) post. The lower strength in the weak-axis direction may prevent the vehicle from ramping up the post during end-on impacts. Also, the post would not introduce any debris into the path of the vehicle that could be hazardous to the stability of the vehicle and the safety of the occupants. Further investigation is required, however, before a decision can be made regarding a selection of a terminal post type.

## **10.2 Conclusions and Recommendations**

Results from all aspects of the study were combined to form the following final set of recommendations for future development of a non-proprietary, high-tension, cable end terminal design:

- Replace the current, high-tension, cable anchor bracket assembly with redesigned anchor bracket assembly;
- further investigate the M4x3.2 (M102x4.8) post or comparable weak-sectioned post for use in the terminal region through simulation, bogie testing, and full-scale testing; and
- further investigate the implications of reduced terminal post torsional stiffness on redirection terminal impacts to determine if a 16-ft (4.9-m) terminal post spacing is still adequate.

A redesigned non-proprietary, high-tension, cable anchor showed promising results in simulations. The redesigned anchor released the system cables when impacted end-on and successfully retained the cable release lever after the impact event. Although the redesigned cable anchor bracket assembly would require physical bogie testing to further evaluate the design, simulation results indicated that the redesigned assembly has potential to improve the safety and crashworthiness of the non-proprietary, high-tension, cable end terminal design.



Based on the study of current cable end terminal systems, it is recommended that further investigation of an alternate terminal post for the non-proprietary, high-tension, cable end terminal design be undertaken. The non-proprietary, low-tension design utilized slip base posts in the terminal region. These post assemblies, however, caused high vehicle roll and yaw angles in full-scale crash testing due to detached post sections interacting with the undercarriage of the test vehicle. In order to prevent system debris from causing vehicle stability issues in future tests, the slip base posts could potentially be replaced with an assembly that does not completely detach from its base, but rather is retained throughout the impact event. Preliminary investigation indicated that an M4x3.2 (M102x4.8) post, weakened S3x5.7 (S76x8.5) post, or similar weak-sectioned post may be viable replacement options. However, these alternatives require further investigation prior to full-scale crash testing.

Finally, a 16-ft (4.9-m) terminal post spacing was utilized in the low-tension, cable end terminal test series (CT series). No issues were discovered during analysis of the crash test series that were directly related to the terminal post spacing. Furthermore, in end terminal simulations the post spacing did not negatively affect the crashworthiness of the system. However, if one of the recommended alternate post sections is selected for use in the terminal region, further investigation may be required. Due to the alternate terminal post's reduced torsional stiffness, as compared with an S3x5.7 (S76x8.5) section, it is unclear whether an M4x3.2 (M102x4.8) post or modified S3x5.7 (S76x8.5) post would be able to adequately support the system cables in a redirection terminal impact.

Other approved, high-tension, cable end terminal designs utilize post spacing of 90 in. (2,286 mm) or less. The benefit of such short post spacing is that the extra posts provide

increased support for the system cables in redirecting impacting vehicles. If larger post spacing is adequate for redirecting impacting vehicles, the system would be cheaper and simpler to install.

Other primary features of the terminal system, such as cable tension and number of system cables, are dependent upon the design of the non-proprietary, high-tension, cable guardrail system, which is still in development. At the time of the research and design of the non-proprietary, high-tension, cable end terminal, the utilized features reflected the latest revision of the high-tension guardrail system.

### **10.2.1 Future Work**

The conclusions and recommendations presented in the previous sections are the result of the conducted research, development, and analysis of high-tension, cable guardrail end terminal components. Although the redesigned, high-tension, cable anchor bracket assembly design exhibited good mechanics in simulation, the design should be subjected to component testing to validate the simulation results and further evaluate its functionality. Other recommendations including certain alternate terminal post types should also undergo component testing to fully assess their strength properties. The following component tests are recommended to further evaluate the proposed designs:

- bogie test with the redesigned cable anchor assembly in abbreviated end terminal with inline orientation;
- bogie test with the redesigned cable anchor with 15-degree impact orientation; and
- bogie tests with the M4x3.2 (M102x4.8) post and S3x5.7 (S76x8.5) post with weakening holes to determine dynamic bending strength properties of each post type so that comprehensive comparison between terminal post options can be made.

Simulation of alternate terminal posts and post spacing can also be used to preliminarily evaluate configurations of posts and post spacing to determine which show potential for use in full-scale crash testing of a new end terminal system.

If no design issues or concerns are exposed during component testing, full-scale testing can be accomplished. Full-scale crash testing of the non-proprietary, high-tension, cable guardrail end terminal design to MASH terminal requirements is necessary for FHWA acceptance. Testing of the terminal's length of need can be utilized to definitively evaluate terminal post spacing. A summary of MASH testing requirements and recommendations for a full-scale testing program with the new, non-proprietary, high-tension, cable end terminal system is shown in Table 12. Note that some tests may be deemed less critical after component testing has been accomplished and evaluated. Only after a full evaluation of the non-proprietary, high-tension, cable guardrail end terminal through full-scale crash testing can the terminal be implemented along state highways and roadways.

Table 12. Recommended MASH Testing

Test No.	Vehicle Type	Impact Speed mph (kph)	Impact Angle (Degrees)	Impact Location	Recommended (Y/N)	Comment
3-30	1100C	62.1 (100)	0	Anchor - 1/4 Point Vehicle Offset	Y	Necessary to evaluate selection of terminal post and redesigned anchor
3-31	2270P	62.1 (100)	0	Anchor - Vehicle Centered	N	Small car stability is more critical test (3-30)
3-32	1100C	62.1 (100)	15	Anchor	Y	Necessary to evaluate small car stability and anchor release mechanics in non-ideal vehicle impact orientation on the anchor
3-33	2270P	62.1 (100)	15	Anchor	N	Small car stability in angled impact is more critical (3-32)
3-34	1100C	62.1 (100)	15	Critical Impact Point	N	Strength test of anchor is more critical (3-34)
3-35	2270P	62.1 (100)	25	Beginning of Length of Need	Y	Necessary to evaluate structural adequacy of the redesigned anchor
3-36	2270P	62.1 (100)	25	Critical Impact Point	N	Evaluation of anchor's structural characteristics more critical (3-35)
3-37	2270P	62.1 (100)	25	Reverse Direction	Y	Necessary to evaluate ability of redesigned anchor and cable release lever to disengage in a reverse direction impact without causing significant snag to vehicle or other potentially hazardous vehicle interaction
3-38	1500A	62.1 (100)	0	Anchor - Vehicle Centered	N	Small car stability is more critical test (3-30)

## 11 REFERENCES

1. Albin, D. and Milton, J., *Improving Highway Safety: Cable Median Barrier*, Washington State Department of Transportation, January 2004.
2. O'Hagan, D.C., *High Tension Cable Barriers*, Roadway Design Bulletin 07-08, Florida Department of Transportation, October 25, 2007.
3. *Guard Cable*, Technical Bulletin, Number 2, Missouri Department of Transportation, 2006.
4. Hitz, R.A., Molacek, K.J., Stolle, C.S., Polivka, K.A., Faller, R.K., Rohde, J.R., Sicking, D.L., Reid, J.R., and Bielenberg, R.W., *Design and Evaluation of a Low-Tension Cable Guardrail End Terminal System*, Final Report to the Midwest States' Regional Pooled Fund Program, Transportation Research Report No. TRP-03-131-08, Midwest Roadside Safety Facility, University of Nebraska-Lincoln, July 2008.
5. Griffith, M.S., FHWA NCHRP Report No. 350 approval letter CC-111 of low tension cable guardrail end terminal, To Dean L. Sicking, Midwest Roadside Safety Facility, Lincoln, NE, August 1, 2010.
6. Ross, H.E., Sicking, D.L., Zimmer, R.A., and Michie, J.D., *Recommended Procedures for the Safety Performance Evaluation of Highway Features*, National Cooperative Highway Research Program (NCHRP) Report 350, Transportation Research Board, Washington, D.C., 1993.
7. *Manual for Assessing Safety Hardware (MASH)*, American Association of State Highway and Transportation Officials (AASHTO), Washington, D.C., 2009.
8. Jacoby, C.H., FHWA NCHRP Report No. 350 approval letter CC-76 of terminal designed for use with a 3-strand cable guardrail, To Dean C. Alberson, Texas Transportation Institute, College Station, TX, August 29, 2002.
9. Baxter, J.R., FHWA NCHRP Report No. 350 approval letter CC-86 of BRIFEN wire rope gating terminal, To Derek W. Muir, Hill & Smith Ltd., Wolverhampton, West Midlands, United Kingdom, January 28, 2004.
10. Baxter, J.R., FHWA NCHRP Report No. 350 approval letter CC-92 of cable barrier terminal designed for use with the Gibraltar cable barrier; To Bill Neusch, Gibraltar, Burnet, TX, June 23, 2005.
11. Baxter, J.R., FHWA NCHRP Report No. 350 approval letter CC-93 of cable barrier terminal designed for use with Safence cable barrier, To Michael Kempen, Safence, Inc., Douglaston, NY, August 16, 2005.
12. Baxter, J.R., FHWA NCHRP Report No. 350 approval letter CC-105 of Armorwire terminal end for wire rope barrier systems, To Dallas James, Armorflex Ltd., North Harbor, Auckland, New Zealand, April 9, 2007.

13. Hallquist, J.O., *LS-DYNA Keyword User's Manual*, Livermore, CA, Livermore Software Technology Corporation, March 2001.
14. Terpsma, R.J., *Modeling and Validation of CT-4 Cable Anchor Bracket*, Mechanical Engineering 950 Term Project, University of Nebraska-Lincoln, December 2010.
15. Hiser, N.R., *Slip Base Modeling for Cable Guardrail Systems*, A Thesis Presented to the Faculty of The Graduate College at the University of Nebraska-Lincoln, April 2003.
16. Reid, J.D. and Coon, B.A., *Finite Element Modeling of Cable Hook Bolts*, 7<sup>th</sup> International LS-DYNA Users Conference, May 2002.
17. Reid, J.D., Hiser, N.R., and Paulsen, T.J., *Simulation and Bogie Testing of a New Cable Barrier Terminal*, International Mechanical Engineering Congress and Exposition, November 2003.
18. Luttig, M. and Lechtenberg, K.A., *Cut Cable Post Bogie Testing, Test Nos. CCP-1 through CCP-11*, Internal Report, Midwest Roadside Safety Facility, University of Nebraska-Lincoln, February 2012.
19. Kuipers, B.D. and Reid, J.D., *Testing of M203.7x9.7 (M8x6.5) and S76x8.5 (S3x5.7) Steel Posts - Post Comparison Study for the Cable Median Barrier*, Final Report to the Midwest States' Regional Pooled Fund Program, Transportation Research Report No. TRP-03-143-03, Midwest Roadside Safety Facility, University of Nebraska-Lincoln, October 2003.
20. Stolle, C.S., *A Concise Model of 3x7 Wire Rope Used in Cable Guardrail Systems*, A Thesis Presented to the Faculty of The Graduate College at the University of Nebraska-Lincoln, May 2010.
21. *DynaMax User's Manual*, Revision 1.75, Instrumented Sensor Technologies, Inc., Okemos, Michigan, April 1993.
22. Society of Automotive Engineers (SAE), *Instrumentation for Impact Test – Part 1 – Electronic Instrumentation*, SAE J211/1 MAR95, New York City, NY, July 2007.
23. Wiebelhaus, M.J., Johnson, E.A., Sicking, D.L., Faller, R.K., Lechtenberg, K.A., Rohde, J.R., Reid, J.R., Bielenberg, R.W., and Rosenbaugh, S.K., *Phase I Development of a Non-Proprietary, Four-Cable, High-Tension, Median Barrier*, Final Report to the Midwest States' Regional Pooled Fund Program, Transportation Research Report No. TRP-03-213-11, Midwest Roadside Safety Facility, University of Nebraska-Lincoln, December 2011.

## **12 APPENDICES**

## **Appendix A. Initial Simulation Results - Metric**



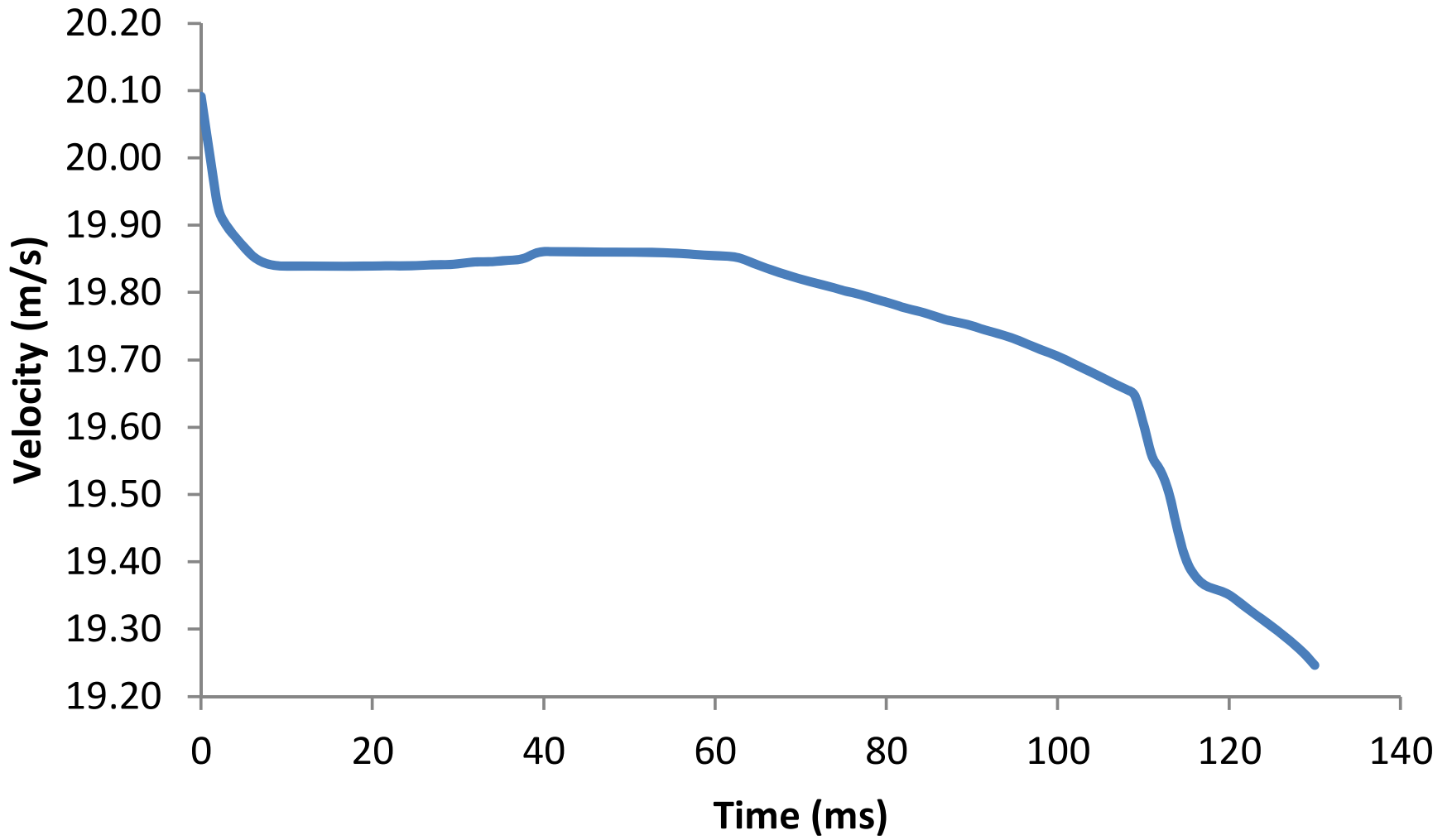


Figure A-1. Bogie Velocity, Initial Simulation

## **Appendix B. Bogie Test Results - Metric**

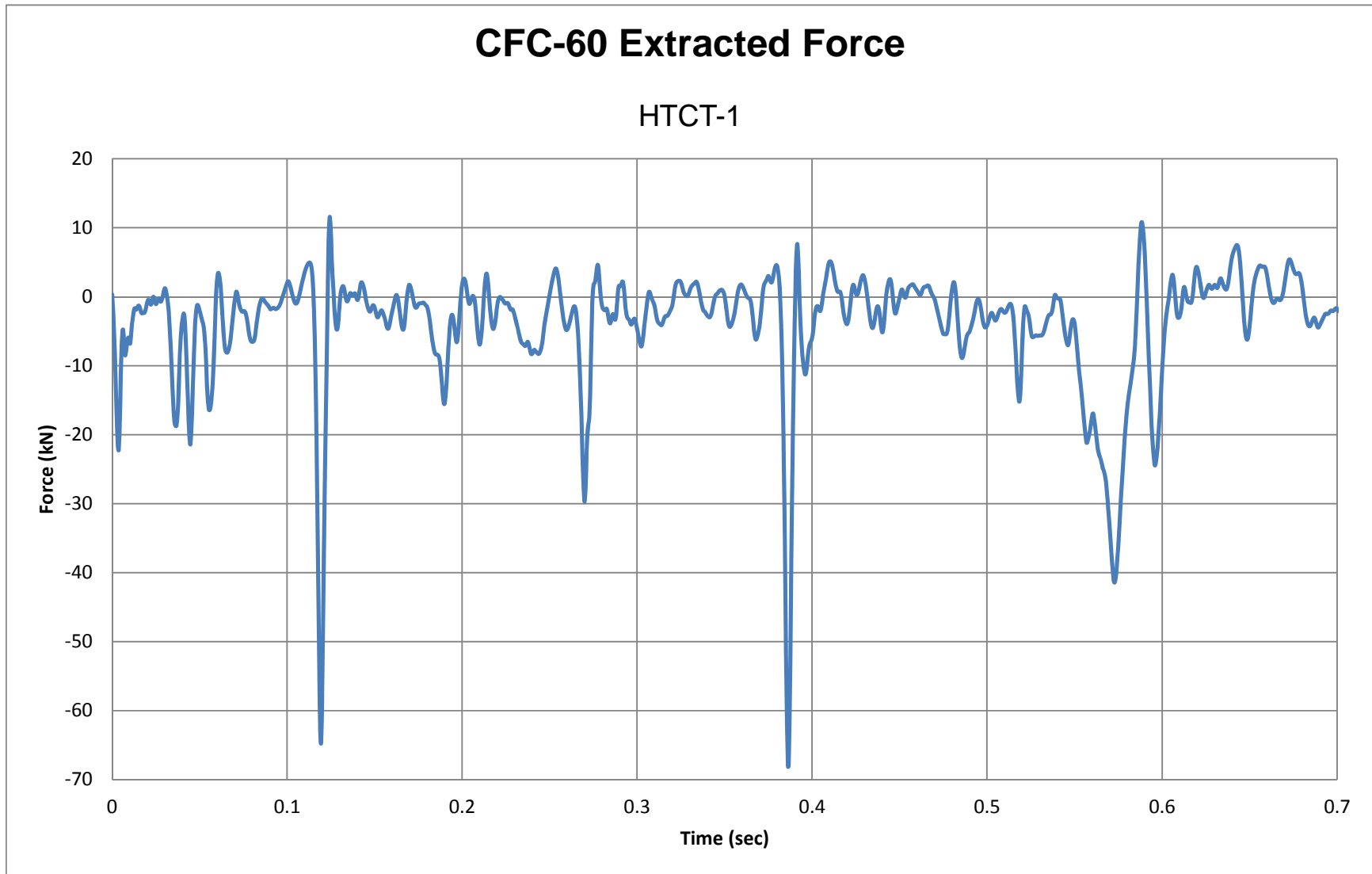


Figure B-1. Force vs. Time, Test No. HTCT-1

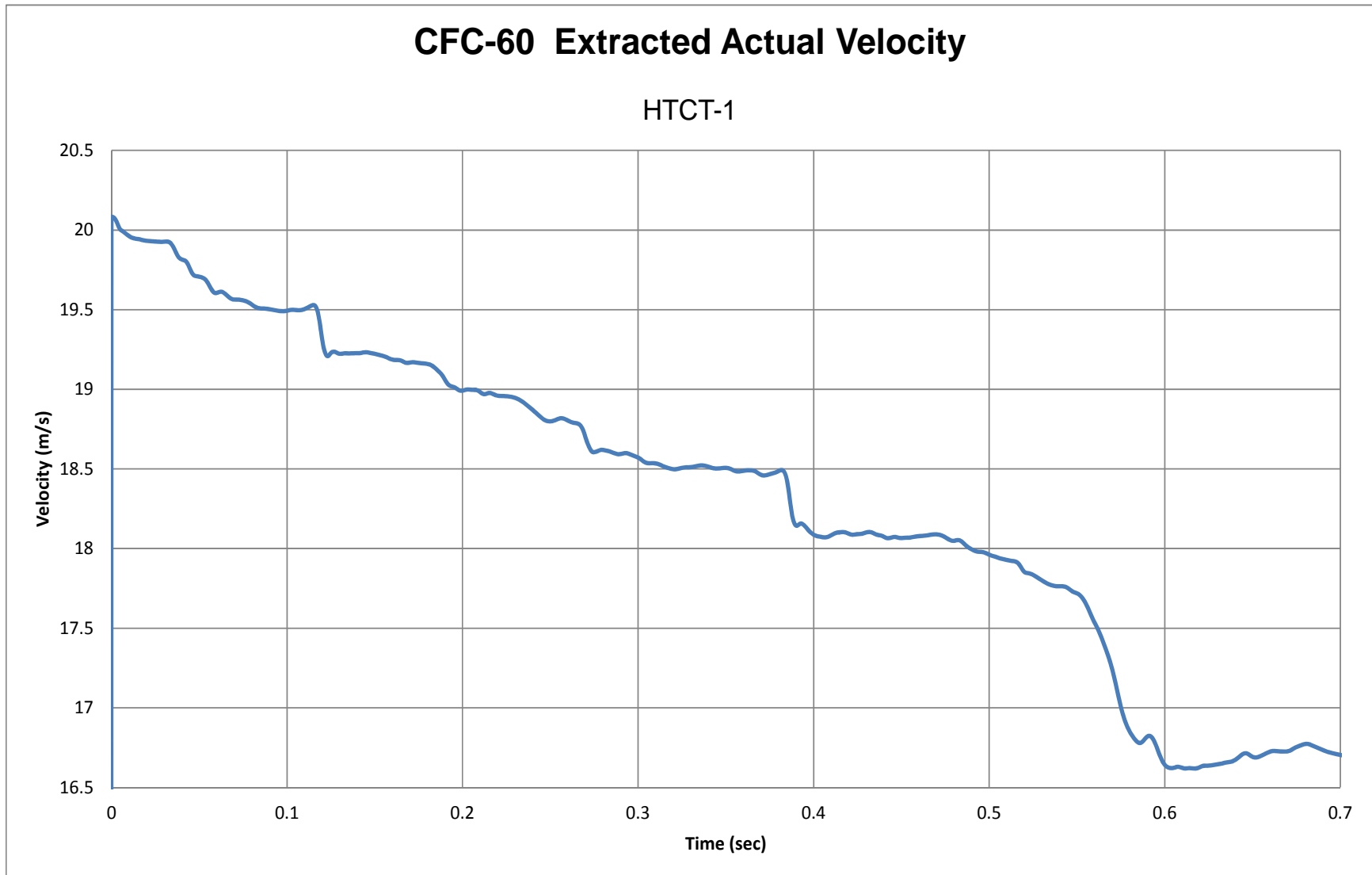


Figure B-2. Velocity vs. Time, Test No. HTCT-1

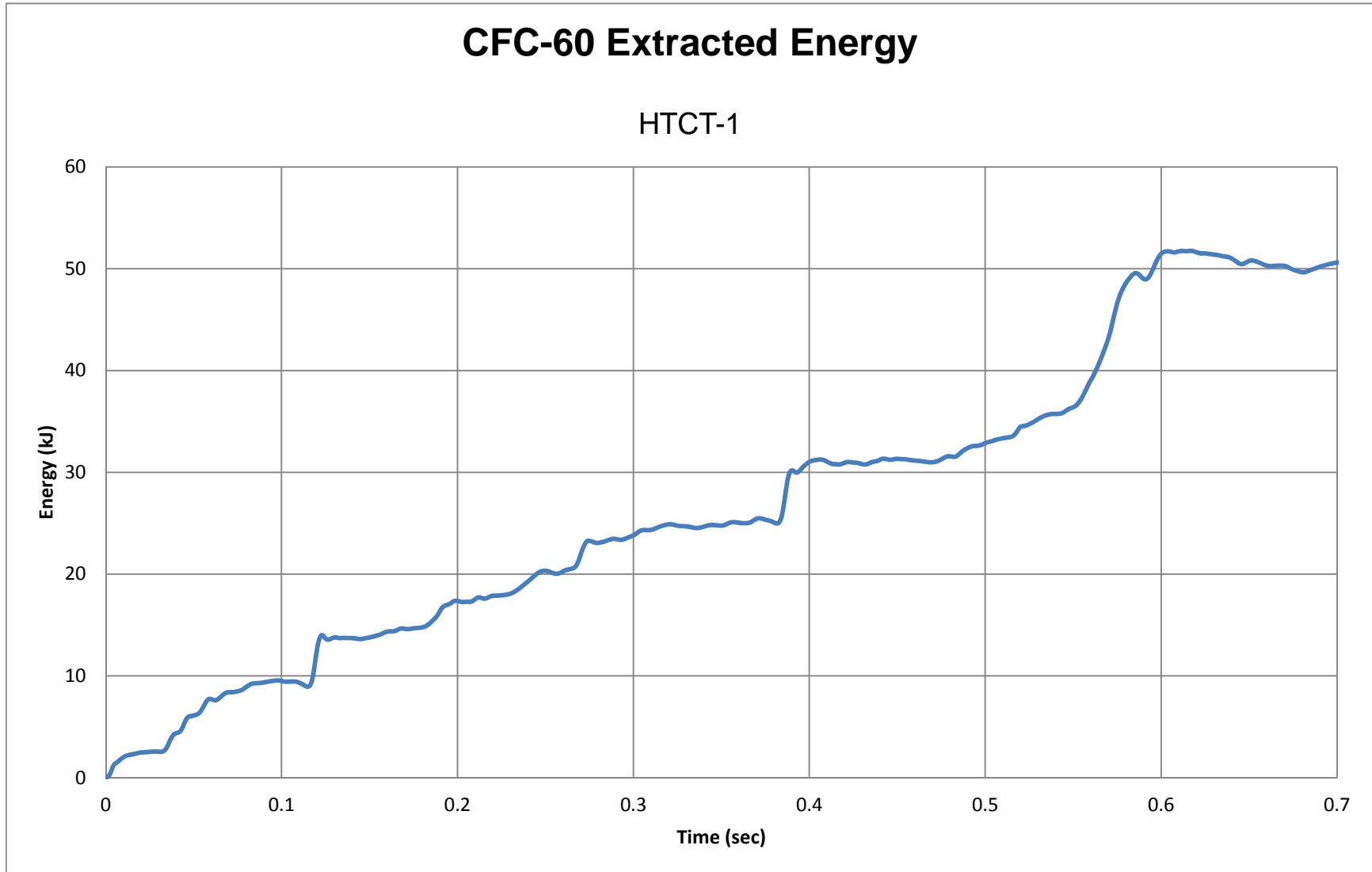


Figure B-3. Energy vs. Time, Test No. HTCT-1

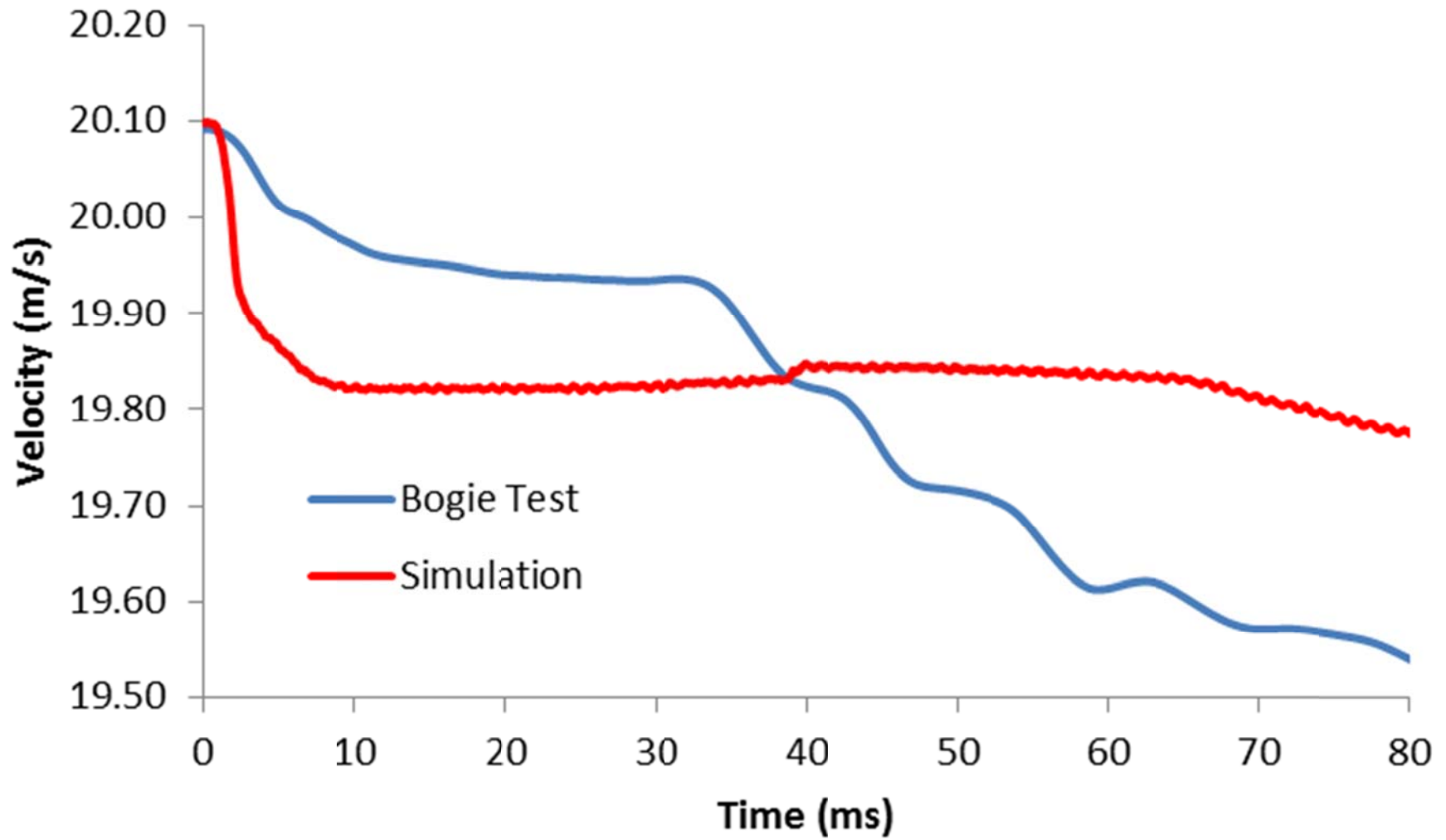


Figure B-4. Bogie Velocity Comparison, Test No. HTCT-1 vs. Simulation

**Appendix C. Standard MwRSF Bogie Test Sheet, Test No. HTCT-1**

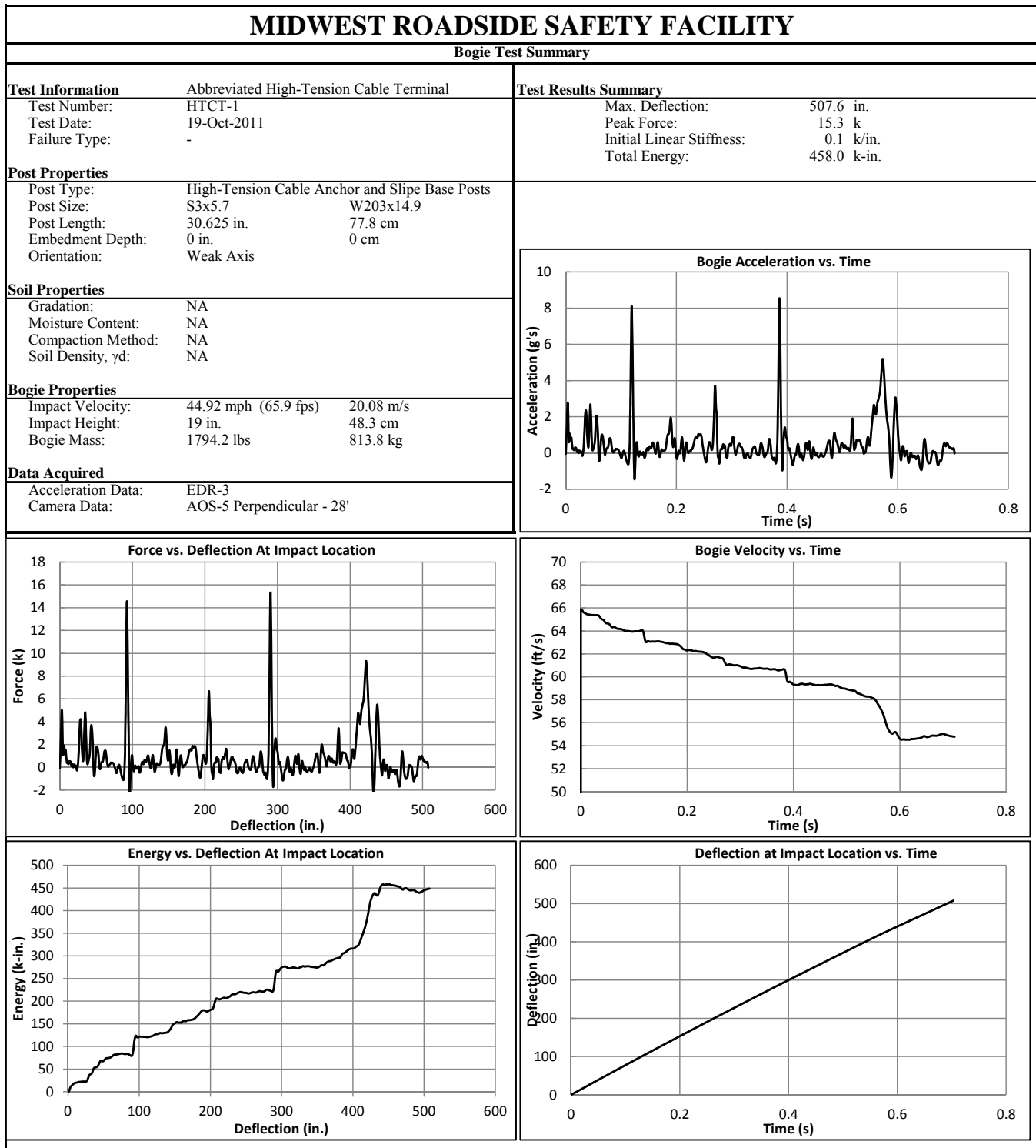


Figure C-1. Results of Test No. HTCT-1 – English



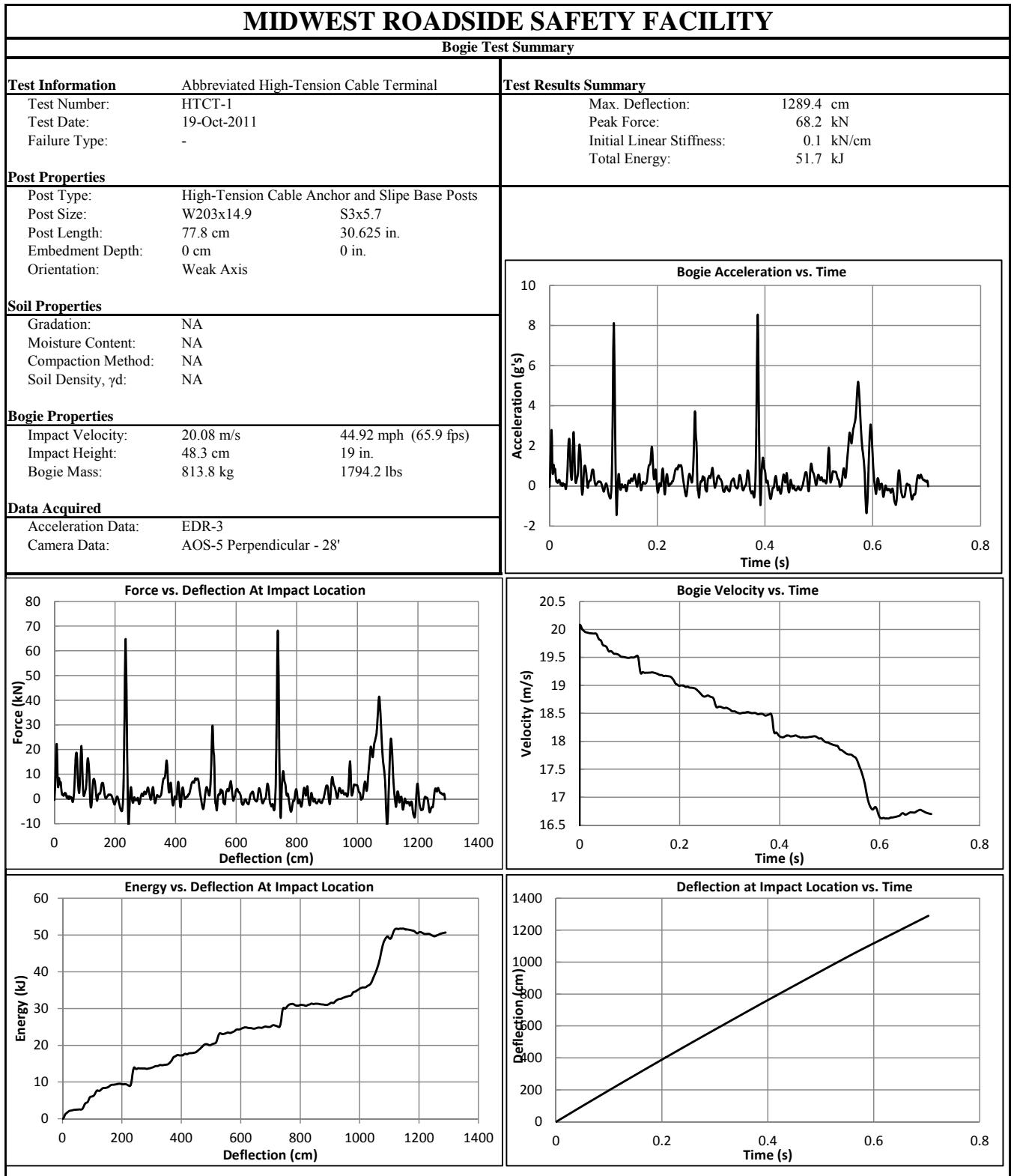


Figure C-2. Results of Test No. HTCT-1 – Metric

**Appendix D. Redesigned Cable Anchor Bracket Simulation Results – Metric**

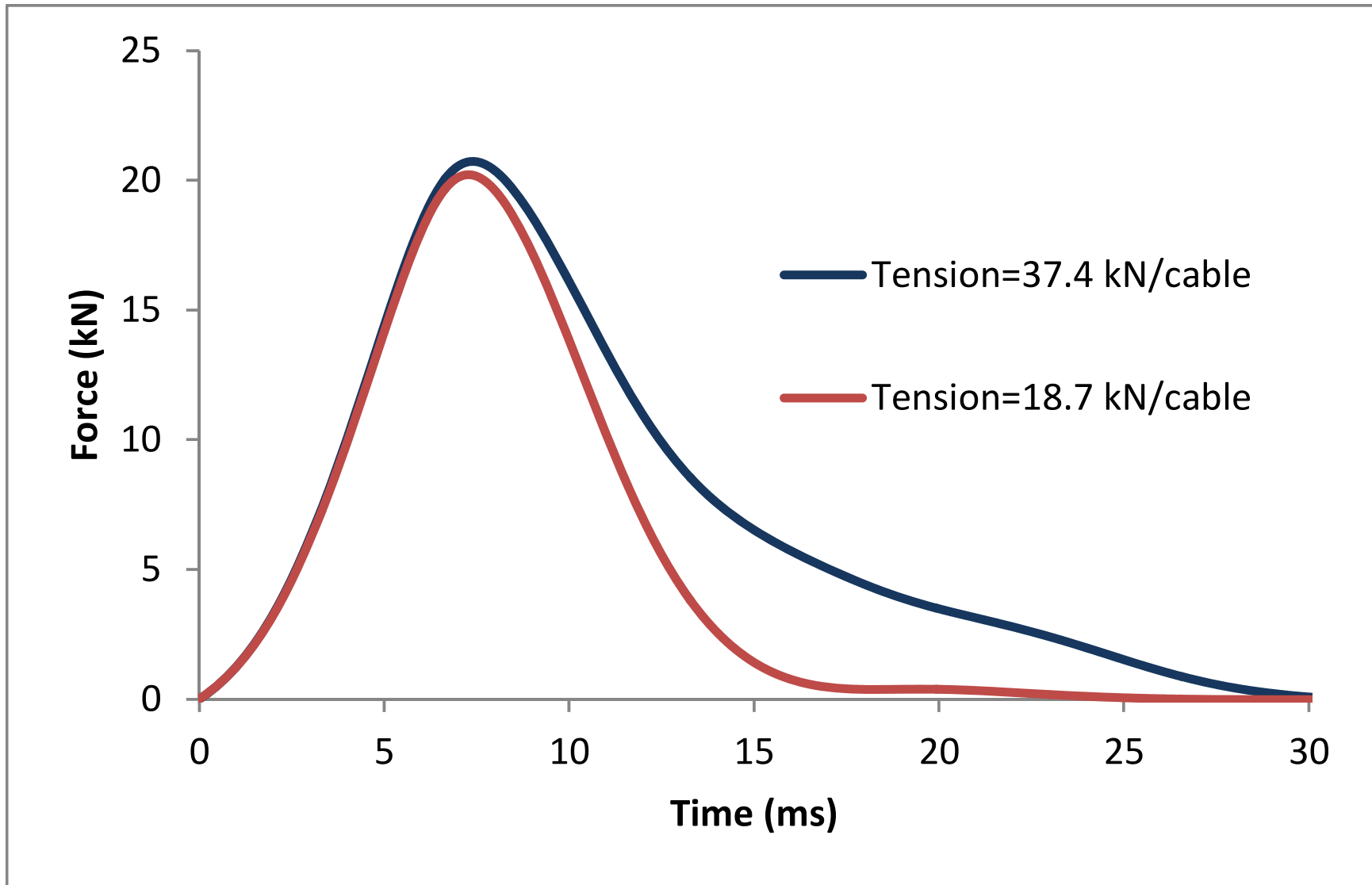


Figure D-1. Impact Force Comparison, Increased Cable Tension vs. Design Tension

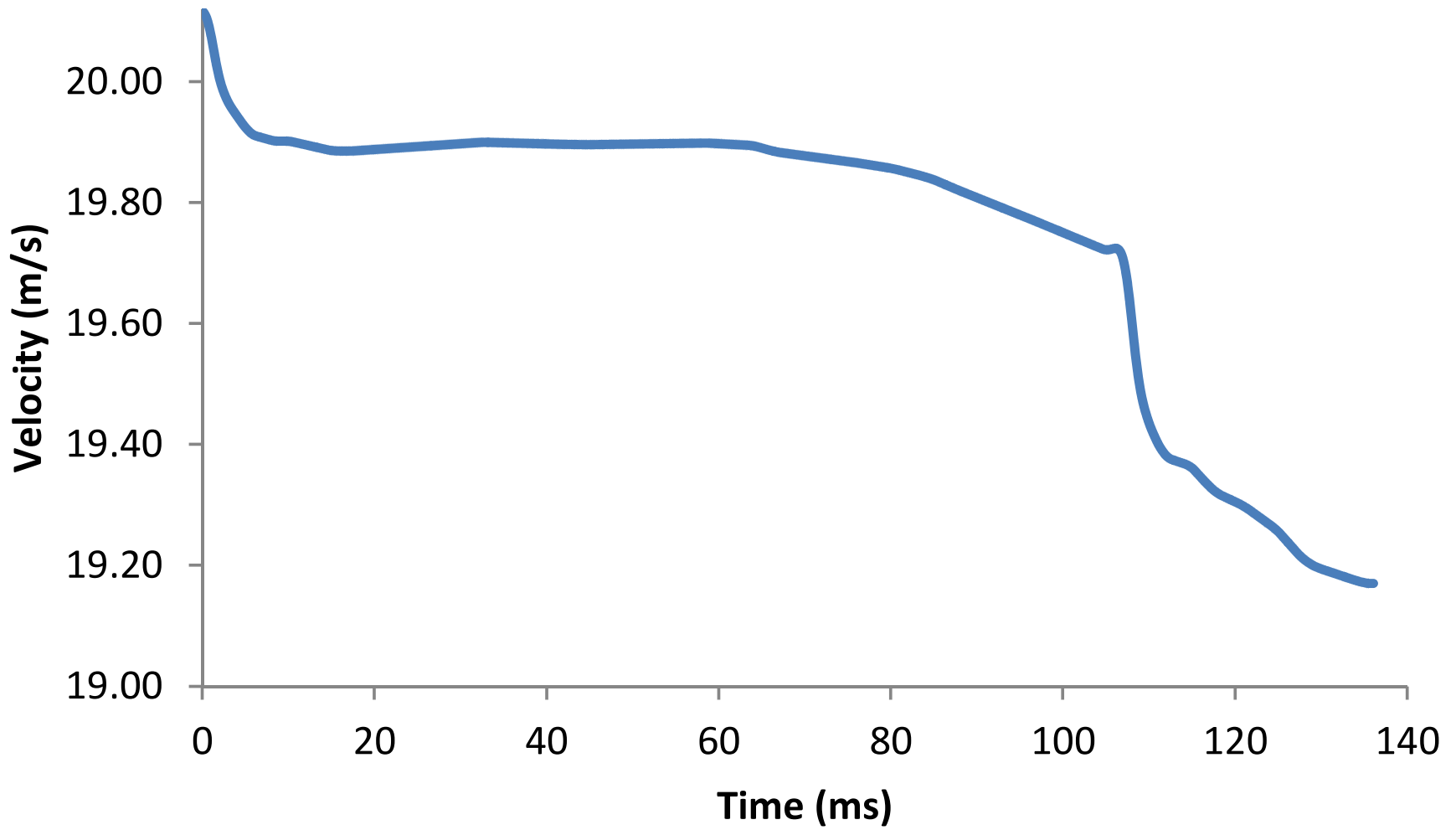


Figure D-2. Bogie Velocity, Final Redesign

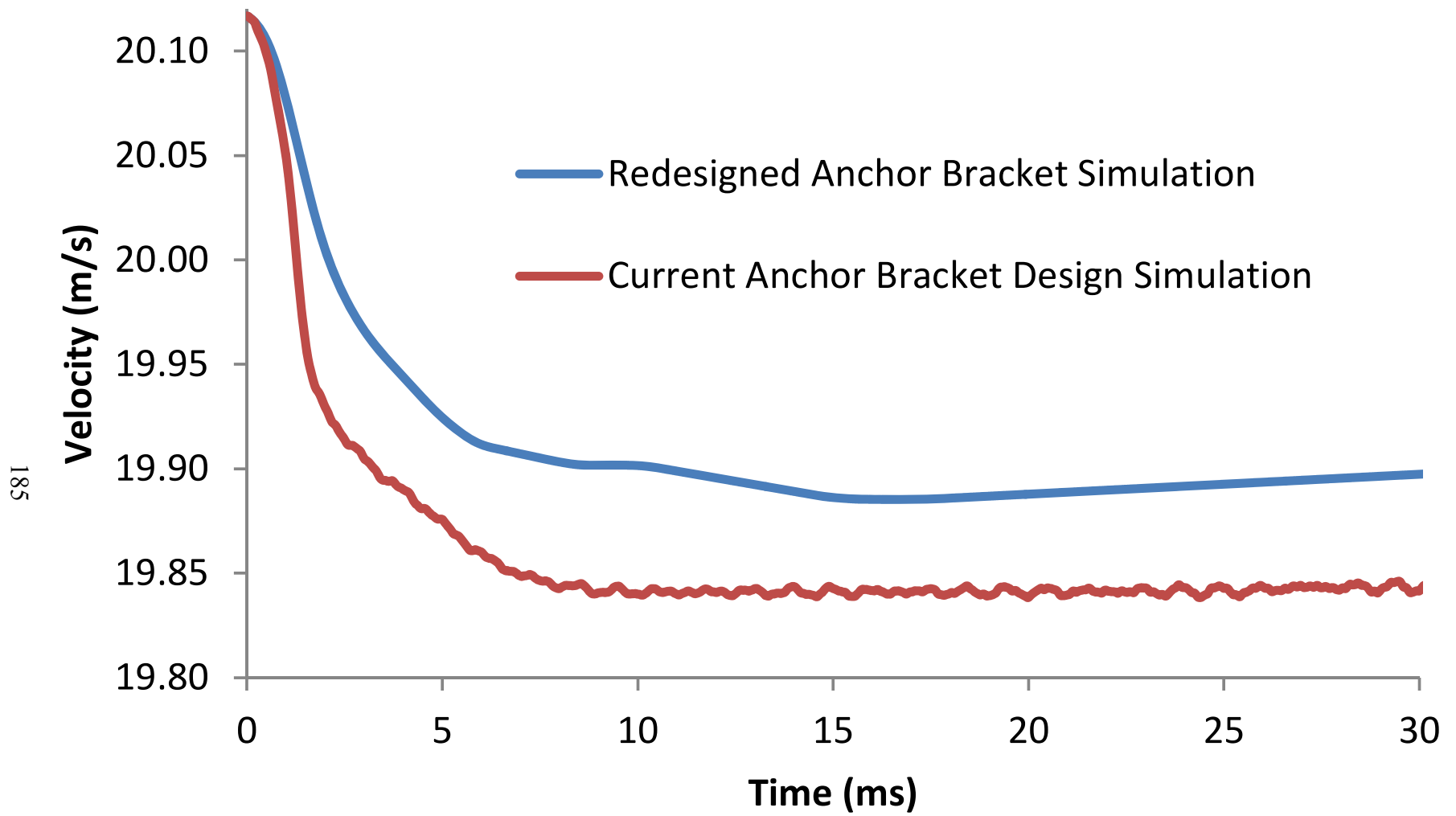


Figure D-3. Anchor Bracket Assembly Simulations Velocity Comparison

**END OF DOCUMENT**